LARGE APERTURE SEISMIC ARRAY

FIRST LASA SYSTEMS EVALUATION CONFERENCE

September 14-16, 1965

ARPA

ADVANCED RESEARCH PROJECTS AGENCY

DISCLAIMER NOTICE

THIS DOCUMENT IS THE BEST
QUALITY AVAILABLE.

COPY FURNISHED CONTAINED
A SIGNIFICANT NUMBER OF
PAGES WHICH DO NOT
REPRODUCE LEGIBLY.

FIRST

LASA SYSTEMS EVALUATION CONFERENCE

SEPTEMBER 14 - 16, 1965

1. PREFACE

The material contained in this conference report consists of a compilation of the papers presented at the First LASA Systems Evaluation Conference.

This conference was intended to serve three purposes: 1. To acquaint all the organizations currently participating in the program with the status of the work; 2. To attempt to formulate the prototype station and network specifications; and 3. To provide a record of the project activities in the conference report.

The papers contained herein have been reproduced as written by the authors without screening for technical errors or omissions. Their reproduction in this report does, therefore, not constitute endorsement of the material by ARPA.

The conference was hosted in the exceptionally well-appointed Board Room of the Institute for Defense Analyces (IDA). I want to extend our appreciation to IDA for providing the conference room, and making all the necessary arrangements to minister to the needs of the attendees.

I would also like to thank Dr. Milton Clauser of IDA for welcoming us to IDA, and Dr. Robert Frosch of ARPA for his introductory remarks, which set the theme for the conference.

H. Sonnemann
ARPA

2. TABLE OF CONTENTS

3. LIST OF ILLUSTRATIONS

x

4. THE LASA SIGNAL ACQUISITION SYSTEM

by
C. B. Forbes, R. Obenchain, and R. McLamore
UED Div., Teledyne, Inc.

1. PREFACE:

In discussing the LASA Signal Acquisition System, the emphasis will be on the appearance and operational characteristics of the system as it exists today, with only casual reference to the process of installing the system.

2. DEFINITION:

The LASA Signal Acquisition System includes those components necessary to convert earth motion to electrical energy and present it at a convenient location in a form suitable for further processing or conditioning.

3. LOCATION AND ENVIRONMENT:

The LASA is located in sparsely-populated southeastern Montana in an area of rolling to moderately rugged topography, as shown in Figure 1. The area is characterized by cold winters and hot, dusty summers. Thunder and lightning storms are frequent in the spring and early summer. Figure 2 shows three geologic cross-sections across the area. The cross-sections are based on published material supplemented by electric logs and sample logs from the 500-foot deep holes which were drilled at the center of each LASA subarray. Even with the vertical scale exaggeration of 20 times the horizontal, Figure 3, the structures shown appear rather gentle. The maximum dip shown is two degrees.

4. LASA CONFIGURATION:

The 525 seismograph or earth-motion sensors that comprise the LASA Signal Acquisition System are segregated into groups of 25 called subarrays. The upper portion of Figure 4 shows: 1)-the relative positions of the subarrays; 2)-the MIT numerical designation of each subarray; and 3)-the plan for alpha-numeric designation of each subarray. In the latter plan the center subarray is designated as A0(A-Zero). NS and EW axes are drawn through A0. The 20 remaining subarrays are then connected by semi-concentric rings (dashed lines in the figure) around A0 The rings are designated by the letters 1 through 7 and the quadrants numbered clockwise with the northeast quadrant being number one. Thus, using this scheme, the subarray which is detailed is designated as F2.

The plan view and alpha-numeric designation of the 25 seismographs in each subarray is shown in the center portion of Figure 4. Referring back to Figure 1 you can observe the pattern

FIGURE 1. AERIAL PHOTO OF SUBARRAY

of broken ground and trails which indicates the location of the cables that connect the seismographs to the Central Terminal Housing.

The relationship between the major units in one leg of subarray is shown schematically in the cross-section at the bottom of Figure 4.

5. PHYSICAL DESCRIPTION OF UNITS WITHIN THE SUBARRAYS:

All electronic components were installed in as protected an environment as possible, while maintaining accessibility and providing for ease of modification.

5.1. SEISMOGRAPH:

The major components of each seismograph are installed in a drilled hole with the seismometer near the bottom of the hole and the amplifier near the top. The 24 radial holes are 5 inches in diameter and 200 feet deep and the center hole of each subarray is 6.5 inches in diameter and

2

LASA
GEOLOGIC CROSS SECTIONS

FIGURE 2   GEOLOGICAL CROSS SECTIONS

3

LASA GEOLOGIC CROSS SECTIONS

FIGURE 3. GEOLOGIC CROSS SECTIONS. 20:1 VERTICAL EXAGGERATION

4
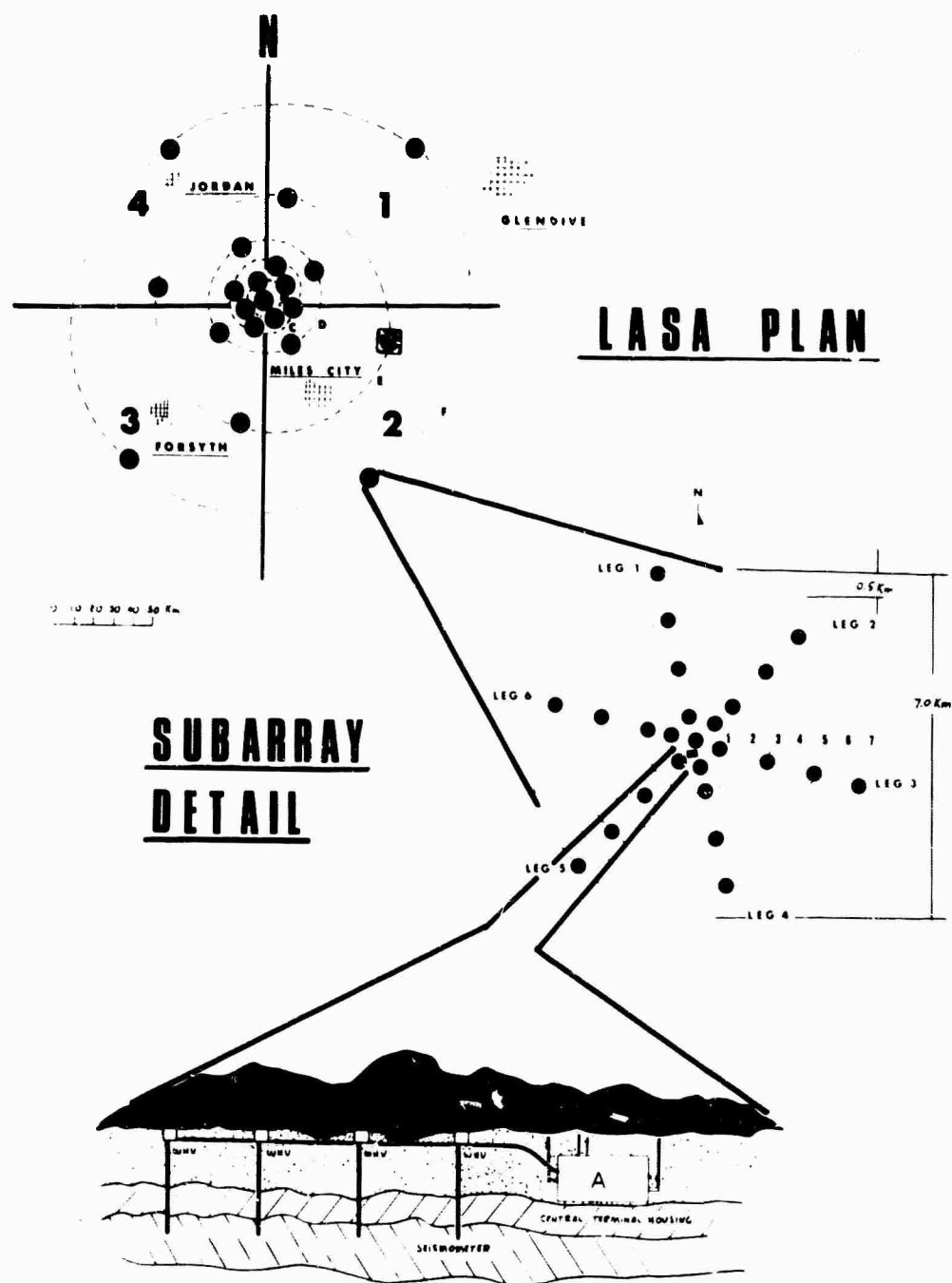
FIGURE 4. LASA CONFIGURATION

500 feet deep. Figure 5 is a schematic representation of a typical installation, and Figure 6 is a photograph of a typical finished installation.

..t the top, there is a three-strand triangular fence surrounding a conical, galvanized iron rain cover called a "coolie hat." This rain cover is held down by three right-angle spikes. The rain cover does not touch any of the components beneath it.
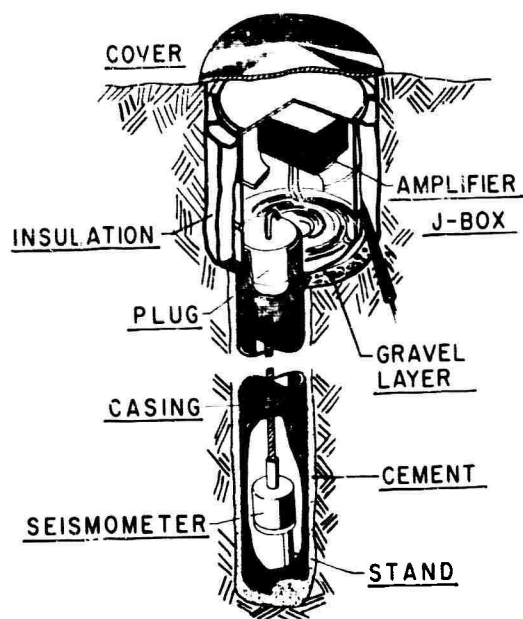
FIGURE 5. WELL HEAD VAULT SITE, TYPICAL BOREHOLE INSTALLATION
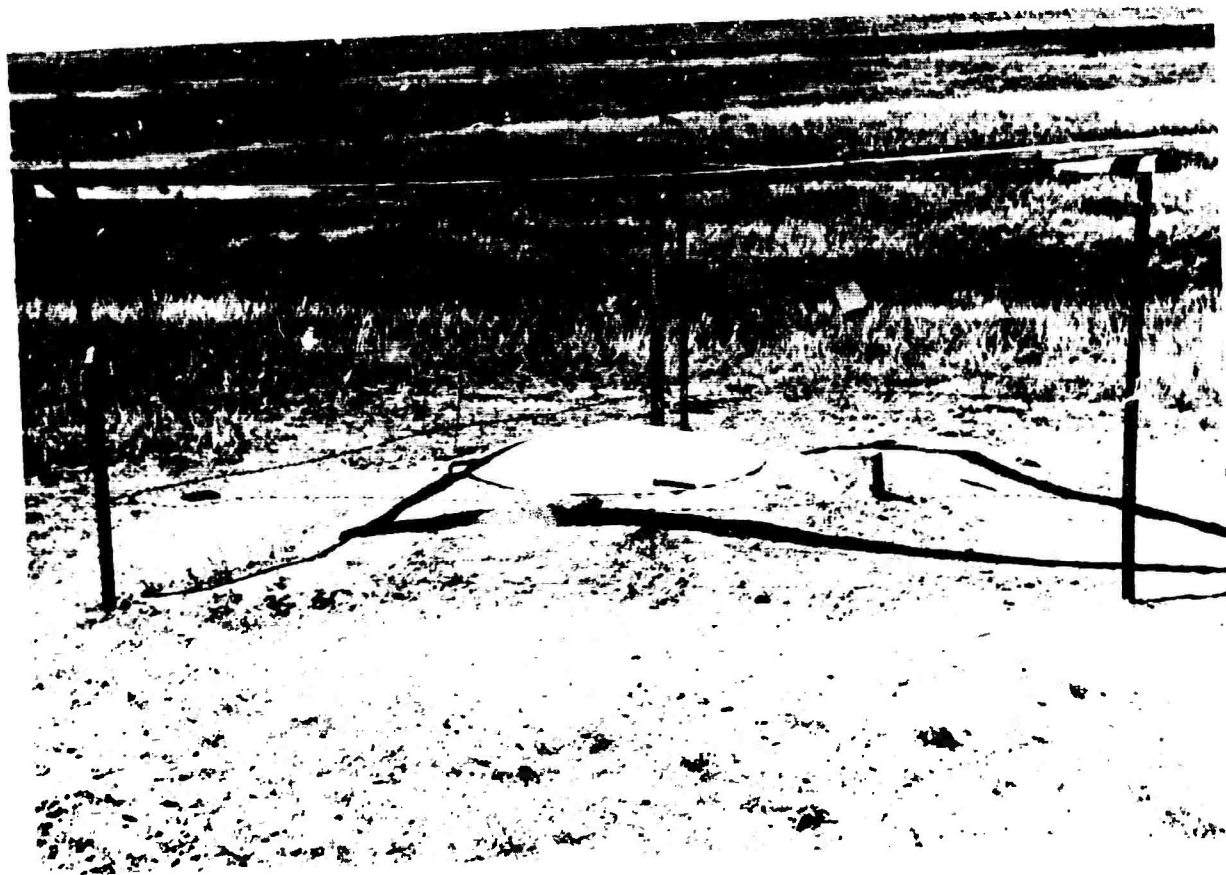
FIGURE 6. WELL HEAD INSTALLATION, SITE PHOTOGRAPH

6

If we remove the rain cover we see the Well-Head vault (WHV), Figure 7. The vault itself is standard designed 55-gallon drum shortened to a height of 24 inches. The gasketed lid is attached by use of a "V"-shaped ring clamp.

A two-inch thick circular pad of Dyfoam insulation is attached to the inside of the lid. The outside of the barrel (WHV) is coated with an asbestos/asphalt preparation to impede corrosion. Polyethylene bags filled with vermiculite are installed around the WHV to provide approximately 5 inches of thermal and acoustical insulation (Figures 5 and 7). The backfilled dirt around the insulation is tamped and graded to drain away from the installation.

Removing the lid from the WHV exposes (Figure 8) the water-and gas-tight Hoffman Junction box that houses the amplifier and related electronic components. The box also contains a sack of dessicant to absorb moisture.

FIGURE 7. TOP OF WELL HEAD VAULT

The Hoffman Box can be lifted out of the WHV if desired. Approximately 10 feet of cable is coiled in the lower half of the barrel to permit such removal if desired, as shown in Figure 9.

A ring of sheet metal spot welded 10 inches below the top of the barrel serves as a shelf to hold the Hoffman Box, and also provides a ground connection (see Figure 9).

The conduit to conduct the cables into the WHV is installed tangentially to the barrel (see Figure 5), to avoid kinking the cable as it is coiled inside the barrel.

A maximum of usable floor space in the barrel is obtained by mounting the barrel off-center on the well casing (Figure 9). The hole is covered and sealed by a tapered, split, rubber plug which aids in maintaining a constant pressure and humidity within the borehole.

A six-inch layer of gravel is emplaced beneath the well-head vault to provide good drainage for ground water that penetrates into the well-head vault area (Figure 5).
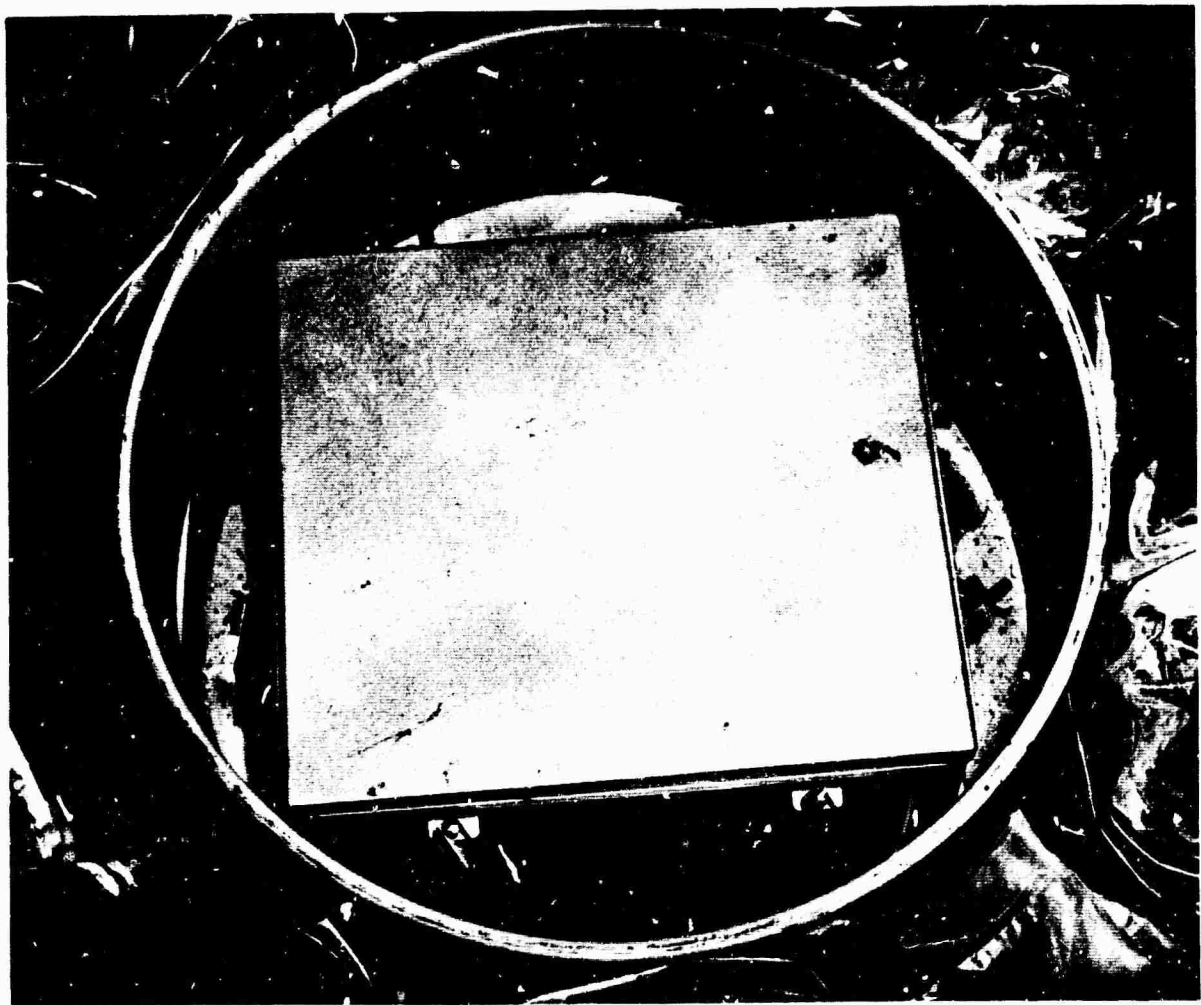
FIGURE 8. HOFFMAN "J" BOX IN WELL HEAD VAULT

8

All of the boreholes, except the 24 radial holes in subarray D1 are cased. The casing is cemented in from top to bottom for stability. A two- or three-foot cement plug in the bottom of the hole provides a water-tight seal (Figure 5).

The earth-motion sensor or transducer is mounted near the bottom of the hole. This unit is the Hall-Sears model HS-10-1 (ARPA) velocity-sensitive seismometer which has a nominal natural frequency of 1 cps and requires near-vertical installation. For this reason all holes were required to be within 6° of vertical. The drilling practices used resulted in an average deviation from vertical of approximately $1 1/2^O$ with a maximum of $3 3/4^O$.

The seismometer was emplaced in a waterproof case for installation. (See Figure 10.) A 5-foot length of pipe, offset from the center, is attached to the bottom of the geophone case by a threaded collar (Figure 5). The offset pipe provides two advantages: 1)-it eliminates the prob-

FIGURE 9. INTERIOR OF WELL HEAD VAULT

9

ability of installing an inverted pendulum, and 2)-it provides for positioning the geophone in the hole on a trial and error basis for minimum deviation from vertical.

2. CABLE:

minimize interference with normal agricultural activities and reduce system maintenance requirements, all cable within the data acquisition system is buried approximately three feet below the surface.

To provide circuit flexibility and low cost, two cables of REA specification PE-23, 6-pair construction were laid together along each radial of each subarray using a typical cable plow. (See Figure 22.) The conductors are encased in a polyethylene jacket, which is in turn encased in a solid, corrugated, .010-inch thick copper shield. An outer polyethylene jacket encloses the shield. Both cables enter each well-head so that all cable conductors and shields are accessible on taper pin terminal blocks inside the Hoffman Boxes

FIGURE 10. SEISMOMETER ASSEMBLIES

10

5.3. CENTRAL TERMINAL HOUSING:

Near the center of each subarray, an underground concrete vault, called the Central Terminal Housing (CTH) is installed as pictured schematically in Figure 11. The CTH serves as the data collection center for the subarray and houses power, communication and signal conditioning equipment.
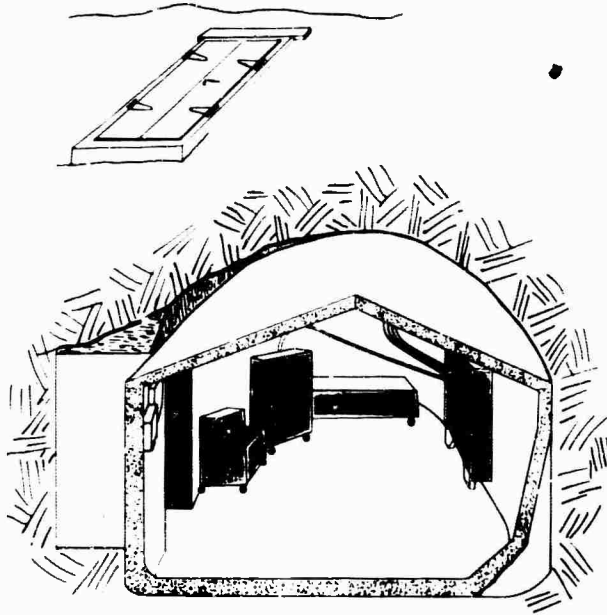
FIGURE 11. CENTRAL TERMINAL HOUSING (CTH)

The CTH is a monolithic concrete structure with at least three feet of earth cover. The approximate inside dimensions of the vault are 12 feet by 10 feet with the dome-shaped ceiling rising from 6 feet at the sides to 6 feet, 8 inches in the center.

Figure 12 is a photograph of the entrance to a CTH. To the left of the open doors, 4 vertical pipes mark the location of the body of the vault. Two of these pipes are for ventilation. The center pipes are to accommodate jumper cables for occasional data users such as an LRSM van.

Figure 13 shows the CTH doors closed displaying the subarray designation and an arrow pointing to the number-one leg.

A total of 16 conduits and vents were provided in the CTH by installing the necessary pipes before pouring the concrete; eight for data transmission cables, two for commercial power, two for telephone lines, and the aforementioned vertical pipe for ventilation and accommodation of temporary data lines.

When we go into the vault and look right, we see the main power distribution and circuit breaker box and the isolation transformer (Figure 14). On the other hand, if we look left we

11

FIGURE 12. ENTRANCE TO CTH

will see in order along the wall (Figures 11 and 15), a dc/ac inverter, a battery charger, and a 30-volt battery of nickel cadmium cells.

Directly across from the entrance we see the gas-tight Hoffman Box housing the central terminal panel (Figure 16). The panel contains lightning protection and all interconnections for power, signals and calibration. Flexibility is provided by the wide use of barrier-type terminal strips. The cables from the seismographs enter the box from the left. The connectors at the upper right are provided for quick connection of the signal conditioning equipment, and for routine calibration signal inputs.

6. INSTRUMENTATION:

Figure 17 is a block diagram of the system. The lower portion depicting the instrumentation in the CTH and the upper portion showing the instrumentation at the well-head.

12

FIGURE 13. CTH DOORS

6.1. POWER:

The commercial power is passed through an isolation transformer for lightning protection. At this time commercial power is used directly for auxiliary uses such as lights and for the signal conditioning equipment that has been installed. By the time all the subarrays have signal conditioning equipment, it is planned that all the instrumentation will be powered from the 30-volt battery as is shown in Figure 17. The batteries are kept fully charged by the battery charger

FIGURE 14. COMMERCIAL POWER DISTRIBUTION UNITS, CTH

on the commercial power line. Output from the batteries is converted into 60-cycle, 115-volt power for the signal conditioning equipment by the dc/ac inverter.

The power required by each of the amplifiers at the well-heads is 8 milliamps at 18 volts. The battery voltage is high enough to permit final Zener regulation of the 18 volts at each well-head, thereby automatically compensating for supply variations due to temperature changes and cable lengths. Partial regulation is provided by isolating resistors on the printed circuit cards
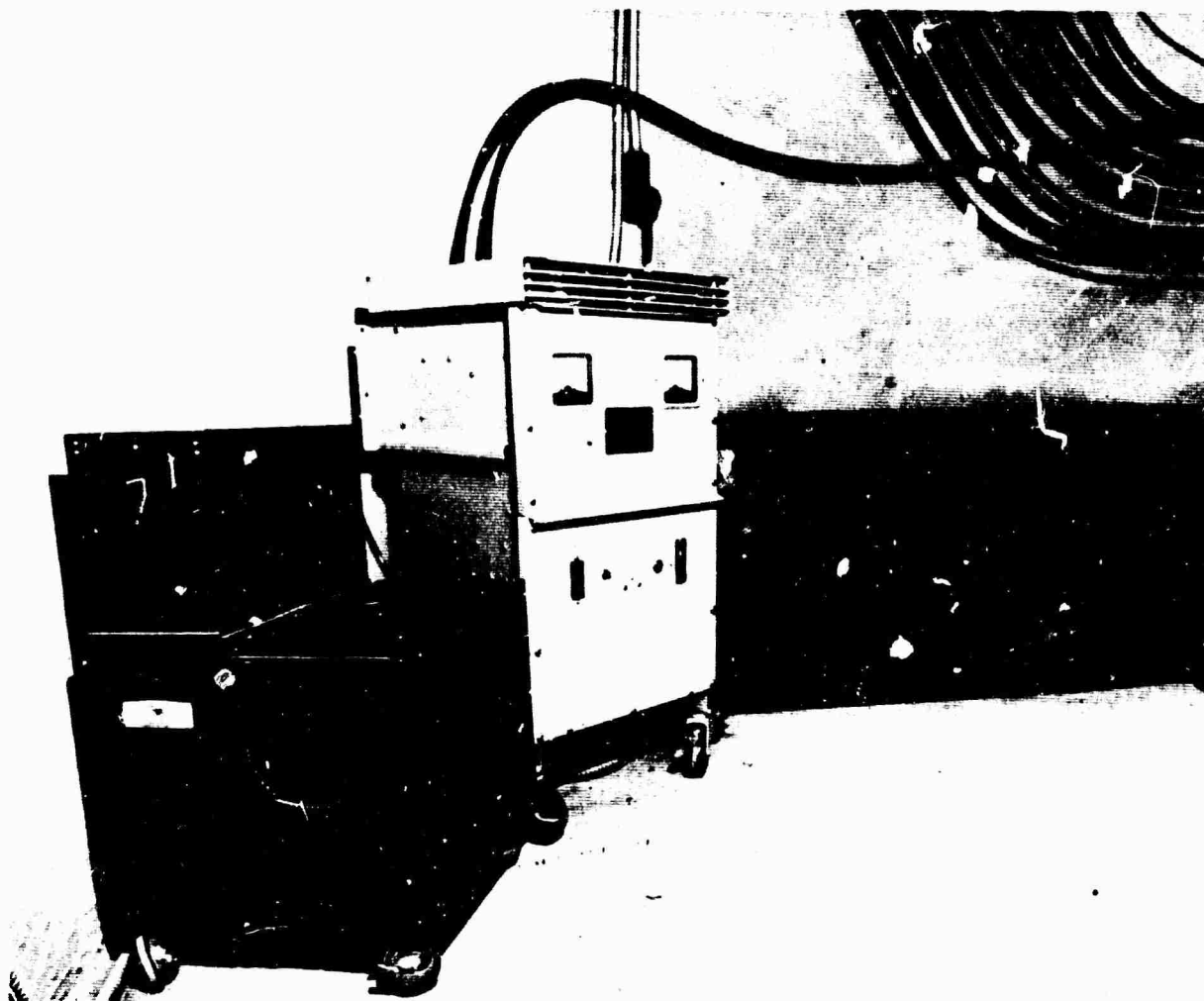
FIGURE 15. STANDBY POWER UNITS, CTH

on the central terminal panel (Figure 16). In the event of commercial power failure, the battery-inverter power system can keep the array operational for a minimum of eight hours.

6.2. WELL-HEAD AMPLIFIER PANEL:

Looking inside the Hoffman Box at the well-head, we see the amplifier panel (Figure 18) assembly. It includes the Texas Instruments RA-5 parametric amplifier, seismometer damping and equalizing resistors, calibration resistors for both the seismometer and amplifier, lightning protectors and terminal strips.

The panel can be quickly removed from the box for replacement or maintenance. All cables coming into the junction box are terminated in an AMP terminal block mounted permanently in the box. The AMP taper pin system provides low impedance connections and eliminates soldering under field conditions. From this taper pin terminal strip, a harness of leads is provided

15
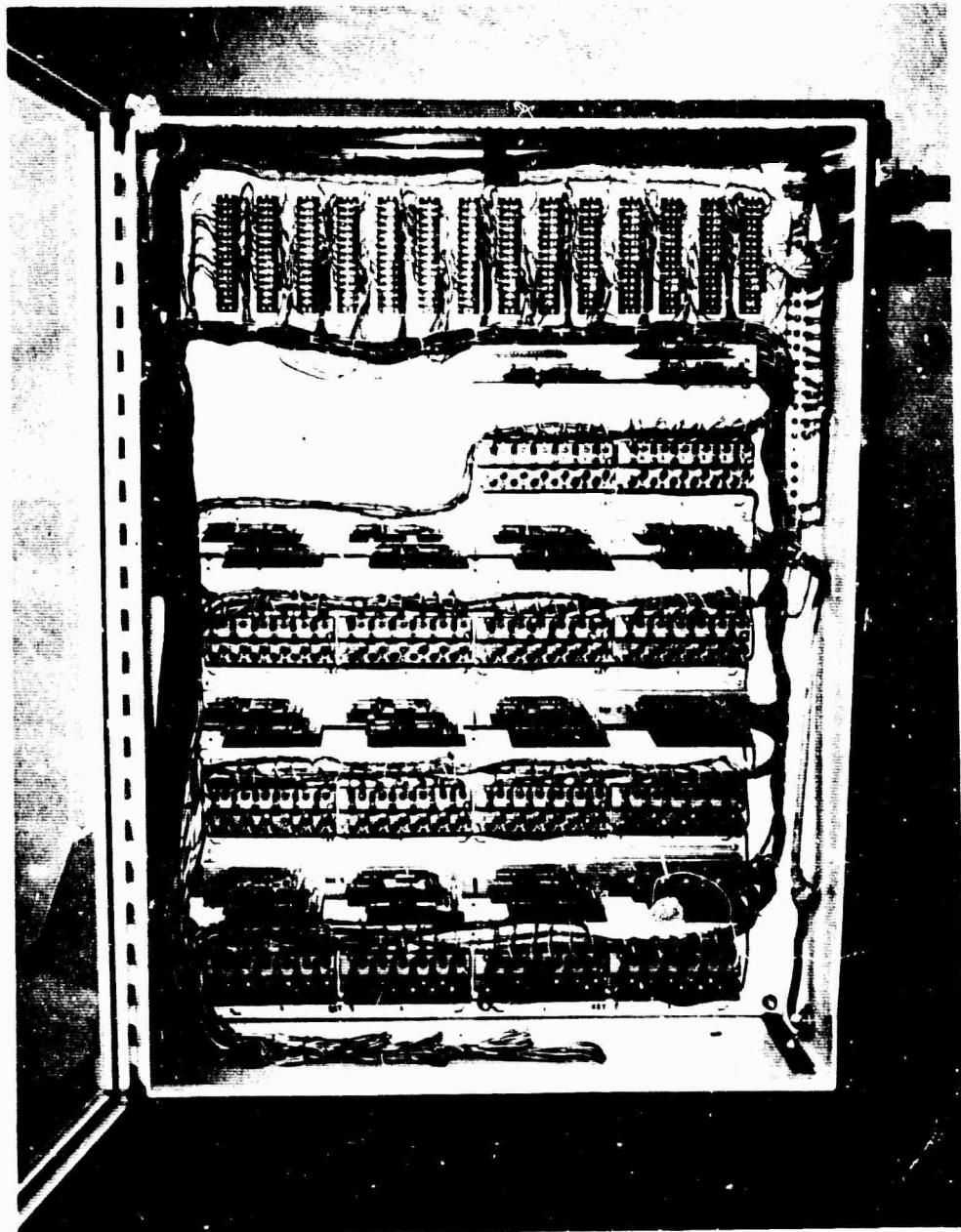
FIGURE 16. CENTRAL TERMINAL PANEL, CTH

which terminates in a connector which matches with a connector on the amplifier panel. Circuit continuity is completed by taper pin jumpers which also provide for temporary circuit changes or future required modifications or utilization of the spare cable conductors which are already installed on the terminal strip.

All small components such as resistors, diodes, and inductors are mounted on one of three printed circuit cards (Figure 18). These cards provide flexibility in test and checkout of the

16
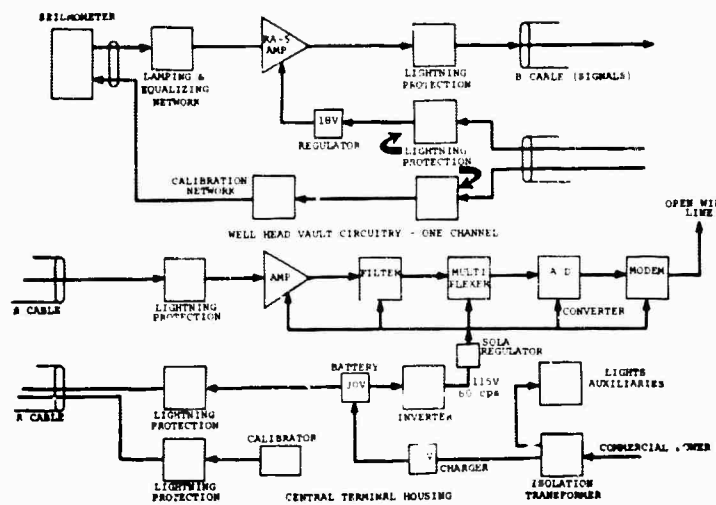
FIGURE 17. BLOCK DIAGRAM OF SIGNAL ACQUISITION SYSTEM

FIGURE 18. WELL HEAD VAULT, HOFFMAN BOX, COVER REMOVED

17

system and ease of replacement of components. The "switch" card allows for "turning off" the seismometer, and also provides an additional 30,000 ohms attenuation in each side of the circuit, if needed, by si. clipping a shunt. A "calibration" card (beside the switch card) provides a variety of damping resistances and allows removal of the damping circuitry from the amplifier input. The "protector" card (next to the amplifier) provides (1) continuity to the calibration coil with the required resistors, (2) some lightning protection circuitry, and (3) voltage regulation circuitry for the amplifier power.

The system sensitivity is specified to be 20 millivolts per millimicron of earth motion at one cycle per second. The sliding resistors (Figure 18) permit adjustment of each system to this condition while driving the seismometer through the calibration circuitry.

The RA-5 amplifier has a flat frequency response from 0.1 cps to over 200 cps, and is operated at a fixed gain of 10,000.

6.3. LIGHTNING PROTECTION:

Protection against voltage transients from the cable terminals to the amplifier circuits is tapered. Two levels of voltage protection were established in the original design, starting with carbon blocks (shown in Figure 18) (375-500 volts) at both ends of the cable, and Zener diodes (13 volts for signal or t each side to common; 18 volts for amplifier power regulation and protection). Subsequent to the completion of the installation, the system suffered considerable damage from lightning. Circuit changes have been made to reduce such damage, including the addition of three-electrode gas tube protectors of 150-200 volts breakdown.

The cable pairs used for signal, power, and calibration are operated in a balanced state. The two separate cables of each spoke are balanced to each other by connecting their shields at every well-head vault and by Zener diode clamping.

Shield grounding is accomplished by deliberately grounding it to wells at every possible point in the system. All shields are grounded to the 500-foot well casing.

6.4. COMPONENT PERFORMANCE:

Clear, meaningful statistics on component performance (failure rate) are not yet available because of the severe damage incurred from lightning prior to the modifications to the lightning protection circuitry. This modification was completed on the last subarray last week (September 8). However, we are encouraged by the following facts:

1. There have been only three seismometer failures si. June 1 out of the 475 installed by Teledyne.
2. No modified subarray has sustained significant lightning damage.

18

3. Less than two percent of the amplifiers on the modified subarrays have given trouble.

4. One splice failure has been the only cable problem to date.

7. INSTALLATION OF THE LASA:

The installation of the LASA was accomplished by dividing the work into three main phases, or fields of effort.

7.1. CONSTRUCTION PHASE:

The construction phase consisted of: producing and casing the boreholes; cementing the casing in place; laying the cable along the spokes of the subarray; and installing the well-head vaults and central terminal housings. A trailer camp shown in Figure 19 was established in the field as a base of operations for the drilling effort. Figure 20 shows typical drilling activity. A total of 12 drilling rigs were used to produce drill holes at the required rate. The drills were operated on a 24-hour/day, seven-day/week basis.

Figure 21 shows the mobile "cement factory" which was used to cement the casing in the hole. The grout mixture was mixed on the spot and pumped down the inside of the casing and forced up the outside until it filled the annulus.

FIGURE 19. FIELD CAMP

19
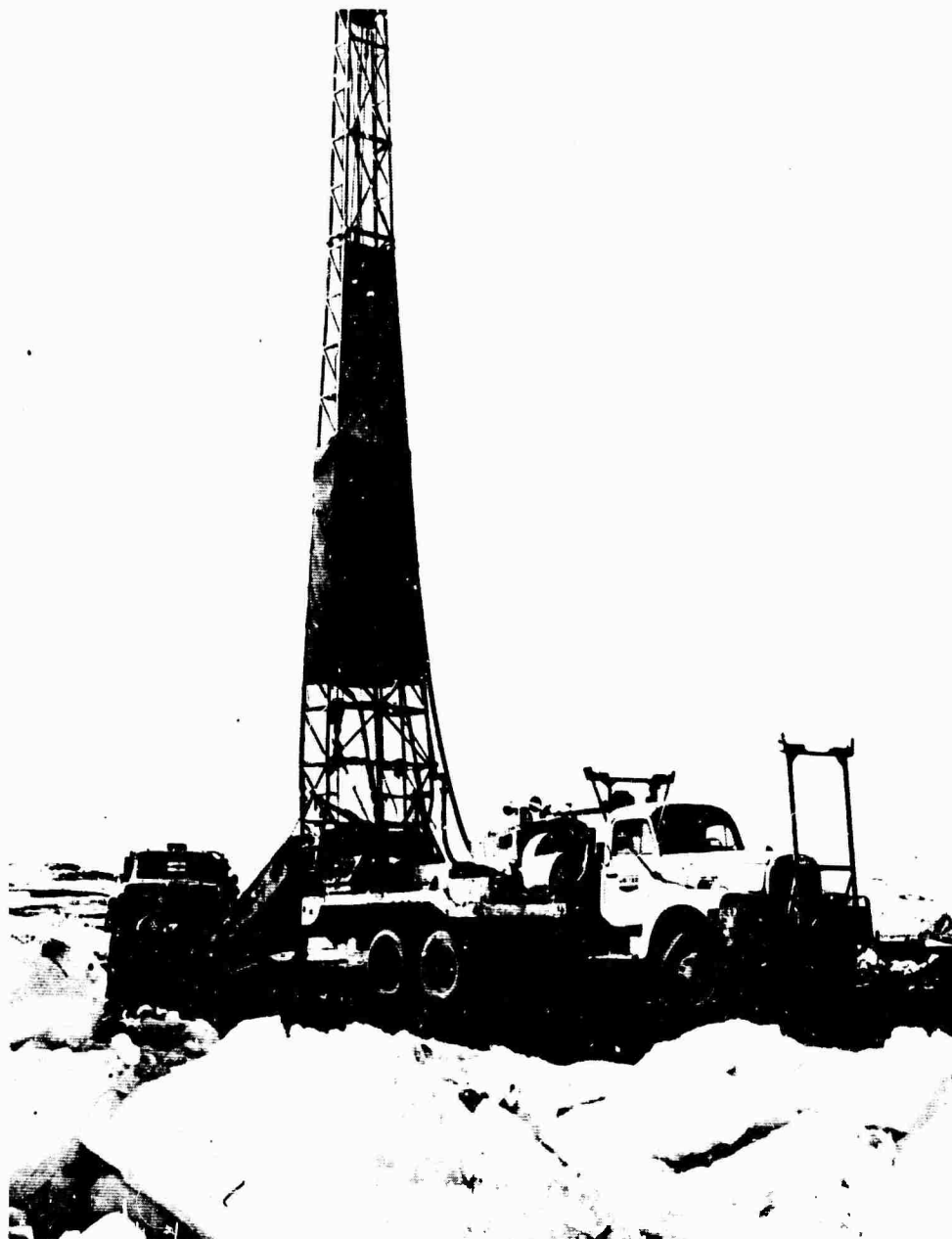
FIGURE 20. TYPICAL DRILLING ACTIVITY

Upon completion of the cementing operation, the casing remained full of water, which was later blown out using compressed air from trailer or truck-mounted compressors. At least two days later the hole was checked for dryness, depth and gage using a dummy seismometer.

Following this check the excavation for the WHV was made, the casing cut off to proper height, and the WHV welded to the casing. Prior to the installation of the WHV, the signal cables had been plowed in using a typical cable plow as shown in Figure 22. During this operation, ap-

20

FIGURE 21. MOBILE CEMENT FACTORY

proximately 100 feet of cable had been left coiled on the ground near each well site. During excavation for the WHV, a short side trench was dug between the excavation and the main cable trench. The cable was laid in this side trench and inserted through the conduit into the WHV. Sealing material was then inserted into both ends of the conduit and the side trench was filled with dirt.

7.2. PHASE 2, ASSEMBLY AND CHECKOUT OF COMPONENTS:

Concurrently with the construction phase, the receiving, checkout and assembly of electronic components was being done at the Miles City facility, shown in Figure 23. All the junction box panels and circuit cards were wired here. Complete operational checks of the amplifiers and seismometers were made both on receiving them and just prior to transporting them to the field. Figure 24 shows the HS-10-1 (ARPA) seismometer before installation into the outer case. The assembly at the top is the calibration coil. In addition to checking the operational characteristics of the seismometer it was necessary to install them in waterproof containers. Figure 25 shows (foreground) a series of waterproof cable entries installed on the cables, and (background) a number of seismometers assembled in their cases, ready for use in the field.

21
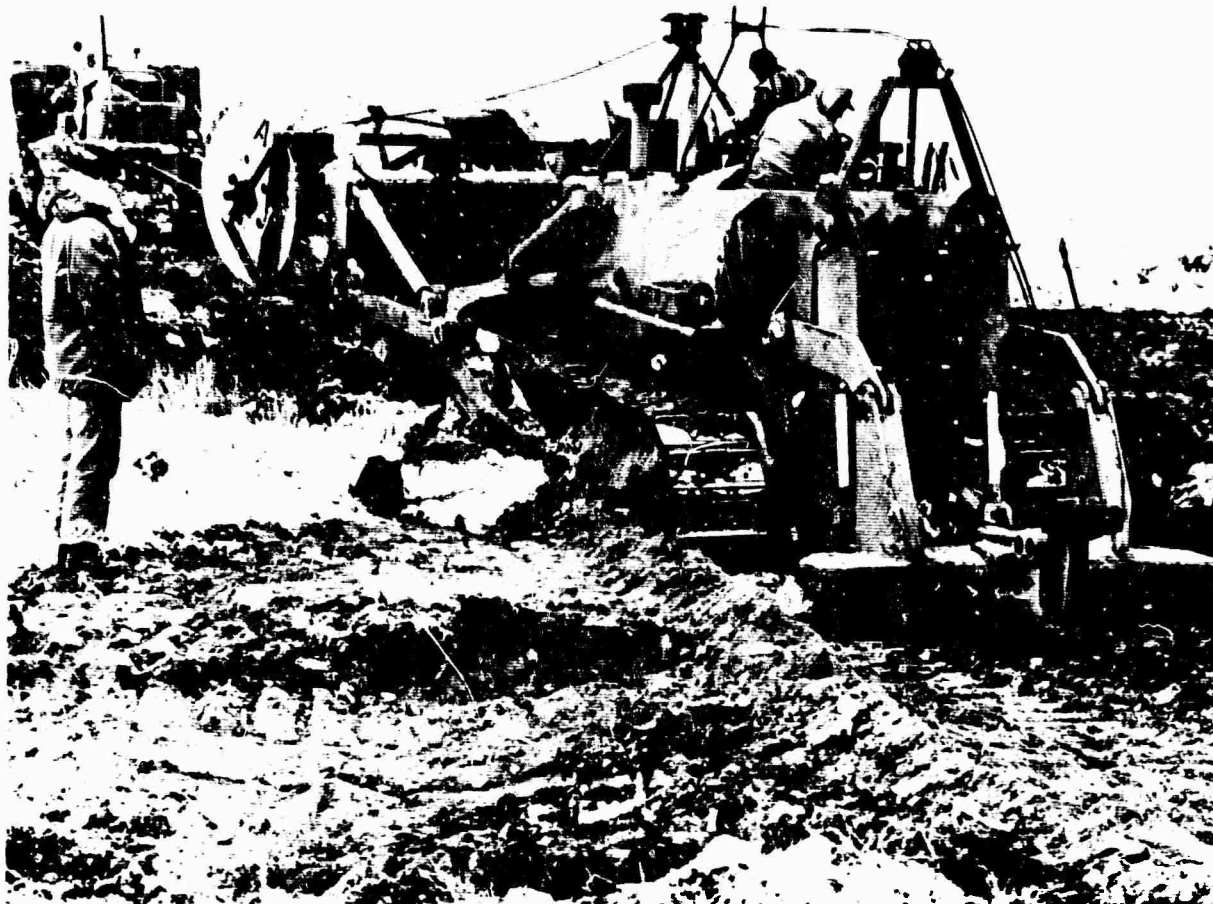
FIGURE 22. CABLE PLOWING OPERATION

The seismometer assemblies were tested for one hour under a hydrostatic pressure of 250 psi before being taken to the field. Figure 26 shows the pressure chambers used.

All necessary components for the installation of a subarray were loaded on a large, shock-mounted van for transportation to the field. Figure 27 shows the interior of a van, loaded and ready to go to the field.

7.3. INSTALLATION— WELL-HEADS:

The installation at the well-heads consisted of lowering the seismometers into the hole as shown in Figure 28 (note the rotating cable stand) and installing the cables into the Hoffman Box (Figure 29) and emplacing the taper pins on the cable.

The taper pins were then installed in the terminal blocks and continuity checks made. After the installation was completed, the entire subarray was equalized and calibrated, and all oper-

22

FIGURE 23. MILES CITY OFFICE AND SHOP

ating parameters were checked from the CTH panel (Figure 50). Seismic signals are then available at the connectors on the side of the Central Terminal Panel J-box and are ready for processing and transmission to the data center, as will be described in the following papers by MIT.

8. CONCLUSION:

In summation, we hope that we have taken advantage of all opportunities to minimize maintenance requirements on the signal acquisition system while permitting ease of access for experimentation and adjustment.

FIGURE 24. HS-10-1 (ARPA) SEISMOMETER

24
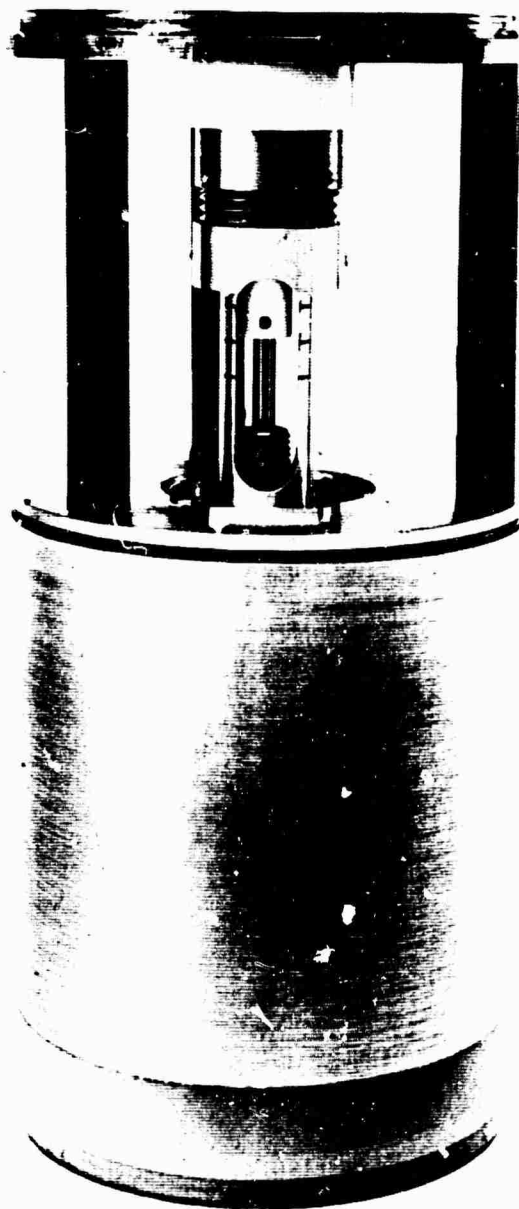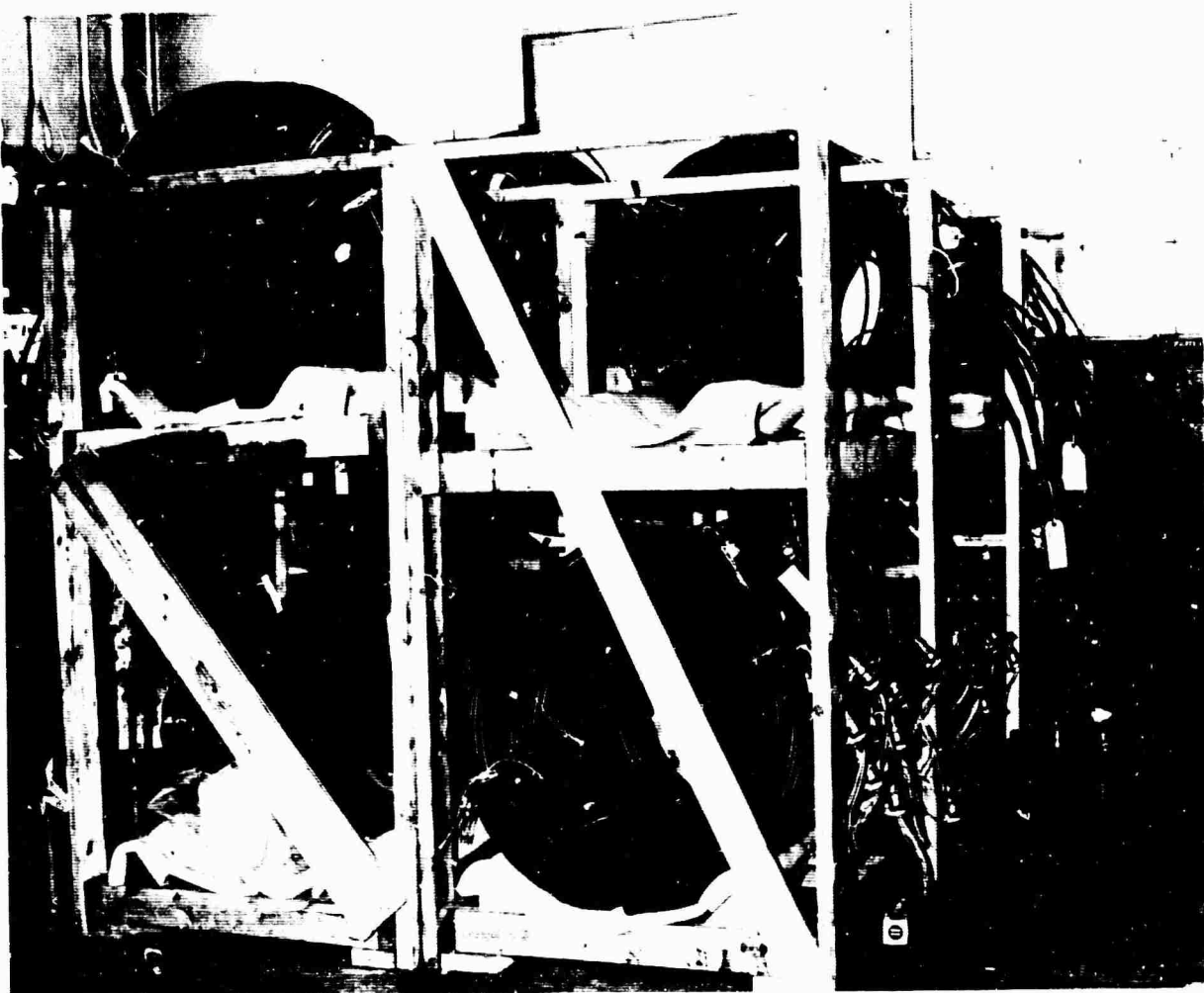
FIGURE 25. CABLE ENTRIES AND FIELD READY SEISMOMETERS

FIGURE 26. PRESSURE-TEST UNIT

26

FIGURE 27. VAN LOADED WITH SEISMOMETERS AND AMPLIFIERS

FIGURE 28. EMPLACING SEISMOMETER IN CASED HOLE

28

F GURE 29. INSERTING CABLES INTO JUNCTION BOX

29
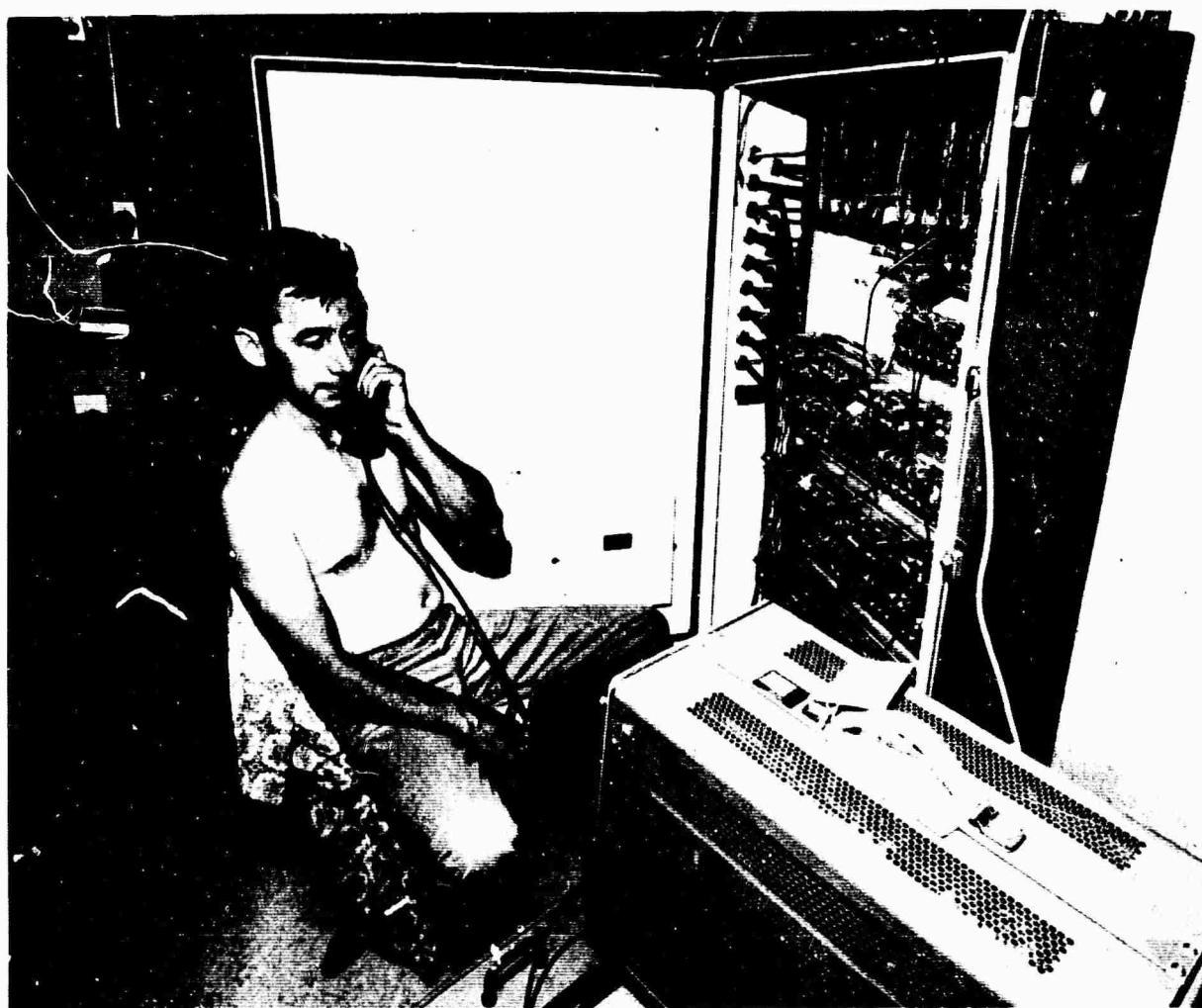
FIGURE 30. TECHNICIAN PERFORMING FINAL CALIBRATION AND EQUALIZATION

5. LARGE APERTURE SEISMIC ARRAY
by
R. G. Enticknap and R. V. Wood, Jr.
Lincoln Laboratory
Massachusetts Institute of Technology
Lexington, Massachusetts

INTRODUCTION

A pictorial diagram of the LASA system is shown in Fig. 31.

The signals from each seismometer, in analog form, balanced with respect to ground, flow through a well head amplifier and then by underground cable to an underground concrete vault. Twenty-five such seismometers arranged in a geometrical pattern, together with the electronics which sample and prepare the signals for transmission constitute a subarray. There are 21 of these.
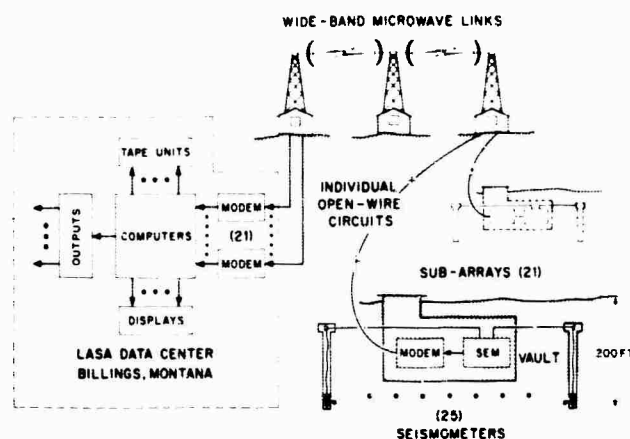
FIGURE 31. LASA SYSTEM

All signals from each subarray are time multiplexed on a single circuit, provided partly by individual open wire construction and partly by frequency multiplexing on wideband microwave radio facilities. From the final radio terminal, there are 21 underground cable circuits into the Data Center in an adjacent building. Here the data are distributed to the various data processing equipment and displays.

I. SIGNAL COLLECTION

The function of the signal collection equipment at each LASA subarray vault is to receive the separate signals from the 25 sensors and to transmit these signals, in suitable form, to the signal recording and display input at the LASA Data Center in Billings.

One Subarray Electronics Module (SEM) is installed in each of the 21 underground vaults in the array. The function of this equipment is to condition the seismometer signals for sampling,

31

periodically sample and digitize the sensor signals, and feed the collected data to the tele facilities. Operation is synchronized by command signals sent from the Data Center to the SEM. Synchronization results in essentially simultaneous (within a 2 msec interval) sampling of all sensors in LASA every 50 msec. The samples are stored in digital form and transmitted to the Data Center in the time interval between samples. The SEM is also capable of operating in a number of test modes on command from the Data Center.

The remote locations of most of the subarrays and nature of the LASA installation area dictate the need for equipment which can operate unattended for long periods in the vault environment and can be easily serviced in the field. To achieve these goals, proven components with known performance records are used and the mechanical operations involved in replacing equipment are minimized. In order to facilitate the maintenance problem, the SEM is provided with means of performing remote troubleshooting. Each major portion of the SEM has a test/operate capability. The Data Center can, by remote control, direct a given portion of any SEM in the array to disconnect from its normal (operate) input and connect to a known (test) input. This remote control feature permits both routine equipment checkout and calibration and the localization of the failed unit in the event of a malfunction.

Figure 32 is a block diagram of the SEM. A set of SEM equipment consists of five sub-assembly "boxes": Control, Output, Multiplexer and Analog-to-Digital (A/D) Converter, and two identical Input Boxes. Physical division of the SEM into subassemblies results not only in interchangeable portions of a SEM and consequent simplified maintenance but also in equipment boxes which one man can easily carry in and out of the underground vaults. Signal flow is from the seismometers to the input equipment which prepares the signals for sampling by the Multiplexer. Under control of the Output portion (which in turn is synchronized to the Data Center), the Multiplexer and Converter equipment samples the signals and produces the signal amplitudes
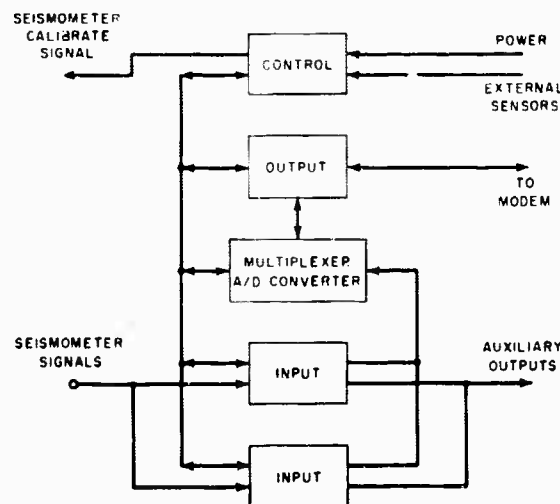
FIGURE 32. SEM BLOCK DIAGRAM

32

in digital form. The Output equipment stores the accumulated samples and formats the data for transmission to the Data Center. The Control equipment contains power sensing and distribution relays, the seismometer calibration oscillator, test signal control relays, and several relays which can be used to telemeter data from binary external sensors. Photographs of the front and back views of the assembl'd SEM are shown in Figs. 33 and 34.

The Input section consists of two identical units each of which is capable of handling 15 signal channels. Expansion from the present 25 sensors in a cluster to a total of 30 can be accomplished with only minor SEM modifications. Two units rather than a single large unit are used to provide pieces of equipment which can easily be handled by one man. Each channel consists of an interface with the seismometer signal cable, a balanced to unbalanced signal amplifier, and a low pass filter. The interface circuitry contains Zener diodes to protect the SEM from undesirably high potentials on the signal cables and coupling capacitors to eliminate the dc bias on the signal lines. An operational amplifier circuit is used to convert the balanced line signal to an unbalanced line prior to filtering. Since the signals of interest are of relatively low frequencies, a low pass filter is used to limit the bandwidth before sampling. The volume and weight involved in packaging 30 passive filters at these low frequencies naturally led to the selection of active filters. The four pole Chebyshev response chosen yields a reasonable compromise between amplitude and phase distortion and out-of-band (above 5 cps) attenuation.

Unlike the other SEM subassemblies, multiplexers and analog-to-digital converters are commercially available. Consequently, a "catalog item" unit modified to interface properly with the input signal levels and control signals is used. To satisfy the need for about 80 db of system dynamic range, 14-bit (sign plus 13 magnitude) quantization is used. The multiplexer input signal range (14 volts peak to peak) will accommodate the maximum amplitude signals the seismometer and associated amplifier are capable of producing.

The Output subassembly is the link between the telephone transmission facilities and the other portions of the SEM. It synchronizes the SEM operating to signals received from the Data Center, controls operation of the Multiplexer and A/D Converter, and stores and formats the digitized data for transmission. A 19.2 kcps clock and a 12-bit command word, transmitted 20 times per second, are received from the Data Center. The command word consists of a 4-bit sync code and 8 control bits. SEM operation is synchronized by this clock word. In order to provide some immunity to noise on the telephone line, a "flywheel" is built into the synchronization circuit so that resynchronization is attempted only after the incoming sync code is not properly detected four consecutive times. The 8 control bits operate relays which place the SEM in the various test modes.

Data are transmitted to the Data Center at a 20-frame-per-second rate. Each frame consists of 32 words of 15 bits (14 data plus odd parity) each. Word No. 29 contains in digital form

33

FIGURE 33. SUBARRAY ELECTRONICS MODULE (SEM), FRONT VIEW

one-half the sum of the signal amplitudes produced by the 25 sensors. Word No. 30 provides a continuous check on operation of the A/D Converter by sampling a locally generated dc voltage (battery) rather than a seismometer signal. The Telemetry Word (31) reports equipment and vault environment status. During the time that the sync word is transmitted, the Multiplexer

34
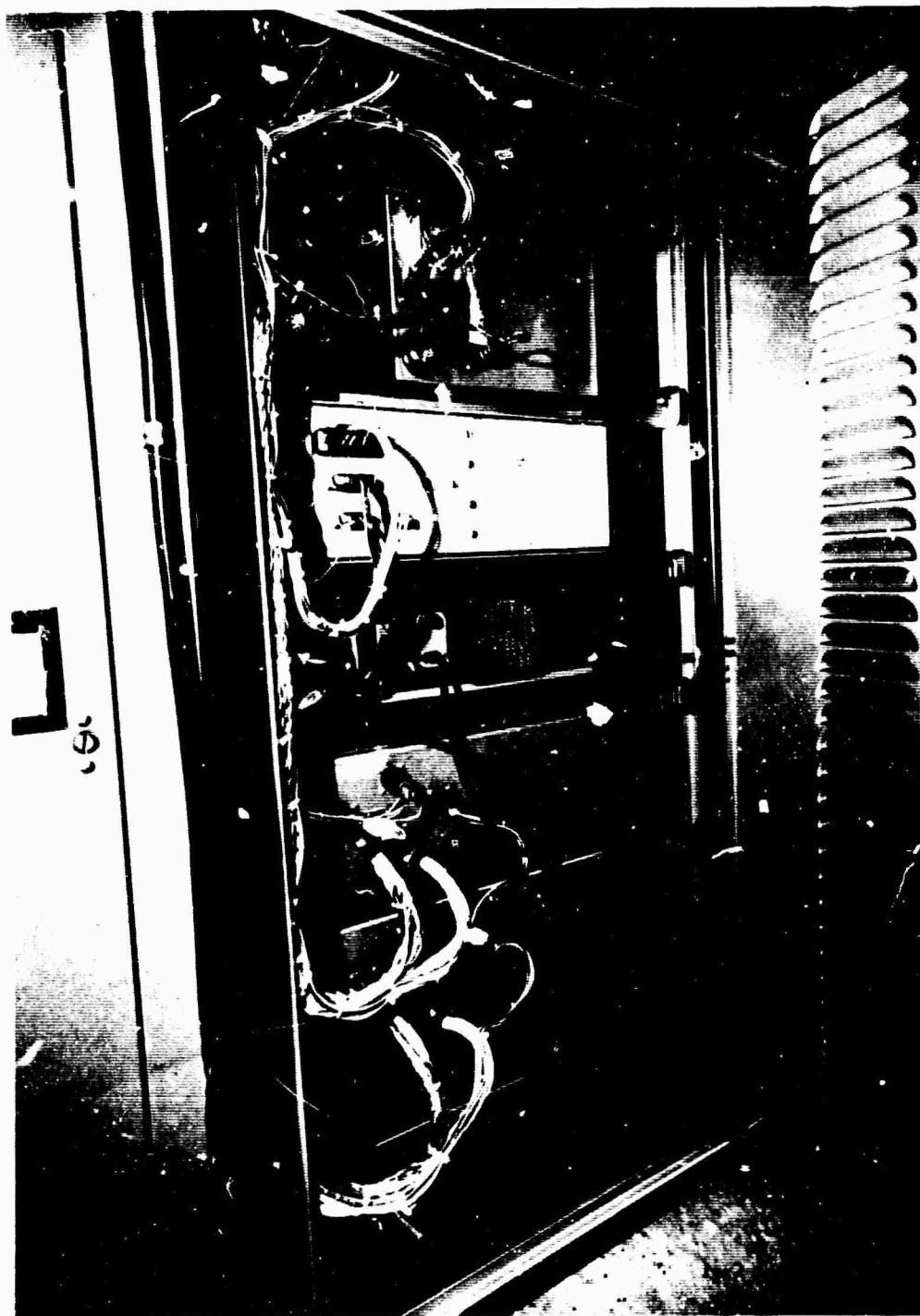
FIGURE 34. SEM, REAR VIEW

and Converter operate to sample and digitize the seismometer signals and forward the data to the Output equipment where it is stored. Since the data rate of 9.6 kcps is half that of the telephone modem operating frequency, each data bit is transmitted as 2 bits. A "one" is represented by 10 and a "zero" is sent as 01. Because this coding scheme insures transitions in the modem

35

input signals, the scrambler normally provided by the telephone company to provide signal transitions is not required.

The Output equipment utilizes micrologic packages which are interchangeable with those used in the Data Center equipment.

The Control Box contains the seismometer calibration oscillator and relays which perform various control functions. The calibration oscillator produces a 1-cycle-per-second 20-volt peak-to-peak signal which is applied to all seismometers in an array on command from the Data Center.

The whole SEM contains a total of 105 plug in printed circuit cards, containing 881 micrologic units and 1800 other active elements.

Two forms of primary power are available in the subarray vault. In addition to the commercial power, a standby source consisting of a battery charger, battery bank, and dc/ac inverter is available. The Control Box contains relays that sense both power sources and report the presence or loss of commercial power via the Telemetry Word. In the event of a power failure, the SEM will operate on standby power until the batteries have discharged to the point where the inverter output is less than 105 volts ac. At this point, the SEM load is disconnected and remains off until commercial power is restored.

The commercial power is routed by pole lines at either 14 kv or 7 kv to each vault as shown in Fig. 35.
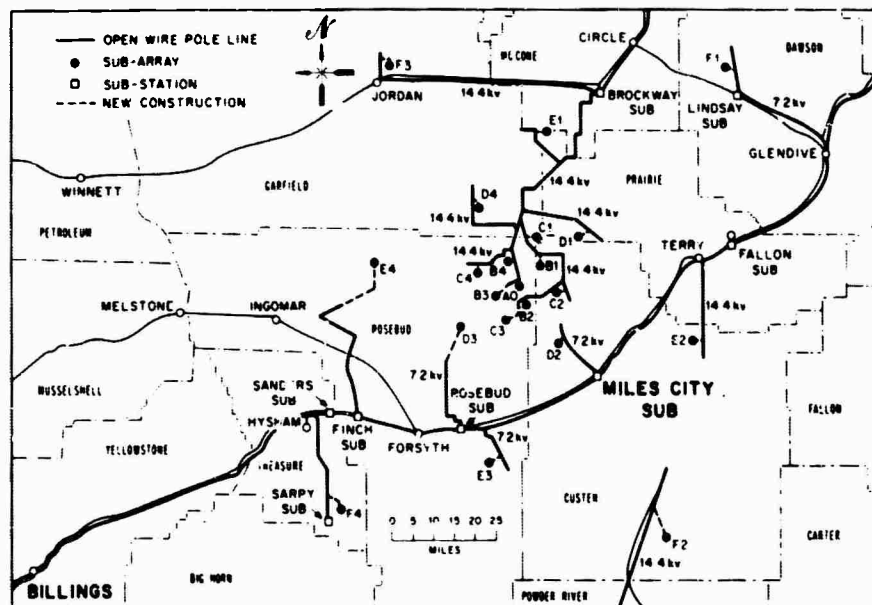
FIGURE 35. LASA POWER DISTRIBUTION

36

II. COMMUNICATIONS AND CONTROL

The choice of communication system for the Montana LASA was only partially contingent on the basic requirements for any such array.

Factors such as data rate. error performance, minimal outage, etc. are a function of over-all system requirements and design and are essentially independent of geographic location.

The choice of facilities, or said another way, the detail of system implementation, must be heavily influenced by local conditions.

The array communications exist to provide voice and data circuits between the 21 LASA subarrays and the Data Center in Billings.

Bearing in mind the very short time available for development, this subsystem was designed to take advantage of existing or planned facilities and local experience as much as possible. In the area of the LASA, existing commercial telephone facilities are very sparse. This situation is to be expected in any area in the United States, or elsewhere, which satisfies the seismic requirements for array location.

Most of the area of the Montana LASA is served by several small telephone cooperatives, again as a direct result of the low population density. The LASA communications facilities had, therefore, to be provided principally by new construction and in large measure by organizations whose resources are not large and whose principal experience is in the area of unsophisticated voice telephone systems.

The LASA requirements for communications entail the following:

A. From Subarray to LASA Data Center (LDC)
   1. Transmission of one quantized sample from each of the 25 seismometers at a rate of 20 samples per second. Each sample is quantized to 14 bits with an additional parity bit.
   2. Transmission of a 15-bit "frame start" pattern per 50 msec frame.
   3. Transmission of 6 extra 15-bit words per frame to provide for the possible subsequent addition of more sensors and for equipment status telemetry.

B. From LDC to Subarray
   1. Transmission of a bit timing signal to synchronize the sampling rate at all subarrays.
   2. Transmission of a frame start signal to each subarray to synchronize the sampling time at all subarrays.

37

3. Transmission of telemetry command signals to facilitate remote control of functions such as seismometer calibration and equipment testing.

C. A two-way voice telephone for maintenance purposes, arranged so that its use does not interfere with the essential data services. This service must have the capability of ringing from either end.

The system provides the following services between each subarray vault and the LASA Data Center:

A. A fixed speed data channel at 19.2 kbps from each subarray to LDC. This channel also provides bit timing (data sampling time).

B. A data channel from LDC to each subarray. This provides (1) a timing signal at 19.2 kbps, and (2) a data stream comprising a 9.6 kcs square wave carrier, capable of being modulated at a n aximum rate of 1.2 kbps.

C. A 3 kc voice channel wi h signaling.

These three basic services are simultaneous and independent.

An obvious topological arrangement for the communications is to bring circuits from the individual subarrays into a concentration point near the geographical center of the array, and from there via a wideband facility to the Billings LDC (see Fig. 36).

In choosing the type of facilities, the following factors were given prime consideration:

A. Early service date
B. Reliability/maintenance
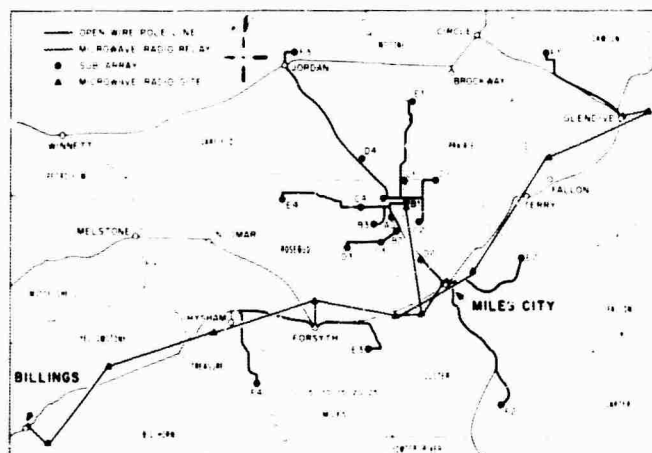
FIGURE 36. LASA COMMUNICATIONS

C. Capacity for growth of requirements

D. Cost

The choice of wideband facilities was straightforward. Basic requirements dictated either coaxial cable or "long-haul" microwave with L carrier or equivalent multiplexing. A suitable microwave facility was already planned for the majority of the route and it was determined that installation could be advanced to meet the service date. A new link from the array center to the planned route was installed, and an existing link from Billings Junction to Billings Main was augmented.

From the circuits to individual subarrays there was a possibility of using (1) lightweight microwave, (2) cable, underground or aerial, and (3) open wire. Open wire was chosen for the following reasons:

A. Excellent transmission characteristics; low loss and wide bandwidth.

B. No repeaters or other active devices are required in even the longest runs found in LASA.

C. Familiarity of all telephone organizations in the area with installing and maintaining this type of facility.

D. No new frequency allocations required.

E. Components readily available.

The data modulation system (MODEM) is a Bell System design and has sufficient capacity, not only for the present information rate, but also for error control coding and/or future expansion should these become necessary.

Each of the 21 subarrays has a single pair of open wires from the site, interconnecting at a suitable junction with a wideband microwave system. Fifteen of the sites have these open wire facilities into a Lenkurt Type 76A microwave terminal located near the center of the LASA at Angela (Fig. 37). One site connects with the TD2 system near Glendive, three with a junction near Miles City, and the remaining two with a junction near Forsyth. The microwave facility at Angela is new and was constructed specifically for the LASA.

The services connecting each subarray and the Billings LDC utilize a one-half group bandwidth.

On the open wire, transmission of the data from the subarray to LDC is in the band 26 to 44 kc. From LDC to the subarray, the band 4 kc and below is occupied by the voice circuit and the band 5 kc to 18 kc by the data signal.

Over the microwave facilities, the signals are transmitted via standard "L" carrier facilities.
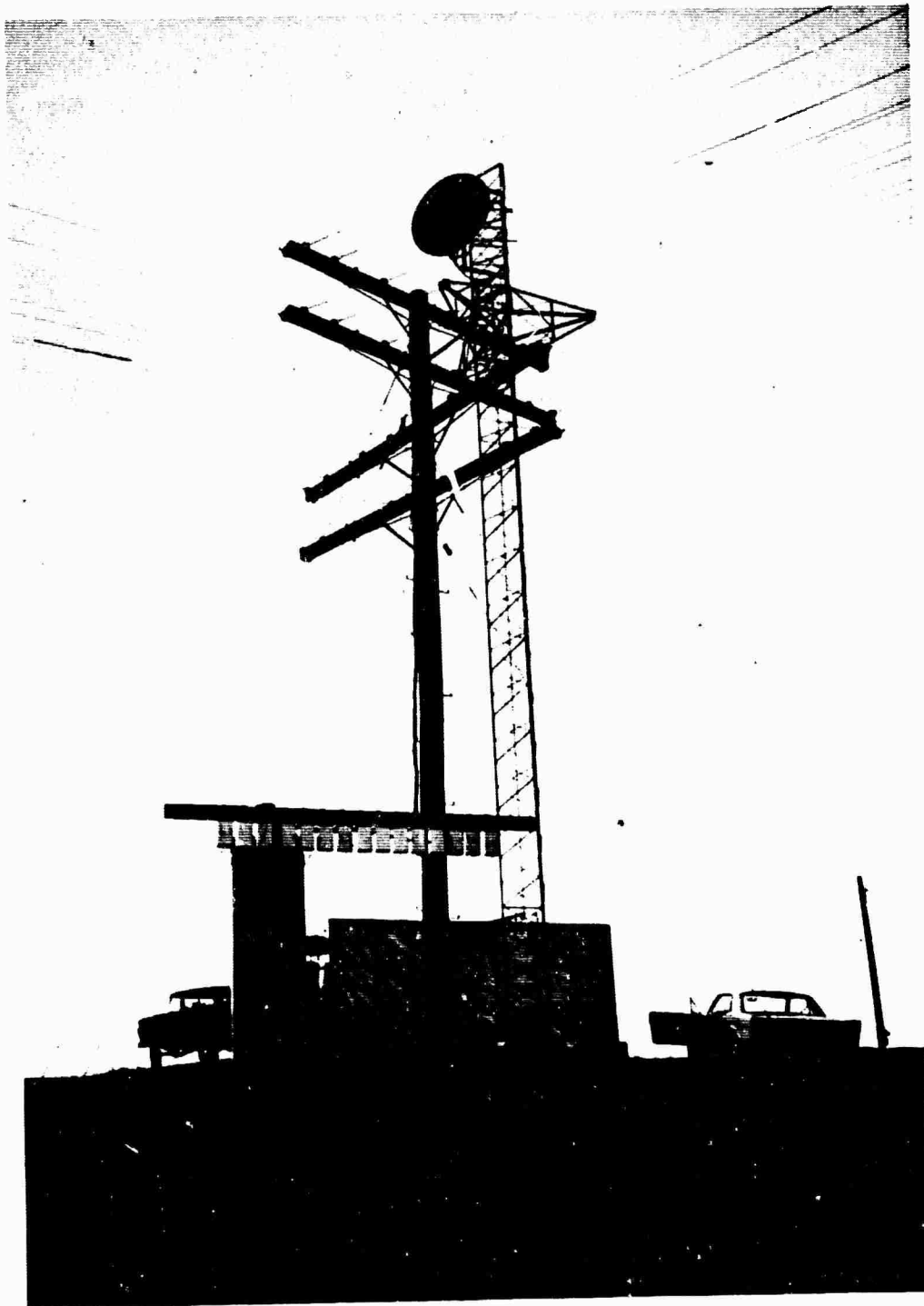
FIGURE 37. ANGELA MICROWAVE SITE

40

The data modems employed are Bell System 303 A 10 used in a fixed speed synchronous mode at 19.2 kbps. From the subarray to the Data Center, the full data rate capability is employed. In the other direction, a mark-space signal (dotting) is sent to provide a timing reference. This signal is modulated by phase reversals, at a maximum rate of 1200 bps. Restricting the rate to 1200 bps, which is generously adequate for telemetry commands, allows the low frequency end of the pass band to be used for the voice circuit.

Electronic control over LASA starts with the Data Center array clock. The clock output consists of the following:

A. GMT, in digital form, for insertion in the digital data tape headers.

B. Timing signals, at various repetition rates, for control of all operations external to the digital computers at the Data Center and in the 21 subarray central vaults.

One timing signal, occurring 20 times per second, is used to control the sampling operation in each of the subarrays. The system requirement is to sample the signals from each of the 525 sensors within LASA during a given 2 millisecond time period. Considering round-trip (Data Center to subarray to Data Center) signal transmission delays for each of the 21 channels, one notes approximately 3.5 milliseconds difference between the shortest and longest delay. Clearly, an attempt to control sampling time at each subarray by sending out 21 simultaneous "frame start" sequences would result in sampling all sensor signals within the allowed 2 milliseconds. However, the digital data representing this array sample would arrive at the Data Center spread out over 3.5 milliseconds. This is undesirable, since it would add unnecessarily to the buffering load at the Data Center. Instead, the "frame start" sequence for each subarray is transmitted with a delay such that the "frame start" sequence returned from each subarray arrives at the Data Center at approximately the same time, within 100 microseconds.

It was mentioned in a previous section that, as an integral part of the LASA system philosophy, remote-controlled trouble-shooting as well as routine calibration and performance checks would be made on subarray equipment from the Data Center, so that maintenance teams would have definite knowledge of the problem facing them before they left the Maintenance Center in Miles City. This feature is achieved by coded digital commands sent from the Data Center to the subarray under consideration. In the SEM, relay decoding networks translate these signals into specific operations on the subarray central vault equipment. Telemetry commands presently in use are as follows:

A. Apply 1 cps constant-amplitude sine wave to the calibration circuit for all 25 sensors in the subarray.

B. Apply test pattern 0101010101 . . . to the communication circuit data input.

C. Replace the normal output of the analog-to-digital converter with a sequence of identical "words."

D. Replace the normal analog-to-digital converter input with signal ground.

E. Replace the normal analog-to-digital converter input with a fixed precision dc voltage.

F. Connect all 31 multiplexer inputs to signal ground.

G. Connect all 31 multiplexer inputs to the fixed voltage used for "E."

H. Connect together, by pairs, the 25 pairs of wires normally connecting the subarray sensors to the signal handling electronics.

It will be seen that, by means of the preceding functions, one may establish remotely, with fair precision the nature of a fault in the subarray electronics.

One of the 32 words making up each "frame" in the continuous sequence from a given subarray to the Data Center is the "telemetry" word. This 15-bit word contains:

A. Acknowledgment from the subarray of any telemetry commands it has received.

B. Information on local conditions at the subarray, (such as: (1) presence or absence of prime power, (2) degree of dampness in the central vault, (3) temperature in the vault, (4) whether the vault door is open or closed).

By means of this information, the Data Center is able to check, automatically or manually, on the more likely physical difficulties at each subarray.

During the initial phases of checking out the array equipment, control of the remote monitoring functions was manual. The maintenance supervisor, seated at a switch panel, selected the subarray and the function desired, then by means of the visible recordings on the chart recorder determined whether the subarray was performing properly in that mode. It is obvious that, with 525 sensors to monitor, the manual process is too time-consuming. In the middle of August, 1965, automatic monitoring was commenced, using a programmed digital computer. This program drives the computer in sequence through all 21 subarrays, applying all of the : above-described telemetry commands to the equipment in each subarray. As part of this program, the computer stores tables of the allowable range of deviation the signal may have for each of the test functions. Signals falling outside the allowable range result in a hard-copy printout from the computer, identifying and locating the fault. The maintenance supervisor may then, by manual means, make a detailed analysis of these faults before calling on the maintenance teams for corrective action. At present, this monitoring program operates continuously, completing a check of all sensors about every half-hour. In the near future, it is expected that the program will be modified so as to operate selectively and on command; that is, the maintenance supervisor may ask for a check on any one or more subarrays. In the absence of a request the program will be inactive.

42

III. SIGNAL RECORDING

The principal components involved with signal recording are:

A. Two general-purpose digital computers.

B. Computer programs

C. Four data display units with a total capacity of 64 channels.

The computer configuration is an interesting one. The two small processors are interconnected by a high speed link, and share a number of tape units. These tape units are used as an on-line bulk data communication media as well as for providing permanent records of interesting events. In normal operation, one computer will receive the seismic data from the Phone-Line Input Systems (PLINS) and will perform some signal processing. It will also record the raw data on magnetic tape for further processing either by the second computer or elsewhere.

The second computer will be employed in data processing of selected data stored on magnetic tape.

There are four tape units connected to the two computers. Either computer can access to any or all tape units but not simultaneously. Again, in normal operation two of these units will be used for raw data storage, the third unit will be used for making output tapes of processed data and the fourth will be used for inter-computer communication.

In the event of a computer failure, the data recording function is not interrupted because the remaining computer will take on that function. The data processing capability will, of course, be reduced, but will not be entirely lost.

The computers chosen for this system are PDP-7's, manufactured by the Digital Equipment Corporation. These are 18-bit, parallel, high-speed, small general-purpose computers. Each computer has an 8000-word memory and a cycle time of 1.75 μsec. The peripheral equipment includes the previously mentioned magnetic tape units plus keyboard, output typewriter, paper tape punch, and reader. In addition, there is an input channel for the telephone circuit data which can be connected to either computer by means of simple cable changes.

The programs associated with the recording and control functions are:

A. A control and interrupt answering program.

B. A seismic data read-in and magnetic tape program to accept input data and write it all on magnetic tape.

C. A detector calibration and test program to examine periodically and sequentially, all seismometers in the array for both calibration and malfunction. The output is recorded on magnetic tape and also presented on a page printer for use by the maintenance personnel.

43

D. A typewriter keyboard input program to handle all types of manual input message. This is a service routine which can be used by other programs in the system.

E. A printing output program which complements the previous input program. This is also capable of serving other programs in the system.

F. A computer checkout program for use by the console operator on core examinations, core changes, etc.

The data display units serve two principal functions. Two 8-channel units provide chart displays for checkout and maintenance purposes of 16 signals selected from among any of the sensor or sum inputs or the processed computer outputs. Two 24-channel units, again with the capability of selection as the 8-channel units, will be used in conjunction with recording devices such as charts, photographic recorders or analog tape units for making permanent records for hum' examination, or in the case of the analog tape records for comparison with seismic recor' de elsewhere.

Each of th ,ial 64 channels is identical in components and function. A channel can be connected to the serial data line of any subarray by means of a patch cord. Thus connected, and utilizing the control and timing signals from the PLINS, a digital word is selected by a switch controlled counter. This word corresponds to a particular seismometer, sum or telemetry word in the data frame. This word is stored in a register until the next sample is received, 50 milliseconds later. The output of the register is connected to its own D/A Converter, whose analog output is presented to the recording device.

A photograph of one of the 8-channel recorders is shown in Fig. 38. It comprises an 8-channel chart recorder, 8 medium gain amplifiers, a zero suppression system, 8 D/A Converters, a patch panel, a word selection panel and also incorporates a telemetry command panel. The 24-channel unit is similar except that the recorder itself is not incorporated nor is the telemetry command panel since this is appropriate only to the maintenance function.

A general view of the Data Center is shown in Fig. 39. A close up of the two 8-channel displays in use by the maintenance personnel is shown in Fig. 40. One of the PDP-7 Computers and two of the digital tape units is shown in Fig. 41.

44
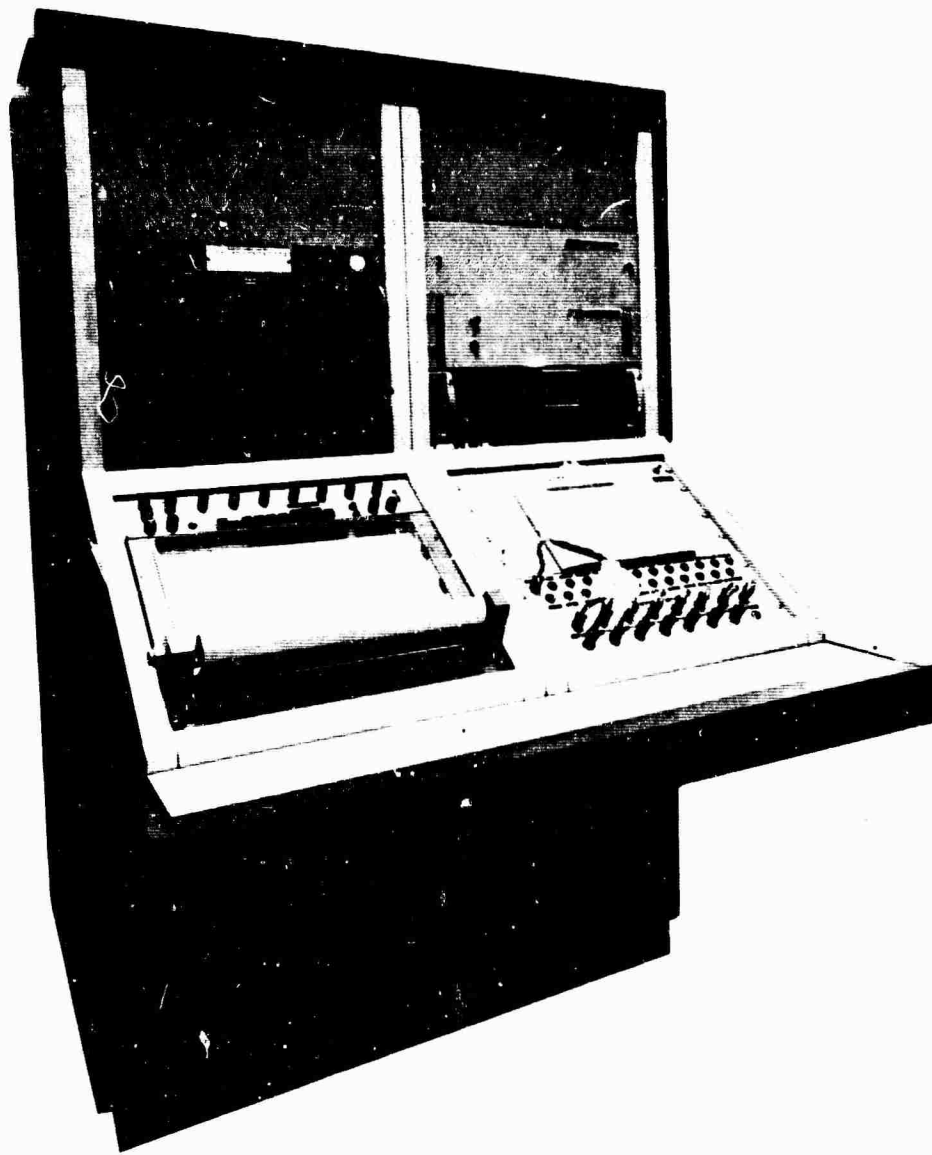
FIGURE 38. EIGHT-CHANNEL DISPLAY CONSOLE

FIGURE 39. LASA DATA CENTER

FIGURE 40. MAINTENANCE CONSOLES

FIGURE 41. PDP-7 COMPUTER

6. PROGRESS REPORT ON LONG-PERIOD INSTRUMENTATION FOR LASA

by
M. G. Gudzin
Geotechnical Div., Teledyne, Inc.

1. INTRODUCTION

Just 5 years ago, long-period (LP) seismographs were commonly operated at magnifications of from 1 K to 2 K at a period of 25 seconds. Magnifications were limited by 6-second microseisms, by thermal effects — both electric and convective, by spurious seismometer resonances, and by the sensitivity of the seismometer to atmospheric pressure changes. Since that time, LP instruments and installation techniques have been improved to such a degree that it is now practical to operate a LP seismograph with a magnification of 100 K at a period of 25 seconds. Most of the development work was done under the VELA-UNIFORM Program. Figure 42 shows a portion of a record made at WMSO by an advanced LP seismograph operating at high magnification. The traces of interest are: ZLH, the high-gain vertical, with a magnification of 100 K; ELH, the high-gain, east-west horizontal, with a magnification of 73 K; and NLH, the high-gain, north-south horizontal, with a magnification of 116 K. Figure 43 shows the frequency responses used in the advanced LP seismograph. The upper curve (with a notch at 6 seconds) is the response of the high magnification channels.
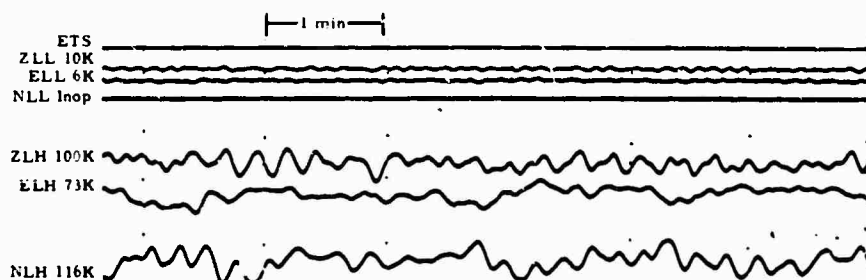
FIGURE 42. ADVANCED LONG PERIOD (LP) SEISMOGRAPH RECORD FROM WITCHITA MOUNTAIN SEISMOLOGICAL OBSERVATORY (WMSO)

This is a report of the work undertaken by the Geotech Division of Teledyne Industries, Inc., to establish a LP detection and recording capability at LASA. It includes a description of the prototype installation, a description of the results of tests with the prototype equipment, a description of work done with parametric amplifiers, a presentation of present plans for the LASA LP seismograph system, and a consideration of studies that might be undertaken using data acquired by the system.

49
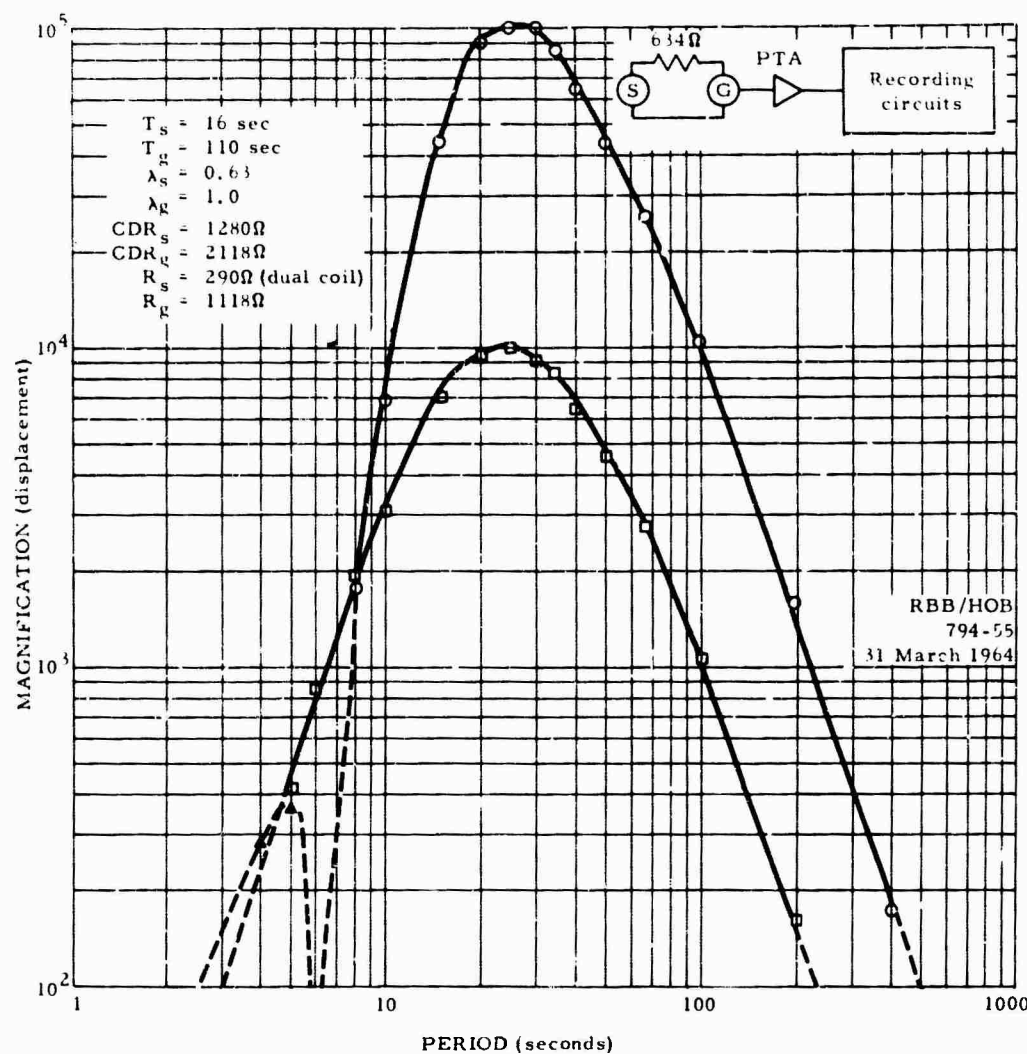
FIGURE 43. ADVANCED LP SYSTEM, TYPICAL FREQUENCY RESPONSE

2. DESCRIPTION OF PROTOTYPE INSTALLATION

The first step in the establishment of a LP detection and recording capability of LASA was the construction of a prototype installation at one subarray. Its objective was to demonstrate the system performance, point out installation and operational problems, and provide a facility for testing various configurations of instruments that might be used.

The prototype installation was made near Hysham, at subarray F3. Its location is indicated in Figure 44. An underground concrete vault (also referred to as a bunker) was constructed there to house the seismometers. It was located remotely (at least 100 feet) from the Long Range Seismic Measurement (LRSM) van and from the other principal structures on the site, and was far enough underground to be covered by 4 feet of overburden. Figure 45 shows the construction details of the concrete vault. Three bottomless metal tanks were cast into individual
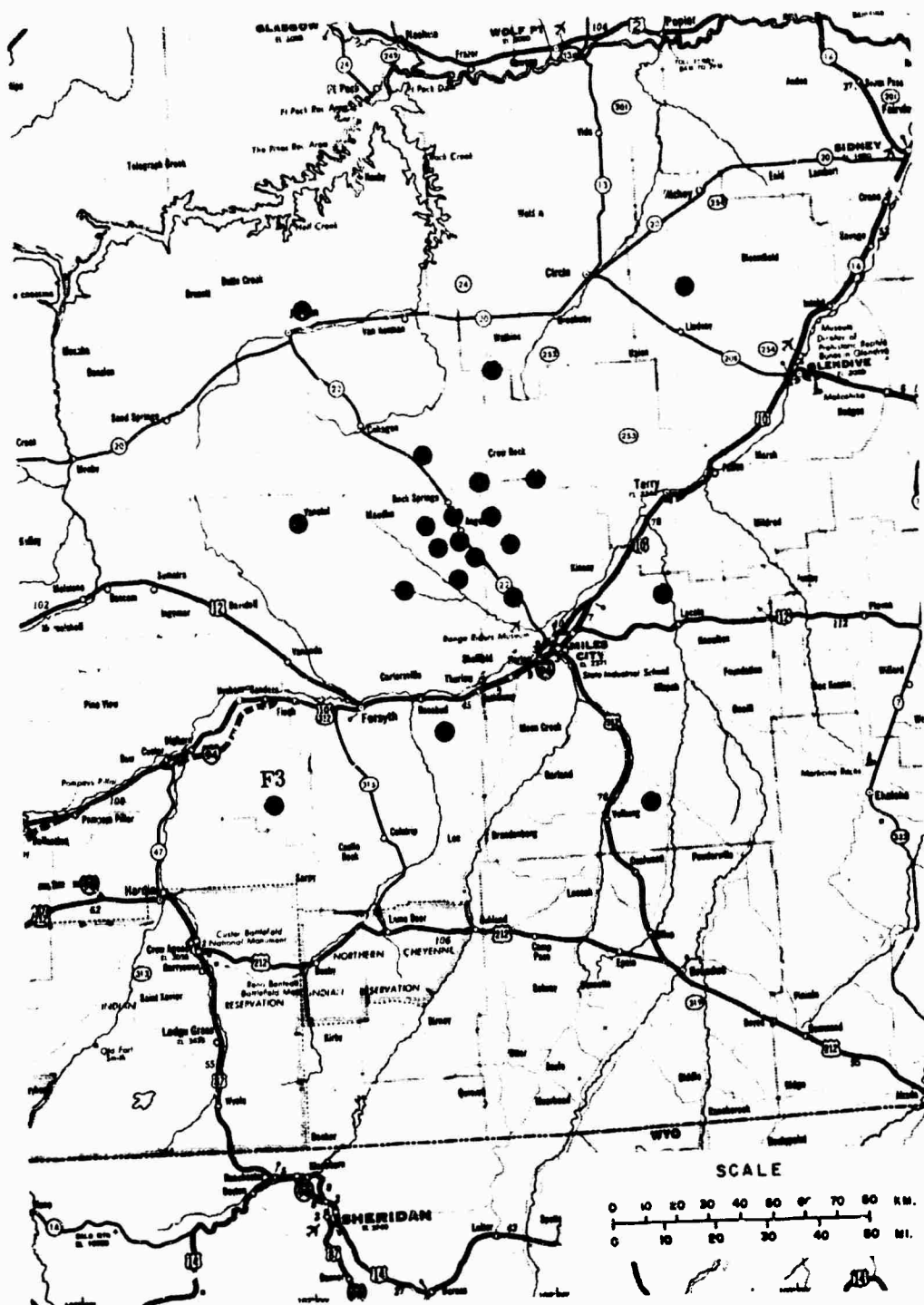
FIGURE 44. LOCATION OF LASA SUBARRAYS
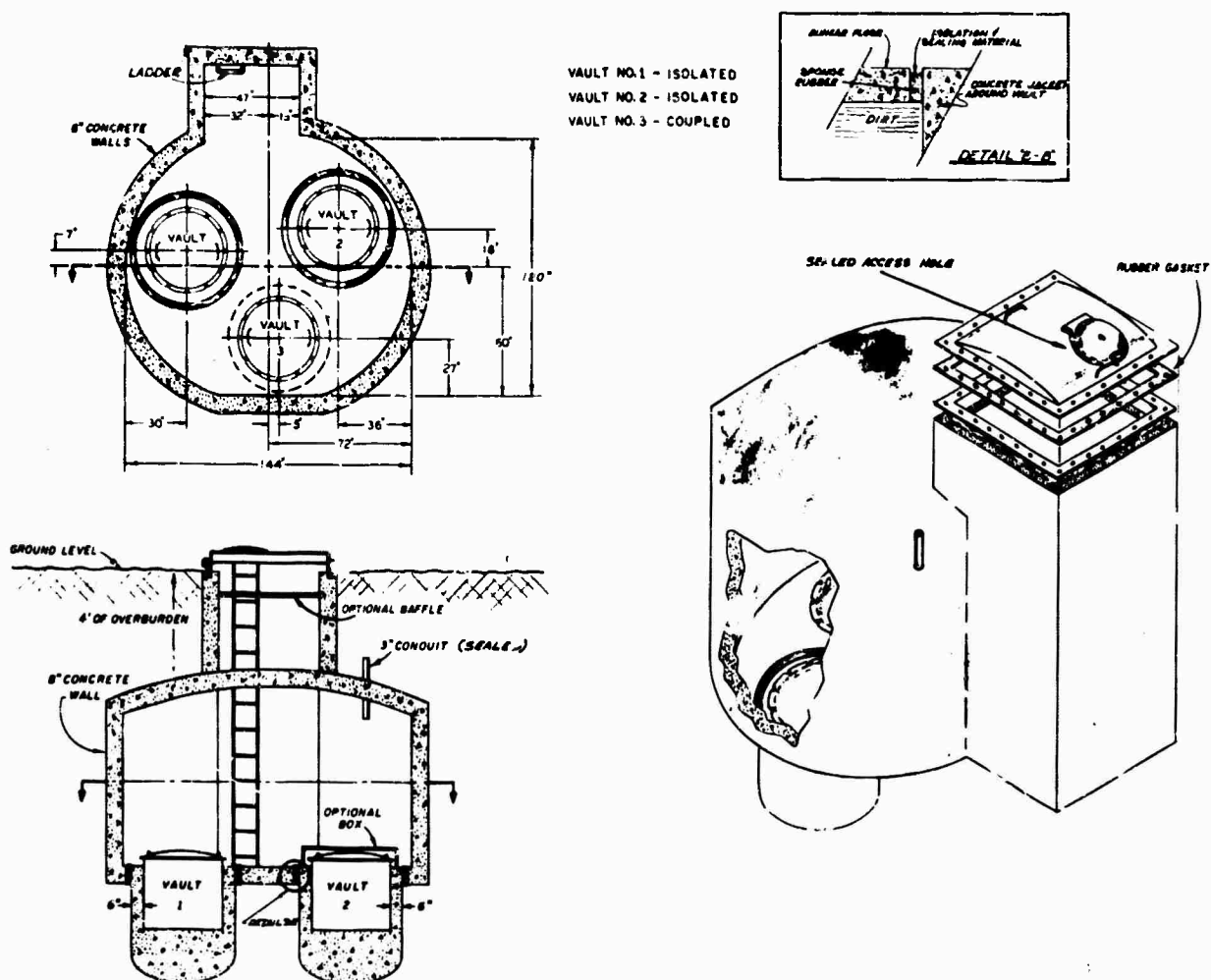
FIGURE 45. BUNKER FOR LASA LONG-PERIOD SEISMOMETER EXPERIMENTS

concrete piers at the bottom of the vault. They were equipped with lids which effectively sealed the interiors of the tanks against changes in atmospheric pressure. Two tanks and their piers (No. 1 and No. 2) were isolated from the concrete floor of the vault with sponge rubber. The pier of the third tank was cast as an integral part of the concrete floor. The concrete vault is equipped with an entryway that can be sealed to isolate the vault interior against atmospheric pressure changes.

Figure 46 shows a partial block diagram of the prototype LP instrumentation. Omitted are a third LP horizontal channel and a short-period channel used during some of the tests. Each of the seismometers shown was installed on one pier—that is, in one metal tank. Its output was amplified by a LP phototube amplifier and an operational amplifier, and was recorded on 35-mm film using a Model 1301A recorder. All cable runs were terminated through lightning protectors, and appropriate damping and gain control circuits were provided. The phototube amplifier (PTA)
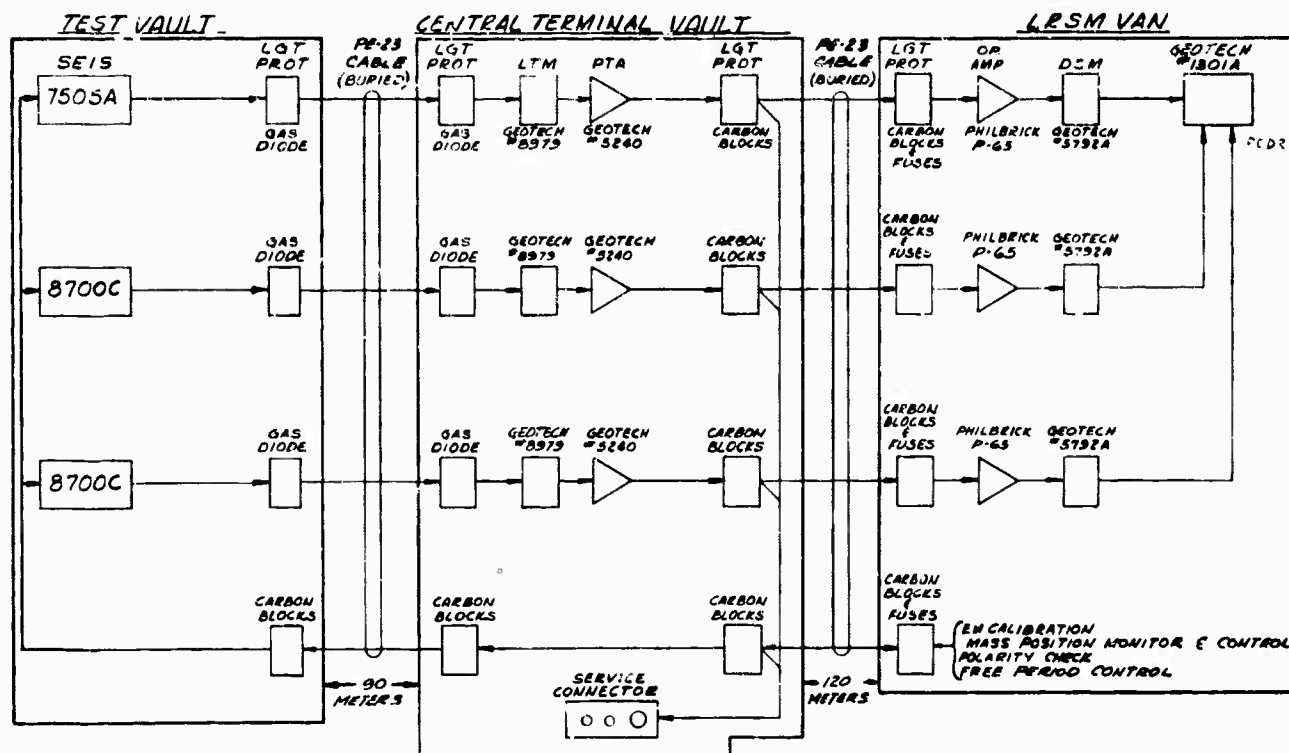
FIGURE 46. EXPERIMENTAL LONG-PERIOD SYSTEM FOR LASA

and its associated circuits were initially installed in the Central Telemetry Vault, and was later moved to the LRSM PTA hut. Recording, calibration and circuit checking were accomplished from the LRSM van on the site.

Figure 47 shows the frequency response characteristic of the prototype system and of the standard LRSM LP instrumentation that was installed nearby to serve as a control.

3. RESULTS OF TESTS AT PROTOTYPE INSTALLATION

As a result of operating the three-component instrumentation in the metal tanks within the concrete vaults as previously described, it was found that the vertical channel can be operated to produce a magnification of over 100 K at 25 seconds. This magnification appears to be limited by propagating seismic noise. At the same time, the horizontal instrument channels are limited to a magnification of about 30 K at 25 seconds. Both of these magnification limits were determined by assuming that the background noise at that magnification should produce no more than 10-mm deflection on the record.

From previous experiences, it was considered likely that the magnification in the horizontal channels was limited by local tilting conditions of the earth and that these tilts could be caused by wind or other phenomena. A series of tests were run to verify that the horizontal instruments

53
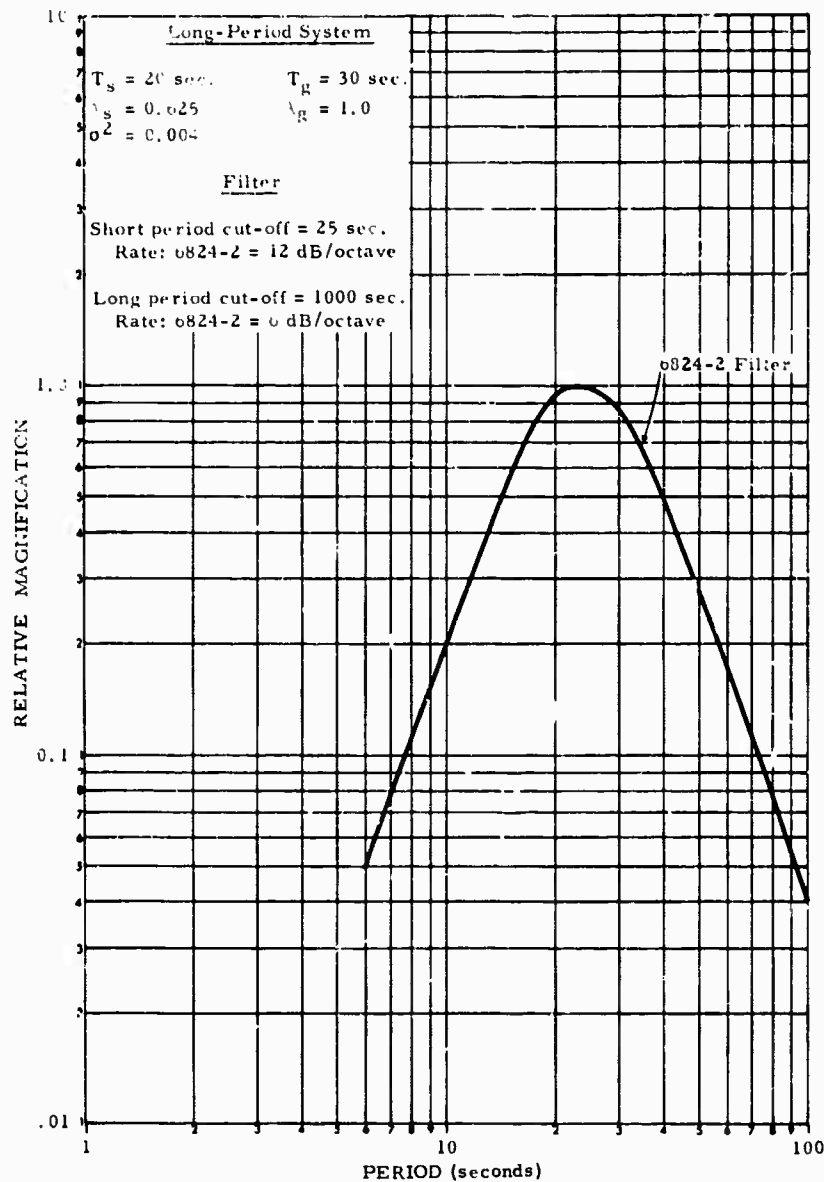
FIGURE 47. RESPONSE OF THE LRSM LONG-PERIOD SEISMOGRAPHS

were indeed affected by local tilts. During the tests, all instruments were oriented in the same direction. In one test, a 5400-pound truck was driven from a large distance (approximately 100 feet) to successive points closer and closer to the center of the vault. Figure 48 shows the results of these tests. All data were normalized to a system magnification of 30 K at 25 seconds. Note that there was a sharp increase in the effect of the load as it was moved closer than 50 feet from the vault. Also note that the effect on the vertical instrument was negligible. A second series of tests were conducted by connecting a rope to the entryway of the concrete vault. This was connected through a spring scale to a truck located 100 feet from the bunker. At each of eight points symmetrically disposed about the vault, a force was applied through the rope and

54
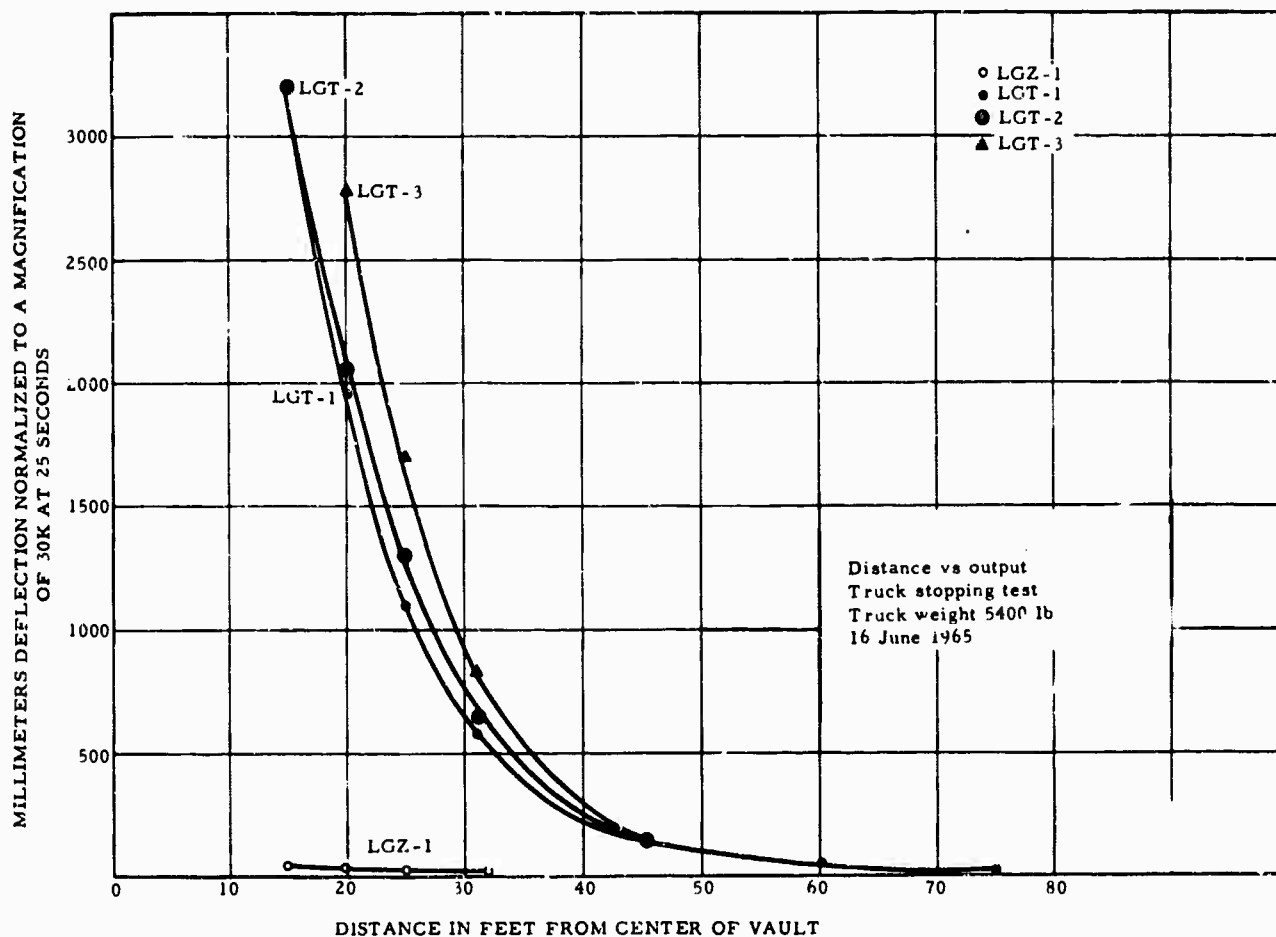
FIGURE 48. RESULTS OF LOAD TEST

spring scale by backing the truck. Figure 49 shows the results of these tests. Note that LGT-3, the horizontal instrument on the floor, was tilted considerably more than LGT-1 and LGT-2 which were located in the metal tanks. Figures 50 and 51 are diagrams of the test setup.

Over long periods of time and under varying weather conditions, the instruments located in sealed tanks in the concrete vault responded approximately 30 percent less to locally generated noise than did the instruments installed nearby in standard LRSM vaults.

The horizontal instruments were operated in the metal tanks and on the floor of the concrete vault. In general, the background noise was approximately 4 db less when the instruments were located in the metal tanks.

Background noise recorded when instruments were located in the coupled tanks was little different from that recorded when instruments were located in the isolated metal tanks. There appears to be no advantage, in this design, to attempt to isolate the tanks (and their piers) from the concrete vault.

55
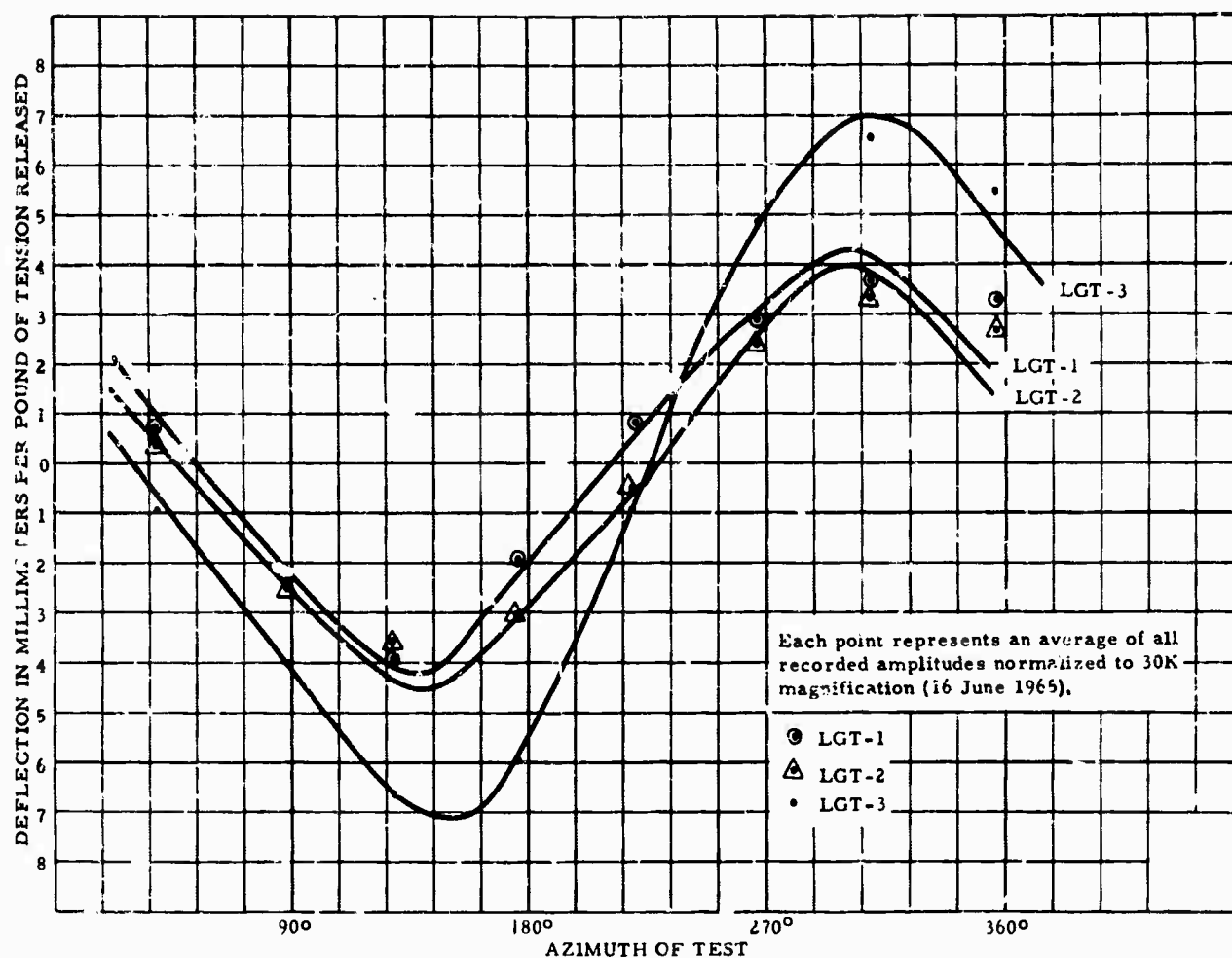
FIGURE 49. RESULTS OF TILT TESTS

There was some evidence that the background noise on the instruments was greater when the concrete vault was sealed than when it was unsealed. It is considered that this may have been caused by buckling of the floor, by movement of the decoupled tanks with respect to the overall vault, or by buoyancy of the concrete vault.

We believe that this condition may not exist in the underground vaults that have all metal tanks directly coupled to the floor and that have a much thicker floor than was provided in the prototype installation.

Short-period noise bursts do not produce spurious responses in the LP seismograph. This was demonstrated by the lack of correlation between short-period noise bursts detected by a seismometer placed in the concrete vault and apparently spurious deflections on the LP record.

It is important that the earth covering and surrounding the LP vault be smoothly streamlined. Sharp changes in elevation or the protrusion of the entryway of the vault will provide a surface against which wind will buffet, producing forces that will tilt the vault and hence produce noise

56
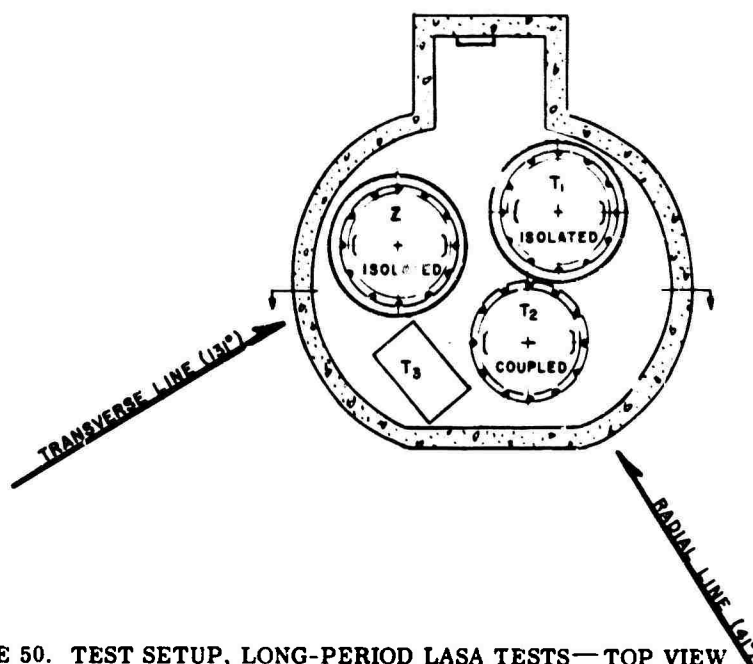
FIGURE 50. TEST SETUP, LONG-PERIOD LASA TESTS—TOP VIEW

1. Arrows indicate direction of earth motion for a positive deflection on the horizontal (T) seismograms.

2. The vertical (Z) seismograph is connected so that upward earth motion produces a positive deflection on the seismogram.

3. Load tests were conducted along the radial and transverse lines at approximate distances of 100, 75, 60, 45, 30, 20, 15, 10, and 5 ft from the center of the bunker.

4. Tilt tests were conducted at a distance of approximately 100 ft.

FIGURE 51. TEST SETUP, LONG-PERIOD LASA TESTS—SIDE VIEW

The temperature stability within the vault proved to be excellent. It was not necessary to heat the instruments at any time during the tests. Of course, these tests were run during the summer months. It is expected that a temperature inversion will occur during the winter. Accordingly, the vaults should be wired for 115 V 60 cycles so that heat may be provided.

4. RESULTS OF TESTS TO PARAMETRIC AMPLIFIERS

During one phase of the tests for the prototype installation, a high-impedance coil (50 K) was installed on a seismometer and a Parameter Amplifier, Texas Instruments Model RA-5, was installed in place of the phototube amplifier to determine its suitability for use in LP circuits. The RA-5 is being used in the short-period LASA channels. Its application to LP chan-

nels would provide a convenient interchangeability and compatibility. It was found that because the flat frequency response of the RA-5 over the long-period passband did not discriminate against 6-second microseisms, these microseisms were recorded at high amplitudes. This caused other data at other frequencies to be obscured by the microseisms.

The operating conditions that prevailed are illustrated graphically in Figure 52, which plots amplifier input voltage as a function of period in response to average background noise (using Brune and Oliver average seismic background data).[1] Note that if the background noise at 20 seconds is recorded at an amplitude 20 db above the amplifier noise, the 6-second microseismic noise will be 57 db above the amplifier noise. Since the total dynamic range of the RA-5 is 72 db, this leaves but 14-db dynamic range for seismic signals. These considerations, of course, are on the basis that the amplifier will not be overloaded. Hence, increasing the seismometer
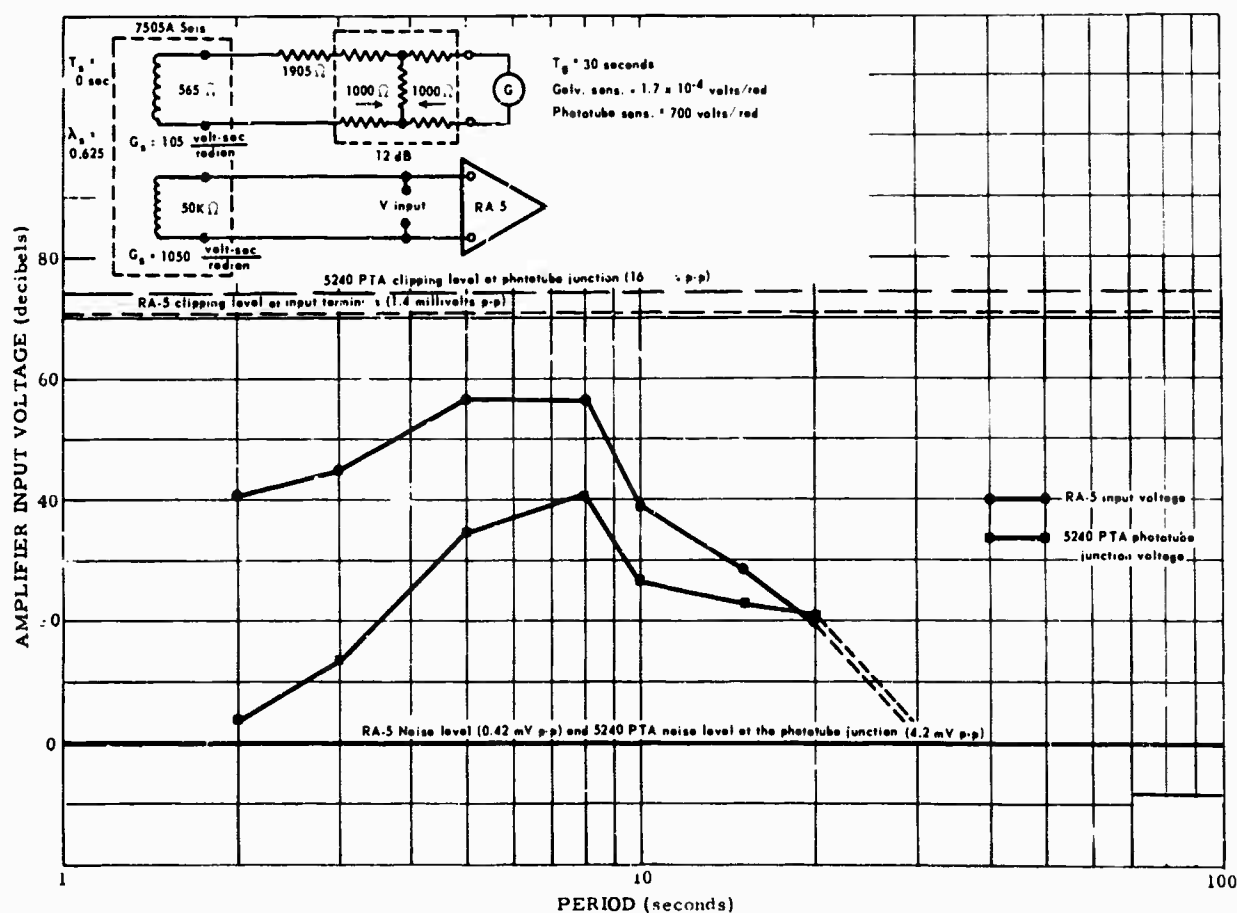
FIGURE 52. AMPLIFIER INPUT VOLTAGE RELATIVE TO AMPLIFIER INPUT CLIPPING LEVEL FOR TWO LONG-PERIOD SEISMOGRAPHS

[1]Brune, J. N. and Oliver, J., "The Seismic Noise of the Earth's Surface," Bull. Seism. Soc. Am., 1959, Vol. 49, No. 4, pp. 349-353.

58

motor constant and applying a filter to the output of the RA-5 will not accomplish the desired results.

An engineering model of the RA-8 parametric amplifier was obtained from Texas Instruments and tested. This amplifier was designed specifically for application to the LP instrumentation system. Although the engineering model had but 90 db of dynamic range, it is understood that developments have made possible the production of this amplifier with 100 or more db dynamic range. Making calculations in the same manner as they are for the RA-5, it is seen that a dynamic range of 42 db above background noise would be available if this amplifier were used in the LP system. This compares favorably with a PTA which has a dynamic range of 33 db above background noise.

Our tests to the engineering model of the RA-8 indicated that it had a high temperature coefficient of drift. It is our understanding that production models of this amplifier will have critical components potted, thereby improving the temperature coefficient of the v . The production model will be called Type II.

5. PLANS FOR THE COMPLETE SYSTEM

Our objective is to furnish the LASA system with a reliable, unmanned, LP seismograph installation that is capable of producing high quality data and is compatible with the short-period LASA system. At present, we are proposing to furnish instrumentation which has the frequency responses shown in Figures 53 and 54. These represent our present thinking of what the system responses should be. These are not final and can be altered as more information becomes avail-
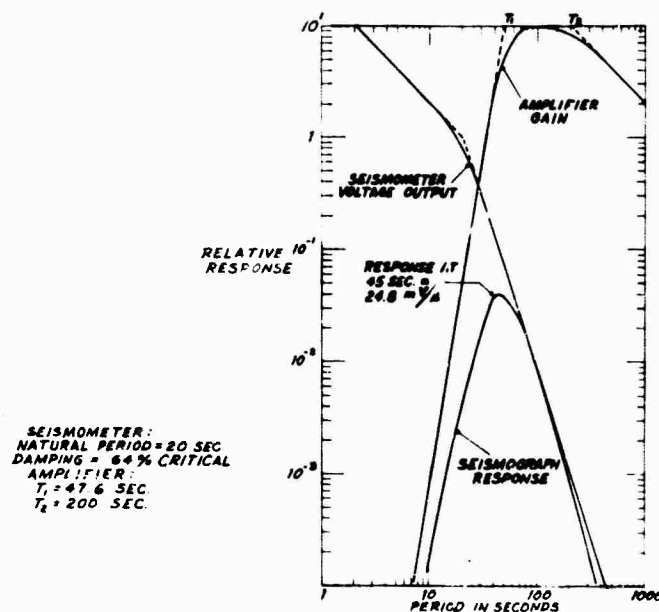
FIGURE 53. SEISMOGRAPH RESPONSE

59
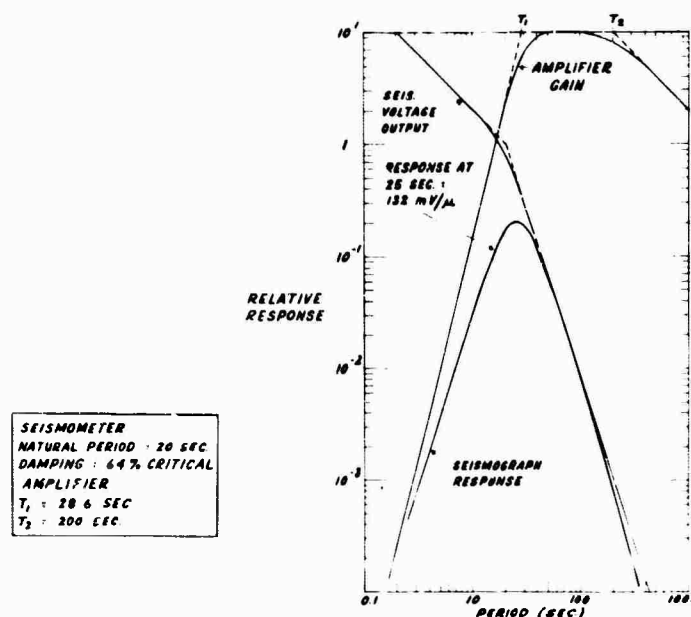
FIGURE 54. SEISMOGRAPH RESPONSE

able by changing filters in the amplifier. One other response that could be provided and might prove useful is the broad-band constant velocity response.

Figure 55 shows a simplified block diagram of the LASA LP system. It will use one vertical and two horizontal seismometers. Their outputs will be amplified by three Type II parametric amplifiers. All three parametric amplifiers will be packaged in a single container. A signal oscillator will provide pump frequency for all three channels. Each data channel will consist of an input section and a detector section, which will constitute the basic amplifier. The output of this basic amplifier will be split into two channels, each containing a filter and an output amplifier. The frequency characteristics of these two filters together with the frequency character-
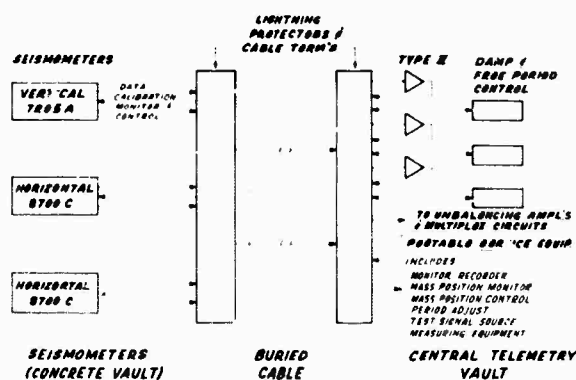
FIGURE 55. SIMPLIFIED BLOCK DIAGRAM LASA LONG PERIOD SEISMOGRAPH

60

istic of the seismometer will determine the response of the overall seismograph. Each filter will be mounted on a separate printed-circuit board that can easily be replaced. The Type II amplifier will be more compatible with other LASA components than the PTA. We expect that some of the PC boards in the Type II amplifier will be interchangeable with those of the RA-5. Furthermore, we expect that the parametric am, 'ifier will require very infrequent adjustment and hence will better meet the concept of an unmanned system than would the PTA. Each seismometer will be equipped with two data coils and a calibration coil. A low impedance (500-ohm) data coil will be used for damping. A high impedance coil (50 K) will be used to drive the Type II amplifier.

A connector will be installed on the cable terminal (the Hoffman Box) at the central teleme' vault to permit the connection of portable service equipment to the system. The portable service equipment will include all equipment needed to provide maintenance and monitor functions to the seismometers without requiring that the seismometer vault be entered. Included will be a monitor recorder, a mass position monitor, a mass position control unit, a period adjust unit, a test signal source, and miscellaneous equipment. These will provide a capability for calibrating the LP instruments from the central telemetry vault.

The seismometers will be installed in sealed metal tanks in the seismometer vault. The vault will have a solid floor in which the metal tanks will be imbedded.

The Type II amplifier will be mounted on the wall in a sealed insulated box located in the central telemetry vault. This will protect its connections from moisture and its circuits from temperature changes.

Three channels of LP data will be connected through the MIT unbalancing amplifiers to the multiplexer and will be transmitted via LASA telemetry circuits to the LASA Data Center in Billings. Interface engineering between LP seismograph circuits and the MIT telemetry circuits is now in the process of being worked out.

It is proposed that LP data be recorded in Billings on both Develocorders and magnetic tape. The Develocorders would present the data in convenient form for visual analysis; the magnetic-tape recorder would provide storage from which data could be extracted for processing. Note that the LP data might be adapted for data pr essing by existing equipment if the sampling rate and playback speed were changed.

6. APPLICATIONS OF LONG-PERIOD SEISMOGRAPHS

Advanced LP seismographs are installed at Witchita Mountain Seismological Observatory (WMSO), Blue Mountain Seismological Observatory (BMSO), Uinta Basin Seismological Observatory (UBSO), Cumberland Plateau Seismological Observatory (CPSO). LP recordings are rou-

61

tinely used in the preparation of the seismological bulletin from the observatories and reports of phases to the USC&GS. The LP data are most useful in the detection and identification of later phases (Figure 56). By the use of LP seismographs, the capability of the observatory is increased by about 50 percent over what it would be if only short-period seismographs were available. The LP seismographs in routine operation at the observatories normally operate at magnifications of about 25K. If routine recordings could be made at 100K, then the LP seismograph would be even more useful. LP recordings are made by each of the LRSM teams on both 35-mm film and magnetic tape. These recordings are routinely used in the preparation of a seismological bulletin and for special studies. In one special study, the similarity of LP body waves across the U.S. was examined (Figures 57 and 58). This was done to determine the feasibility of an array of LP seismographs. The recordings are aligned in accordance with the J-B travel time curve. It can be seen that there is a remarkable similarity in wave shape between stations spaced thousands of kilometers apart.

Overall Relative Phase Detection Capability
for Each WMSO System, by Phase

| Type of earthquake | Phase | Seismograph | | | | | |
		SP	IB	BB	LP	JM20	SIE
Teleseism	P or P'	1	3	5	6	2	4
	PP	1	3	6	4	2	5
	pP	1	3	4	6	2	5
	PcP	1	4	5	-	2	3
	PPP	4	3	2	1	-	-
	S	2	4	3	1	-	-
	PS & SP	3	4	2	1	5	-
	PPS & SPP	3	4	2	1	5	-
	SS	-	-	2	1	-	-
	PKKP	1	3	--	-	2	4
	P' P'	1	3	-	-	2	-
	SKP	1	3	5	-	2	3
	SKS	2	4	2	1	5	-
	SKKS	2	3	4	1	-	-
	Love	-	-	-	1	-	-
	Rayleigh	3	4	2	1	6	5
Regional	P	1	3	2	1	6	5
	Lg	1	3	5	5	2	3
Local and near-regional	P	2	4	-	-	1	3
	S	1	4	-	-	2	3
	Lg	1	4	-	-	2	3

(Note: 1 indicates greatest capability; 2 indicates second greatest capability, etc.)

SP = Short Period   LP = Long Period
IB = Intermediate Band   JM = Johnson-Mathieson
BB = Broadband   SIE = SIE Company Seismograph

FIGURE 56. OVERALL RELATIVE PHASE DETECTION CAPABILITY FOR EACH WMSO SYSTEM BY PHASE

DH-NY	Dist. = 48.1°
BR-PA	Dist. = 49.4°
LC-NM	Dist. = 68.8°
JE-LA	Dist. = 56.5°
HN-ME	Dist. = 46.8°
MN-NV	Dist. = 78.5°
HL2ID	Dist. = 75.8°
SUM (Attenuated)	

Time Base: 1 cm. = 10 secs.
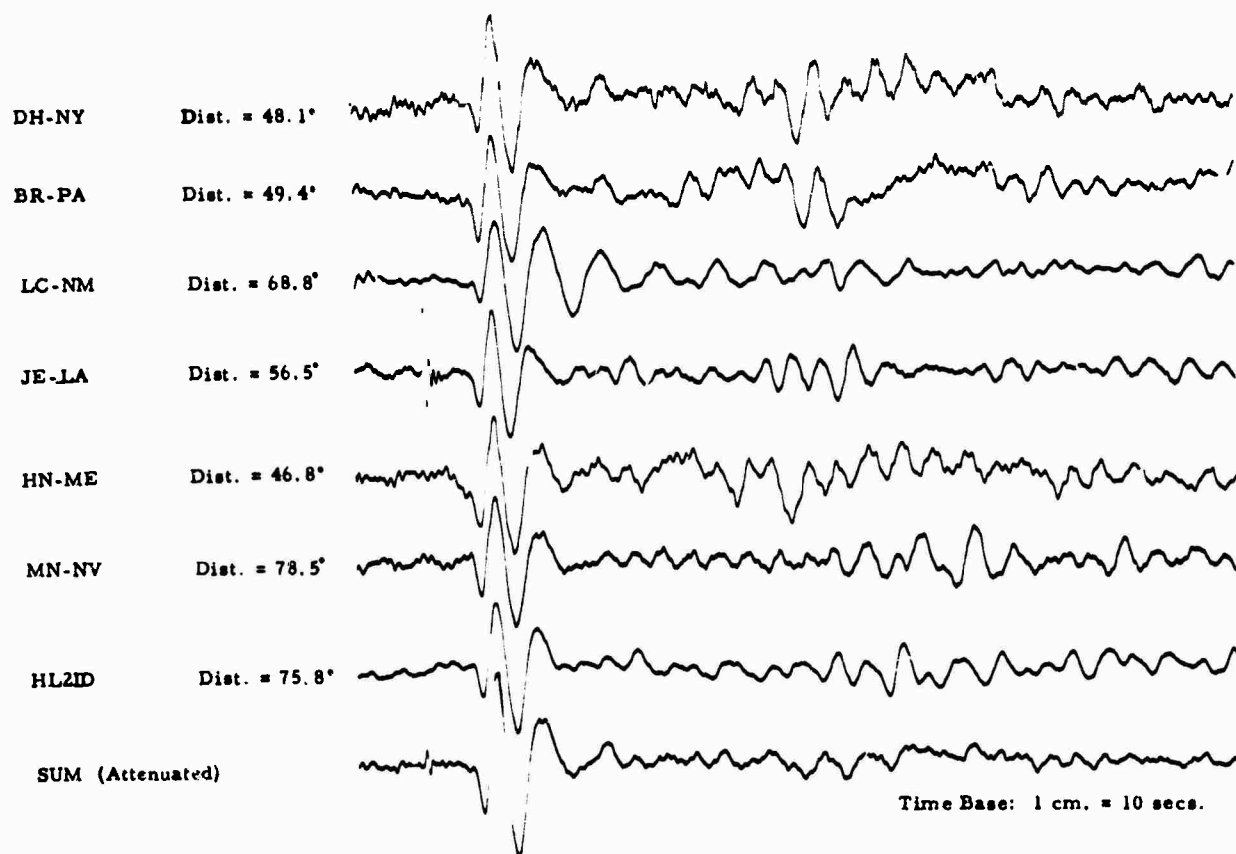
Long-period teleseismic P phase time-shifted for alignment according to Jeffrey--Bullen Seismological Tables, then summed. Earthquake occurred 4 September 1964 along the Central Mid-Altantic Ridge. Depth was approximately 22 km, magnitude about 5.4. Distances were calculated on a digital computer, based on epicenter data from USC&GS

FIGURE 57. SIMILARITY OF LP BODY WAVES ACROSS THE U. S.

A study of LP body waves has also shown that more consistent results in the determination of magnitude can be obtained than when using short-period body waves. One interesting possibility is that the use of LP seismographs appears to improve the detection of body waves in the shadow zone. This is probably due to the fact that LP waves defract around the core, whereas short-period waves are cut off more sharply (Figure 59).

Long-period waves are generated by all earthquakes. Their detectability decreases continuously and almost linearly with magnitude. This is shown graphically in Figures 60 and 61. Figure 60 shows the relative capability of two LRSM teams for detecting LP surface waves. One team was located at Las Cruces, New Mexico (LC-NM); the other team was at Maryville,
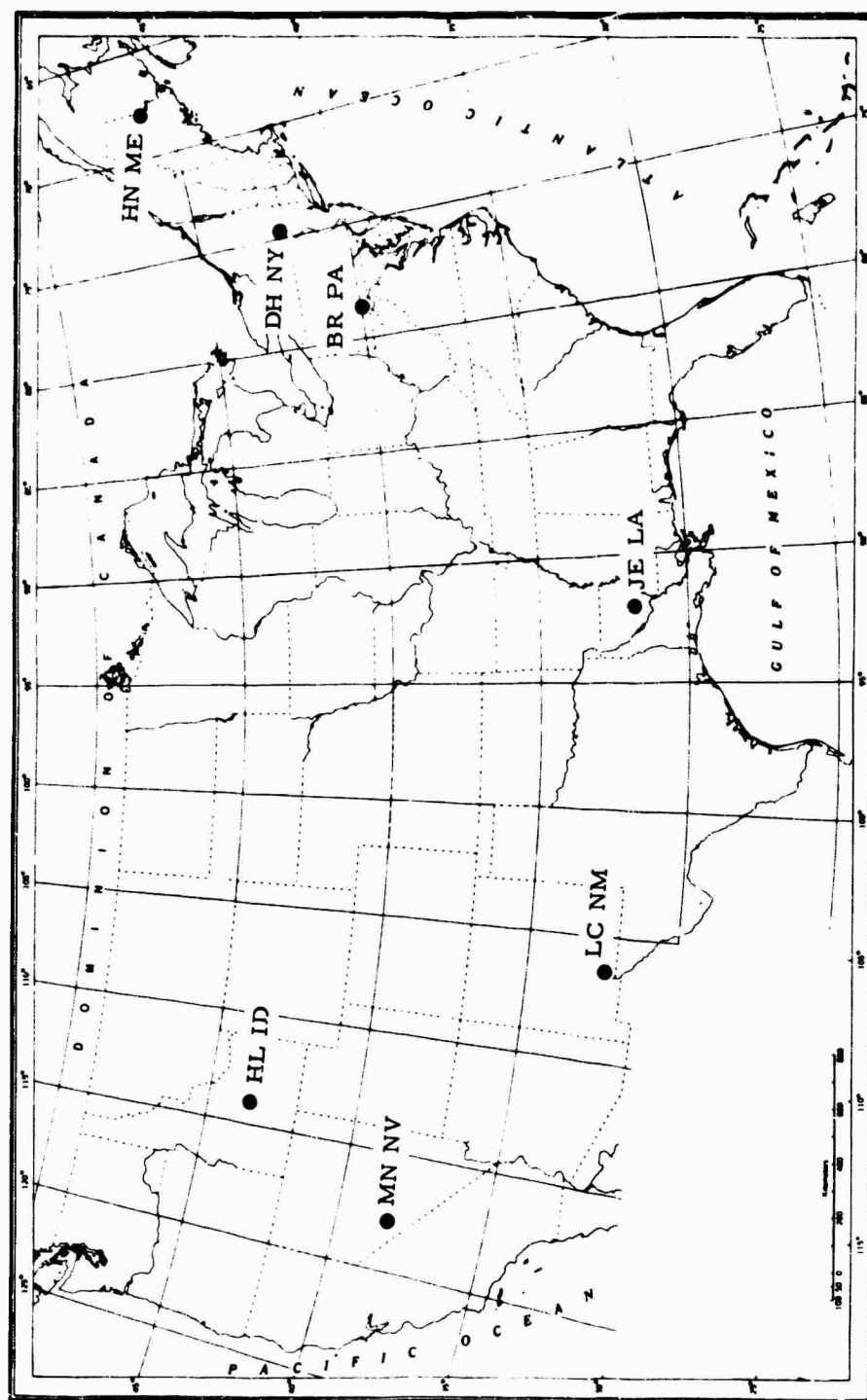
FIGURE 58. LOCATIONS OF SITES USED FOR LP ARRAY STUDY

64

Distance	No. of events recorded by short period	Percent recorded by long period[1]
20-100°		11
95-100	315	26
101-105	73	60
106-110	71	38
111-11:	91	26
116-120	121	12
121-125°	191	3
126-130	108	5
131-135	46	11
136-140	29	31

[1] Percent of P phases detected by the LRSM short-period seismographs which were also detected by long-period seismographs.

FIGURE 59. DETECTION OF LONG-PERIOD BODY WAVES AS A FUNCTION OF EPICENTRAL DISTANCE

California (MV-CL). Figure 61 shows the probability of detection of Rayleigh waves using LP data and is based on the study of over 22,000 earthquakes.

It is anticipated that the addition of LP seismographs to LASA will provide the capability for extending these studies and undertaking new ones.
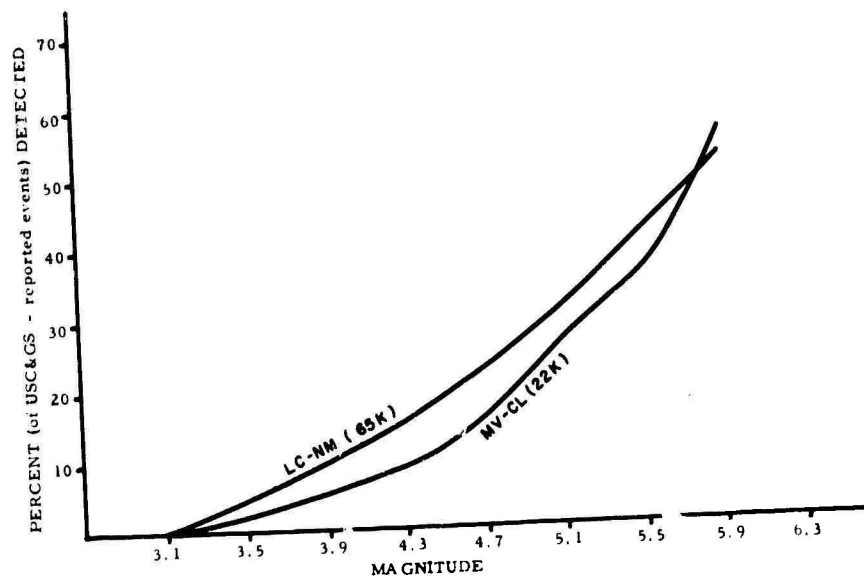
LC-NM (65K) vs MV-CL (22K)
(For all distances - depth restricted to 50 km or less)

FIGURE 60. RELATIVE DETECTION CAPABILITY FOR LP SURFACE WAVES

66
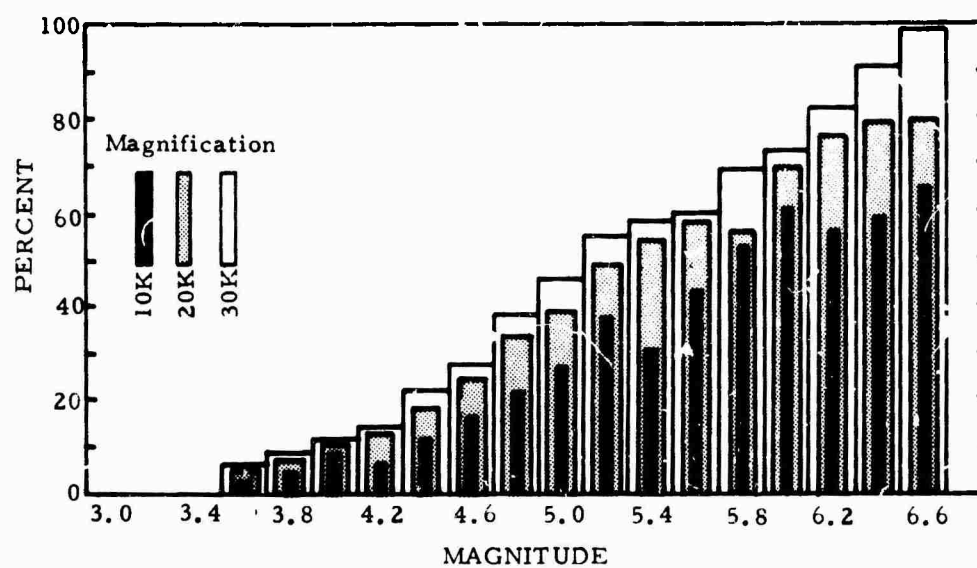
FIGURE 61. PERCENT DETECTION OF RAYLEIGH WAVES (ALL MAGNIFICATIONS)

7. ANALYSIS OF FILM RECORDINGS AT ANGELA AND HYSHAM SUBARRAYS (B1 and F3)
by
Carl F. Romney
AFTAC/VELA SEISMOLOGICAL CENTER

Mobile stations from the Long Range Seismic Measurements (LRSM) program were installed at the centers of Subarrays B1, Angela, Montana, and F3, Hysham, Montana. These LRSM vans were each equipped with a Develocorder, which made it possible to record a number of traces from the shallow hole array instruments in addition to the standard three-component surface instruments. The LRSM teams also installed a 500-foot deep Benioff seismometer and a 200-foot deep Hall-Sears 10-1 seismometer at the two subarray centers in addition to the normal 25 array detectors. The objectives were to obtain a comparison between the signal-to-noise ratios recorded at the surface and in the shallow holes and to obtain preliminary estimates of the effectiveness of the unphased sum of all instruments in each subarray. Preliminary conclusions from the analysis of these recordings are reported in the following paragraphs.

SIGNAL-TO-NOISE RATIOS AT SUBARRAY B1

A study was made of the teleseisms recorded at Angela during January 1965. Forty-four earthquakes were selected which had suitable signal-to-noise ratios on all traces of interest. Signal amplitudes and periods were measured on the Develocorder records and converted to approximate ground displacement by using the instrumental response curves and assuming the signals to be roughly sinusoidal. Noise data were also obtained for each instrument or sum of instruments by measuring amplitudes of noise pulses having periods in the range from 0.3 to 1.4 seconds at several hundred regularly spaced time intervals throughout the month, and computing the probability distribution curves. The 50 percent noise value for each channel was then used in the signal-to-noise estimates.

Data were obtained from the following instruments:

SPZ	Surface short-period Benioff vertical at array center.
DW1	500-foot deep short-period Benioff vertical at array center.
DW2	500-foot deep Hall-Sears 10-1 at array center.
DW3	200-foot deep Hall-Sears 10-1 at array center.
Sum or Summation	Sum of twenty-four 200-foot deep Hall-Sears 10-1.
Sum 1-6	Sum of 200-foot deep Hall-Sears 10-1 instruments in rings 1 through 6.

Some uncertainties exist in the Angela data because the recordings were made before all calibration procedures had been developed for the array instruments. The surface instruments

and the 500-foot deep well Benioff, however, were well calibrated and relative calibrations of other instruments were obtained from this reference where necessary. The summation channel in particular was calibrated exclusively by comparing the 6-second microseisms with those recorded by the surface instrument. Subsequent investigations established that the magnification values computed by this means were reasonably accurate.

Figure 62 shows the individual data plots and the least squares fit through each set of data. On the graphs shown, the curves would have 1 to 1 slopes if the signal-to-noise ratios of signals recorded from the borehole instruments were identical to those recorded by the surface instruments. Equations of the least squares lines are given on Figure 63, which also shows the same curves on a common abscissa to facilitate comparison of the improvement in borehole and summation channel signal-to-noise ratios relative to surface values. It may be seen that the signal-to-noise improvement of the borehole instruments ranged from a factor of 1.15 (~1 db) for DW3 to 1.47 (~3 db) for DW1 with respect to the surface instrument. These modest improvements result chiefly from reduction of relatively high frequency noise below the surface; it will be noted that the improvement increases with depth.
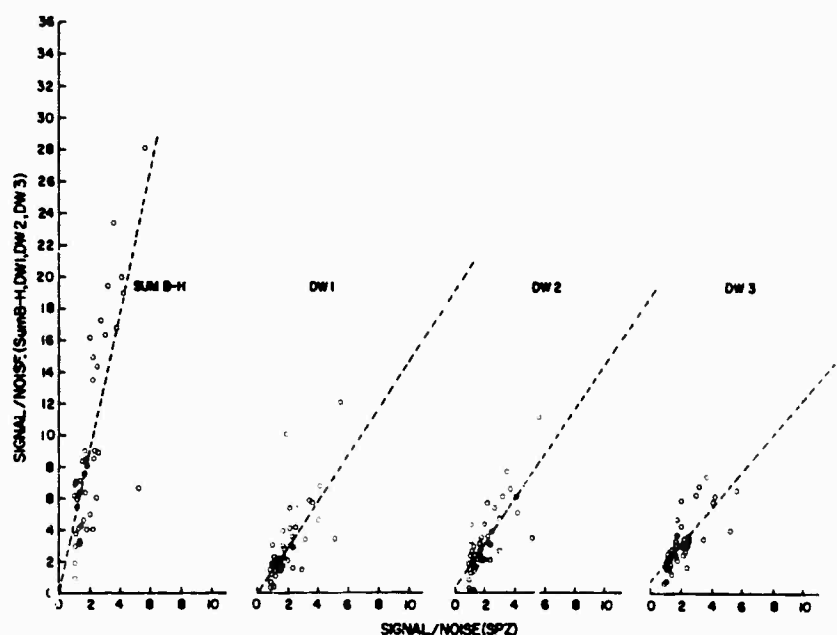
FIGURE 62. LASA B1 BOREHOLE S/N vs SURFACE S/N

In addition to the improvement in signal-to-noise ratio with depth, a further improvement was found by summing the 24 detectors of the 200-foot deep array. This improvement amounted to a factor of 3.8 (~12 db) with respect to a single instrument at the same depth (DW3). This may be compared with a signal-to-noise improvement of 4.9 (or $\sqrt{24}$) which would result from an array of this number of instruments recording coherent vertical signals and random noise.

69
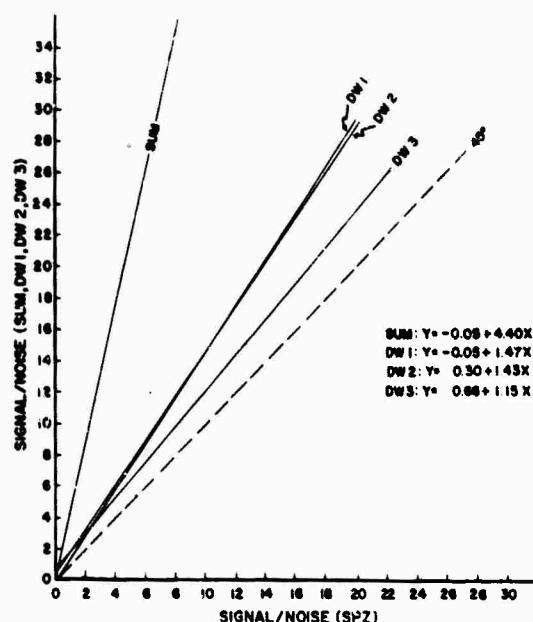
FIGURE 63. LASA B1 BOREHOLE S/N vs SURFACE S/N

It should be recognized that there is no a priori reason to expect $\sqrt{n}$ signal-to-noise improvement for this particular array. The improvement could be greater or smaller, depending on the actual properties of the signals and the noise. The combined result of the improvement due to the array and the improvement due to the 200-foot burial of the instruments gave a total improvement in signal-to-noise ratio of 4.4 over that obtained by a single instrument at the surface.

SIGNAL-TO-NOISE RATIOS AT SUBARRAY F3

A similar analysis of Develocorder records from Hysham, Montana, (Subarray F3), is summarized in the data plots shown in Figure 64. These data were recorded during April and 35 signals were selected for analysis.

In addition to the sum of all detectors in the array, an analysis was made using subsums consisting of instruments in rings 1 through 4 and 1 through 6 (the summation of all instruments includes rings 1 through 8). It is noted that for this particular analysis, the 500-foot Benioff seismometer registered a better signal-to-noise response than did the 500-foot deep Hall-Sears 10-1 instrument. It can also be seen that the sum channels show varying signal-to-noise improvements with the 19-element sum, rings 1-6, providing the best performance. A comparison of the best sum performance relative to a single 200-foot instrument, DW3, revealed a factor of 3.5 improvement. The best improvement at Angela, as previously mentioned, was 3.8.

70
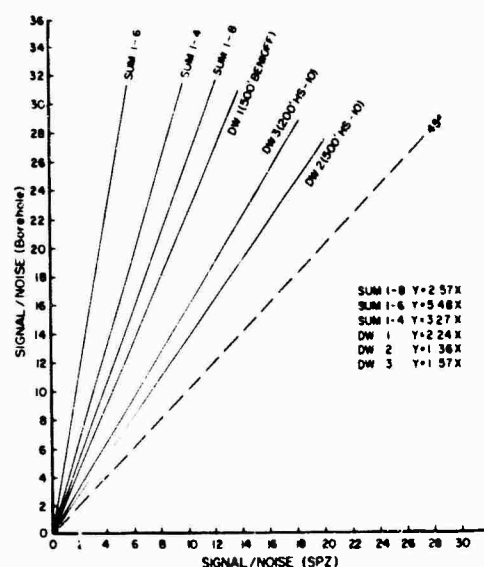
FIGURE 64. LASA F3 BOREHOLE S/N vs SURFACE S/N

VARIATION IN SIGNAL AMPLITUDE BETWEEN ANGELA AND HYSHAM

Ideally, we would hope that teleseismic signals are identical in waveform and amplitude at the various subarrays of the LASA. If not identical, we would hope that there is at least a constant ratio between amplitudes or a fixed operator which would equalize signals arriving from all paths. The Developcorder data obtained from the two LRSM vans are sufficient for preliminary investigation of amplitude variations, leaving waveform studies to be conducted when magnetic tape recordings are available. Accordingly, an analysis was made of 117 earthquakes which were satisfactorily recorded at both Angela and Hysham. To correct for small differences in distance, the magnitudes were computed at each station and the differences in magnitude (Δm) were tabulated. All measurements were made from the 500-foot deep Benioff recordings, which were probably the best calibrated. The differences were large, ranging from +0.6 to -0.7 magnitude units, where the positive sign indicates that the Angela signal was larger than the signal at Hysham.

Figure 65 illustrates the variability in the recorded amplitudes. The upper two traces show signals from an event in the Aleutian Islands and the lower two traces show recordings of an earthquake from the South Pacific, approximately 6 minutes later. The magnifications of the instruments at 1 cps are indicated on the recordings and it will be noted that the gain at Angela (ANMA) is only about 5 percent higher than the gain at Hysham (HYMA). The signal from the Aleutian Islands is larger at Angela, whereas the relative amplitudes are reversed for the South Pacific event, the Angela recording being smaller than that at Hysham. Occurring, as they do,

71
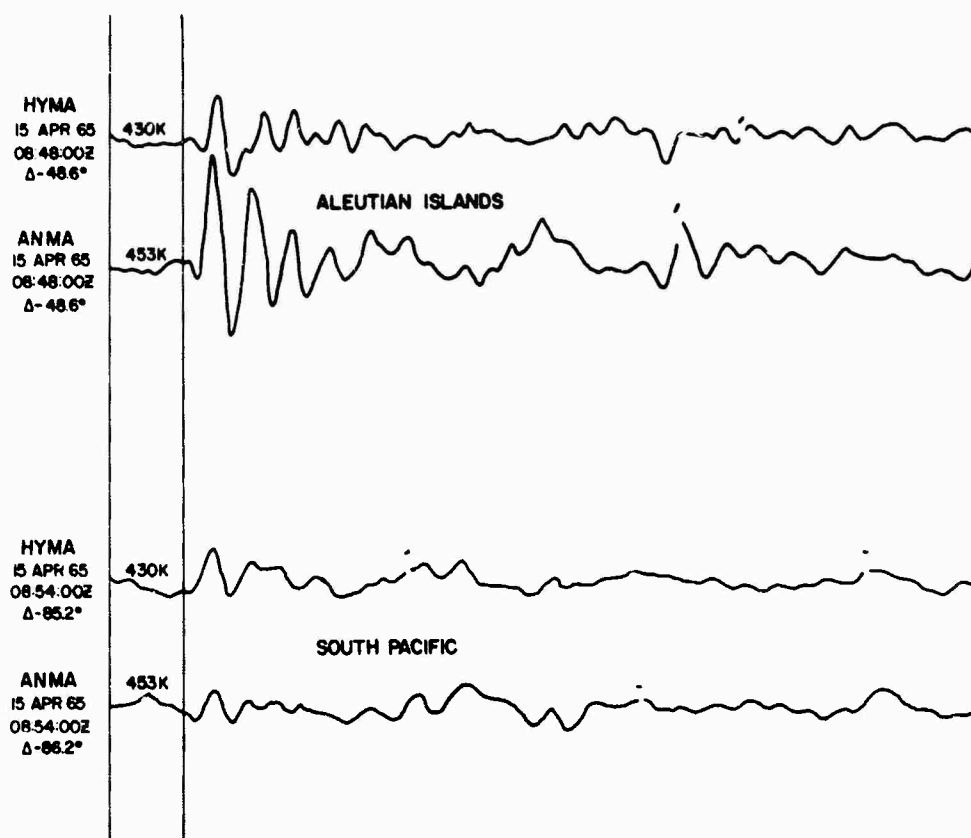
FIGURE 65. DW1 SIGNALS AT ANGEL₄ AND HYSHAM

within a few minutes of one another on the records, there is no possibility that these signal variations are caused by errors or changes in the instrumental gains.

The observed magnitude differences were analyzed in an attempt to determine any dependence upon distance or azimuth, but no simple relationship was found. However, there does appear to be some correlation in the magnitude differences for signals from particular regions. This is perhaps best illustrated by referring to the table on the next page. We can infer from these results that the signal variability is both real and large and that it is either a very complex result of local effects at the recording sites, or is (and I think more probably) introduced to an important degree in the near-source and mantle portion of the paths. The consequence of this variability on array performance remains to be seen.

A NOTE ON CALIBRATION

Variable seismometer performance, as illustrated in Figure 66, causes difficulties in interpreting data and reduces the precision of estimates of the kind previously described in this paper. As an example, a spot check of system response of instruments at Hysham (relative magnification versus period) which was made from 13 April logs revealed that the re-

	Area	Δ m Average (ANMA-HYMA)	Standard Deviation	Number of Events	Extremes of Δ m
1.	Alaska and Aleutians	+.16	±.25	27	(+.6, -.4)
2.	Kuriles, Kamchatka, and Japan	-.13	±.17	23	(+.1, -.4)
3.	South Pacific, Samoa through Carolines	-0.3	±.24	21	(+.3, -.6)
4.	Central America and Caribbean	-.05	±.23	16	(+.4, -.5)
5.	South America	-.26	±.21	27	(+.1, -.7)
6.	Mediterranean Area	-.10	±.14	3	-
	Average, all areas	-.07	±.26	117 (total)	

sponse for DW2 was approximately 2 db below the average response at 3 cps. The DW3 response was approximately 2.5 db higher than the average response at 3 cps. Normally, these variations are not known to the analyst from a routine single frequency calibration. In most cases, the best that can be done is to refer to a standard response curve in reducing trace motion to ground movement.

The signal periods observed from the Angela and Hysham data ranged from 0.5 to 1.1 seconds. The average period was about 0.7 seconds. Some of the noise had periods as low as 0.3 seconds. The relative gains for signals and for noise may not have been properly accounted for in estimating the signal-to-noise ratios because the full frequency response of each instrument was unknown. This effect could account for part of the reported differences in the effectiveness of various instruments.

ACKNOWLEDGMENT
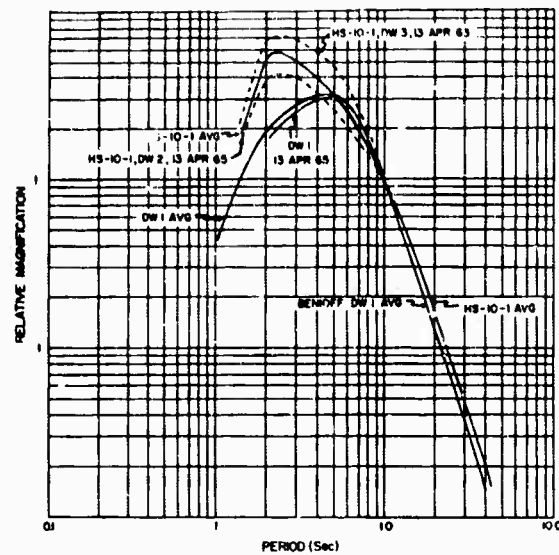
FIGURE 66. DEEP WELL BENIOFF (DW1) AND HS-10-1 RESPONSE CURVES

8. EXPERIENCE AT TFSO EXTENDED ARRAY: TRAVEL-TIME ANOMALIES

by

E.F. Chiburis

Seismic Data Laboratory, Teledyne, Inc.

Any process for aligning signals across an array requires a knowledge of significant travel-time anomalies which may be associated with any of the array elements.

To test whether such anomalies exist and whether they could be used to align signals over a large array, we measured P-wave arrival times at the extended array stations (Figure 67) for more than 300 teleseisms from two directions. The key questions of the study were:

1.   Are there significant travel-time anomalies associated with particular sites?
2.   Are they consistent for all events from one particular region?
3.   How large are they?
4.   Are they necessary to improve P-signal alignments across the array?
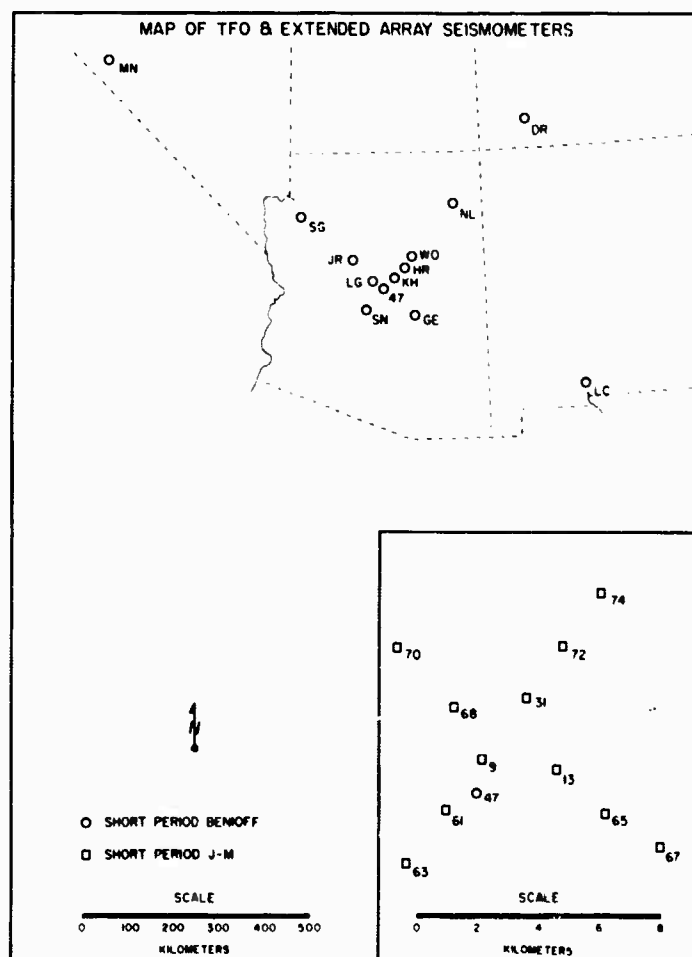
FIGURE 67.   TONTO FOREST OBSERVATORY (TFSO) INSTRUMENT CONFIGURATION

75

5. Are they sufficient (together with Herrin travel times) to align signals or are there other factors?

All travel-time anomalies were made relative to arrivals at the center of TFSO. P-onset times for some events were difficult to measure. On the other hand, picking a later characteristic feature, first peak or trough, of the P-phase was fairly easy and provided a measure of travel-time intervals between sites. For this reason, relative rather than absolute anomalies were measured. The questions of phase-distortion or instrumental-response errors when using these later phases were substantially answered by analyzing several shocks with well-recorded impulsive first arrivals. The anomalies obtained by using first arrivals were in good agreement with those obtained from later motions.

Herrin travel times for P-arrivals from the given epicenter to all stations were computed and subtracted from the observed travel times of a particular feature of the P-phase. Then this time difference at Z-1 was subtracted from all other differences for that event, yielding relative (to Z-1) travel-time anomalies.

Examples of the results of relating anomalies to epicentral distance for northwesterly and southeasterly directions at two of the LRSM sites are shown in Figures 68 and 69.

To show that it is necessary to know the anomalies, Figure 70 compares the alignment of a Kurile Island event recorded at TFSO using velocity only with the alignment using velocity plus the travel-time anomalies. This event is one used in deriving the average travel-time anomalies. The prominent feature lined up in Figure 70 was the one chosen to read P-arrivals for this event. The fact that this feature does line up at most of the sites when the travel-time anomalies are used indicates that the travel-time anomalies are important and that the alignment of this feature of this event agrees with the alignment of similar features on other events. With the exception of one site (WO AZ) all of these prominent features (largest trough) seem to be within 0.1 second of each other when travel-time anomalies are applied.

The northwest-azimuth results show much less scatter than the results from the southeast. It is significant that the northwest results were obtained almost entirely from aftershock sequences rather than unrelated events. The significance here is epicenter location errors. If a main shock is not correctly located, the aftershocks are usually mislocated also but not with respect to the main event. Therefore, all of the anomalies calculated from the sequence will have about the same value but will contain a constant but unknown error.

Errors in epicenter location can produce quite large errors in the calculated anomalies. To show this, Figure 71 depicts the geometry. The error in anomaly is simply the error in relative epicentral distance to the station pairs for the two epicenters divided by the velocity

76
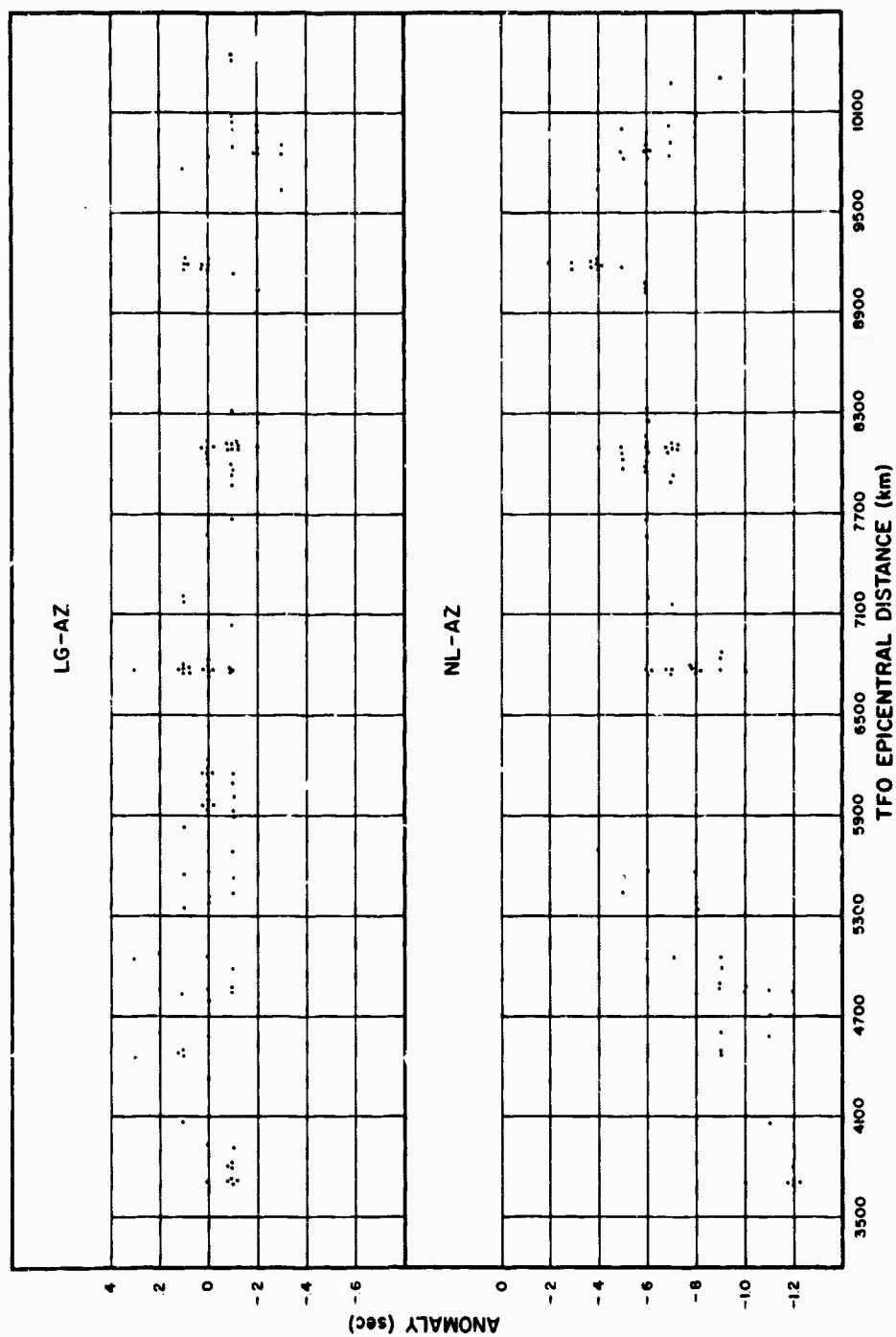
FIGURE 68. TRAVEL-TIME ANOMALY AT TFSO SITE A vs EPICENTRAL DISTANCE

77
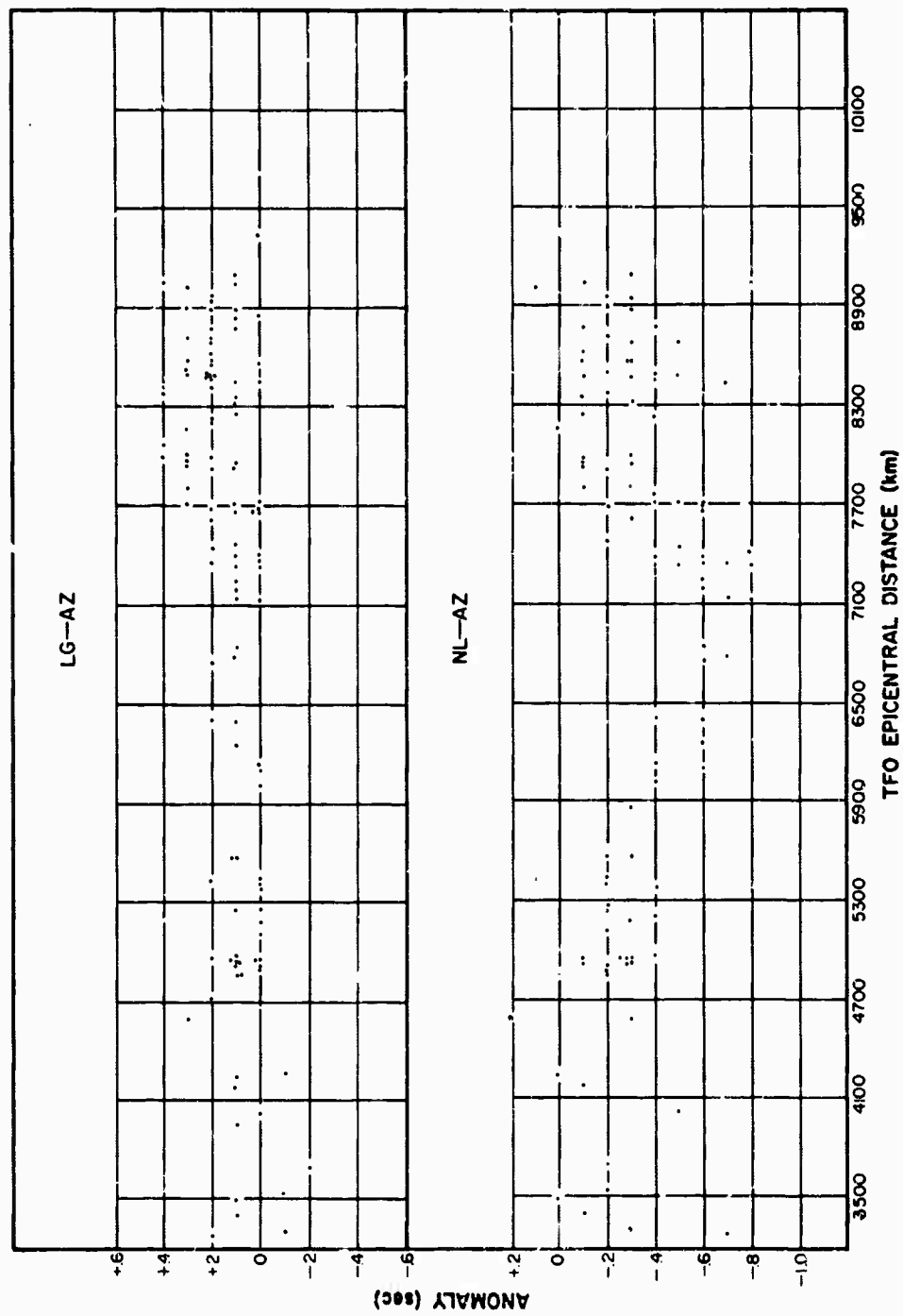
FIGURE 69. TRAVEL-TIME ANOMALY AT TFSO SITE B vs EPICENTRAL DISTANCE

78

Without Travel Time Anomalies   With Travel Time Anomalies

SG-AZ	0.0 sec.	
LG-AZ	-0 1 sec.	
WO-AZ	0.0 sec.	
KH-AZ	+0.3 sec.	
SN-AZ	-0.3 sec.	

10 sec.   10 sec.

Event: 31 May 1964, 43.5°N 146.8°E, 00:40:36.4Z
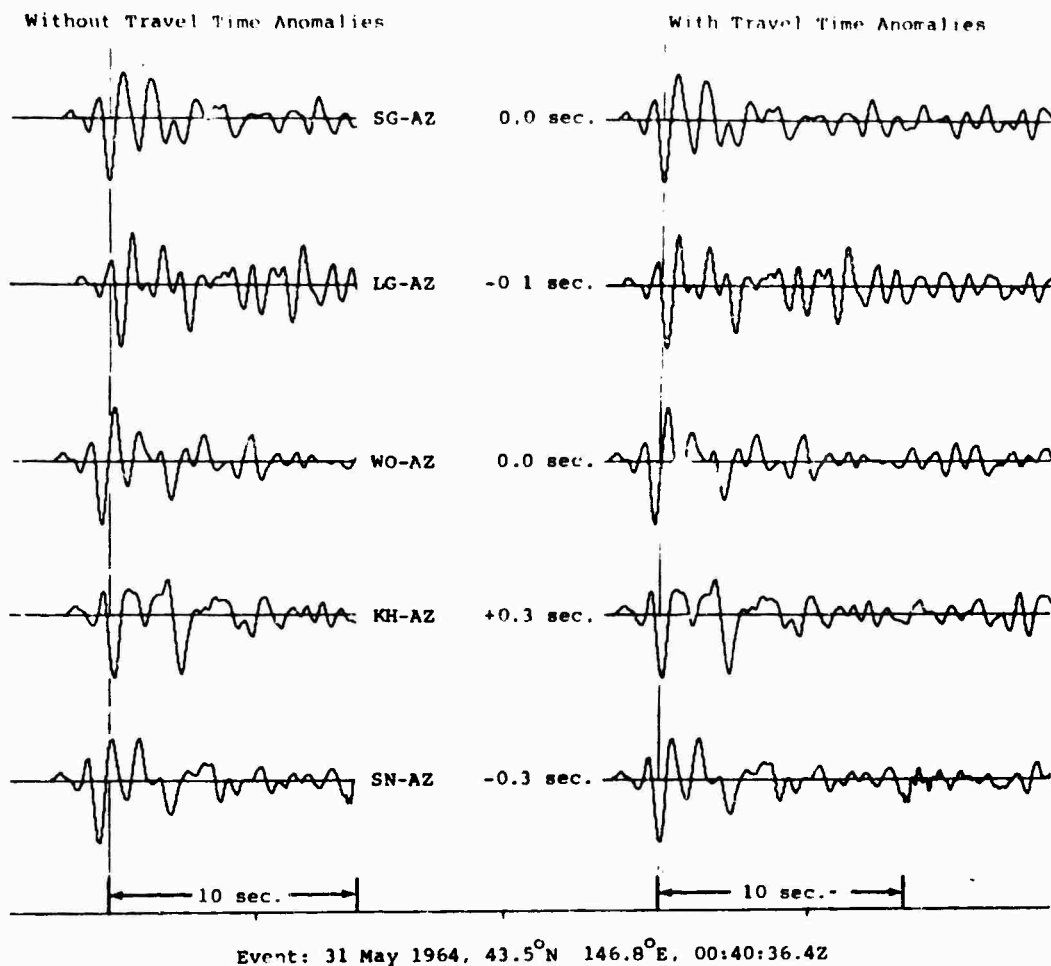
FIGURE 70. SIGNAL ALIGNMENT OF A KURILE ISLAND EVENT WITHOUT AND WITH TRAVEL-TIME
ANOMALY CORRECTIONS

at that epicentral distance; that is

$$\text{Anomaly error} = \frac{(\Delta_a - \Delta_o) - (\Delta'_a - \Delta'_o)}{V(\Delta)}$$

An example actually computed is shown in Figure 72. The event is a Columbian shock on
January 24, 1965 at Δ_o = 4956 km. The location error was assumed to be 1° in latitude or
longitude or both. Although this location error is probably high, it serves to show the possible
result. It is clear that epicenter location errors can produce anomaly errors larger than the
anomaly itself. We are presently devising a program with which epicenters can be relocated
on the basis of the observed average anomalies. This program assumes that the original
epicenters are mislocated randomly; if they are not, we should be able to obtain an indication
of this bias.
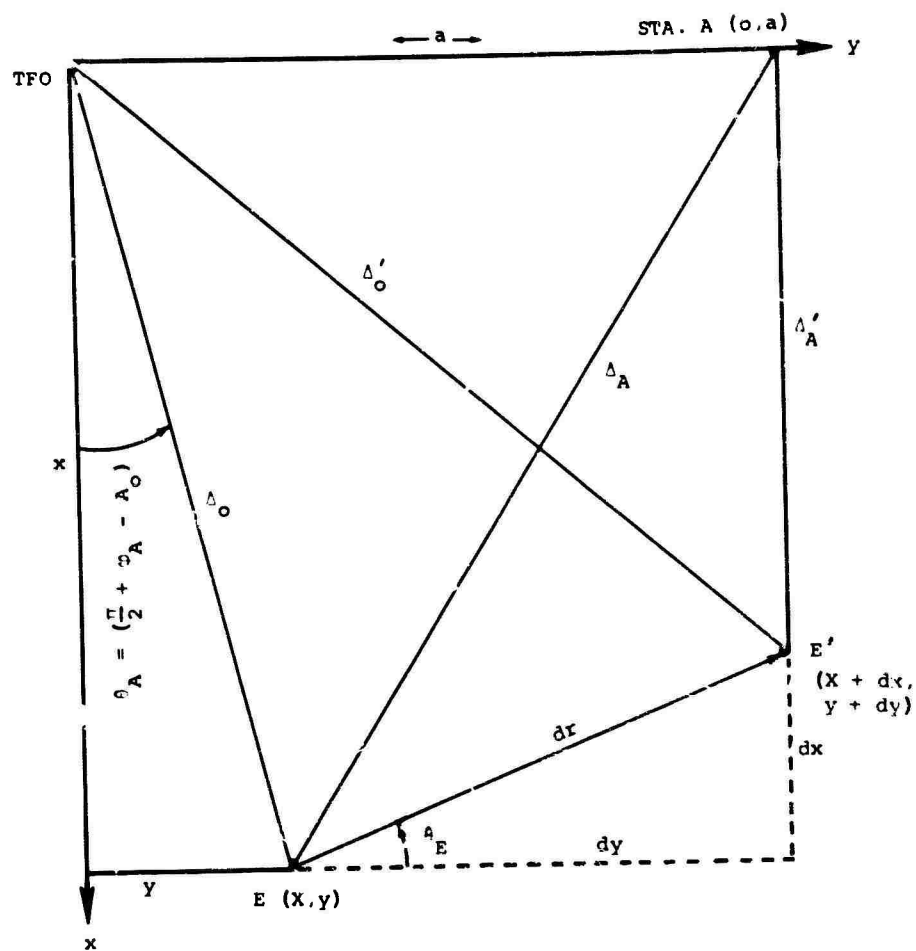
79

TFO

STA. A (o,a)

$\leftarrow$ a $\rightarrow$

Δ_o'

Δ_A'

Δ_A

x

$\theta_A = (\frac{\pi}{2} + \theta_A - A_o)$

Δ_o

E'
(X + dx,
y + dy)

dr

dx

θ_E

dy

Y

E (X,y)

x

Anom. Error, $\delta T = \dfrac{(\Delta_A - \Delta_o) - (\Delta_A' - \Delta_o')}{V(\Delta)}$

where $\Delta_A = \left[\Delta_o^2 + a^2 - 2_a \Delta_o \sin \theta_A\right]^{1/2}$

$\Delta_o = \Delta_o$

$\Delta_A' = \left[\Delta_o^2 + dr^2 + a^2 + 2\Delta_o dr \right.$

$(-\cos \theta_A \sin \theta_E + \sin \theta_A \cos \theta_E) - 2a (\Delta_o \sin \theta_A + dr \cos \theta_E)\left.\right]^{1/2}$

$\Delta_o' = \left[\Delta_o^2 + dr^2 + 2\Delta_o dr (-\cos \theta_A \sin \theta_E + \sin \theta_A \cos \theta_E)\right]^{1/2}$

FIGURE 71. GEOMETRY FOR TRAVEL-TIME ANOMALY ERROR COMPUTATIONS

80
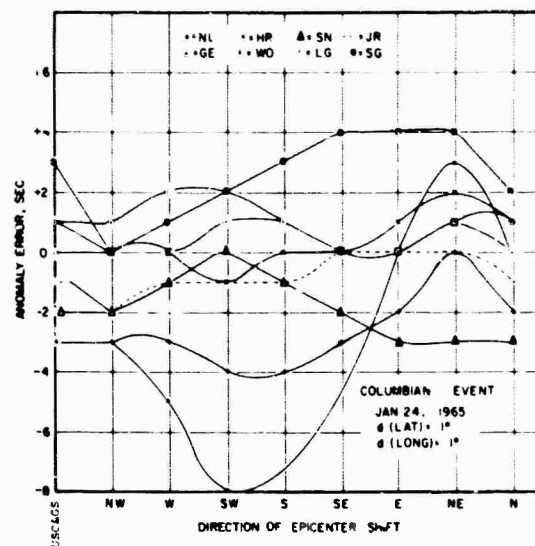
FIGURE 72. ANOMALY ERROR AS A FUNCTION OF DIRECTION OF EPICENTRAL SHIFT

The cause of the anomalies is presently unknown, although site geology appears to be the most important. Station elevations alone are inadequate to explain the anomalies.

Several conclusions have been drawn from this study and are as follows:

1. There are significant relative travel-time anomalies associated with the TFSO extended array stations.

2. The anomalies are consistent for all events from a particular region but vary slowly with distance and azimuth.

3. Knowledge of the anomalies is necessary and probably sufficient to improve signal alignments using the expected velocity across the extended array.

4. Differences in station elevation are insufficient to fully explain the anomalies.

5. Epicenter location errors cannot be assumed to be negligible when determining the anomalies.

6. Aftershock sequences should not be used to determine the anomalies.

7. Many shocks from many regions are necessary to determine the average anomalies.

8. The techniques used at TFSO can and must be used at LASA to determine if relative travel-time anomalies exist there also.

81

9. NOISE & SIGNAL CHARACTERISTICS IN THE VICINITY OF MONTANA LASA

by
H. Lake
Texas Instruments, Inc.

This paper presents results of a study to determine those noise and signal characteristics in the vicinity of the Montana LASA which are pertinent to the operation of a large diameter seismic array. Most of this material is presented in greater detail in the report referenced below.*

Before discussing the noise characteristics which were observed in the vicinity of Montana LASA, it is important to point out one of the main problems which are discovered during the investigation. This problem concerned phase and amplitude variations between instruments within the same array.

Figure 73 presents data which gives an indication of maximum amplitude variations observed for instruments in the Angela and Hysham arrays. The data shown was obtained by calibrating all 25 instruments simultaneously at the indicated frequencies. As can be seen, these variations are 5 to 8 db after being corrected at one cycle per second. Figure 74 gives an indication of the maximum phase variations that were observed. The variations shown indicate the variation in phase between instruments observed from this single simultaneous calibration. It is noted that below one cycle per second, variations are on the order plus or minus 20°. Above one cycle per second (the approximate damp resonant frequency) the variations are less. This suggests the possibility that the observed phase variations can be related to the differences in damped resonant frequency of the instruments within the array. Figure 75 presents data which gives an indication of the time variation of phase response of instruments in the array. The instruments were calibrated at one cycle per second three different times within a 14 day period. The bars here indicate maximum variation of each within the 14 day period. As can be seen these variations are on the order of 4°. It should be pointed out that the observed variations may be attributed to the measurement technique. That is, the variations seen might be due to a difference in setting of the signal generator to one cycle per second. In any case the observed phase variations are an order of magnitude less than observed static phase variations between instruments within the array.

Figure 76 presents the measured damped resonant frequency for each of the instruments within the Angela and Hysham arrays. These values are representative except for the D2 instrument in the Angela array which was replaced.

---

*Large Aperture Seismic Array Final Specification, Texas Instruments, Inc., August 1965.
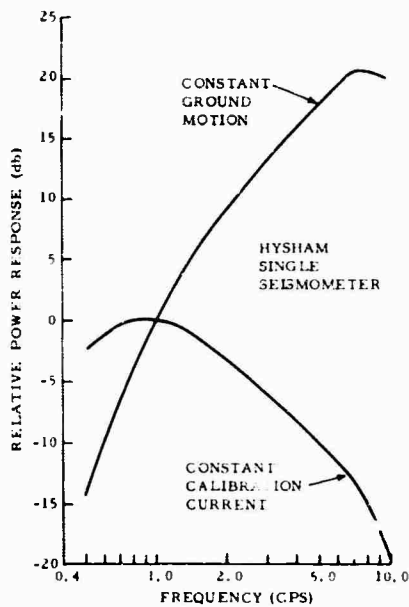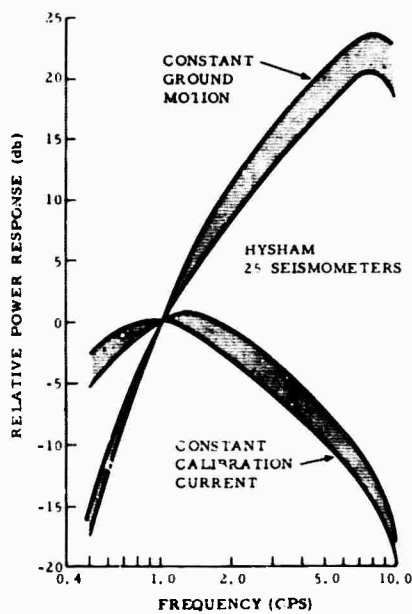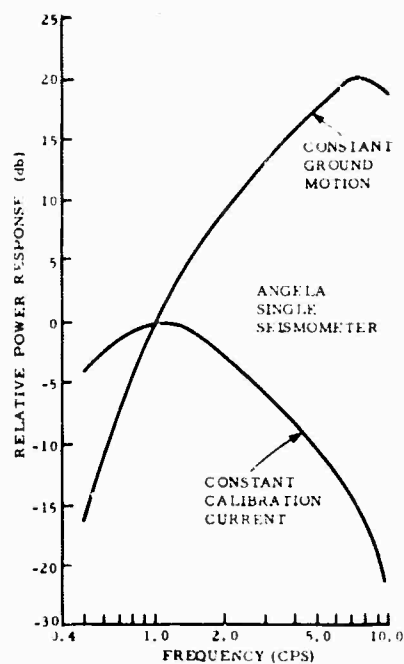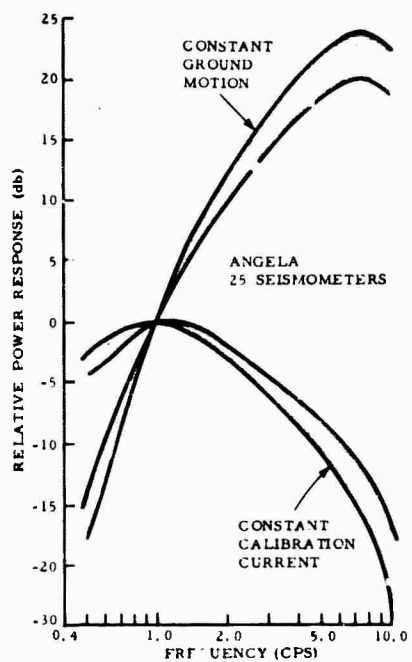
FIGURE 73. ANGELA AND HYSHAM SEISMOMETER FREQUENCY RESPONSES FOR A SINGLE SEISMOM-
ETER AND FOR 25 SUBARRAY SEISMOMETERS

83
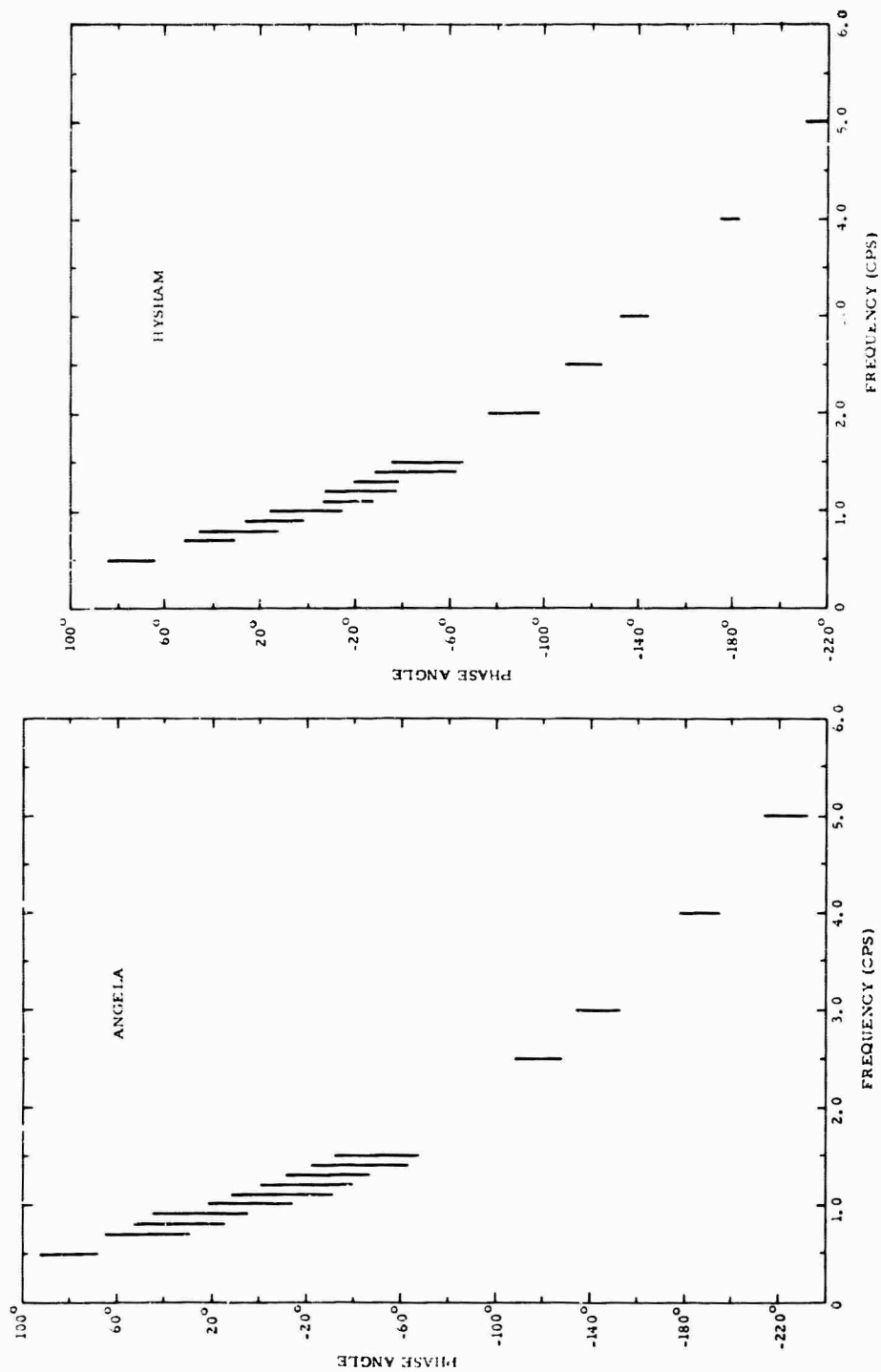
FIGURE 74. SEISMOMETER PHASE RESPONSE OF THE ANGELA AND HYSHAM 25 ELEMENT SUBARRAYS

84
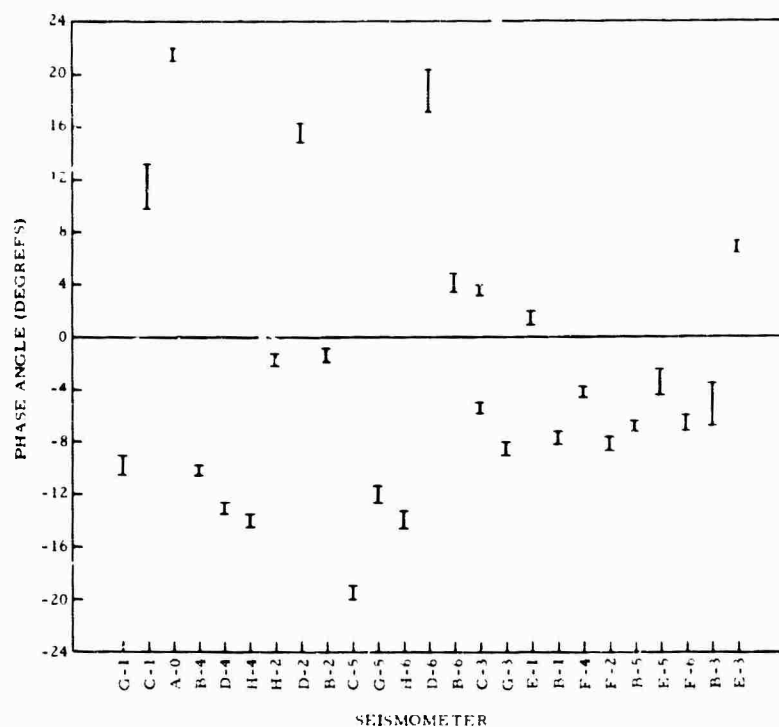
FIGURE 75. SEISMOMETER PHASE RESPONSE FOR THE ANGELA SUBARRAY OVER A 14-DAY PERIOD

Variations in phase and amplitude response having magnitudes observed at the Angela and Hysham subarrays can critically affect the array gain that can be realized with LASA. Further studies should be undertaken to determine the effect of this problem on each of the various proposed types of processing for LASA.

Figure 77 presents a block diagram related to the system noise measurements that were made at Angela. In this diagram, system III includes the recording system used to measure the system noise, subsystem II includes subsystem III and the MIT equipment. Subsystem I includes II, III and all the cable and amplifier equipment to the well head.

Figure 78 shows measured power density spectra of each of these system components. The system noise was obtained by replacing the inputs to each subsystem by an equivalent resistance. The system noise through the amplifier is approximately 30 db below the ambient seismic noise at 1.0 cps. Therefore the system is far from system noise limited.

Studies were included to determine the effect of burial on the ambient measured noise spectra. Figure 79 presents the results of computing power density spectra at various depths in the same approximate area. Holes were drilled at 10-foot separation. As can be seen, below 1 to 1.5 cps there is no apparent benefit to be obtained by burying the instrument at 200

85

ANGELA		HYSHAM	
Channel	Frequency (cps)	Channel	Frequency (cps)
B1	1.05	B1	1.05
C1	1.15	D1	1.05
E1	1.10	F1	1.10
G1	1.10	H1	1.15
B2	1.20	B2	1.05
D2	1.40	C2	1.00
F2	1.05	E2	1.15
H2	1.15	G2	1.15
B3	1.05	B3	1.10
C3	1.20	D3	1.10
E3	1.20	F3	1.10
G3	1.10	H3	1.05
B4	1.05	B4	1.20
D4	1.00	C4	1.15
F4	1.10	E4	1.05
H4	1.00	G4	1.20
B5	1.00	B5	1.00
C5	0.95	D5	1.10
E5	1.05	F5	1.05
G5	1.00	H5	1.30
B6	1.15	B6	1.00
D6	1.40	C6	1.15
F6	1.00	E6	1.00
H6	1.00	G6	1.15

FIGURE 76. SEISMOMETER DAMPED RESONANT FREQUENCY

rather than 50 feet. However, above this approximate frequency range, 3 to 9 db improvement with deeper burial was observed depending upon frequency. Figure 80 presents the results of measuring the noise at the surface and at 200-foot depth. In this example some gain is made as low as 1 cycle per second with significant gain above 1 cycle per second.

Figure 81 presents power density spectra for different stations, CPO, TFO, UBO and Angela with all spectra corrected for instrument response at 1 cycle per second. The solid curve is a plot of the 0 db line and is essentially the Johnson-Matheson response curve. The

86
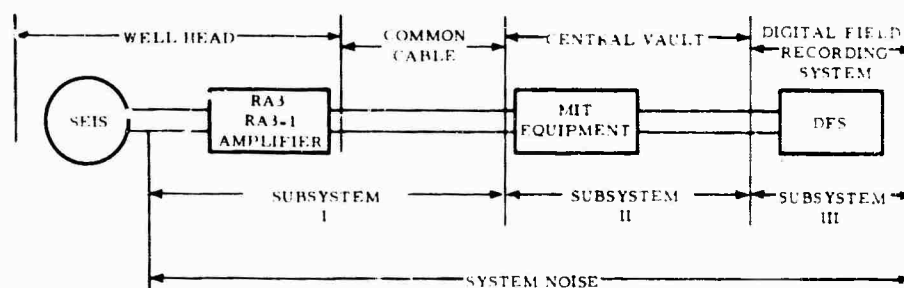
FIGURE 77. ARRAY TRANSMISSION AND RECORDING SYSTEM

spectral data in this figure were corrected to a Johnson-Matheson response. As can be seen, CPO is the highest with UBO and Angela approximately equal up to 1 to 1.25 cycles per second. Above this frequency the Angela noise spectrum is higher out to approximately 4 cycles per second. The lowest spectrum in the figure is from TFO where it has been shown that the majority of the noise is high velocity noise. Included in this set of curves is the mantle P-wave noise spectrum obtained at UBO.* It is pointed out, that in the .5 to 1.5 cps range where TFO is thought to be mantle P-wave noise limited, the ambient measured noise spectrum compares quite closely with the UBO mantle P-wave noise spectrum. The point of interest here is that the hypothetical lower noise level that can be reached with a small subarray is the high velocity mantle P-wave noise. If a universal curve of this type were available, it would give an indication of the improvement that could be obtained with a small array. That is all stations could be corrected to, or have noise levels as low as P-wave noise by subarray processing. As can be seen, the indication is that the mantle P-wave noise spectrum at UBO is on the order of absolute noise level at TFO. On the other hand the noise at Angela, UBO and CPO can be reduced from 8 to 15 db if mantle P-wave noise is universal.

An attempt was made to characterize the seismic noise in terms of frequency wave number power density spectra. This work was hampered by the observed phase differences between instruments. Due to these phase differences it was necessary to discard those instruments which indicated extreme phase variations. Using this approach of discarding instruments, 11 to 13 instruments were left to use in computing frequency wave noise for Angela and Hysham. Two different sets of simultaneous noise were used in computing frequency wave number spectra.

Figure 82 presents two of the array configurations used in computing the wave number spectra.

Figure 83 presents the resultant spectral window for the Hysham array shown in Figure 82 and it can be seen that side lobes occur which are within 6 db of the main lobe so that

_____
*Roden, R. B., "1965 Vertical Array Experiments at Uinta Basin Seismological Observatory," 35 Annual SEG Convention, 1955.
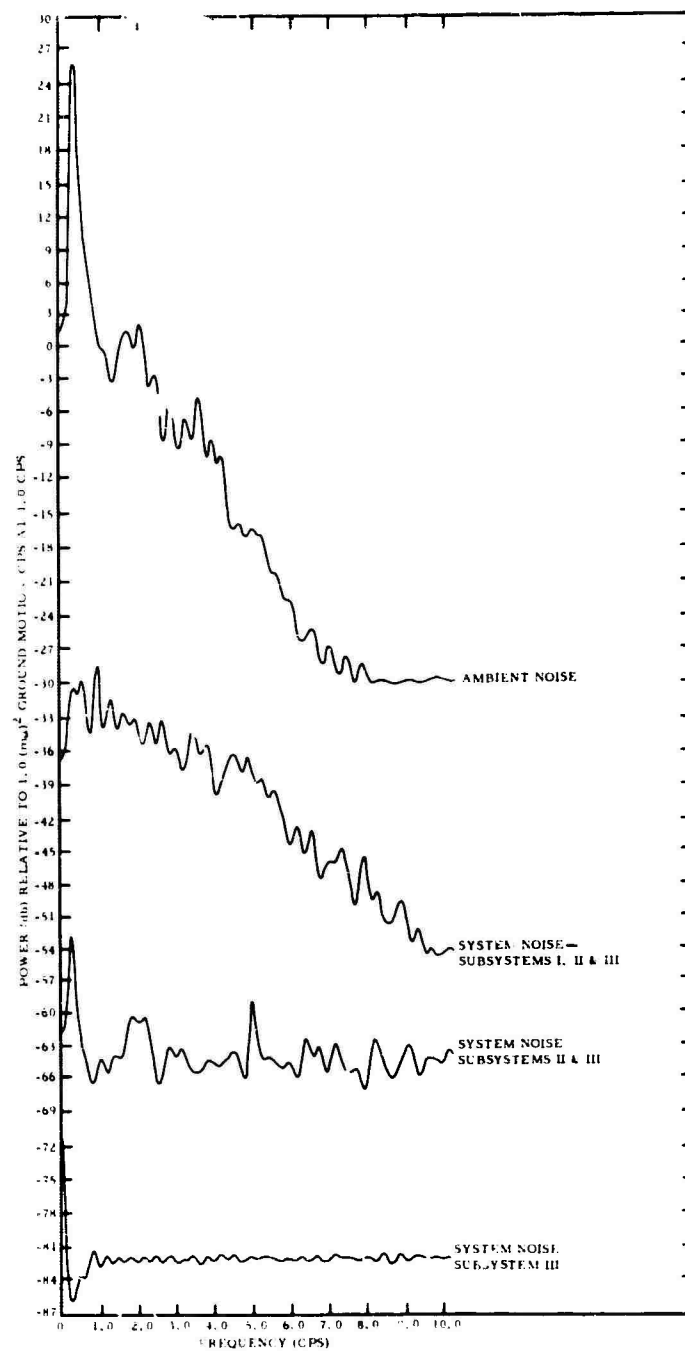
FIGURE 78. POWER DENSITY SPECTRA OF SYSTEM NOISE TESTS
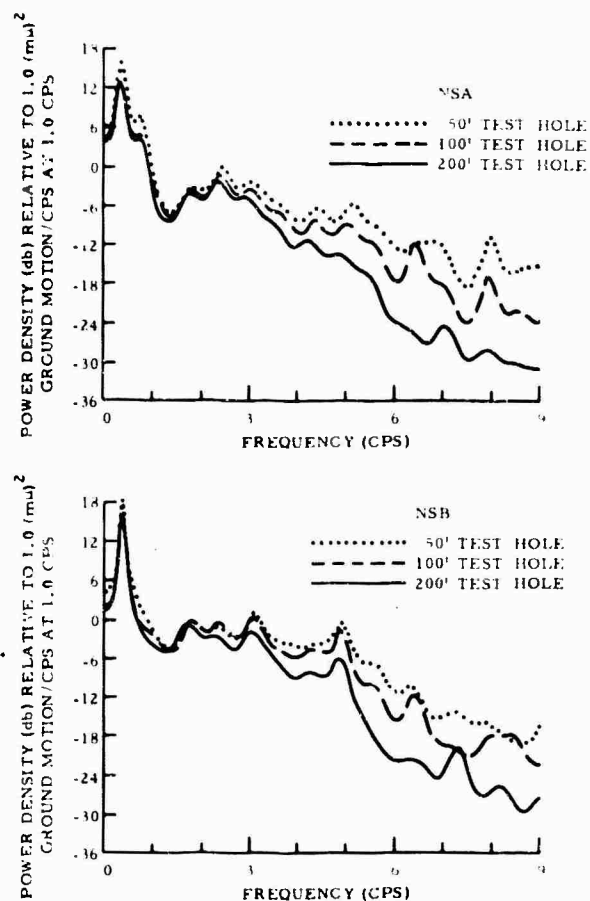
FIGURE 79. POWER DENSITY SPECTRA FOR 50 FT, 100 FT, AND 200 FT SIMULTANEOUSLY RECORDED AMBIENT NOISE
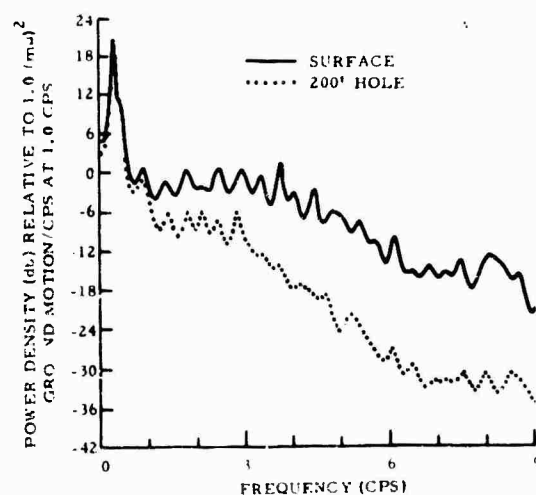
FIGURE 80. POWER DENSITY SPECTRA FOR SURFACE AND 200 FT SIMULTANEOUSLY RECORDED AMBIENT NOISE
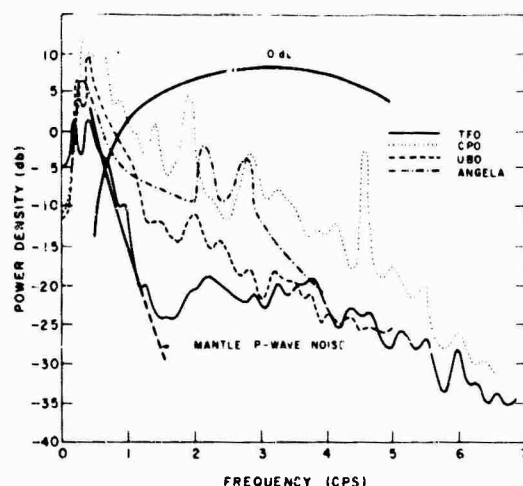
FIGURE 81. COMPARISON OF AMBIENT NOISE SPECTRA AT TONTO FOREST OBSERVATORY (TFO), CUMBERLAND PLATEAU OBSERVATORY (CPO), UINTA BASIN OBSERVATORY (UBO), AND ANGELA

the true spectra that we are trying to measure will be convolved with this rather undesirable spectral window.

An attempt was made to minimize the observable effect of the spectral window by not shading those portions of the f-k spectrum which could be interpreted as side lobes of a predominate peak in the spectrum.

Figures 84 and 85 present typical f-k spectra that were observed. A complete set of these spectra are presented in the previously mentioned report. As can be seen the predominate energy in both spectra is around zero wave number indicating high velocity energy. In both examples the main lobe is much larger than the spectral window indicating that in addition to the high velocity energy, a contribution is being made to the f-k spectra from energy of around 4 to 8 km/sec. A check of the surface wave velocity from a quarry blast indicated a surface wave velocity of approximately 3.5 km/sec which is close enough to be estimated as 4 to 8 km/sec energy in the rough f-k spectra obtained.

During the study carried out it was attempted to evaluate the signal-to-noise improvement that could be obtained with optimum multichannel filtering and straight summation. Multichannel filters were developed for the limited arrays (again limited by the phase variation problem). Figure 82 presents typical array configurations used in these studies. Arrays used varied from 10 to 13 elements.

Figure 86 presents a noise power density spectrum for the four samples used. The solid curve is a single instrument power density spectrum of the noise. The other two curves presented in each of the figures are the power density spectrum after straight summation and the

90
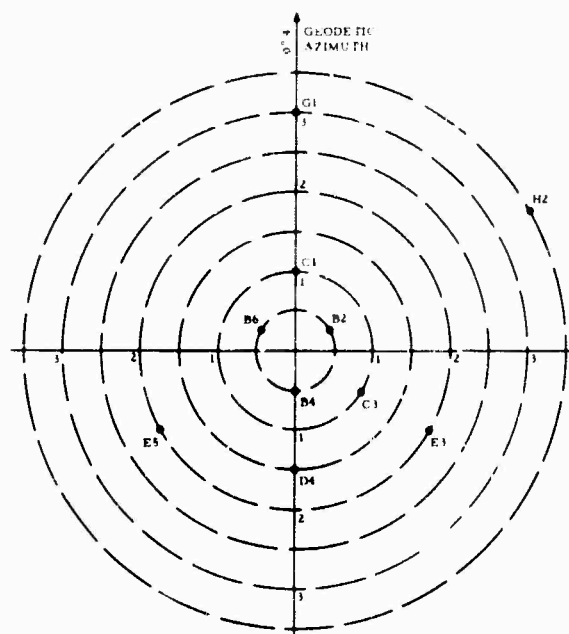
10 ELEMENT ARRAY USED FOR
ANGELA NOISE SAMPLE A
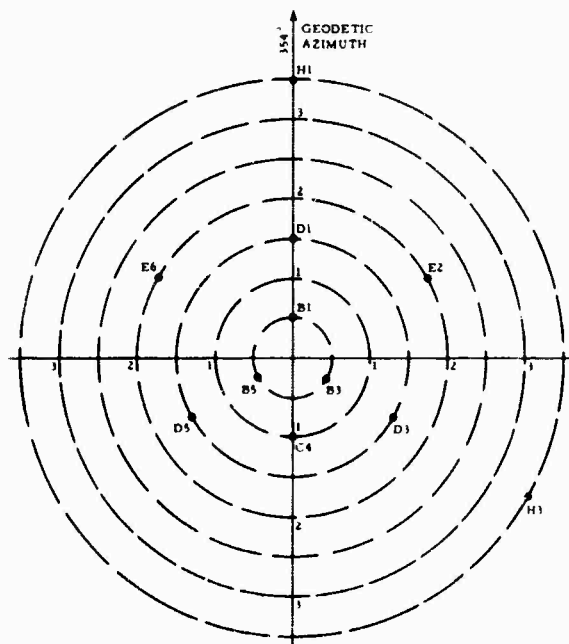
11 ELEMENT ARRAY USED FOR
HYSHAM NOISE SAMPLE A

FIGURE 82. ARRAY ELEMENTS USED IN NOISE STUDIES

91
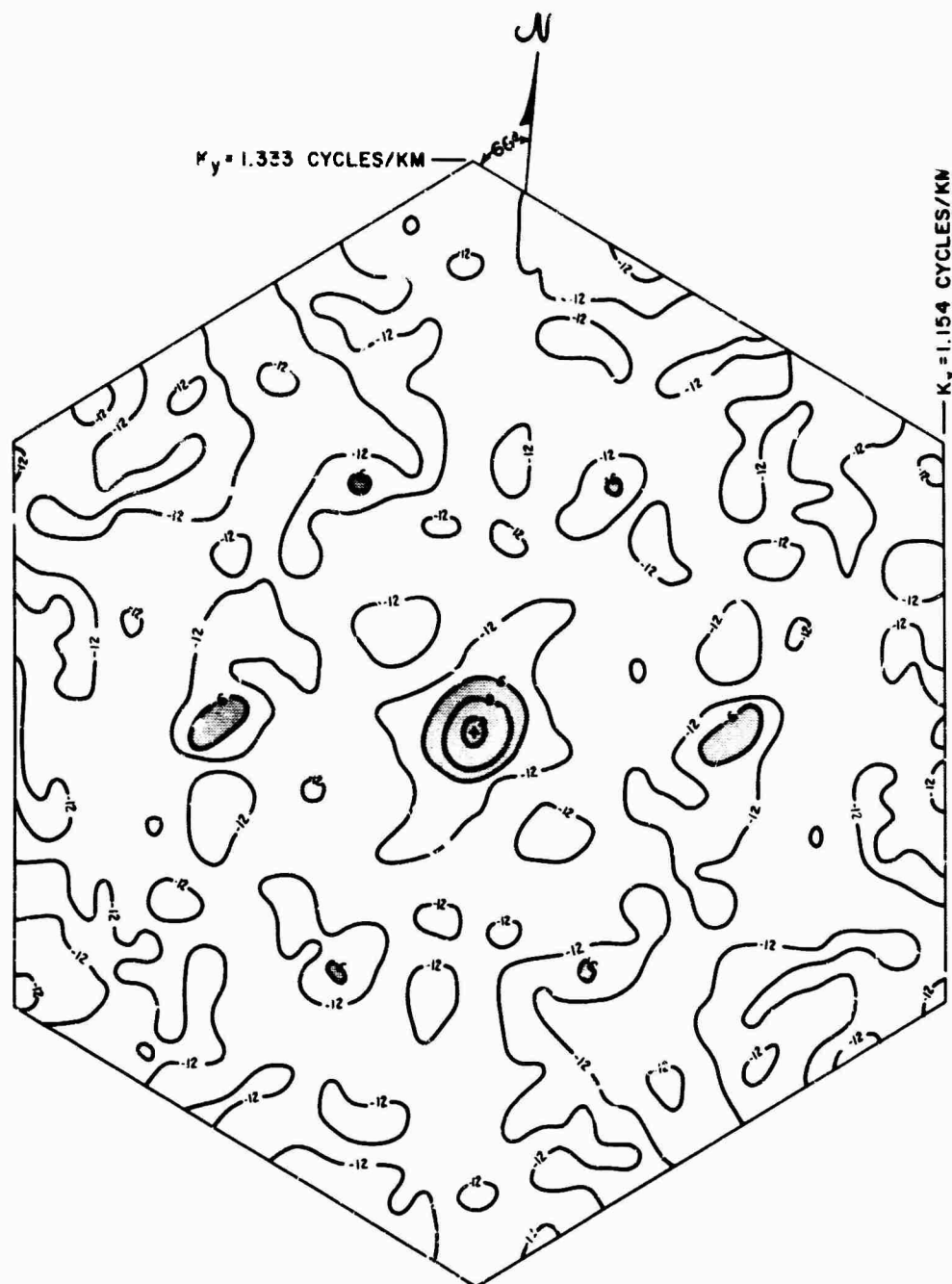
FIGURE 83.   FREQUENCY WAVE NUMBER SPECTRAL WINDOW FOR HYSHAM NOISE SAMPLE A
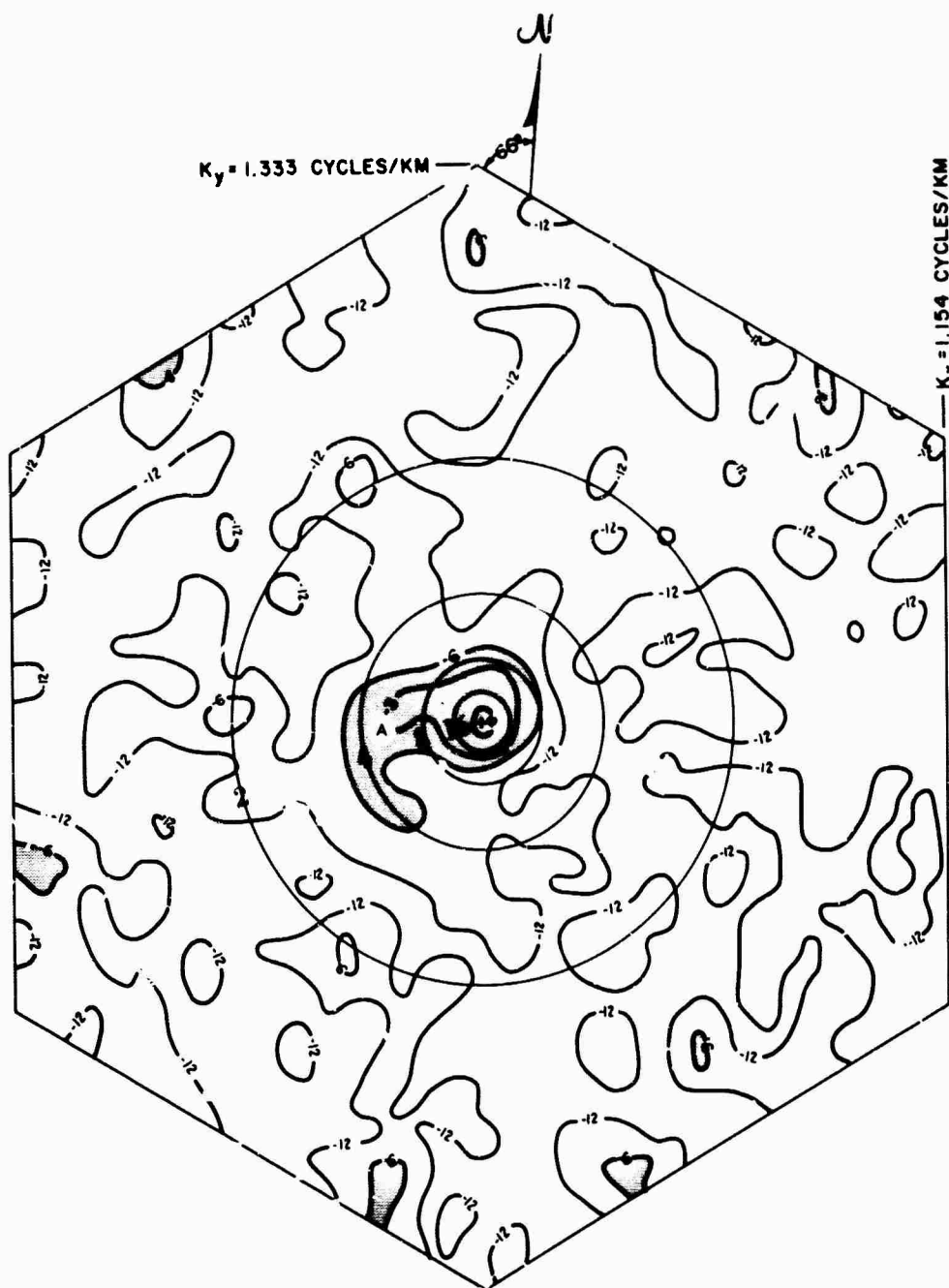
FIGURE 84. HYSHAM NOISE SAMPLE A: WAVE NUMBER SPECTRAL ESTIMATE AT f = 1.25 cps
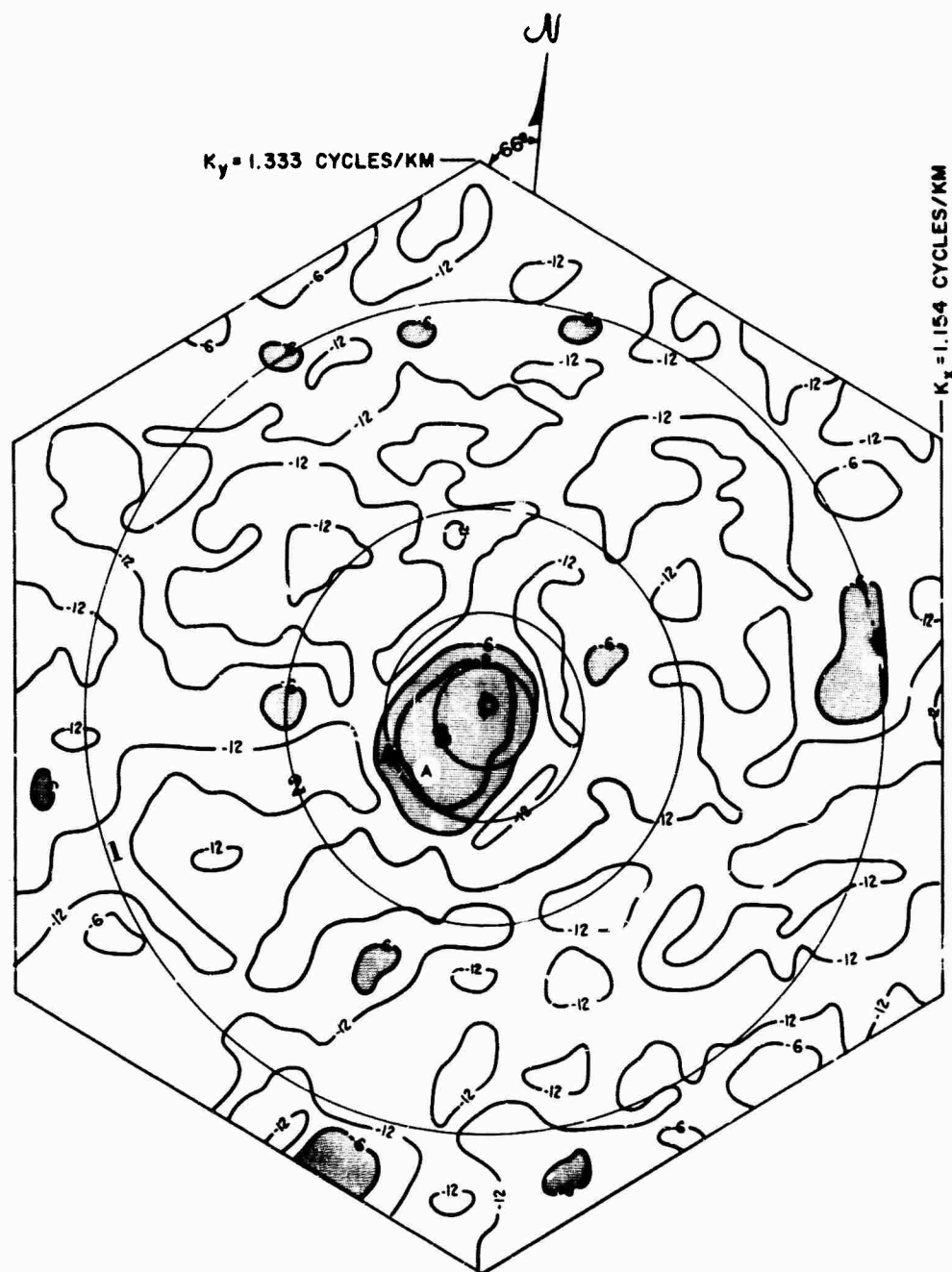
FIGURE 85. HYSHAM NOISE SAMPLE B: WAVE NUMBER SPECTRAL ESTIMATE AT f = 1.0 cps

94
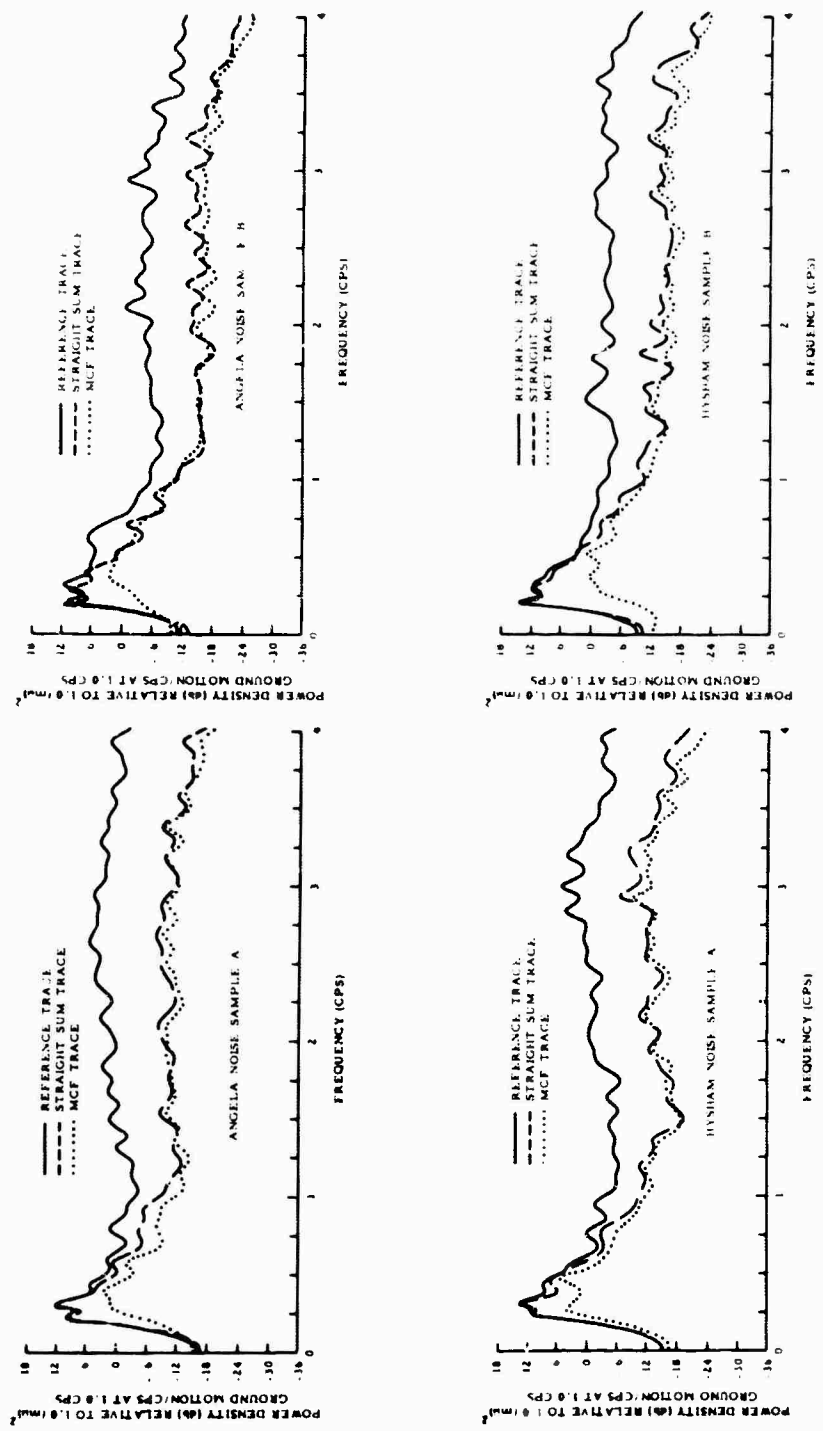
FIGURE 86. POWER DENSITY SPECTRA FOR ANGELA AND HYSHAM NOISE SAMPLES A AND B

95

noise power density spectrum after multichannel filtering. As can be seen in all four curves most of the improvement of multichannel filtering over straight summation is in the region of .25 to .5 cycle per second. Above .5 cycle per second to 1 cycle per second the gain observed is on the order of 3 to 4 db in some of the spectra. Figure 87 presents the noise spectra from sample A at Hysham and Angela with more information as to predictability and with respect to the mantle P-wave spectrum that was shown for UBO earlier. If the mantle P-wave spectrum is taken as the limiting value it is indicated that the multichannel filter is removing most of the ambient noise down to mantle P-wave noise up to a frequency of approximately .6 to .7 cps. Above .7 cps it is indicated that there is 2 to 6 db of improvement still possible with
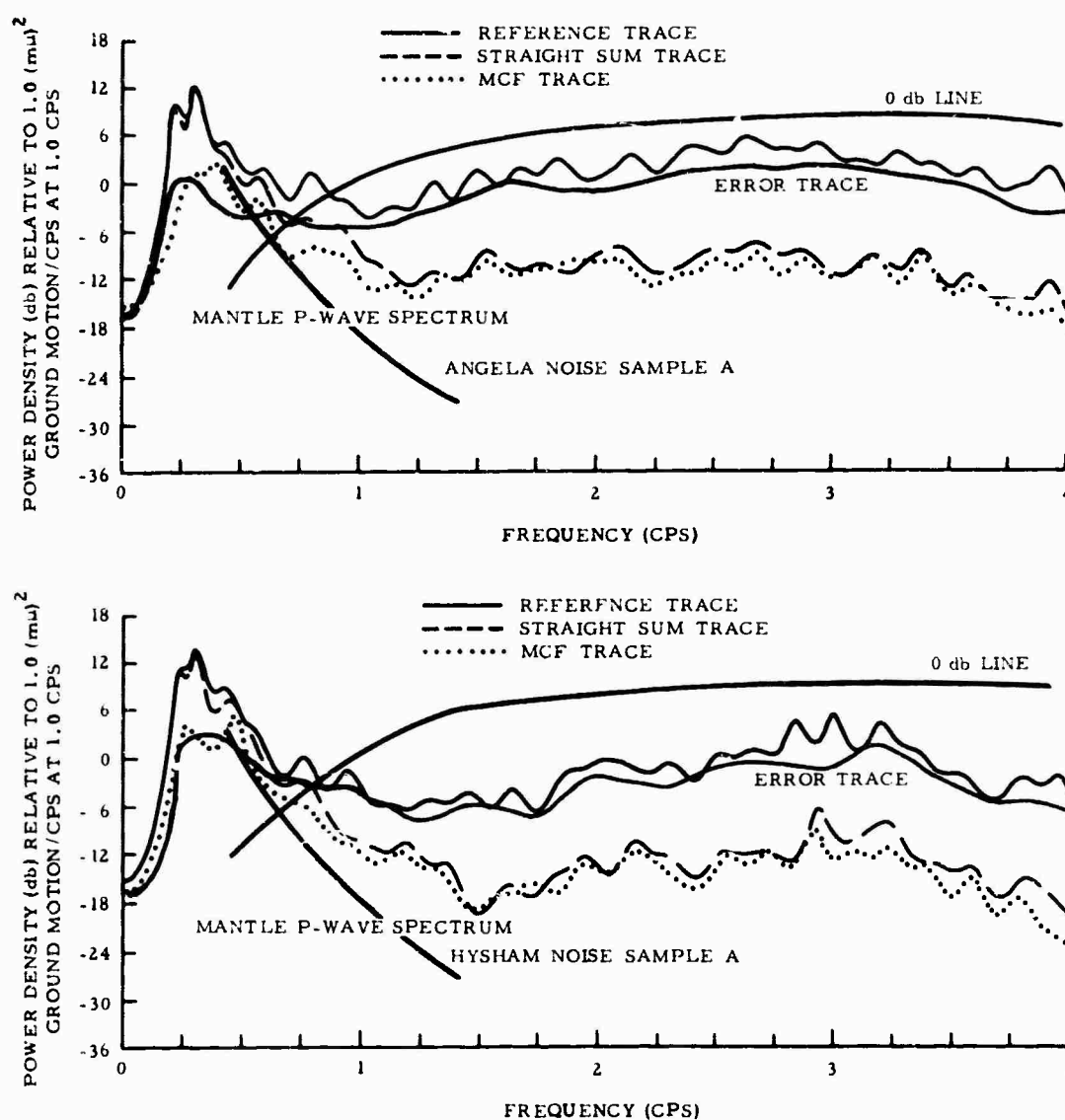
FIGURE 87. POWER DENSITY SPECTRA FOR ANGELA AND HYSHAM NOISE SAMPLE A

96

the subarray to 1.0 cps. Above 1.0 cps the possible improvement is larger. With the high velocity noise that was observed (3.5 to 4.0 km/sec) at these two stations, it was not possible for the multichannel filter to pass the desired signal model (an infinite velocity signal model) and reject the high velocity noise using only 11 to 13 element arrays. However with the use of all instruments, it should be possible to make improvements on the order of 6 to 8 db above 1 cycle per second up to as high as 1.25 cycles per second. Included in these curves is an error spectrum. This curve was obtained by developing a set of multichannel filters to predict a single element of the array. The error curve is the spectrum of the trace obtained by subtracting the predicted trace from the reference trace. Predictability here gives a measure of the spatial organization. As can be seen the energy was primarily predictable in the range .25 to 1.0 cps with very little predictability above 1.0 cps. Again the response curve is plotted as a 0 db line in this figure.

Figure 88 presents the improvement of multichannel filtering over straight summation in another form for all four arrays and four noise samples. As was indicated in figure 86 and 87, the multichannel filter is making significant improvement over the straight summation in the frequency range of .25 to .5 cps with less improvement in the .5 and 1.0 cps range and very little improvement above 1 cps. Again it should be emphasized that this data was using 10 to 13 elements and a significantly greater improvement of multichannel filtering over straight summations should be observed when the full diameter of the array is used.

Comparison tests were carried out to determine signal similarity between earthquake signals received at the Angela subarray and the Hysham subarray. Sixteen and seventeen element arrays were selected on the basis of minimum static phase variation between instruments. These arrays were then beam steered for the earthquake of interest. Figures 89 through 96 present the processed signals. The resulting signals were aligned and selected intervals of both signals were crosscorrelated. The purpose of crosscorrelation was to attempt to determine signal similarity. If the signals were similar, crosscorrelation functions should be symmetric and appear as an autocorrelation function. Non-similarity of the signals would show up as a non-symmetric correlation function. The selected intervals are shown by the scale beneath the signals. The crosscorrelation labeled A, corresponds to crosscorrelating the two signals using only the interval A from the signal, likewise crosscorrelation B corresponds to crosscorrelating only the interval B from the two signals. As can be seen in nearly all cases where only the first cycle was used in crosscorrelating, the correlation functions appear to be symmetric. In most signals where only the first two cycles were used the correlation functions appear to be symmetric, however, beyond two cycles the majority of the signals do not show significant similarity. It should be pointed out that this lack of similarity defeats detection in

97

two ways. Although the signals may be similar over the first half cycle so that coherence may be obtained across the large array upon summation, the first cycle is often not the largest in an earthquake. The fourth or fifth cycle may be as large as five times the first half cycle. Thus by not maintaining similarity over a number of cycles one destroys possibly 10 db of detectability. Additionally, one loses the ability to integrate over several cycles thus possibly destroying another 4 or 5 db detectability so that it is conceivable that if the signals are not similar over the first five to ten cycles one could be losing up to 15 db of detection capability. Thus, it appears that some sort of cross-equalization filter between subarray cutputs will be necessary to obtain the maximum performance of a large array.

98
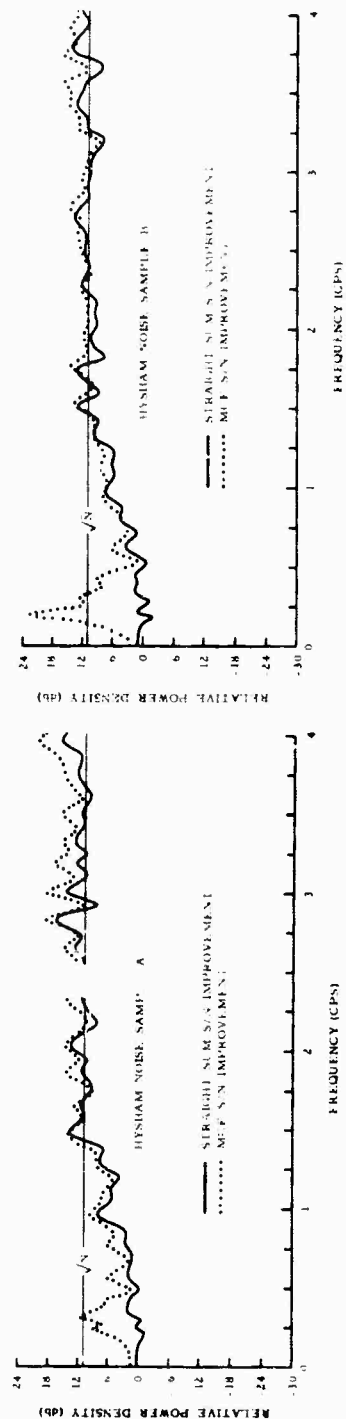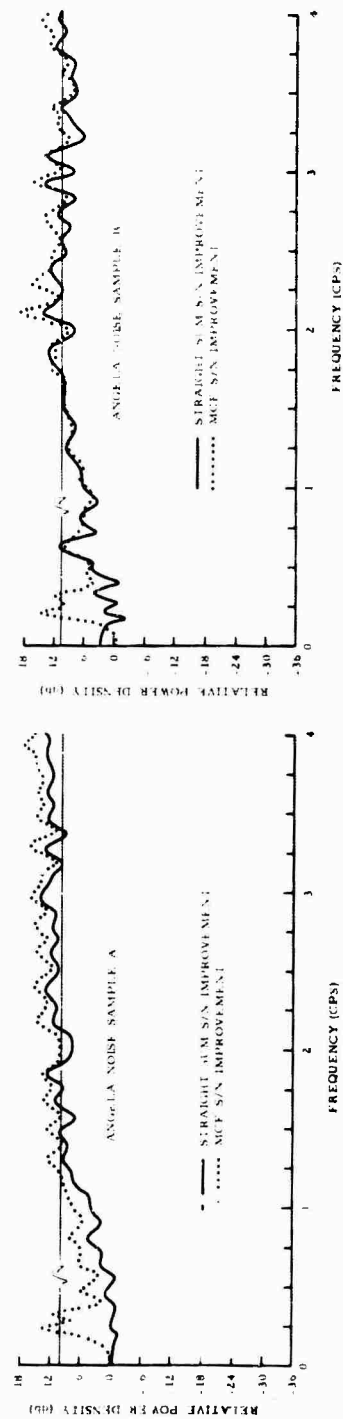
FIGURE 88. SIGNAL-TO-NOISE IMPROVEMENT FOR ANGELA AND HYSHAM NOISE SAMPLES A AND B OBTAINED FROM STRAIGHT SUM AND INFINITE VELOCITY MULTICHANNEL PROCESSING

99
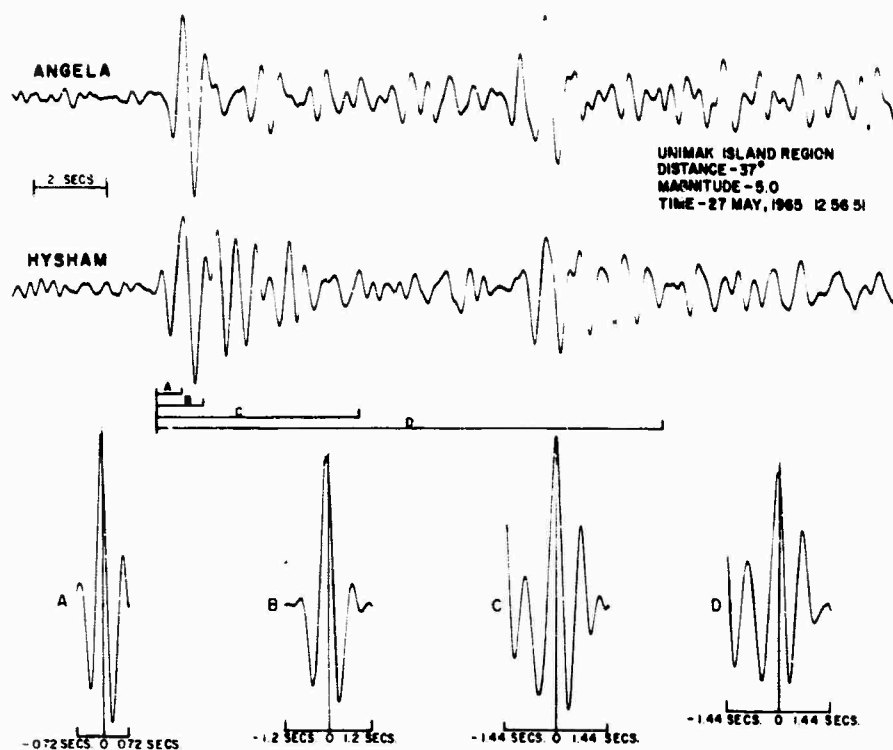
FIGURE 89. CROSSCORRELATION OF UNIMAK ISLAND EVENT RECORDED SIMULTANEOUSLY AT ANGELA
AND HYSHAM
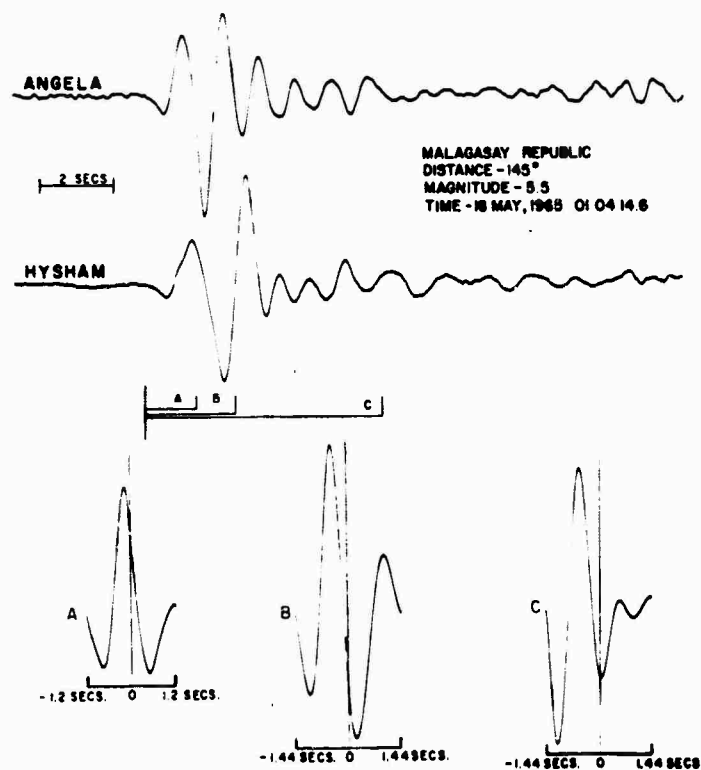
FIGURE 90. CROSSCORRELATION OF MALAGASAY REPUBLIC EVENT RECORDED SIMULTANEOUSLY
AT ANGELA AND HYSHAM
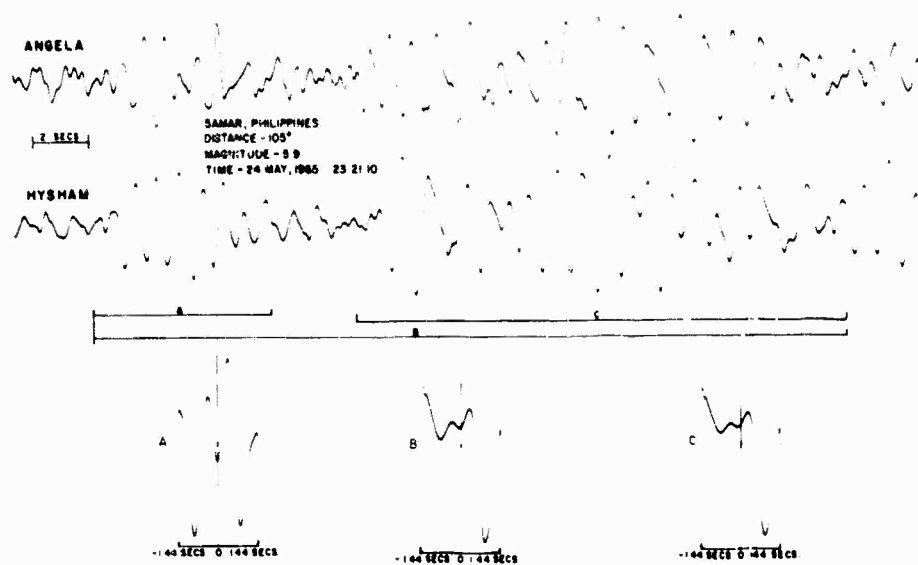
FIGURE 91. CROSSCORRELATION OF SAMAR, PHILIPPINES, EVENT RECORDED SIMULTANEOUSLY
AT ANGELA AND HYSHAM
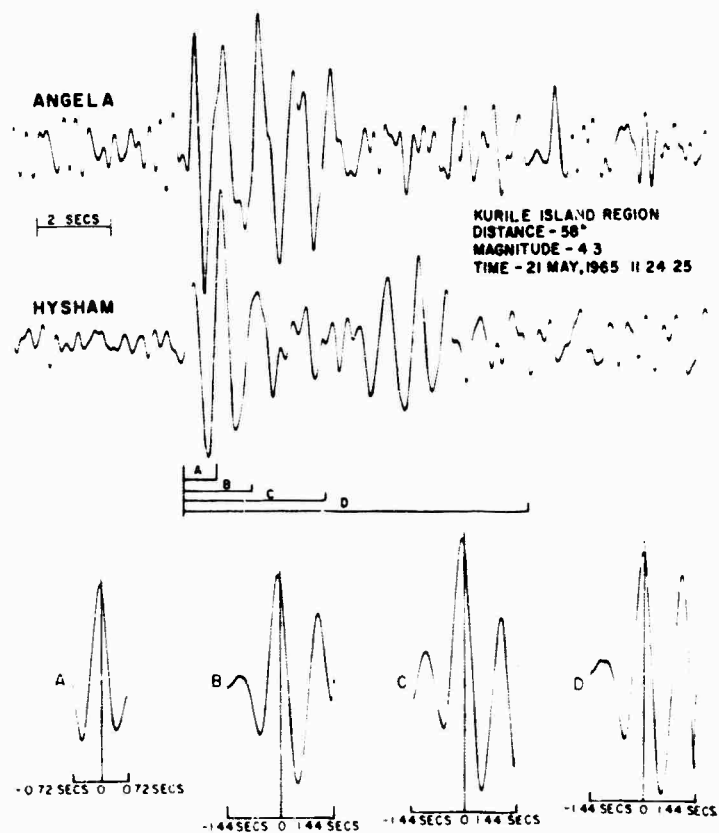
FIGURE 92. CROSSCORRELATION OF KURILE ISLAND REGION EVENT RECORDED SIMULTANEOUSLY
AT ANGELA AND HYSHAM

101
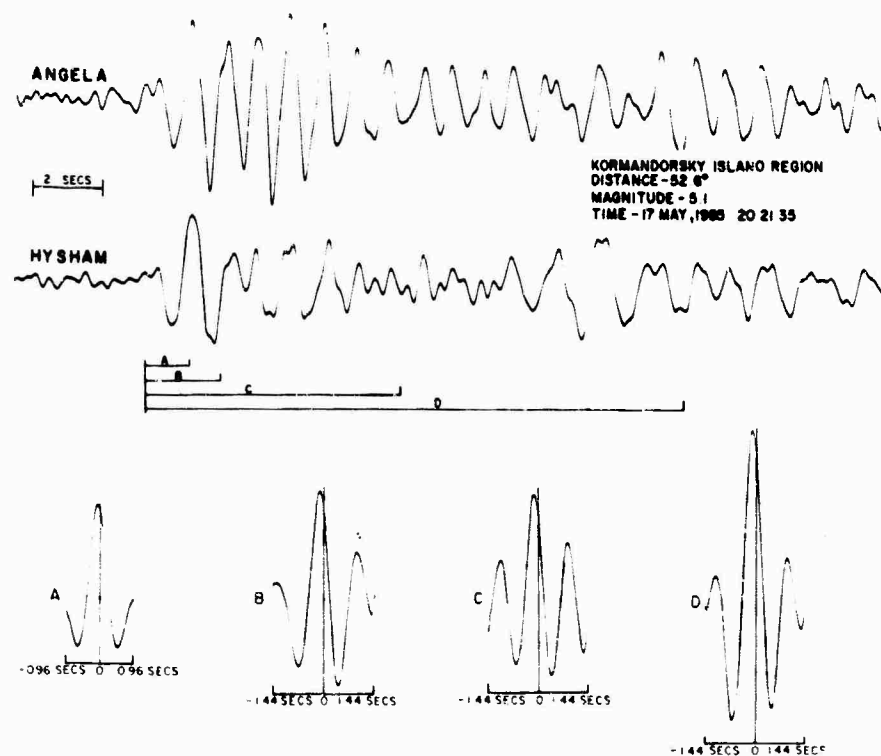
FIGURE 93. CROSSCORRELATION OF KORMANDORSKY ISLAND REGION EVENT RECORDED SIMULTA-
NEOUSLY AT ANGELA AND HYSHAM
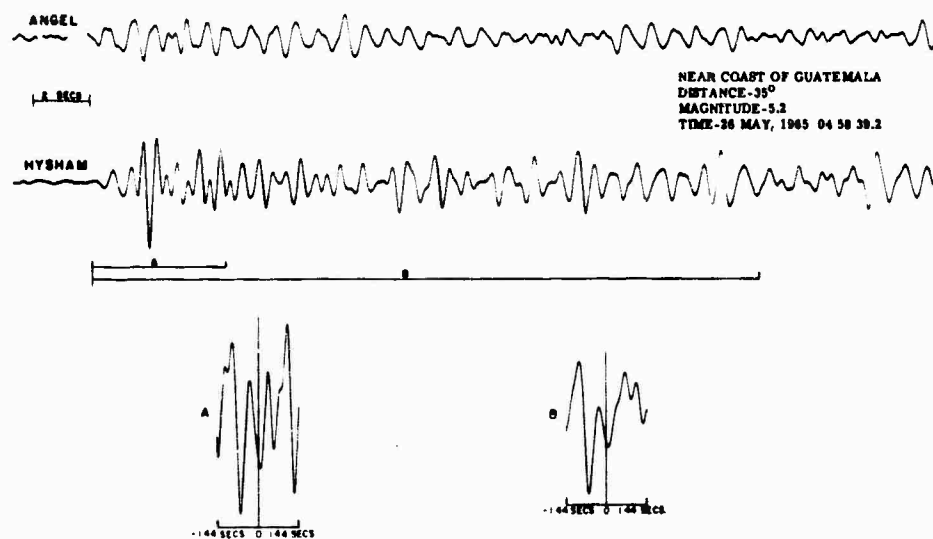
FIGURE 94. CROSSCORRELATION OF EVENT NEAR COAST OF GUATEMALA RECORDED SIMULTA-
NEOUSLY AT ANGELA AND HYSHAM

102
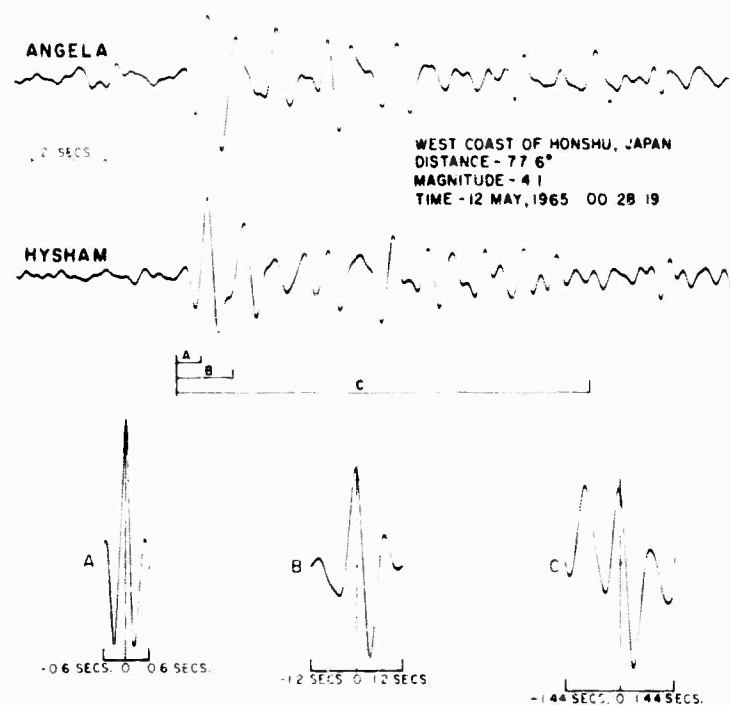
FIGURE 95. CROSSCORRELATION OF EVENT ON WEST COAST OF HONSHU, JAPAN, RECORDED SIMULT.NEOUSLY AT ANGELA AND HYSHAM
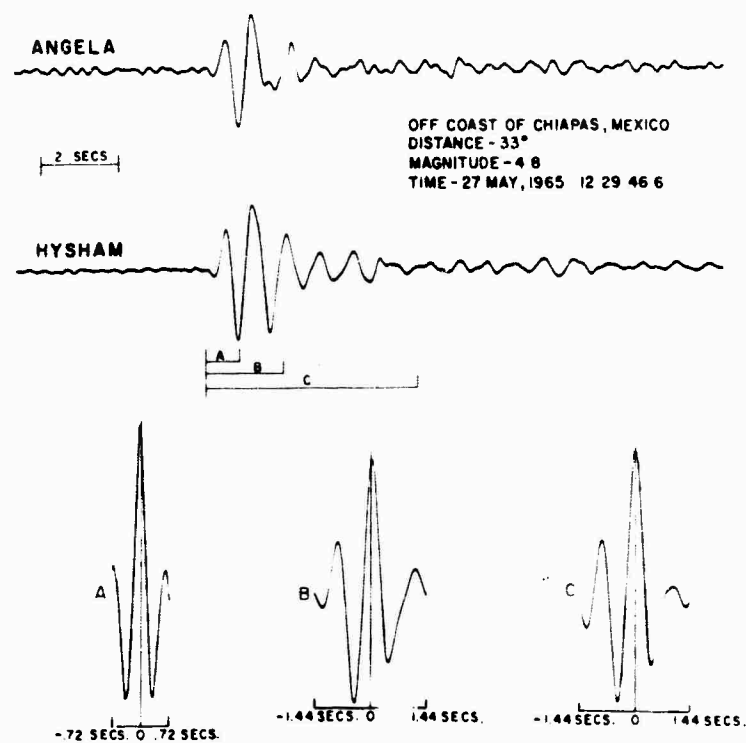
FIGURE 96. CROSSCORRELATION OF EVENT OFF COAST OF CHIAPAS, MEXICO, RECORDED SIMULTA-NEOUSLY AT ANGELA AND HYSHAM

103

10. RESULTS OF PRELIMINARY SEISMIC STUDIES
by
E. J. Kelly
Lincoln Laboratory, MIT

I. INTRODUCTION

Preliminary studies on the characteristics of the LASA site have so far been made in
comparison with our experience with Tonto Forest Seismological Observatory (TFSO) data.
We have investigated the detectability of small events by manual and automatic means, the
coherence of signals across the array, and the relative station corrections to arrival times
between subarrays. Analytical work is in progress in preparation for studying the frequency-
wave number properties of the noise. Each of these is briefly discussed below.

II. DETECTION

Results to date, based on about two hundred events, indicate that LASA has the same single-
trace detection threshold as TFSO. To make this statement meaningful, we must describe the
detection procedures used in some detail. TFSO data was recorded in two forms: a) three
short-period instruments (the three components of motion) were recorded on a Helicorder at
0 5 mm per second, while b) these and LRSM van instruments were recorded on Develocorder,
with viewing at 1 cm per second. Helicorder traces were scanned visually to pick rough times,
at a high false-alarm rate, and these times examined on the film record. All events reported
by U.S.C. and G.S. were sought on the records at first, until rough thresholds were established,
and then only misses which were marginal, or should have been seen, were looked up. It soon
became possible to do very nearly as well without prompting by U.S.C. and G.S. data as with-
out. Results are shown in Figure 97 as a scatter diagram of several hundred events, giving
the reported (U.S.C. and G.S.) magnitude vs epicenter distance. Hits, marginals, and misses
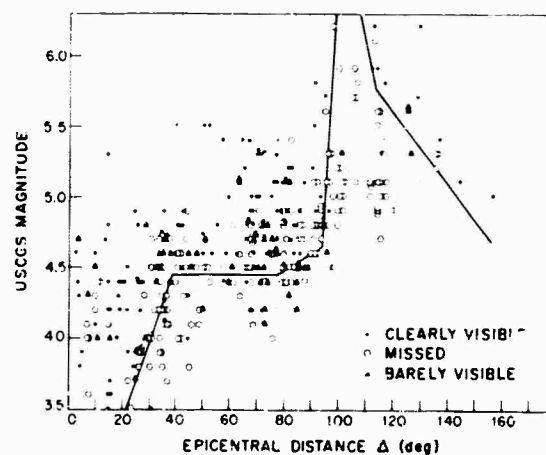
FIGURE 97. TFSO SINGLE SENSOR DETECTABILITY STUDY (375 EVENTS)

104

are indicated, and a simple empirical curve evolved representing a detection threshold. This threshold is constant at about m = 4 5 for distances of 40° to 80°.

A similar diagram has been prepared from the LASA data reaching Lincoln Laboratory by telephone line for a two-month period beginning in late April. This data consisted of one trace from Site B1 and one trace from Site F3, usually the deep central seismometer A0, recorded only on film. All events reported by U.S.C. and G.S. for this time period were sought on the film recordings and hits (either station showing the signal) and misses recorded. These results, all prompted by U.S.C. and G.S. reports are also shown as a scatter diagram of magnitude vs distance in Figure 98. Performance of the 500-foot sensors is shown separately from 200-foot sensors. The improvement due to deep burial is not striking in this small data sample. The empirical curves obtained from the two locations (TFSO and LASA), Figure 99, do not differ significantly from one another. The actual arrival times at LASA were usually within 1-2 seconds of that predicted from U.S.C. and G.S. epicenters, which is also in agreement with the behavior of TFSO. The performance of the automatic detector is not inferior to these curves, as shown for a small number of events in Figure 100.

FIGURE 98. LASA SINGLE SENSOR DETECTABILITY STUDY (224 EVENTS)

III. COHERENCE

The coherence of signals across the LASA area is being studied qualitatively by collecting prints of high signal-to-noise ratio events seen on single seismometers at each of several subarrays. The only meaningful quantitative measure of coherence is the performance of array processing itself, when that processing is designed on the assumption of perfect coherence. Such a measure will be illustrated in a later paper. However, even visual comparison should be useful in judging the improvement brought about by careful matching of seismometer response, site-to-site equalization, etc. The coherence for seven events seen at seven of the subarrays is fair; quite comparable to that to which we have become accustomed over similar

FIGURE 99. COMPARISON OF TFSO AND LASA SINGLE SENSOR DETECTABILITY

FIGURE 100. AUTOMATIC DETECTOR PERFORMANCE

distances at TFSO. The signal oscillations usually correspond closely at all sites for the first few peaks, while rapidly becoming quite different thereafter. Often, the actual shape of the first significant half-cycle is similar in the various traces. It should be kept in mind that good coherence of P and pP over their respective first half-cycles alone would bring the full array processing gain to bear on first motions, permitting full array accuracy in epicenter and depth determination. The possible utility of waveform discrimination criteria, such as complexity in time or frequency domain, depends critically, of course, on the attainment of high coherence (through accurate equalization and deconvolution) over a much longer portion of the P waveform.

106

are indicated, and a simple empirical curve evolved representing a detection threshold. This threshold is constant at about m = 4.5 for distances of 40° to 80°.

A similar diagram has been prepared from the LASA data reaching Lincoln Laboratory by telephone line for a two-month period beginning in late April. This data cons'sted of or ? trace from Site B1 and one trace from Site F3, usually the deep central seismometer A0, recorded only on film. All events rer rted by U.S.C. and G.S. for this time period were sought on the film recordings and hits (either station showing the signal) and misses recorded. These results, all prompted by U.S.C. and G.S. reports are also shown as a scatter diagram of magnitude vs distance in Figure 98. Performance of the 500-foot sensers is shown separately from 200-foot sensors. The improvement due to deep burial is not striking in this small data sample. The empirical cur es obtained from the two locations (TFSO and LASA), Figure 99, do not differ significantly from one another. The actual arrival times at LASA were usually within 1-2 seconds of that predicted from U.S.C. and G.S. epicenters, which is also in agreement with the behavior of TFSO. The performance of the automatic detector is not inferior to these curves, as shown for a small number of events in Figure 100.

FIGURE 98. LASA SINGLE SENSOR DETECTABILITY STUDY (224 EVENTS)

III. COHERENCE

The coherence of signals across the LASA area is being studied qualitatively by collecting prints of high signal-to-noise ratio events seen on single seismometers at each of several subarrays. The only meaningful quantitative measure of coherence is the performance of array processing itself, when that processing is designed on the assumption of perfect coherence. Such a measure will be illustrated in a lat paper. However, even visual comparison should be useful in judging the improvement brought about by careful matching of seismometer response, site-to-site equalization, etc. The coherence for seven events seen at seven of the subarrays is fair; quite comparable to that to which we have become accustomed over similar

FIGURE 99. COMPARISON OF TFSO AND LASA SINGLE SENSOR DETECTABILITY

FIGURE 100. AUTOMATIC DETECTOR PERFORMANCE

distances at TFSO. The signal oscillations usually correspond closely at all sites for the first few peaks, while rapidly becoming quite different thereafter. Often, the actual shape of the first significant half-cycle is similar in the various traces. It should be kept in mind that good coherence of P and pP over their respective first half-cycles alone would bring the full array processing gain to bear on first motions, permitting full array accuracy in epicenter and depth determination. The possible utility of waveform discrimination criteria, such as complexity in time or frequency domain, depends critically, of course, on the attainment of high coherence (through accurate equalization and deconvolution) over a much longer portion of the P waveform.

106

IV. STATION CORRECTIONS

Fundamentally, the accuracy of determination of epicenters for first-order event location by a network, such as that formed by the outer square and central element of LASA, is limited only by the size of the network and the accuracy of the picking of arrival times at sites being used for triangulation. However, this accuracy will not even be approached if the bias introduced by relative station anomalies is not first removed. The removal of this bias requires a knowledge of relative station corrections for all epicentral regions, and may require the statistical analysis of hundreds or thousands of events. The relative station corrections must also be accurately known in order to form precisely steered beams. The systematic study of a few hundred events recorded at TFSO and the outlying Long Range Seismic Measurement (LRSM) vans has shown the feasibility of this approach. Rough station corrections have been determined for stations there (LRSM vans relative to TFSO) as functions of bearing only for teleseismic P arrivals. These corrections are van-TFSO times measured minus van-TFSO times implied by U.S.C. and G.S. epicenter. Corrections up to 0.7 seconds were obtained. Using these corrections on a smaller set of events, we computed epicenters from TFSO data alone and compared them with the U.S.C. and G.S. data. We attained an r.m.s. error of 2.3^O. Expressed as a steering accuracy in wave-number space at a fixed frequency (≈ 1 cps), this corresponds to about four times the size of the resolution cell of an array the size of LASA.

Comparable data have been available from LASA only from two subarrays: B1 and F3. Relative station errors for this pair have been measured for some seventy P arrivals. The results, shown in Figure 101, indicate somewhat smaller effects than at TFSO. One group of 42 events in the bearing range 280° to 340° exhibits a mean relative error of $+0.22 \pm 0.03$ seconds (F3 late compared to B1). Very recent data on many more subarrays using advance tentative epicenters from U.S.C. and G.S. indicates the possibility of somewhat larger corrections at other sites.
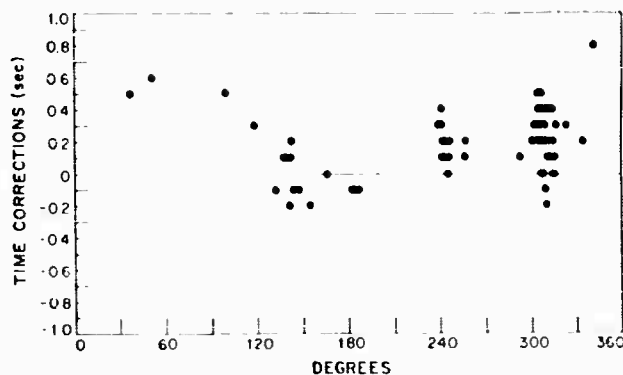
FIGURE 101. STATION CORRECTION OF LASA SITE B1 WITH RESPECT TO F3

107

Some attempt is being made to interpret the station effects observed at both LASA and TFSO in terms of crustal and upper mantle structure under the arrays. It seems to be difficult to explain the magnitude of the effects in terms of one or more dipping layers, and the results may prove to be more compatible with known lateral variations in upper mantle P velocity.

V. NOISE STUDIES

An integral part of the maximum-likelihood form of processing, applied to subarrays, is the measurement of the cross-correlation matrix for subarray elements on periods of noise preceding events. By Fourier transforming these correlation matrices using suitable space and time tapers, one can obtain the spectral density of the noise in frequency-wave number space. The analytical aspects of this problem have been studied, useful tapers evolved and a computer program written for this computation. Data from full subarrays has just become available and no results are available as yet. We also plan to combine outputs from some 25-30 elements chosen from the five central subarrays (A0 and the B-ring) to provide spectral density measurement with higher resolution in wave number (about 0.05 cpkm). This resolution would permit a clear definition of the low-order Rayleigh modes, if present, and a fair decomposition of the structure of the mantle P-wave noise. In addition to providing independent information about crustal structure at LASA, it is hoped that the noise may exhibit some stationary characteristics (e.g., dominant excitation of a particular trapped mode) which would permit the design of non-adaptive array filters which could provide a useful degree of processing gain.

It should also be mentioned that corollary outputs of the maximum-likelihood program provide simple measures of the long-term stationarity of the noise in space and time.

11. DEVELOPMENT OF WIDE BAND BEAM PATTERNS USING THE MONTANA LASA

by

Harry Lake

Texas Instruments, Inc.

For the developments made in this paper, a large aperture seismic array is assumed to consist of 21 outputs, each output representing the center of one of the 21 subarrays. The subject to be dealt with concerns the manner in which these outputs are combined to yield a desired beam response. The simplest approach that has been suggested is simple time shift and summation. Using this approach one is unable to exercise any control over placement of sidelobe structure. Additionally, it is impossible to construct a given beam to pass the contour shape of any specified area of the world using a single beam.

In a companion paper entitled "Noise and Signal Characteristics in the Vicinity of the Montana LASA" it was indicated that it may be necessary to apply cross-equalization filters to the outputs of each of the 21 subarrays. If it is necessary to apply cross-equalization filters, hardware for applying convolution operators will be necessary. It is therefore conceivable that this same hardware could be used in applying filters which would be useful for wide band shaping of the main beam from the LASA output. Such beam shaping could include specifying regions where sidelobes are to be held to a minimum, and specifications for regions which should be passed, such as a specific beam to pass all of the seismic energy coming from Russia.

In this paper response curves are presented which result from optimum beam shaping. These beams are developed by Wiener optimum criteria, in that desired regions of k space were passed, and selected regions in k space were specified for rejection. The technique allows a set of frequency dependent weightings to be developed for each seismometer output (or for each subarray output in this consideration). The process is wideband, in that a specified velocity band is selected for rejection over the frequency range of interest, and another velocity band is specified to be passed over the selected frequency range.

Figure 102 presents a map of the world in wave-number space centered on the Montana LASA. As can be seen much of the circum-Pacific Belt lies on the edge of the core shadow. Figure 103 presents the noise model that was used in developing optimum beam patterns. It should be pointed out that the noise model simply specifies that area in wave-number space in which the sidelobe pattern is to be held to a minimum.

In actual practice the energy to be rejected in this region is from earthquakes. However, for the purpose of developing filters the regions to be passed are specified as signal regions or signal models and the regions to be rejected are specified as noise models or noise regions. Selection of these types of noise models allow several sets of first order Bessel functions to

109
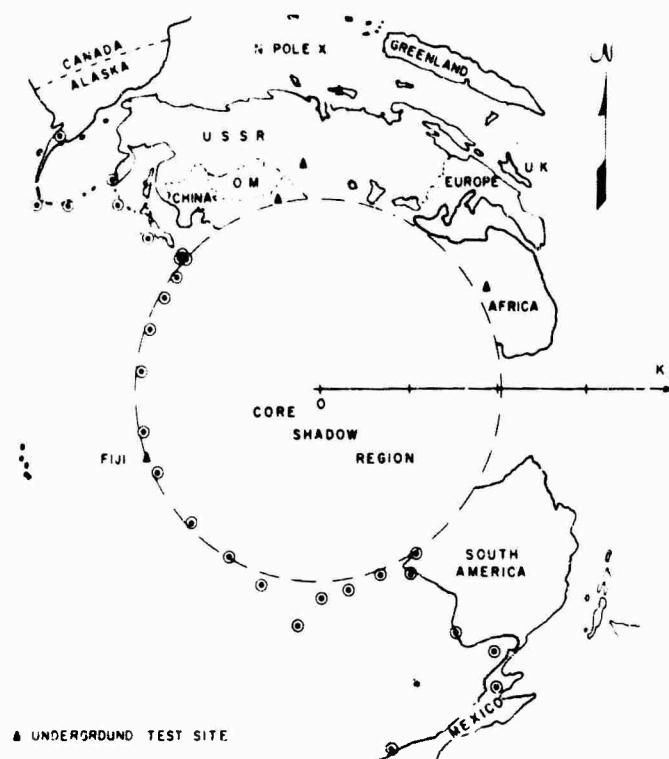
FIGURE 102. WAVE NUMBER MAP OF THE WORLD AS SEEN FROM MONTANA LASA
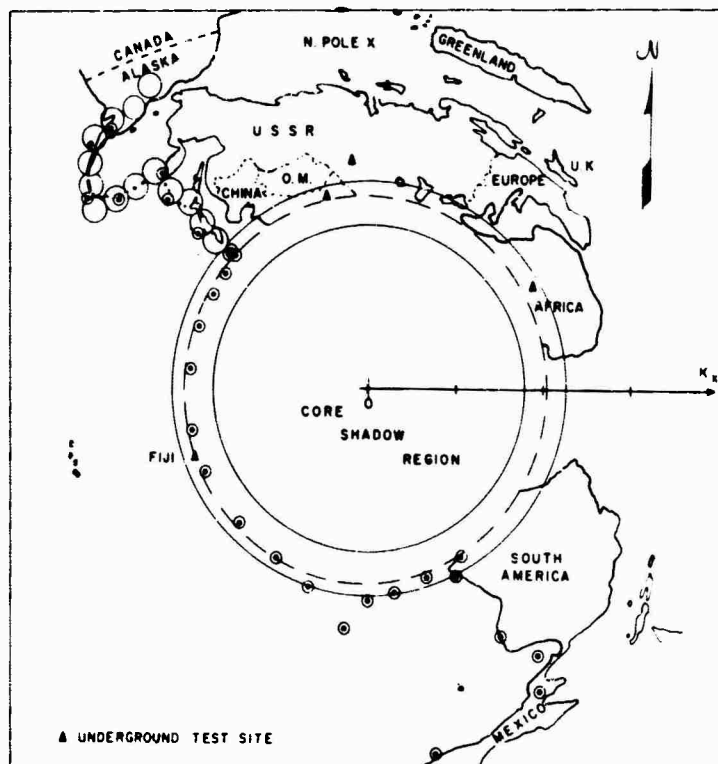
FIGURE 103. WAVE NUMBER MAP FROM MONTANA LASA FOR NOISE MODEL B

110

be combined to formulate the interchannel correlation functions between subarray outputs which corresponded to signal energy in k space occupying the region shown. Each of the small circles in the Aleutian Island chain represented a set of interchannel correlation functions (first order Bessel functions) and the large disc with center at the Montana LASA was another set of interchannel correlation functions developed by combining first order Bessel functions.

Figure 104 presents the first signal model to be considered. This model was simply a shifted cone in three-dimensional f-k space with the cone shifted to center over Novaya Zemlya. Figure 105 presents the response in k space at a frequency of .5 cycle per second of the filters which were designed to reject this specified noise model and to pass the Novaya Zemlya signal model. As can be seen the signal region appearing in the plane as a circle is passed with 0 db response. The noise region is 18 db down at a few points on the large disc and between -18 and -24 db down on the rest of the disk and all the Aleutian Island chain. Figure 106 presents the response of the same set of filters at 1.0 cps. The signal model is still passed with 0 db and the Aleutian Islands chain has one point at which the response gets up to 12 db. However, the majority is -18 to -24 db down. The large disc indicates a point of -6 db due south from Montana. However, the majority of the response is -12 to -18 is down throughout the large diameter disc. The response of the filters are shown only in the specified
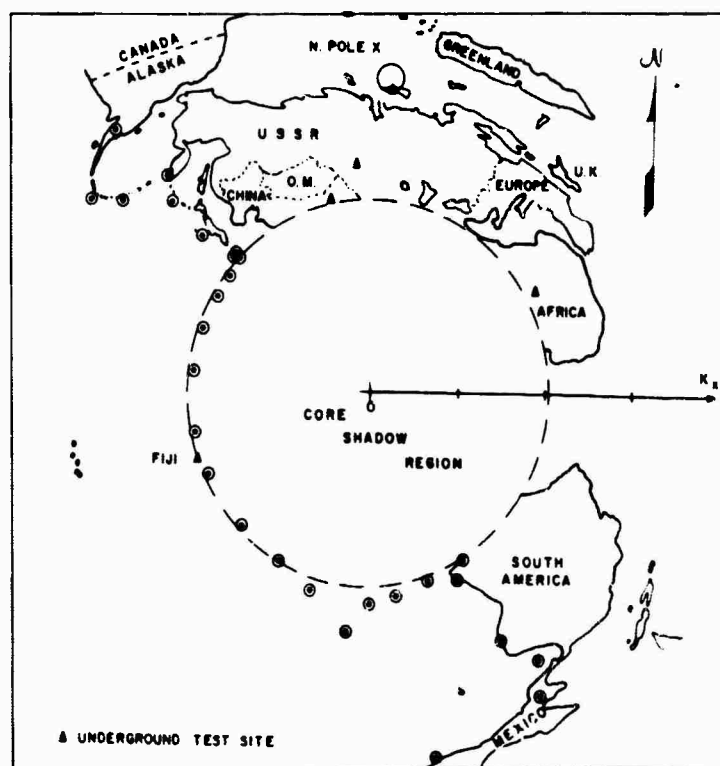
FIGURE 104. WAVE NUMBER MAP FROM MONTANA LASA FOR NOVAYA ZEMLYA SIGNAL MODEL

111
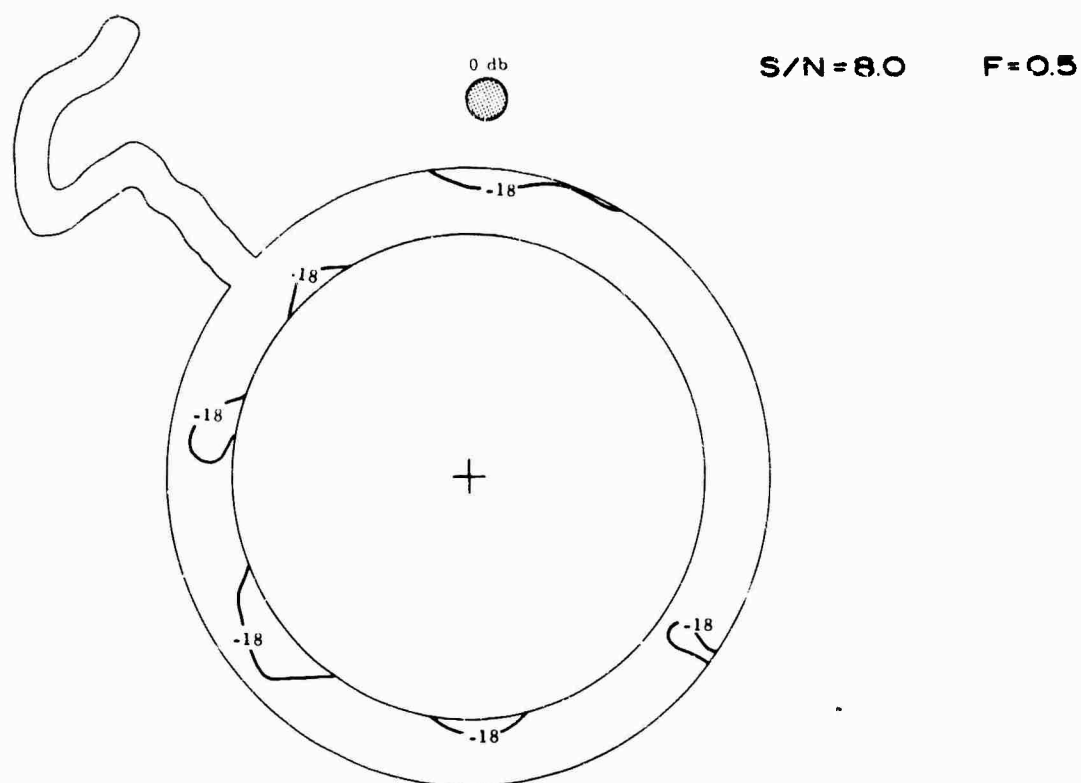
FIGURE 105. k-SPACE RESPONSE AT 0.5 cps FOR FILTER REJECTING NOISE MODEL B AND ACCEPTING NOVAYA ZEMLYA SIGNAL MODEL
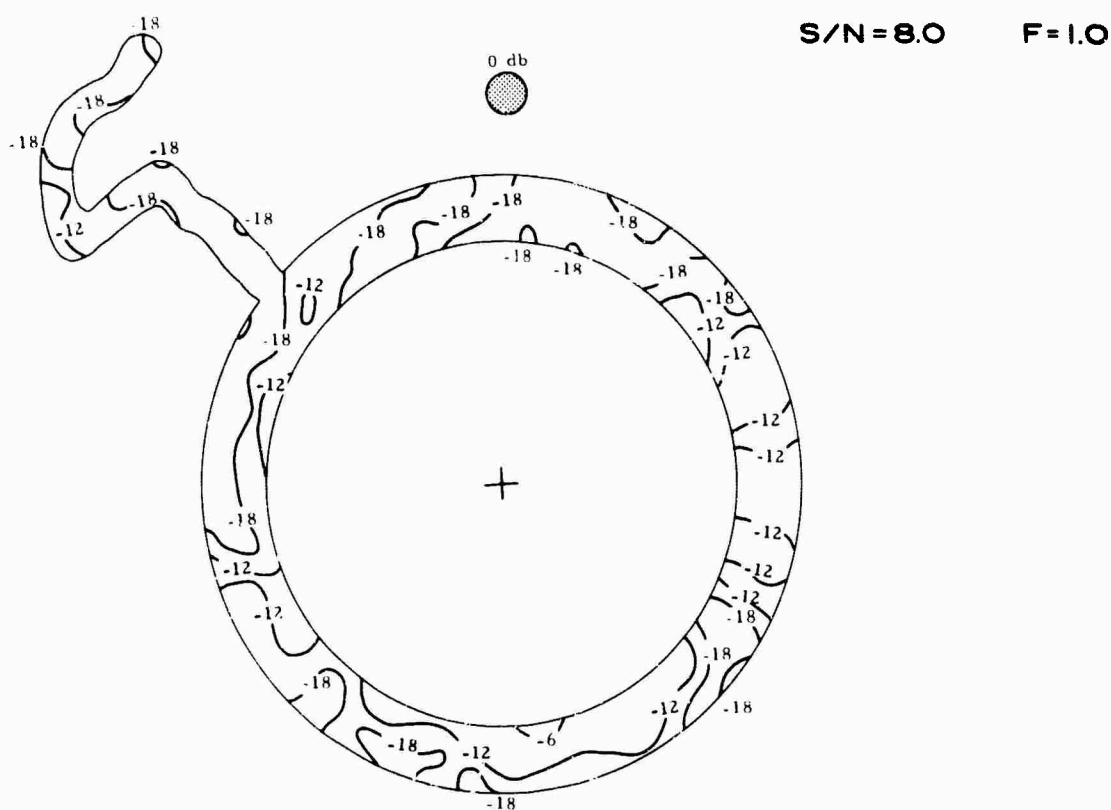
FIGURE 106. k-SPACE RESPONSE AT 1.0 cps FOR FILTER REJECTING NOISE MODEL B AND ACCEPTING NOVAYA ZEMLYA SIGNAL MODEL

112

noise and signal regions since these were the only regions of interest specified in the filters.
It is not intended to indicate that there are other regions which are not just as important, this
presentation is a demonstration of design and when used in practice more realistic noise re-
gions may be specified. If, for instance, due south was an area of extreme importance in mon-
itoring some particular signal region, it would be possible to place more weight in the noise
region shown to be -6 db down. This would force the filters to reject this region more heavily
letting the response come back up at some other point in the k plane which was not as important.
The important point to be demonstrated is that a specified region can be held up in response
while another specified region can be reduced in response thus allowing a tool for shaping the
beam in an optimum manner. Figure 107 presents the response at 2.0 cps. The majority of
the signal region is still passed with 0 db response down, the rest being between 0 to -3 db
down. The Aleutian Islands chain still has a small -12 db response area but the majority of it
being -18 db down. Additionally, there is a small -6 db region in the upper portion. The large
diameter cone now shows several regions where the response is popping up to -6 db. Again
these regions could be reduced further, if desired, by specifying a stronger weighting of the
noise model at these points.
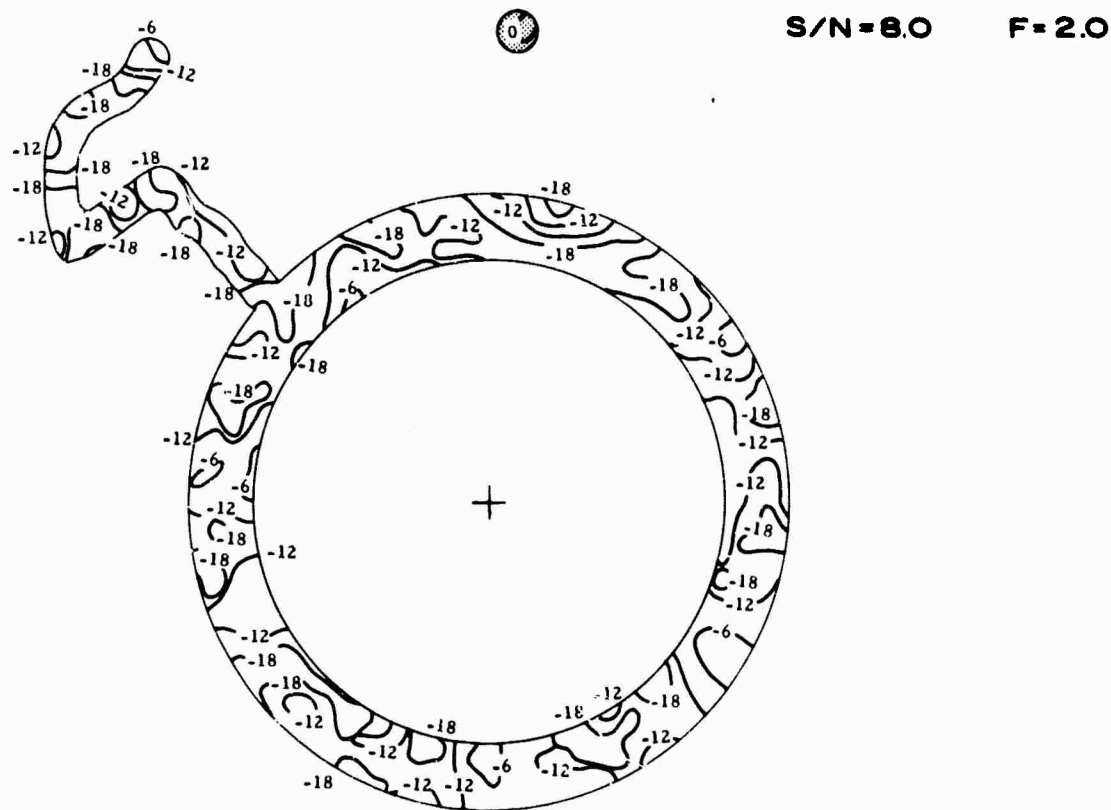
FIGURE 107. k-SPACE RESPONSE AT 2.0 cps FOR FILTER REJECTING NOISE MODEL B AND ACCEPT-
ING NOVAYA ZEMLYA SIGNAL MODEL

113

It should be kept in mind that the response figures shown indicate only a first attempt at optimum beam shaping. The same noise and signal models might well be better rejected and passed respectively with further tailoring, that is adding more emphasis to the noise regions which are coming up in response in the figures shown and more emphasis to the signal region where it indicates it is falling below 0 db.

Figure 108 presents the second signal model that was used. This consisted of a series of time shifted cones to cover the signal energy coming from that portion of China which is within approximately 90° of Montana LASA. This signal model was used in conjunction with the previously shown noise model. Figure 109 presents the response in k space at .5 cps to a set of filters designed to pass the China signal model and reject the noise model that was shown previously. As can be seen, a small portion of the Aleutian Islands chain is at a -12 db response. However it should be noted how rapidly the response goes from a broad area of 0 db response in the China signal model to an area of -12 to -18 db response through the Aleutian Islands chain. The majority of the large diameter disc is -12 to -18 db down in response. Figure 110 indicates the response of the same set of filters at a frequency of 1.0 cps. It is noticed that the response through the Aleutian Islands chain is still -12 to -12 db down primarily. However, a small area of -6 db has shown up due south of Montana LASA again as happened in the pre-
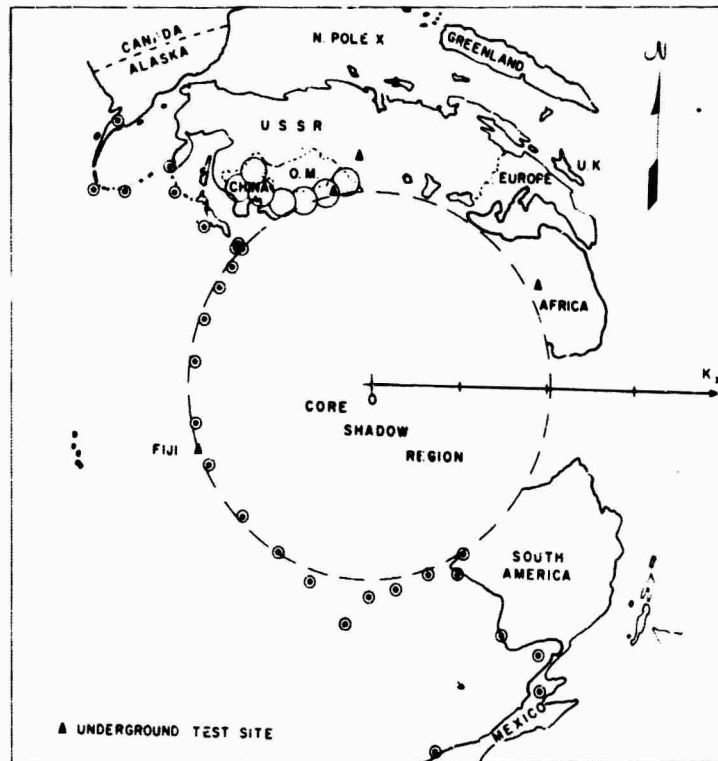
FIGURE 108. WAVE NUMBER MAP FROM MONTANA LASA USING CHINA SIGNAL MODEL
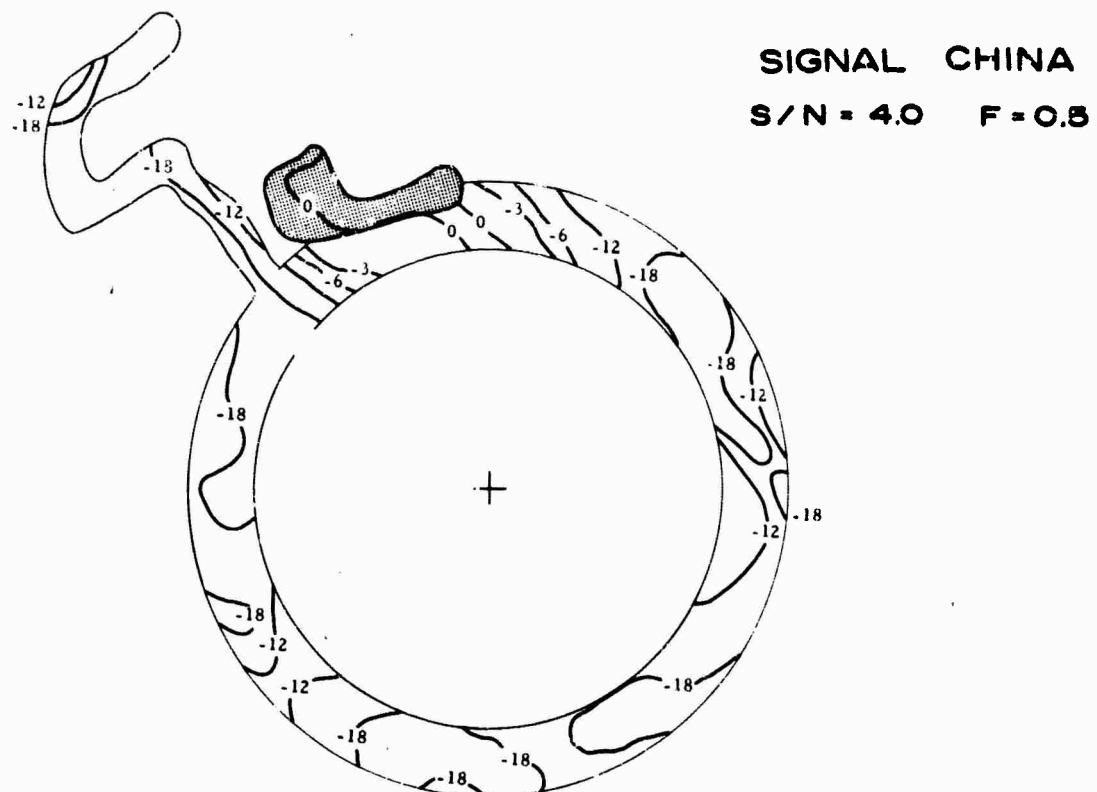
FIGURE 109. k-SPACE RESPONSE AT 0.5 cps FOR FILTER REJECTING NOISE MODEL B AND ACCEPT-
ING CHINA SIGNAL MODEL
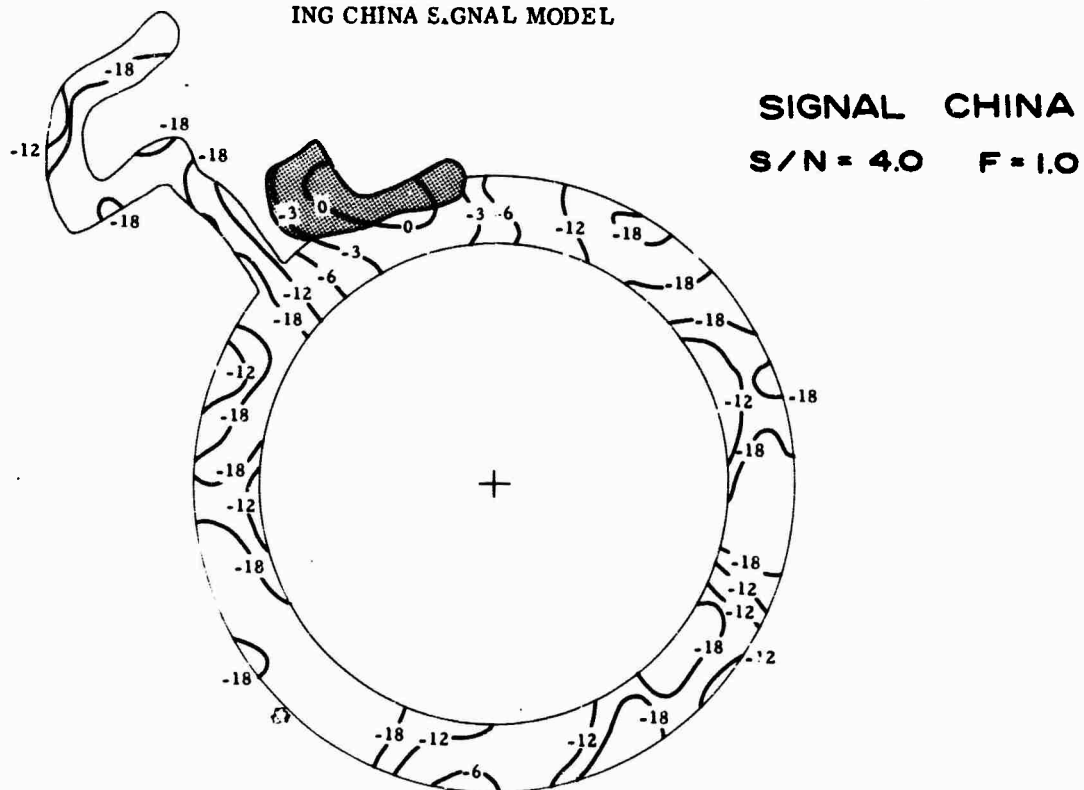
FIGURE 110. k-SPACE RESPONSE AT 1.0 cps FOR FILTER REJECTING NOISE MODEL B AND ACCEPT-
ING CHINA SIGNAL MODEL

vious signal model. It is also noticed that the portion of the large diameter disc which overlaps the indicated signal model is passed. This region is passed in favor of passing the signal model as opposed to rejecting part of the signal model in order to reject the noise model. This is accomplished by weighting the signal model heavier in k space than the noise model. If it was more desirable to reject the noise than it was to pass the signal it would have been possible to do so by weighting the noise model heavier than the signal model through this region. Possibly more constraint could be placed on this region by special noise model additions around the edge of China. Finally Figure 111 presents the response of the same set of filters at 2.0 cps. The Aleutian Islands chain still exhibits the -12 to -18 db down response with -6 db lobes occurring at a few places within the major disc model. All of the portion of China shown is still passed with a 0 db to a -3 db response.

Figure 112 presents the signal model used to cover Russia. As can be seen, this model is made up of different time shifted velocity cones in three-dimensional f-k space. Figure 113 shows the response at .5 cps of a set of filters designed using the signal model shown in Figure 112 and the noise model shown previously. As can be seen, the majority of the noise region is of order -18 to -24 db with the only region occuring above -18 db lying very closely to the specified
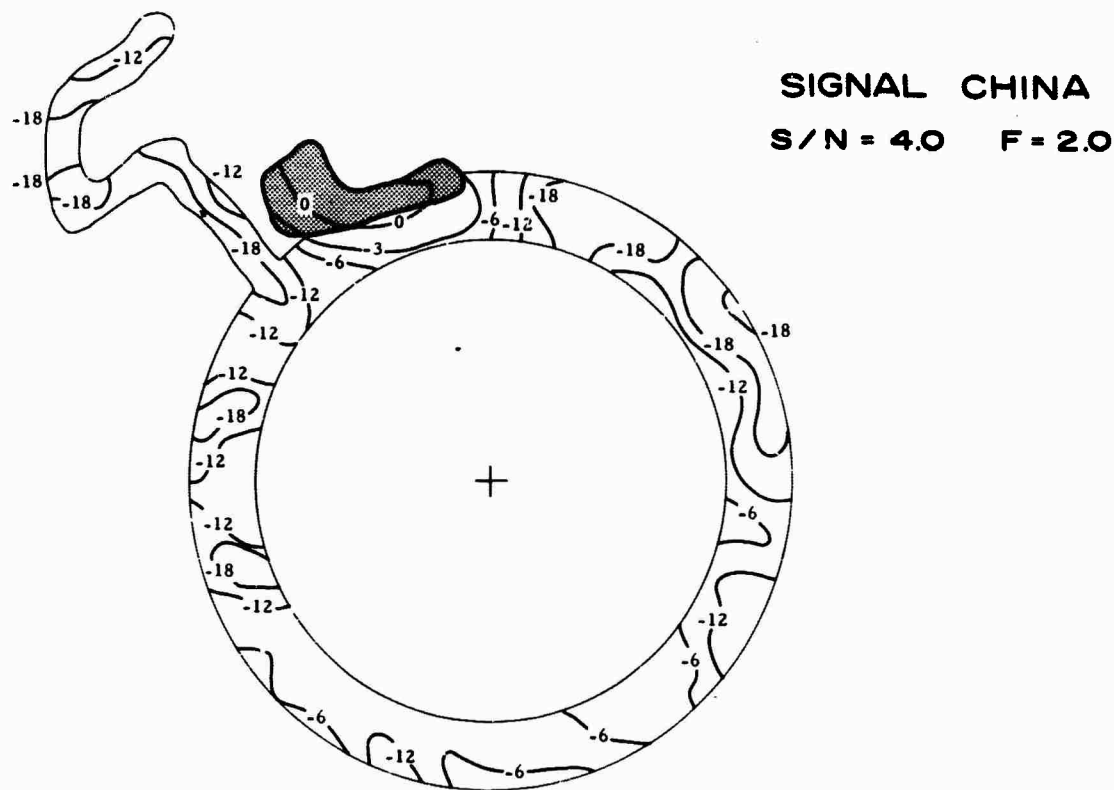
FIGURE 111. k-SPACE RESPONSE AT 2.0 cps FOR FILTER REJECTING NOISE MODEL B AND ACCEPT-
ING CHINA SIGNAL MODEL
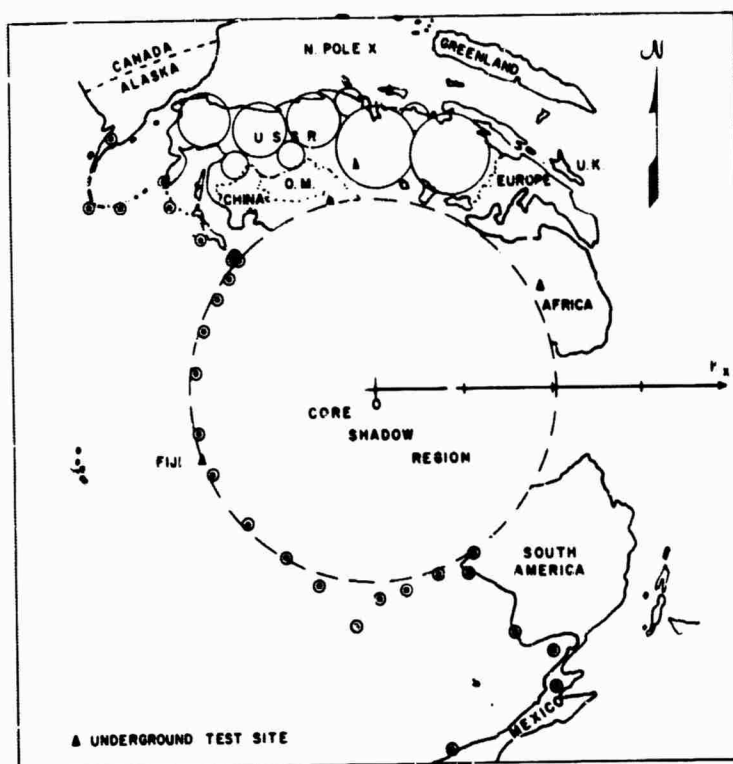
FIGURE 112. WAVE NUMBER MAP FROM MONTANA LASA USING RUSSIA SIGNAL MODEL
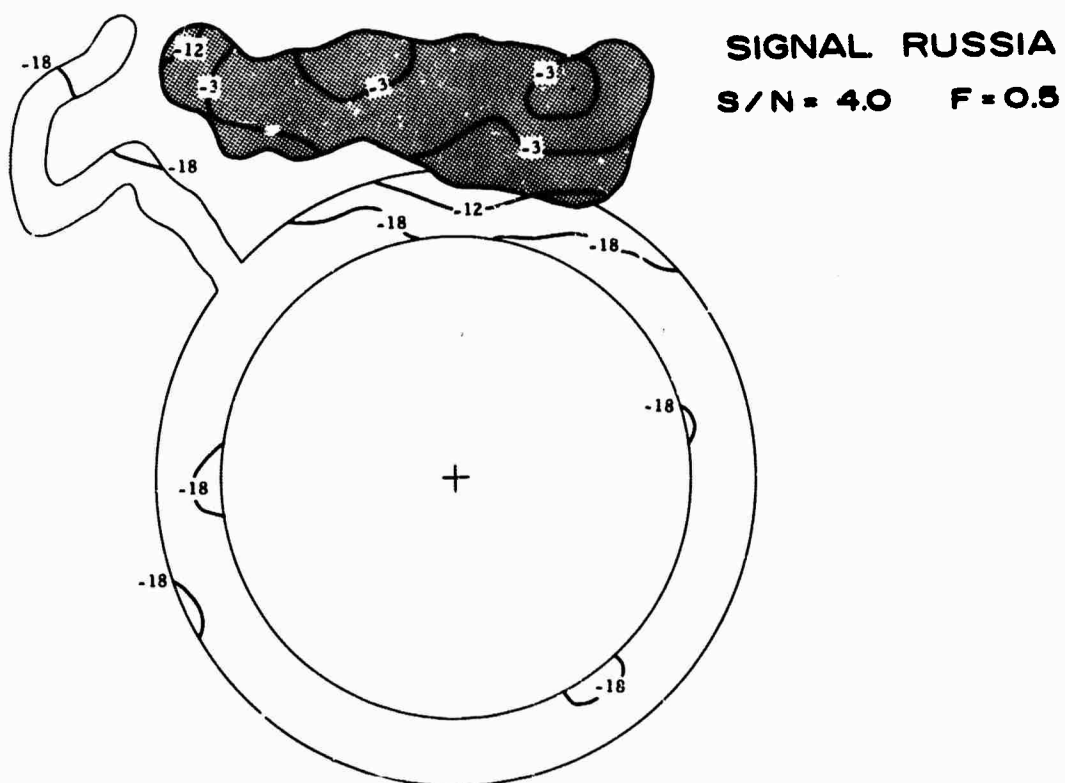
FIGURE 113. k-SPACE RESPONSE AT 0.5 cps FOR FILTER REJECTING NOISE MODEL B AND ACCEPT-
ING RUSSIA SIGNAL MODEL

117

signal region. Again the signal region is covered by contours on the order of -3 to 0 db with a few small areas of -12 db where the signal model very closely approaches the noise model. Figure 114 indicates the response of the same set of filters computed at 1.0 cps. Again the majority of the noise region is down -18 to -24 db with -6 db sidelobes occuring almost south of Montana again and -6 and -3 db occurring in the major disc where the signal model overlaps the noise model. Finally Figure 115 presents the response of the same set of filters at 2.0 cps. As can be seen the response over the signal model holds up very well, 0 to -3 db. The Aleutian Islands chain is down for the most part on the order of -18 to -24 db with the major disc model varying -12 to -18 db but coming up to 0 db in a few places. Again it should be pointed out that if these are undesirable areas to let the model have high response, the areas could be forced down by placing heavier noise weighting in these regions.

At this point the conclusions that can be drawn from the data presented are that:

a) The main beam from a large array can be selectively broadened as a function of velocity to encompass any specified signal region by properly weighting the outputs of the individual subarrays and

SIGNAL RUSSIA
S/N = 4.0   F = 1.0
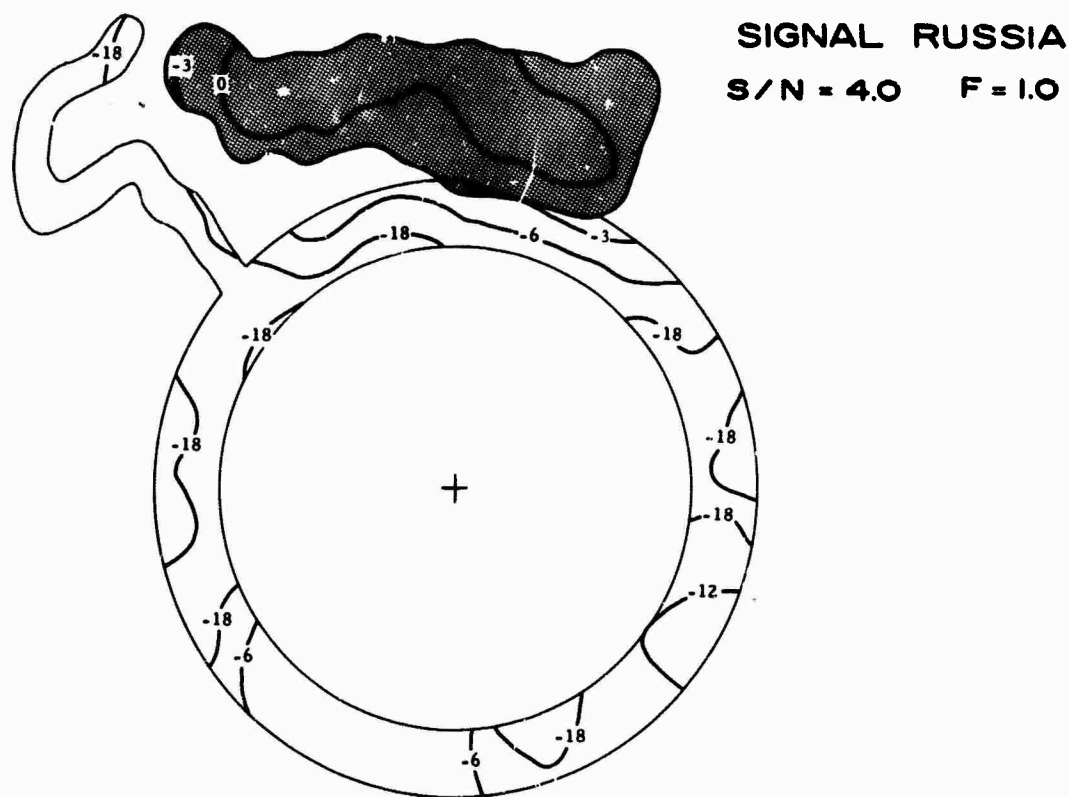
FIGURE 114. k-SPACE RESPONSE AT 1.0 cps FOR FILTER REJECTING NOISE MODEL B AND ACCEPT-
ING RUSSIA SIGNAL MODEL

118

b) Specified noise regions can be rejected by selecting the proper correlation set when developing optimum weightings.

The response curves presented are only intended to demonstrate the technique and are not suggested as final operational response models. Much more detailed weighting and shaping of the signal models should be attempted in determining weighting functions that would be used in an on-line or operational condition.
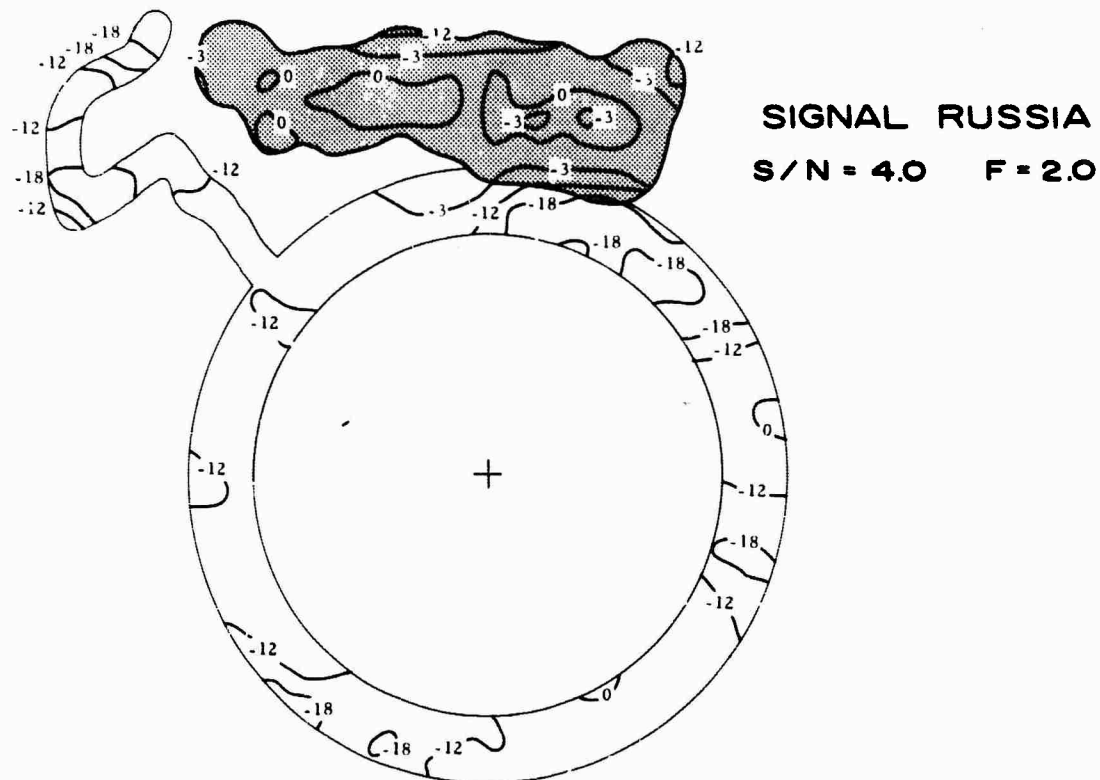
FIGURE 115. k-SPACE RESPONSE AT 2.0 cps FOR FILTER REJECTING NOISE MODEL B AND ACCEPT-ING RUSSIA SIGNAL MODEL

12. LARGE APERTURE ARRAYS
by
Walter J. Davis
AFTAC/VELA Seismological Center

INTRODUCTION

An array, when operated as a velocity-phase simple summation, is a wave number filter. The filter passes events corresponding to the phasing velocity and attenuates all other events. If the phasing velocity is constant over the array, the response of the wave number filter is a function only of the array geometry. In this short note we will examine critically the wave number response of the Montana Large Aperture Seismic Array (LASA) and suggest an alternative geometry for any subsequent LASA development.

MONTANA LASA

1. The Montana installation is an array of 21 subarrays. If each subarray has identical geometry, the response, in decibels, of the large array is the sum of the responses of one of the subarrays and of the array of 21 center points of each subarray. While the subarrays of the Montana LASA are not exactly identical, the variation among the subarray geometry, including orientation, does not affect the total response of the LASA for wave number $|\bar{k}|$ less than 0.20 km^{-1}.

2. Figure 116 shows the response of the 21-point Montana LASA along three profiles. The convention used here is that points on the 65° profile, for instance, represent events propagating in the direction N65°E. The response is a rapidly varying function of vector wave number. The 65° and 146° profiles cut through two of the principal side lobes of the response. The 105° profile misses the main side lobes although it does tend to peak up at 0.06 km^{-1}. Generally, the response is down not more than 12 db over approximately 50 percent of the square $|k_x| = 0.1$ km^{-1}, $|k_y| = 0.1$ km^{-1}. The effect of the response of the subarrays is to provide an additional attenuation of 3 db at $|k| = 0.1$ km^{-1} and 6 db at $|k| = 0.14$ km^{-1}.

3. The profiles indicate a tendency for the response to peak for $|k|$ between 0.05 and 0.06 km^{-1}. From the 2-dimensional response,[1] one finds that in the annulus between $|k| = 0.05$ km^{-1} and 0.06 km^{-1} the response is down less than 12 db over about 50 percent of this area with a significant percentage down less than 9 db. Further, the main beam has strong azimuthal asymmetry. Finally, the principal side lobes ranging in wave number from about 0.08 to 0.15 km^{-1} are broad, flat, and down typically 10 db, including the effect of the subarrays, relative to the main beam.

---

[1]Technical Note VSC-19, AFTAC/VELA Seismological Center, 12 July 1965.
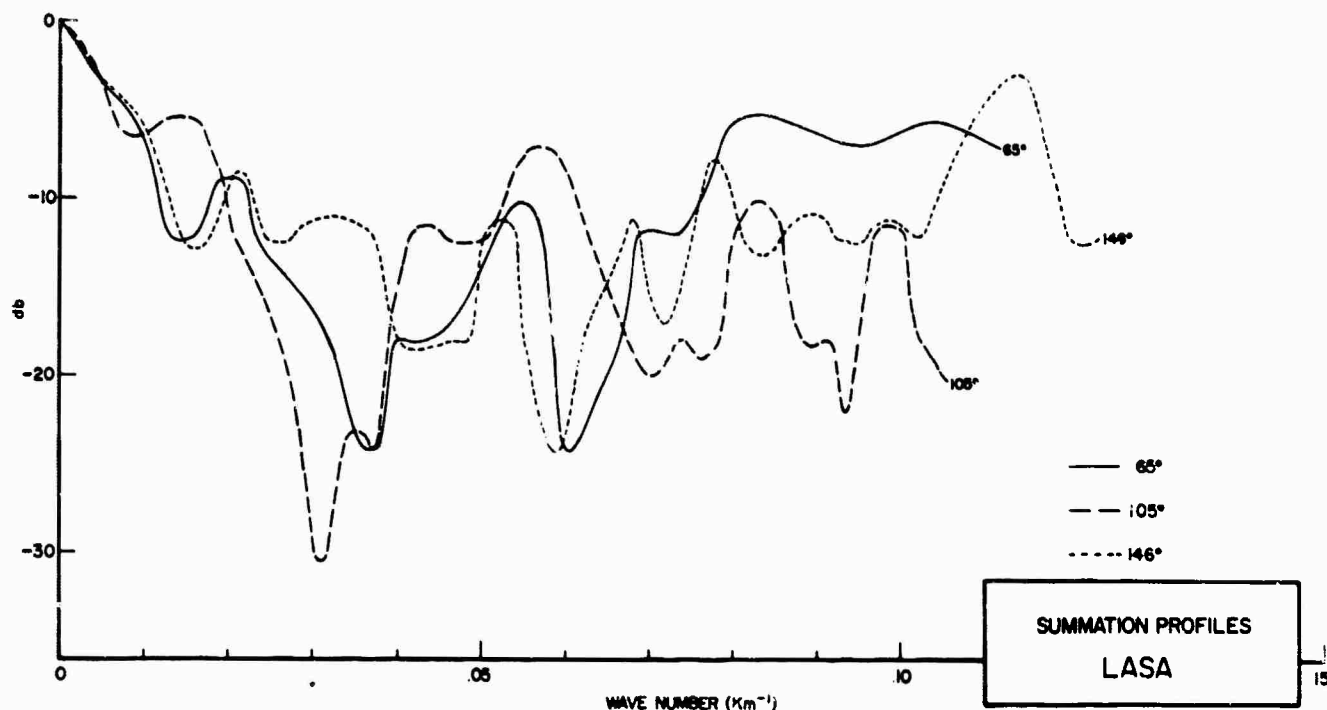
FIGURE 116. RESPONSE OF MONTANA LASA AS A FUNCTION OF WAVE NUMBER FOR SELECTED PROFILES

4. Since a difference of one half of a magnitude unit corresponds to 10 db, the significance of the preceding discussion is obvious. The question that arises is, "Is there a better filter (array configuration) and what are the trade-offs?"

HEXAGONAL LASA

1. Figure 117 shows the wave number response of two regularly spaced hexagonal arrays.[2] The wave number is expressed in units of the reciprocal subarray separation d km. Two profiles, the best and the worst, are shown. The solid-line profiles are symmetrical about the axis $k = (1/\sqrt{3})d^{-1}$. The dashed-line profiles are symmetrical about the axis $k = (2/3)d^{-1}$. The nearest principal side lobes lie at $k = (2/\sqrt{3})d^{-1}$. We note that the average response for the 19-element array between the main lobe and the side lobes is down approximately 18 db. Further, the side lobes have shape and size similar to the main lobe. However, the response at the side lobes may be reduced because of the subarray response. Also, the main beam possesses azimuthal symmetry.

2. The resolution of the main lobe and the separation between the main lobe and the side lobes are a function of the subarray separation, Figure 118. If one desires to have side-lobe

---

[2] VELA T/077 Phase I Final Report, Texas Instruments, Incorporated.

121
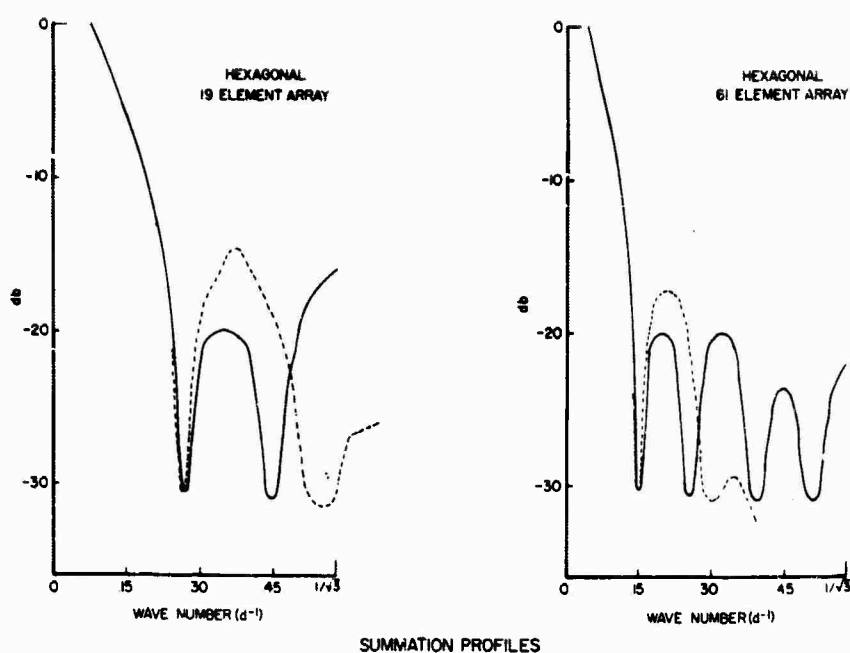
FIGURE 117. WAVE NUMBER RESPONSE OF TWO HEXAGONAL ARRAYS
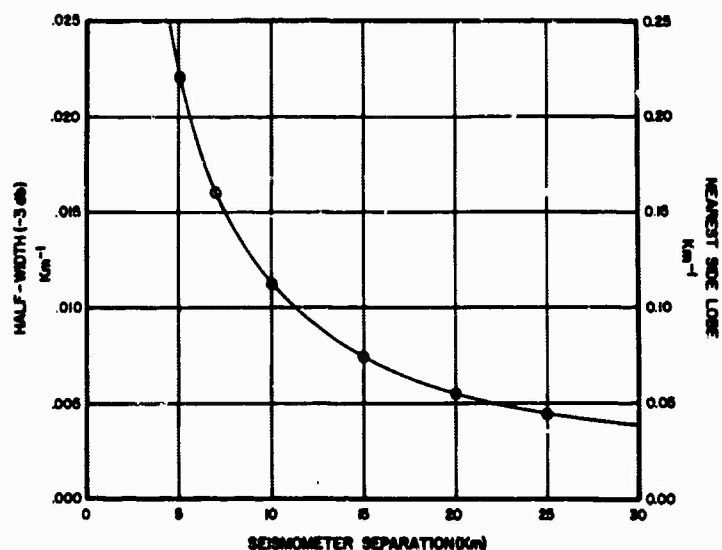
FIGURE 118. MAIN LOBE RESOLUTION, AND SEPARATION BETWEEN MAIN LOBE AND SIDE LOBE AS A FUNCTION OF SEISMOMETER SPACING FOR 19-ELEMENT HEXAGONAL ARRAY

separation similar to the Montana LASA ($|k| = 0.1$ km^{-1}), then the main lobe will cover about four times the area of the Montana LASA. If one desires the same resolution, then the side lobe moves in to $|k| = 0.05$ km^{-1}.

122

DISCUSSION

1. The particular feature of a LASA is the width of the main beam. Whereas small arrays pass all teleseismic P-phase arrivals equally well, the LASA can be used to discriminate against (or separate out) some of these P-phase arrivals. A beam width at 1 cps of 0.00012 km^{-1} would be required to separate P, pP, and sP on the basis of wave number. The corresponding array would be about 6000 km in diameter. To separate phases like P, PP, PcP, and PKP requires beam widths of the order of 0.01 km^{-1} corresponding to apertures of 100 to 200 km. In order to provide a beam width of 0.01 km^{-1} down to 0.5 cps, the beam width at 1 cps must be less than 0.005 km^{-1} at 1 cps. Thus, we are led to choose an array spacing of about 22 km for a 19-element hexagonal array. With 22 km spacing the nearest side lobes will be centered at $|k| = 0.05 \text{ km}^{-1}$.

2. The Montana LASA cannot be expected to provide, on the basis of velocity-phased summation, more than about 12 db separation on the average between interfering events. Generally, additional off-line processing will be necessary. One proven technique for separating events off-line is multichannel filtering with vector velocity as the separation parameter.[3] If the side lobes are well removed from the main beam (i.e., 5 to 10 beam widths), the velocity filter can reject very strongly even events coinciding precisely with a side lobe. This condition is fulfilled for the 19-element hexagonal array for all spacings. On the other hand, velocity filtering will not significantly narrow the main beam. Thus, the structure of the main beam of the Montana LASA limits the capability to separate the various P-phase arrivals of a given event as well as two nearby interfering events.

3. The construction of a regularly spaced hexagonal LASA may not be feasible at many potential sites because of topographical or cultural geographical considerations. The required 7 km diameter subarray sites at regularly spaced points can be expected to eliminate many otherwise desirable LASA locations. As an alternative to the LASA and it horizontally distributed subarrays, one can consider an extended array of vertical arrays buried in a borehole. Here one achieves suppression of the random surface noise by taking advantage of the very rapid (generally) attenuation of this noise with depth. The trapped mode noise can be attenuated by multichannel filtering where the separation parameter is now the depth dependence of the amplitude of each mode. The typical vertical array would contain six seismometers with 0.3 km spacing and with the upper instrument buried from 0.3 to 0.6 km deep. A vertical subarray would require only a few hundred square feet of surface area.

---

[3] Velocity filtering is an optimum process in the Wiener sense.

123

SUMMARY

Since I believe that techniques more sophisticated than simple velocity phasing will be required in order to fully utilize the potential capability of a LASA, I consider it important that the wave number response of the array, and therefore the array geometry, be carefully controlled. In particular, the structure of the main beam should have azimuthal symmetry, should have steep skirts, and should have a small half-width. All of these features can be obtained with a regularly spaced hexagonal array.

13. BEAM PATTERNS

by

Felix Rosenthal
International Business Machines Corporation
Federal Systems Division

REQUIREMENTS OF LASA SKELETAL* ARRAY BEAM PATTERN

Regions in frequency-wave number space in which significant noise may be expected at LASA are shown in Figure 119.[1] This figure indicates that one or another of the noise types shown can occur at almost any value of wave number difference, ΔK, between the signal and the noise. Therefore, a desirable beam pattern for the LASA skeletal array would show significant loss everywhere from the main lobe to values of ΔK at which the subarray beam pattern itself provides adequate loss.
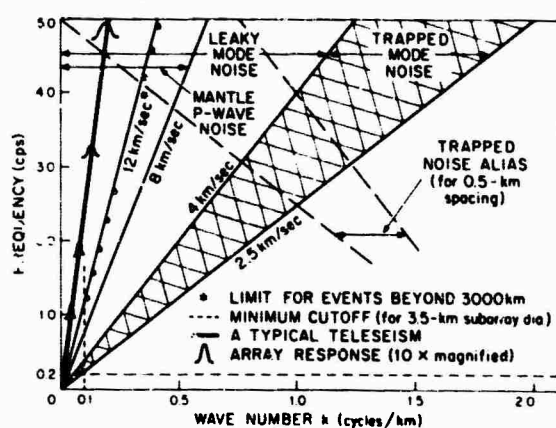
FIGURE 119. REPRESENTATION OF NOISE, REVERBERATION, AND A TYPICAL P-WAVE SIGNAL IN A SPACE FREQUENCY vs HORIZONTAL WAVE NUMBER

A tentative criterion which one might set as a goal would be to try to make the sum of the LASA skeletal array and subarray losses about 10 db everywhere outside the main lobe. As shown in Table 1, the present subarray design achieves subarray loss of 10 db for $\Delta K = 0.18$. The subarray side lobes should not be troublesome, because they (a) correspond to rather high frequencies not present in the signal, and (b) they will be smoothed because of the variation of subarray orientation. Therefore, the beam pattern of the skeletal array should be considered for values of wave number deviation from $\Delta K = 0$ to 0.18. If possible, the gain should be sufficiently far down in this range to meet the suggested 10 db down criterion.

---

*The skeletal array assumes one omnidirectional sensor at each of the subarray centers.

[1] From Seismic Discrimination, Semi-Annual Technical Summary by P. E. Green, Jr., et al., Lincoln Laboratory, Massachusetts Institute of Technology, 31 Dec. '61.

TABLE 1
Subarray Beam Pattern

ΔK	Subarray Loss, db
0.00	0.0
0.02	0.1
0.04	0.6
0.06	1.3
0.08	2.3
0.10	3.6
0.12	5.1
0.14	6.9
0.16	8.6
0.18	10.2

PRESENT STATUS

Neither the present LASA skeletal array design, nor any other design we have studied quite meets this goal. However, the preliminary studies which have been completed indicate that:

a. Some significant side lobes of the present array can be slightly reduced by the addition of perhaps two well-placed subarrays.[2]

b. For any future arrays, assuming that logistic considerations still require a clustered or subarray layout, an array design based on a regular polygon possessing an odd number of sides shows promise. In particular a pentagon may show side lobe characteristics somewhat superior to either the basically square design of the present array, or a hexagonal design which has also been considered. The reason for this seems to be that the odd number of sides assures that a wave front traversing the array sees a different set of periodicities leaving the array center from those encountered while approaching it, and this avoids some degree of "aliasing" inherent in an array geometry based on an even number of sides.

APPROACH

Two computer programs have been written and are described in detail.[2] Both are based on conventional steering, on the assumption that optimum processing would significantly affect only the subarray beam pattern. The simpler of the two programs has been used to provide beam patterns of the kind shown in this report. It suffers from the disadvantage of neglecting the effects of frequency averaging due to the finite signal bandwidth. This bandwidth will in fact tend to smooth some of the peaks in the beam pattern observed for a single frequency. Furthermore, this program is arranged to calculate power loss at equal increments in radius and equal increments in azimuth, thus yielding sparser data as the radius increases. It has the

---

[2]Large Aperture Seismic Array, Signal Processing Study, IBM Final Report to ARPA, 15 July '65, Contract No. SD-296.

advantage of being less expensive to run than the bandwidth program and is quite good for a preliminary analysis of the kind presented here, before making final studies on the bandwidth program. The bandwidth program, on the other hand, has the advantages of being adaptable to an automatic contour plotting routine and of providing more detailed information.

RESULTS

The worst nearby side lobe of the present array is only 4 db down at $\Delta K = .015$. This lobe can be reduced to about 6 to 7 db down, by the addition of two subarrays. These subarray loca- tions were found by trying out a number of possible locations based on an attempt to reduce the occurrence of repeated distances (aliasing) seen by a wave front. Before thinking of adding actual subarrays, this study needs to be carried further to try to obtain greater side lobe re- duction if possible, and to check that the improvement of the near lobe has not degraded the pattern for larger values of ΔK.

Figure 120 presents a comparison of beam patterns of the present LASA skeletal array with what appears to be one of the better pentagonal configurations: a 21-element log-periodic spiral array, with successive pentagon radii in a ratio of 2 to 1, a maximum radius of 100 km, and with each pentagon rotated 24° with respect to its neighbor. The graph of the least loss

Approximate Beam Patterns at Worst Azimuth
———— LASA Skeletal Array
— ·· — ·· — Subarray
● ● ● ● ● ● ● Skeletal Pentagon, Log Periodic 24 Degree Spiral, Ratio = 2.0
Skeletal Array Sampling Grid: ΔK : Every 0.001 KM^{-1}
Azimuth: Every 3°, $0 \le \Delta K < .06$; Every 1.5°, $.06 \le \Delta K \le .12$
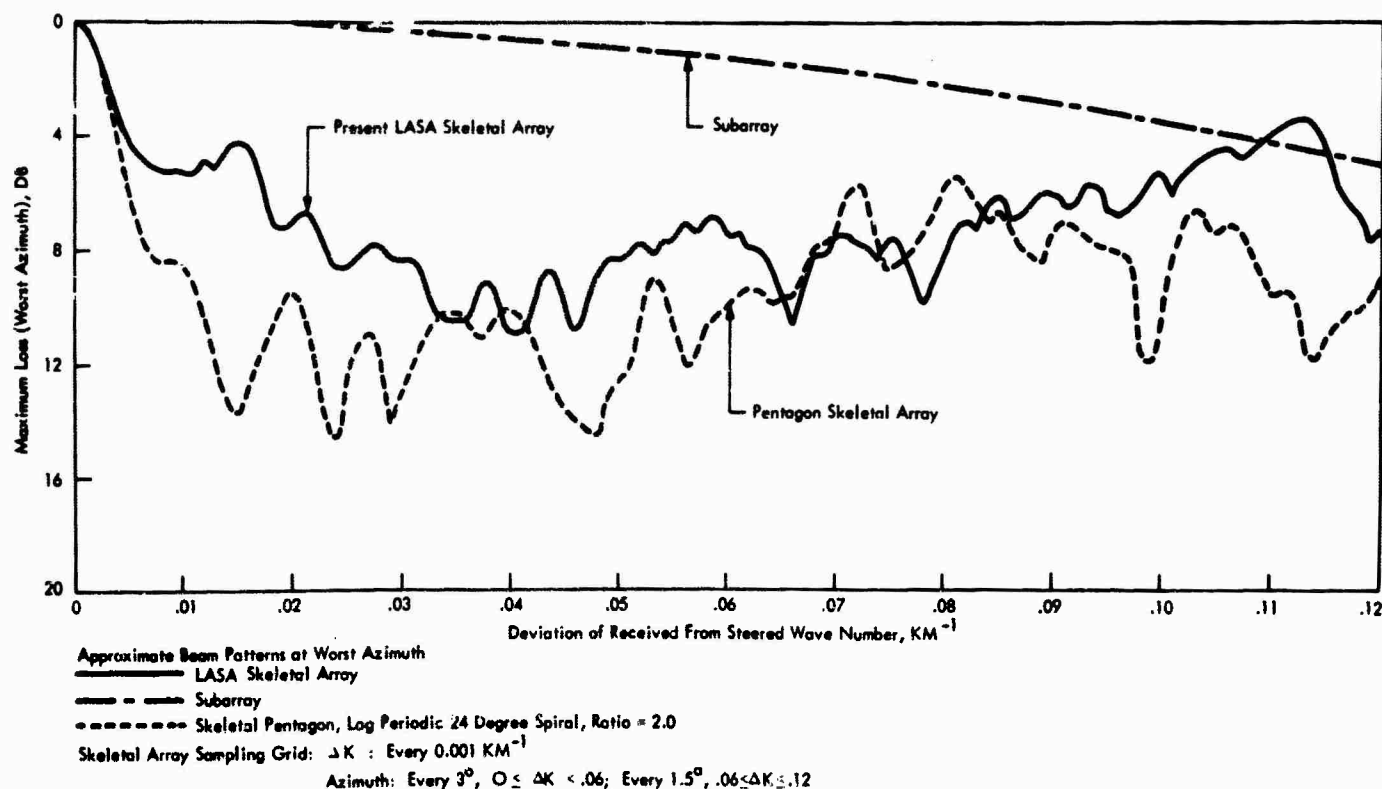
FIGURE 120. LASA, PENTAGON, AND SUBARRAY BEAM PATTERN

127

(as a function of azimuth) versus the wave number deviation, out to $\Delta K = 0.12$, shows that the pentagon array meets the previously suggested 10 db criterion everywhere in the range, except between $\Delta K = .066$ and $\Delta K = .086$, where it becomes as bad as about 7 db at worst. Because of time limitations, the patterns have not been explored beyond $\Delta K = 0.12$. Furthermore, the grid which has been used in preparing the charts was rather coarse (at worst, increments of ΔK of about .003 in the azimuth direction) so that the summits of at least some of the peaks have undoubtedly been missed in both the LASA and the pentagon patterns. More comprehensive studies, yielding contour plots and using bandwidth signals are required.

The log-periodic spiral used in the present LASA array helps to suppress farther out side lobes, of course at the expense of getting a somewhat fatter main lobe than in a linear spiral. Figure 121 shows a comparison of the 24^0 log-periodic spiral shown previously, with a linear 36^0 spiral, which was about as good as any of the linear spirals studied. The advantages of the log-periodic structure are evident.
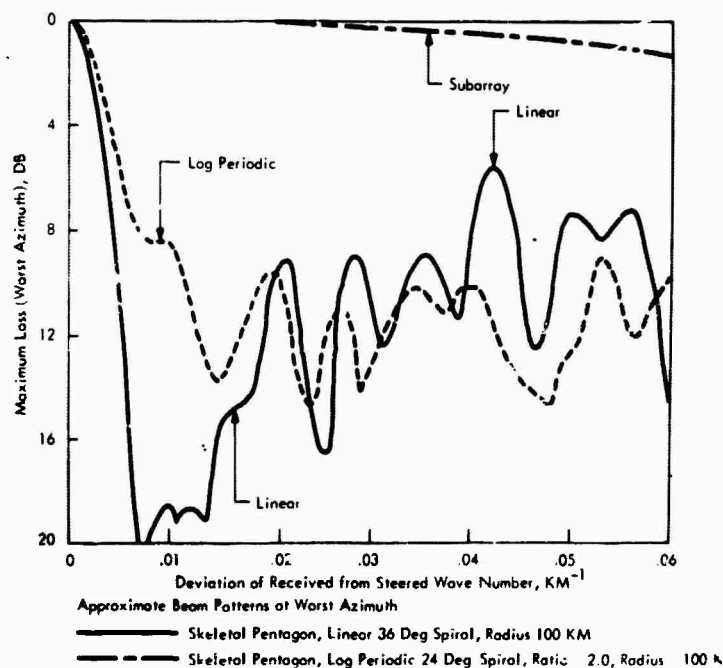
FIGURE 121. LINEAR AND LOG-PERIODIC PENTAGONS

CONCLUSIONS

a. The LASA skeletal array beam pattern is capable of at least limited improvements by the addition of two, or perhaps more, well-chosen subarray locations. Further study is required to assure best results.

b. Assuming that logistics for any future arrays still call for a clustered or subarray design, a pentagon array design shows promise of having a better side lobe pattern than a basically square or hexagonal design. More detailed examination of the beam pattern of a number of log-periodic spirals is recommended.

BEAM PATTERN FORMULAS

A. Single Frequency

(1) Replace (x_i, y_i) by $(x_i - \bar{x}, y_i - \bar{y})$;

$$\bar{x} = \frac{\sum w_i x_i}{\sum w_i} , \bar{y} = \frac{\sum w_i y_i}{\sum w_i} .$$

(2) Using the new x_i, y_i,

$$L = -10 \log_{10} \left| \frac{w_i \exp\left[2\pi j (x_i \Delta K_x + y_i \Delta K_y)\right]}{\sum w_i} \right| .$$

B. Bandwidth

u_x, u_y = reciprocal velocity components;

$\Delta K_x = f(u_x - \hat{u}_x), \Delta K_y = f(u_y - \hat{u}_y)$;

$\wedge$ means "steered."

(1) Correlation coefficient, nth to mth receiver: $R_{nm} = \dfrac{\sin \pi BT}{\pi BT} \cos 2\pi ft$, where

$$T = \frac{1}{f}(\vec{K} \cdot \vec{\Delta x}) = u_x(x_n - x_m) + u_y(y_n - y_m).$$

(2) $L = -10 \log_{10} \dfrac{\displaystyle\sum_{n=1}^{L} \sum_{m=1}^{L} w_n w_m R_{nm}}{\left(\displaystyle\sum_{n=1}^{L} w_n\right)^2} = -10 \log_{10} \dfrac{\displaystyle\sum_{n=1}^{L} w_n^2 + 2 \sum_{n<m} w_n w_m R_{nm}}{\left(\displaystyle\sum_{n=1}^{L} w_n\right)^2}$

129

$$= -10 \log_{10} \frac{\sum_{n=1}^{L} w_n^2 + 2 \sum_{n=2}^{L} \sum_{m=1}^{n-1} w_n w_m R_{nm}}{\left(\sum_{n=1}^{L} w_n \right)^2}$$

where B = bandwidth, cps

f = center frequency, cps

w_m = weight attached to mth receiver

130

14. BEAM PATTERN AND GEOMETRY STUDIES

by
E. J. Kelly
Lincoln Laboratory
Massachusetts Institute of Technology

I. ARRAY GEOMETRY

The performance of an array depends upon its geometry and the combining scheme used
in processing the data and can only approximately be discussed in terms of these factors sep-
arately. The problem of choosing a geometry so that reasonable beams can be formed is
typical of a class of problems involving the choice of a function in one domain so that its Fourier
transform, in a conjugate domain, has desirable properties. Hence array geometry in real space
is inevitably bound up with performance, i.e. patterns, in wave-number space. The chief geo-
metric design parameters are (1) maximum spatial extent of the array, (2) minimum spacing
between array elements, and (3) density of elements through the array. The extent of the array
determines the wave-number resolution attainable, the minimum spacing sets the scale for
wave-number aliasing (or near-aliasing), and the density distribution governs the possible
degree of side-lobe control achievable.

The aperture of LASA, roughly 200 km across, was chosen to provide about twenty times
the wave-number (or angular) resolution of existing arrays. The actual LASA array can achieve
a main lobe 10 db beam half-width of .007 cpkm in wave number which corresponds, for example,
to 0.5^O in epicentral distance at 80° (for signals at 1 cps). The minimum spacing, represented
by many seismometer pairs, is one-half kilometer which provides a fold-over wave number of
about 1 cpkm. This will provide alias-free processing if there is no noise at velocities lower
than 1 km/sec at 1 cps, 10 km/sec at 10 cps, etc. A uniform density at this spacing would
require more than 10^5 elements, hence some drastically non-uniform placement was required.
In any case, it is not of vital importance that all nearest neighbors be at the minimum spacing,
hence it is reasonable, and enormously more practical, to group the seismometers in subarrays.

The subarray geometry adopted, as proposed by Texas Instruments, Inc., consists of 25
elements placed on six radial arms, as shown on Figure 122, which also shows the layout of
subarrays in the array itself. The original idea was to place subarrays in rings, with a few
subarrays per ring, and with successive ring radii increasing exponentially. In fact, each ring
radius is roughly double that of the next smaller ring, and it was decided to place four subarrays
on each ring in order to have four remote sites which, together with the site at the center, would
provide a reasonable network for on-line epicenter determinations. The original orientations
of the squares was as shown, but their actual placement has been seriously modified by siting
problems. One, purely theoretical motivation for the exponentially-thinned (or log-periodic)
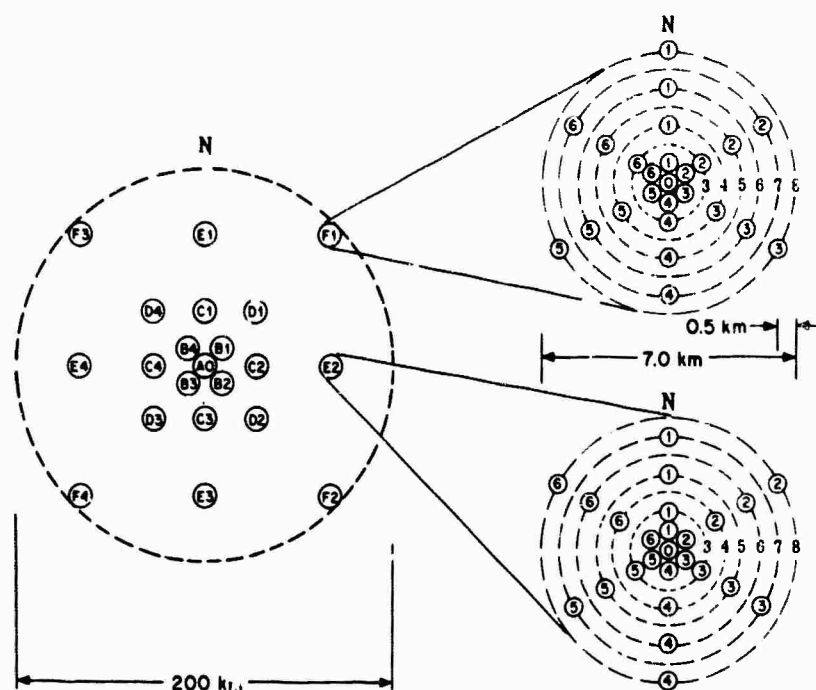
FIGURE 122. GEOMETRY OF LASA ARRAY AND SUBARRAYS

array was the desire to obtain comparable performance in angular resolution over a wide band of frequencies. In fact, if the full array has a certain beam shape at a given low frequency, the array obtained by deleting the outer ring should have nearly the same beam shape at double frequency, and so on. In addition. many practical reasons dictate a greater density of subarrays near the center. For example, signal coherence may be insufficient to realize full signal enhancement at full aperture, hence it seemed unwise to compromise the performance at the central portion of the array by spreading subarrays uniformly out to maximum radius. Also, the present pattern gives us a well-filled array out to about 30 km for side lobe control and noise spectral density measurement on an array smaller than LASA.

II. BEAMFORMING AND ARRAY PROCESSING

Given an array, there are many more forms of combining, or processing, than is suggested by the classification into beamformers and array processors. It is therefore necessary to describe a number of these, briefly, and then make an arbitrary classification. We limit ourselves to linear processors, listed in Figure 123.

The simplest combining scheme is delayed summation, in which the array is pointed at a fixed spot on the surface of the earth by inserting appropriate time delays in each seismometer channel and adding the resulting traces. These time delays are found by computing the distance from the fixed spot to each subarray and looking up the travel times from standard tables.

132

NON-ADAPTIVE	ADAPTIVE
STRAIGHT SUM	WEIGHTED DELAY AND SUM
DELAY AND SUM	FILTER AND SUM
WEIGHTED DELAY AND SUM	
FILTER AND SUM	

FIGURE 123. LINEAR ARRAY PROCESSING METHODS

Empirical station corrections are then applied to these times. The term steered sum is also used, and the special case of zero delays (pointing to the antipode of the array) is called straight summation. Delayed summation forms a beam in wave-number space which is usually characterized by good resolution and poor side lobes. By weighted delayed sum we refer to the modification in which the delayed traces are multiplied by constant (in time) weights before addition. This is simply spatial tapering, carried out to improve the shape of the beam in wave-number space. In order to produce beams of different shape at different frequencies, the weights must be frequency-dependent, or, in time-domain, each trace is filtered (which includes steering) before summation. This may be called filtered summation, and we shall arbitrarily interpret "array processing" to mean this class of schemes, while beamforming will refer to the previously described frequency-independent techniques. Figures 124-127 illustrates the beam structures attainable with these schemes in a rough way.

ARRAY   DIRECTIVITY PATTERN
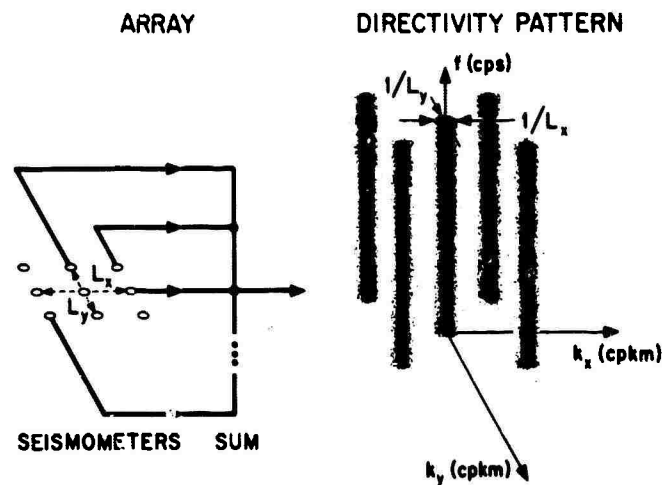
FIGURE 124. BEAM STRUCTURES FOR SEISMOMETER SUMS

In the weighted-sum and filtered-sum cases, the weights or filters can be fixed (i.e., preassigned), or adaptively determined in response to the changing environment. The beamforming methods familiar in the early days of phased-array radars are examples of non-adaptive weighted summation; the techniques of maximum-likelihood and multichannel Wiener filtering are examples of adaptive filtered summation. Finally, any of these schemes may be used on

133

ARRAY

DIRECTIVITY PATTERN
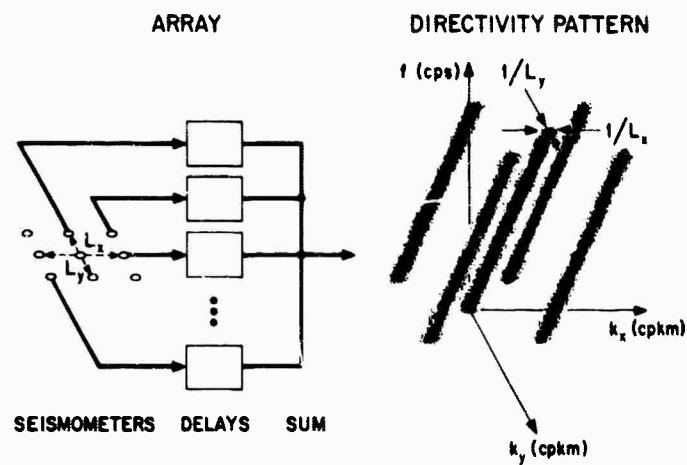
FIGURE 125. BEAM STRUCTURES FOR DELAYED SUMS

ARRAY

DIRECTIVITY PATTERN
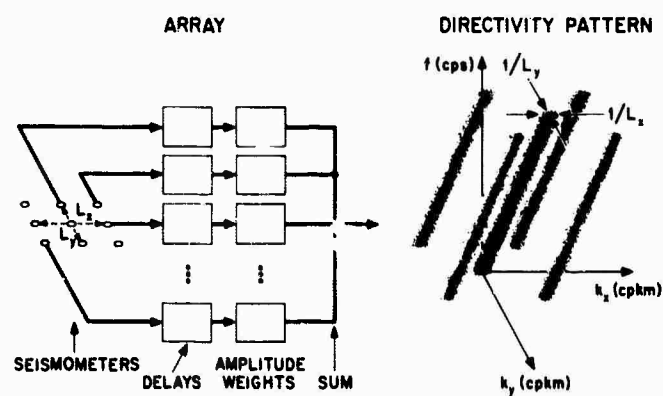
FIGURE 126. BEAM STRUCTURES FOR DELAYED AND AMPLITUDE WEIGHTED SUMS

ARRAY

DIRECTIVITY PATTERN
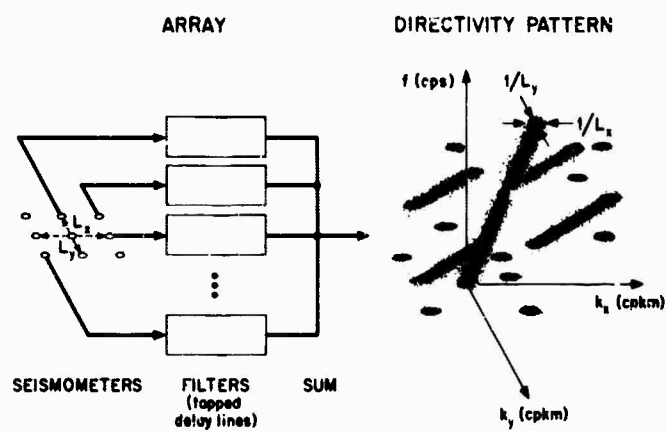
FIGURE 127. BEAM STRUCTURES FOR DELAYED, FILTERED SUMS

134

subarrays, clusters of subarrays, or in order to combine single processed subarray outputs
to form full array beams, and they may be used in a predetection or post-detection context.

Our general philosophy for predetection processing will be discussed in Briscoe's paper.
The simplest version of our post-detection philosophy is to process subarrays so as to reject
low-velocity noise and then to combine processed subarray outputs to form array beams with
reasonable main- and side-lobe structure, in order to reject unwanted events and high-velocity
noise. We have given principle attention to adaptive filtered summation processing for sub-
arrays, and non-adaptive weighted delayed summation of processed subarray outputs. The
former technique will be discussed by Green; here we shall comment only on beamforming
schemes for subarrays and the full array.

III. SUBARRAY BEAMS

The LASA subarray has a radius of 3.5 km and a straight-sum beamwidth (10 db) of 0.15
cpkm. At 1 cps, this corresponds to a velocity of about 6 km/sec hence the subarray can only
be expected to reject low-velocity noise, even at signal frequencies. Actual subarray perform-
ance has been evaluated at LASA and, for comparable small arrays, at TFSO, using delayed
summation, adaptive weighted delayed summation, and the maximum-likelihood technique. The
adaptive weighted sum consists of that set of weights, or one-point (i.e., no memory) filters,
which minimize the noise variance while adding up to unity to pass the signal unattenuated. To
find the appropriate weights, the zero-delay cross-correlation matrix of the noise is measured
just prior to the event. The results of several runs of nine-element "subarrays" at TFSO and
LASA are shown in Figure 128. The following processing gains are typical: (1) Delayed sum-
mation, 3 db; (2) Adaptive weighted delayed sum (the so-called "modified sum"), 6 db; (3) Maxi-
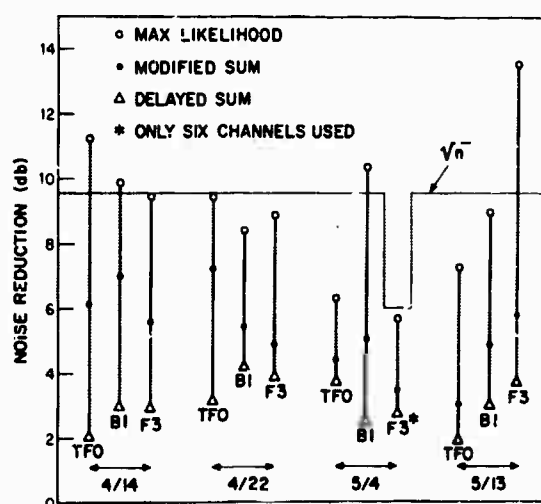
FIGURE 128. NOISE REDUCTION ACHIEVED WITH NINE-ELEMENT "SUBARRAYS" AT LASA AND TFSO
FOR VARIOUS PROCESSING METHODS

135

mum-likelihood, 11 db. For nine sensors, $\sqrt{N}$ voltage gain is 9.5 db. Similar results are found for actual subarrays of 25 sensors, where $\sqrt{N}$ corresponds to 14 db: (1) Steered sum, 5 db; (2) Modified sum, 8 db; (3) Maximum-likelihood, 16 db.

The failure of delayed summation to achieve anything like $\sqrt{N}$ performance is a simple expression of the fact that we are not dealing with independent white noise in our sensors. The modified sum processing would presumably be better than it actually is if the noise were really distributed over low-velocity modes. Actually, of course, the noise differs significantly from the signals in frequency content and the delayed sum and weighted delayed sum has no frequency filtering. Recent repetitions of some of these runs with high-pass filtering of each trace before combining has yielded delayed sum gains approximating that of the maximum-likelihood processor, which introduces no frequency distortion. The implication of this, together with the fact that the maximum-likelihood processor gains little more than $\sqrt{N}$, is that much of the noise is travelling at too high a velocity to be effectively rejected by subarray velocity filtering, and that most of the gain of the maximum-likelihood processor is being obtained in frequency. However, maximum-likelihood processing of the prefiltered data provides still better gain, significantly in excess of $\sqrt{N}$, as will be discussed by Green.

IV. ARRAY BEAMS

It may well turn out that one would like to combine all the elements of the inner nine, or thirteen, subarrays into one array, and process accordingly, without making the subarray-array distinction. However, for the present, we shall discuss only the "factored" forms of processing in which single processed subarray outputs are combined to form array beams. The fine-structure of such a beam is determined by the pattern obtained by treating the subarrays as points in a steered or weighted sum. The actual array pattern is, of course, only equal to the product of this pattern with the subarray pattern for identical, identically processed subarrays. Another limitation on the interpretation of these patterns is that they are functions of wave number, fixed in frequency, while signals occupy a range of frequencies at fixed velocity. Thus, a wide-band plane wave signal has a smeared spectrum in wave number, which mitigates the effect of pattern side lobes in some cases.

The unweighted steered sum over subarrays produces an irregular main beam with a 10 db beam width of about 0.02 cpkm (in the worst direction) and assorted side lobes as bad as 5 db in interesting regions of the wave-number plane. It seems that both the main lobe width and the side-lobe level could be improved by weighting the terms in the steered sum. A first attempt in this direction, using weights based on treating the sum as an approximation to a particular integral (which in turn gives a good pattern) has improved the main lobe, making it much more nearly circular in cross-section, and bringing the 10 db contour in to .007 cpkm, a value quite

136

consistent with the physical size of the array. However, in this attempt, some of the side lobes were made worse, although some were improved, as shown in Figures 129-131, which show the lower right quadrant of the k-space plot. The origin is in the upper left corner. Considerable experimenting will be necessary to find satisfactory beam shapes, and this is now in progress.
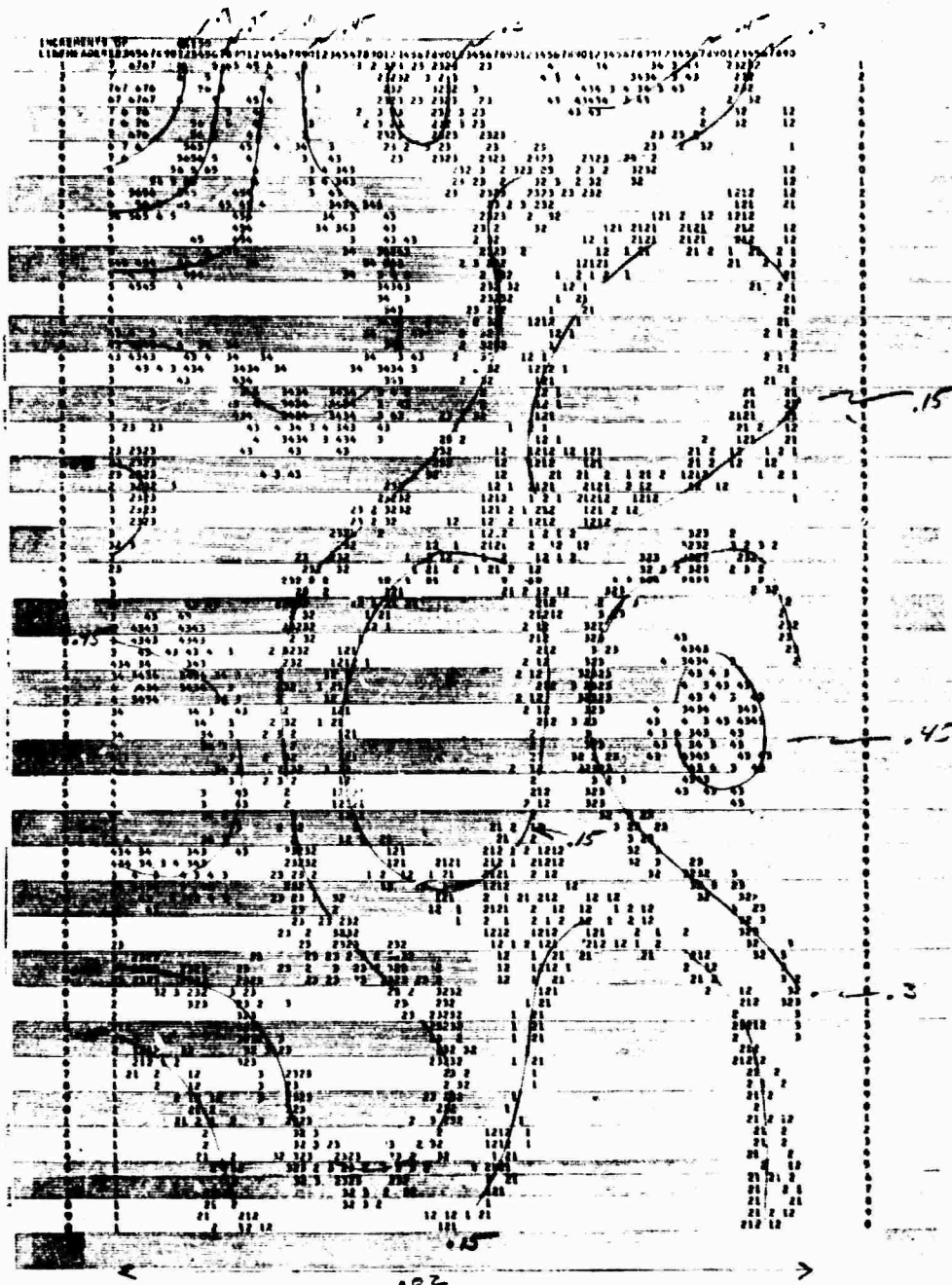
FIGURE 129. k-SPACE PLOT OF WEIGHTED STEERED SUMS, MODEL A
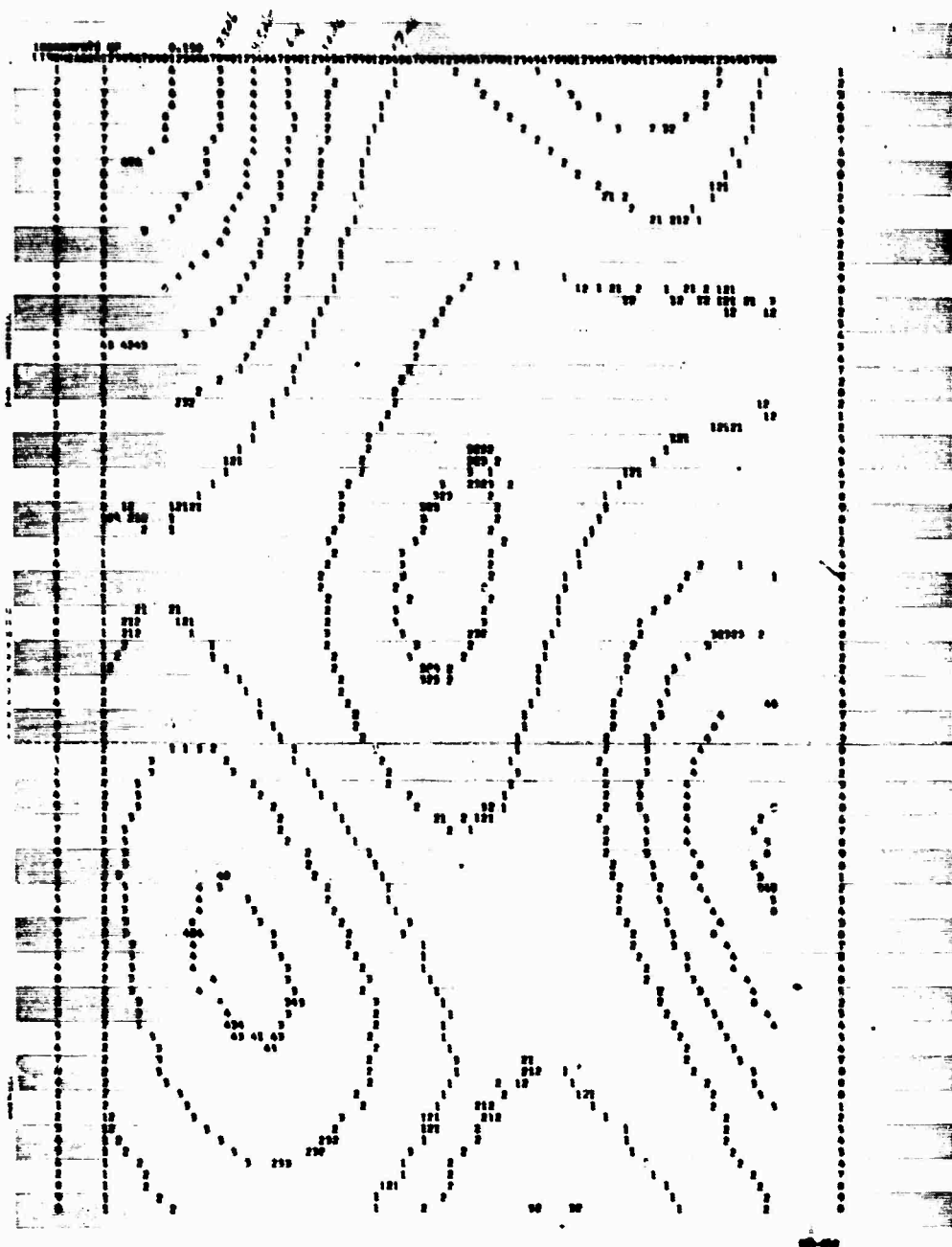
FIGURE 130. k-SPACE PLOT OF WEIGHTED STEERED SUMS, MODEL B

138
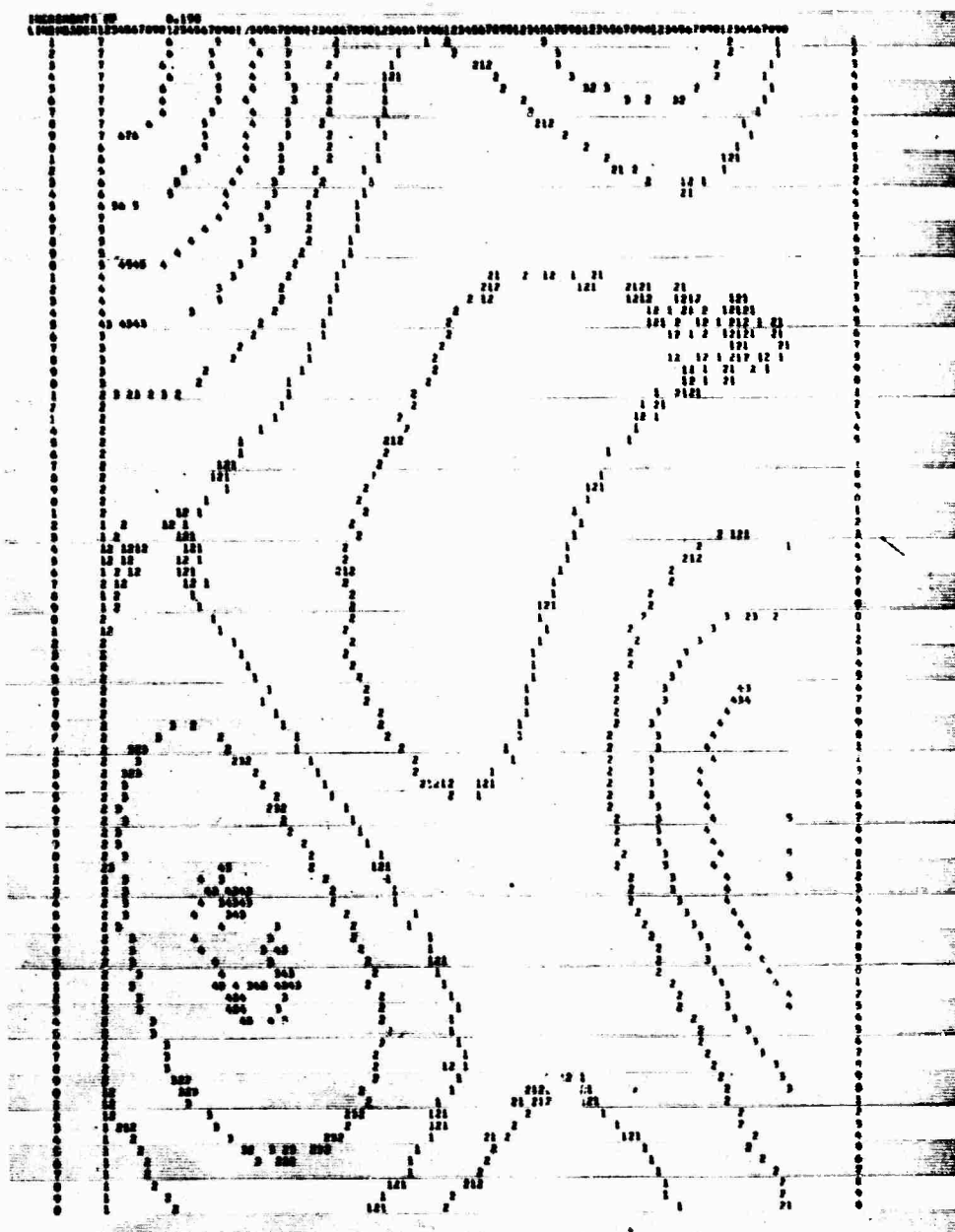
FIGURE 131. k-SPACE PLOT OF WEIGHTED STEERED SUMS, MODEL C

15. LARGE APERTURE TELESEISMIC ARRAY THEORY
by
Bernard D. Steinberg
General Atronics Corporation

I. INTRODUCTION

Three topics in the theory of large seismic arrays are discussed. The first is the theory of formations of beam patterns in an idealized earth, and the derivations of parametric expressions relating the more important properties of the beams with measurable design parameters.

The second topic deals with spatial coherence of seismic signals and of noise across an aperture. It includes the theoretical dependence of array performance upon signal and noise coherence and measurements of the pertinent quantities.

The third topic deals with the dependence of array performance upon travel-time residuals.

A summary of our work on these topics is given in this report. On the first topic enough has been done to warrant a technical report, and this is in process. This work includes a first order theory of beam formation and derives the beamwidths in three dimensions at the focal point. The theory is developed in terms of distance in the array, distance in the focal plane and travel-time parameters. Considered also are the use of phases other than P, the response of an array to transients, and certain side-lobe properties.

Work on the second topic is still in process. The theory from which the pertinent measurable quantities are determined is complete, and is reported herein. Twenty-eight selected events are currently in numerical analysis. This work is expected to produce enough data to complete this topic. A report will be issued as soon as the work is done. To date six events have been partially analyzed. Their results are given in this report.

The third topic has an easy part and a difficult part. The easy part has been done and is reported. It is the theoretical dependence of array performance upon travel-time residuals. The hard part is the measurement of the irreducible minimum uncertainty over various and appropriate seismic routes. This work is left to others.

II. BEAM THEORY

A. Single Frequency

Figure 132 shows an array located at a pole of a spherical earth. Two perpendicular meridians are drawn. The beam is focused at point P which is located on one of the meridians at latitude $\pi/2 - \Delta_o$. This means that the elements in the array have time delays built into them which exactly correct for the differential travel times from P to the array elements. The

140
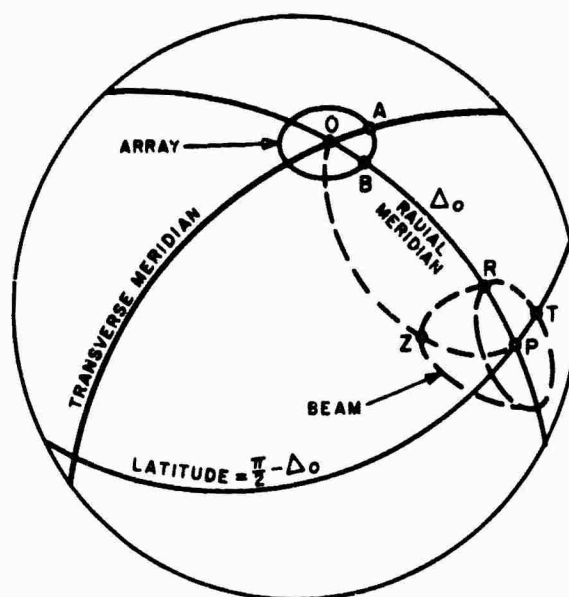
FIGURE 132. GEOMETRY OF TELESEISMIC ARRAY AND BEAM

meridian containing P is called the radial meridian. The other meridian is called the transverse meridian.

Shown also is a distorted ellipse containing P. This ellipse is an array gain contour. The radial extent of the beam is twice PR, the size of the ellipse on the radial meridian. The transverse extent of the beam is twice PT, the size of the ellipse on the latitude line containing P.

This constant gain contour is the intersection of a distorted constant gain ellipsoid with the surface. The "vertical" axis is along the seismic path. The depth of field of the array is twice PZ, the extent of the beam from the focal point to the constant gain contour along the seismic ray path.

For a surface focus half of the distance covered by the depth of field is outside the earth and therefore not pertinent. Thus the depth of field could be very sensibly defined as the distance PZ, rather than twice it. However, for deep focal points the alternate argument would prevail. For generality, therefore, the depth of field is taken as twice PZ.

It can be shown that the transverse extent of the beam 2PT is dictated by the transverse size of the array, twice OA, which is the extent of the array long the transverse meridian. Similarly, the radial size of the array twice OB dictates PR and PZ.

Following these comments we define the following quantities:

τ = dominant period of the seismic signal (sec)

γ_t = transverse extent of the array (radians)

γ_r = radial extent of the array (radians)

141

η = aperture efficiency. This quantity, typically 2/3 to 3/4, represents beam broadening beyond the theoretical minimum due either to amplitude weighting or spatial taper in the aperture, normally dictated by side lobe tolerance or by economics.

θ_t = transverse extent of beam within 3 db contour (radians)

θ_r = radial extent of beam within 3 db contour (radians)

Δx = transverse extent of the beam within 3 db contour (km)

$$= \frac{2 \times 10^4 \theta_t}{\pi}$$

Δy = radial extent of the beam within 3 db contour (km)

$$= \frac{2 \times 10^4 \theta_r}{\pi}$$

Δh = 3 db depth of field (km)

T = travel time (sec)

Δ = great circle distance variable (radians)

Δ_o = value of Δ from array center to beam focal point (radians)

h = depth variable (km)

h_o = depth of focal point (km)

$$T_\Delta = \left. \frac{\partial T}{\partial \Delta} \right|_{\Delta_o} \quad \text{(sec/rad)}$$

$$T_{\Delta\Delta} = \left. \frac{\partial^2 T}{\partial \Delta^2} \right|_{\Delta_o} \quad \text{(sec/rad}^2\text{)}$$

$$T_{h\Delta} = \left. \frac{\partial^2 T}{\partial \Delta \partial h} \right|_{\Delta_o, h_o} \quad \text{(sec/rad km)}$$

From the beam theory we find

$$\theta_t = \frac{\tau \sin \Delta_o}{\gamma_t \eta T_\Delta} \text{ (rad)}$$

$$\theta_r = \frac{\tau}{\gamma_r \eta T_\Delta} \text{ (rad)}$$

$$\Delta h = \frac{\tau}{\gamma_r \eta T_{h\Delta}} \text{ (km)}$$

The simplicity and similarity of these expressions permit universal plots to be made as in Figure 133, where it is shown for the P wave.[1] Δ is the independent variable. The dependent variable contains the beam size, the effective array size $\gamma\eta$ and the dominant period τ. For convenience the vertical scale is in terms of km degrees rather than square radians. Its units are km deg/sec. To obtain beam size in km multiply the ordinate by the dominant period in seconds and divide by the effective array size in degrees. For a one-degree array and one-second instruments, the vertical scale gives the beam dimensions directly in km. The depth of field curve pertains to a surface focus, $h_o = 0$. The 3 db contour extends below the surface only to one half the depth of field.
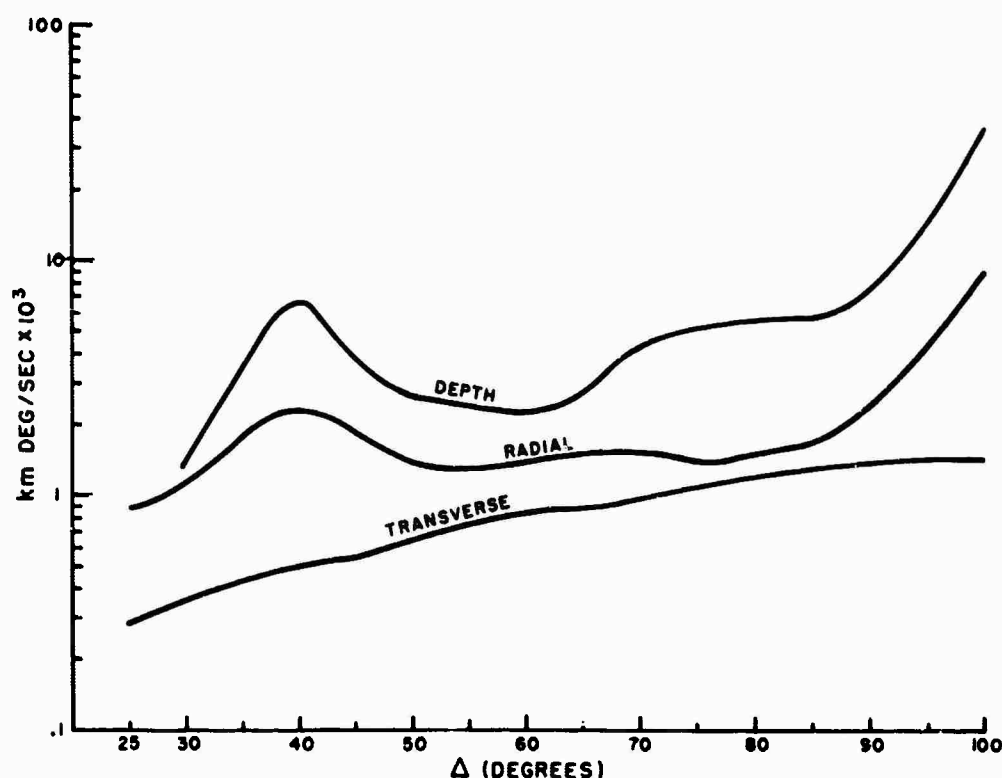
FIGURE 133. DIMENSIONS OF P-WAVE BEAM OF TELESEISMIC ARRAY

When applied to the LASA/Montana installation the following results are obtained:

Assuming an aperture efficiency of 3/4 and a dominant period of one second, the 200 km aperture when focussed at $\Delta = 70^o$ has a transverse cross-section of 760 km, a radial cross-section of 1130 km and a depth of field of 3080 km.

---

[1] Jeffreys, H. and Bullen, K. E., 1958. Seismological Tables. Office of the British Association, London.

A quantity which measures the distortion in the beam cross-section is the ellipticity, the ratio of the radial to the transverse beamwidths. This quantity is plotted in Figure 134.

B. Phases Other Than P

Figures 133 and 134 pertain to P-wave propagation only. Seismological interest in other phases, however, invites comparison. The theory relates to the seismic phase only through the travel-time derivatives. Hence a comparison of travel-time derivatives specifies completely the beamwidth ratios between phases.
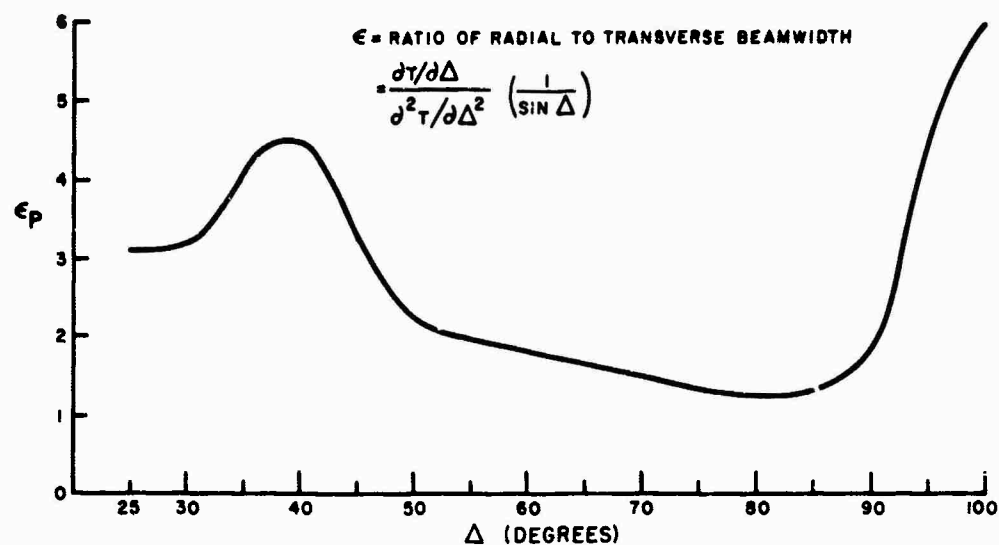
FIGURE 134. ELLIPTICITY OF BEAM CROSS-SECTION OF P WAVE

The table below shows $\partial T/\partial \Delta$ for three distances and several selected phases. The first derivative is smaller for P than for any of the other phases, and therefore the transverse P-beamwidth is correspondingly larger. The mean ratio of transverse beamwidth for the other phases relative to P is also given in the table.

Δ	T_Δ (/deg)					
	P	PP	PPP	S	SS	SSS
30º	8.8	13.0	13.7	15.8	23.5	24.6
70º	6.1	8.5	9.7	11.7	15.5	17.5
100º	4.5	7.7	8.7	8.4	13.8	15.5
Nominal transverse beamwidth relative to P	—	0.72	0.60	0.54	0.38	0.33

144

For the other beam dimensions the beamwidths of the various phases are neither consistently larger nor smaller than for P. Hence no single set of nominal ratios suffices. Figure 135 gives approximate beamwidth ratios relative to P in the radial dimension.

Δ	PP	PPP	S	SS	SSS
30^{0}	1.0	2.2	0.8	0.6	1.5
40^{0}	C `	1.2	0.5	0.i	0.8
50^{0}	0.9	1.4	0.8	0.4	0.8
60^{0}	2.0	0.4	0.7	1.6	0.2
70^{0}	2.3	1.4	0.5	1.8	0.4
80^{0}	2.3	1.4	0.5	1.2	1.0
90^{0}	1.3	2.0	0.3	0.8	0.8
100^{0}	0.7	0.7	1.0	0.4	2.0

FIGURE 135. BEAMWIDTH RATIOS RELATIVE TO P

C. Side lobes

A "filled" array is one having array elements about one-half wavelength apart. If the area is A and the wavelength is λ, the number of elements

$$N = \frac{4A}{\lambda^{2}}$$

A "thin" array has a much larger mean interelement spacing and, therefore, a smaller number of elements. If two such arrays cover the same area, their main beams have about the same cross-sections. Their side-lobe patterns, however, would be considerably different. In the former case it would be well determined in all directions and controllable to an extent predictable by antenna design theory. In the latter case, assuming a random distribution of elements, the side-lobe structure is specifiable only in statistical terms. Banta [1961][2] has shown that the mean asymptotic side-lobe level is N^{-1}. Lo [1963][3] has shown that for large N the probability is the order of 10% that few lobes, if any, rise more than 10 db above this level.

Large seismic arrays are likely to be thin arrays. A large aperture is one that is large compared to wavelength. The crustal wavelength for the P wave is 5-7 km. Hence a large seismic aperture is measured in hundreds of kilometers. This large distance from array elements to the beamforming site creates costs which tend to minimize the number of elements.

[2]Banta, 1961, "Far Field Properties of Wideband Planar Arrays with Nonlinear Processing," IRE International Convention Record, Part 1, pp. 95-100.

[3]Lo, Y. T., 1963, "A Probabilistic Approach to the Design of Large Antenna Arrays," IEEE Trans. on Antennas and Propagation, Vol. AP-11, No. 1, January.

Clustering the elements, or the formation of subarrays no larger than about one wavelength, only marginally helps the side-lobe problem. Subarrays as used in LASA are designed to suppress noise with a large horizontal propagation component. In the LASA design the number of clusters is 21. Hence the expected mean asympototic side-lobe level is -13 db.

Figure 136 shows the radial beam pattern for LASA when looking due north and focussed at 80° (see the solid curve). A steady state P wave of one-second period is assumed. The pattern was calculated from travel-time tables [Jeffreys (1958)] using the actual cluster locations.
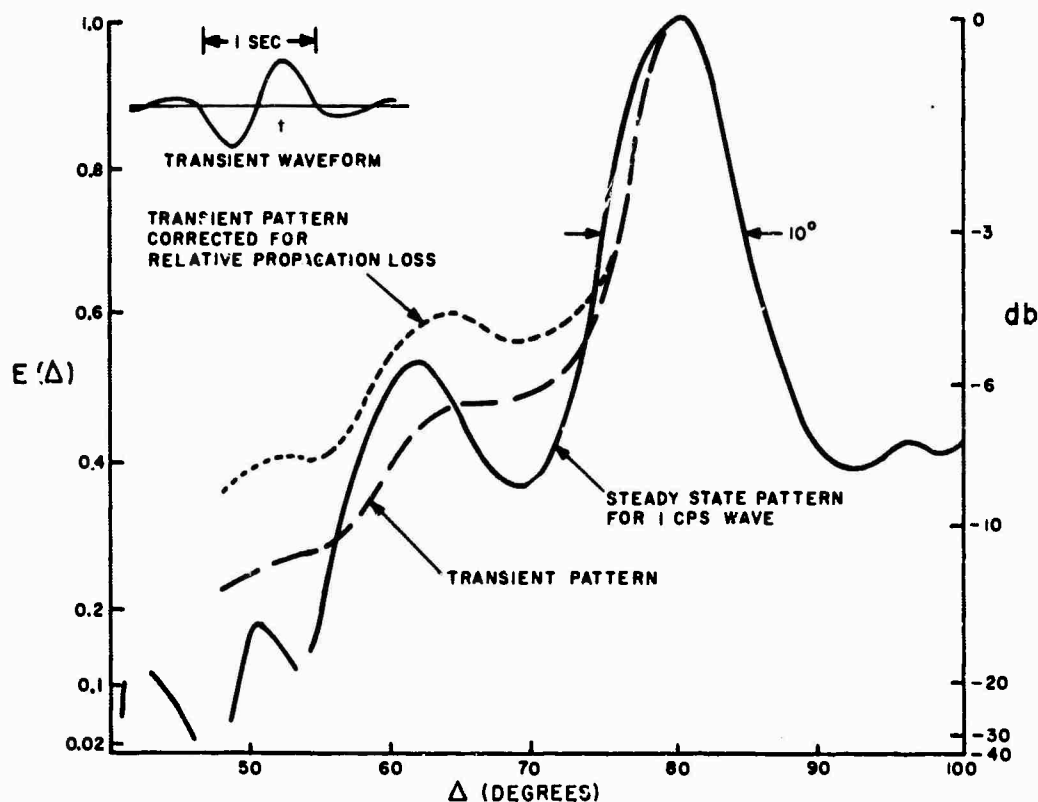
FIGURE 136. LASA-RADIAL BEAM PATTERN AMPLITUDE FOR 80° DISTANCE DUE NORTH, DECAY
AND SUM

The beamwidth is 10°, which is quite consistent with the theory (Figure 133). The side-lobe pattern falls toward the expected -13 db, but disappointingly lingers about -7 db near the main lobe.

Clever redistribution of array clusters will help. Increasing the number of clusters will help more.

D. Array Response to a Transient

The P wave has a transient waveform which is very different from the steady state sinusoid of 1-second period assumed for the beam pattern calculation. A less unrealistic waveform is

the transient shown in Figure 136. This waveform is synthesized from five sinusoids having periods 3/5, 3/4, 1, 3/2 and 3 seconds and relative amplitudes 0.31, 0.71, 1.0, 0.99 and 0.62, respectively. This wideband signal should narrow the main beam and smooth the side lobes.

The peak response of the LASA to this transient has been calculated and is shown as the dashed curve in Figure 136.

E. Propagation Loss Correction

Let a standard source liberate energy at $\Delta = 80^O$ due north, and let the peak response to the P wave be measured. Imagine the same source moved to $\Delta = 40^O$. The peak response relative to the first measurement presumably would be about that given by the dashed curve, namely approximately -14 db.

This estimate is considerably in error, however. The distance dependence of the propagation loss in the teleseismic region appears to be consistent with spherical spreading [Carpenter (1964)].[4] Hence at $\Delta = 40^O$ the attenuation is 6 db less than at $\Delta = 80^O$, and the radial side-lobe pattern should reflect this factor. This correction is introduced into the dotted curve in Figure 136.

F. Test of the Theory

During the coming months an attempt will be made to test the theory from experimental earthquake data.

III. SPATIAL COHERENCE

A. Theory

Let N stations record an event. Let $f_i(t)$ be the record of the ith station. Let $f_i(t) = s_i(t) + n_i(t)$ contain a signal part s and a noise or interference part n. The signal could be the P wave in which the noise is largely microseismic noise. Or the signal could be pP, in which case the interference could be P coda.

Consider the set of N records over some common period of time T relative to P onset. The cross-correlation between two records over this interval is defined by

$$\rho_{ij} = \frac{\int_T (f_i(t) - \overline{f}_i)(f_j(t) - \overline{f}_j)\,dt}{\left[\int_T (f_i(t) - \overline{f}_i)^2\,dt \int_T (f_j(t) - \overline{f}_j)^2\,dt\right]^{1/2}} = \rho_{ji} \qquad (1)$$

---

[4] Carpenter, E. W., 1964, Teleseismic Methods for the Detection, Identification, and Location of Underground Explosions, Univ. of Michigan Report 4410-67-X, VESIAC Report No. 7744VU, April, p. 11.

147

where

$$\bar{f}_i = \frac{1}{T} \int_T f_i(t) \, dt. \qquad (2)$$

Given N stations there are N^2 values of ρ_{ij} of which N, the ρ_{ii} are unity. Define the average correlation by

$$\bar{\rho} = \frac{1}{N^2 - N} \sum_{i \neq j}^{N^2 - N} \rho_{ij} = \frac{2}{N^2 - N} \sum_{i=1}^{N-1} \sum_{j=i+1}^{N} \rho_{ij} \qquad (3)$$

Designate by subscript s or n mean correlations for signal and for noise. Then it can be shown that the available signal enhancement in noise (gain in signal/noise power ratio) is

$$G = \frac{\bar{\rho}_s(N - 1) + 1}{\bar{\rho}_n(N - 1) + 1} \qquad (4)$$

An interesting observation is immediately available. With N large, signal correlation high and noise correlation so close to zero that $\bar{\rho}_n N \ll 1 \ll \bar{\rho}_s N$

$$G \approx \bar{\rho}_s N \qquad (5)$$

This is the normal and expected result; i.e., array gain grows linearly with the number of elements.

However, when the noise correlation is not near zero as is likely to be the case where the "noise" is P coda and the signal is pP, the gain will grow approximately linearly with N, as in (5), only so long as $\bar{\rho}_n N \ll 1$. Thus

$$
\begin{aligned}
G &\approx \rho_s N, \quad \text{when } N \ll \frac{1}{\bar{\rho}_n} \\
G &\approx \frac{\bar{\rho}_s}{\rho_n}, \quad \text{when } N \gg \frac{1}{\bar{\rho}_n}
\end{aligned}
\quad \text{and } N \gg \frac{1}{\bar{\rho}_s} \qquad (6)
$$

In the latter case additional array elements do not increase array signal gain significantly relative to interference. This is illustrated in Figure 137 in which array gain is plotted against N for three pairs of $(\bar{\rho}_s, \bar{\rho}_n)$ = (0.9, 0.2), (0.8, 0.1), (0.9, 0.05).

B. Measurements

Twenty-eight selected events are currently in numerical analysis. Distributions of ρ_{ij} will be examined as functions of event magnitude, epicentral distance, distance between stations, back

148
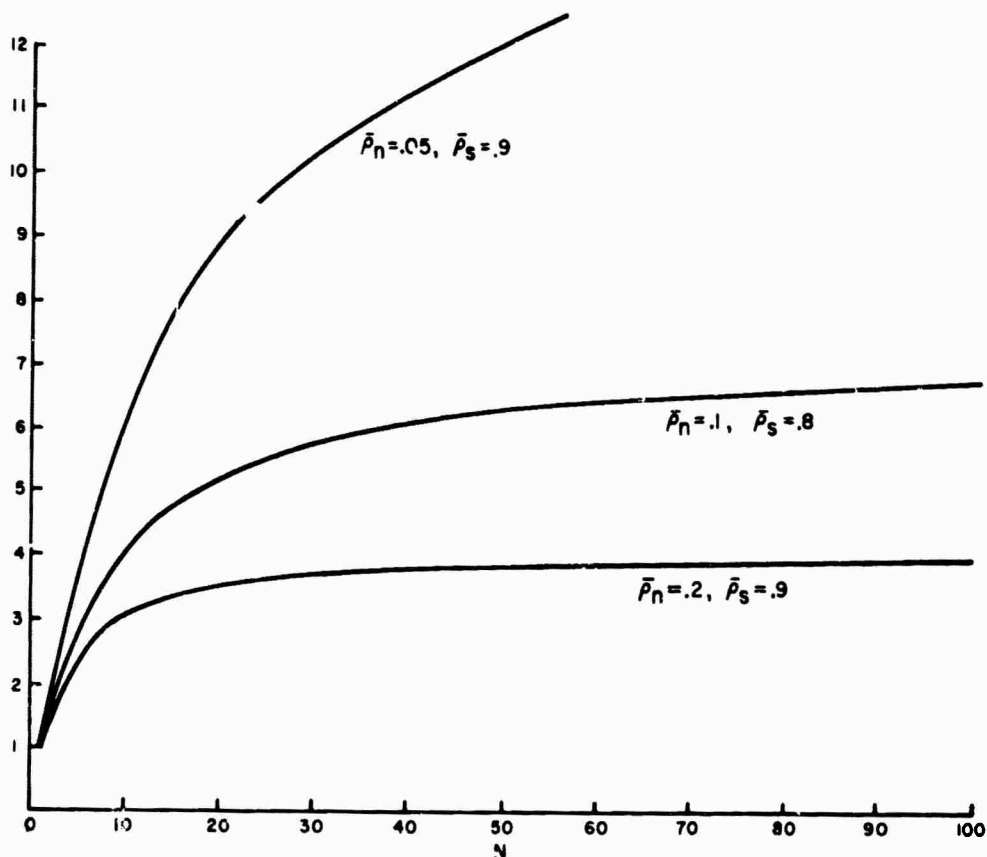
FIGURE 137. POWER GAIN OF ARRAY vs NUMBER OF ELEMENTS FOR 3 PAIRS OF $(\bar{\rho}_s, \bar{\rho}_n)$

azimuth from array, and angle between seismic paths to stations. Values of $\bar{\rho}$ will be obtained for as large a set of conditions as the data will permit. To date six events have been partially analyzed; measurements of $\bar{\rho}$ have been made for signal (P and pP) and noise (microseismic noise and P coda). Subscripts P, p, μ, and c pertain to P, pP, microseismic noise and P coda. The nominal size of the array varies from 2800-3800 km and the number of elements from 5-14.

It is evident that P correlation is uniformly high (0.73 to 0.94) and microseismic noise acceptably low (-0.13 to +0.10). Hence if these numbers prove typical, P-signal gain relative to microseismic noise can be made to grow arbitrarily with the number of elements N, as in (5).

Less can be said with confidence at this time about pP and P-coda correlation. First, the pP correlation data are very fragmentary (two readings only, 0.69 and 0.67). Second, there is reason to believe that the mean correlation of pP is larger ..... that shown, and possibly as large as $\bar{\rho}_p$. This is because the calculations were based on P-coda contaminated data, which can only degrade the computed correlation. This suspicion is consistent with the correlation hypothesis

149

drawn from the seismic propagation model described in the preceding report [General Atronics, 1965].

Regarding P-coda correlation the spread in the six samples is too broad to permit conclusion. However, unlike the correlation of microseismic noise, the six samples suggest a positive bias. If such a bias does exist then, from (6), there is an upper limit to the useful number of array elements for the buildup of pP in coda. This matter will be pursued further.

IV. TRAVEL TIME RESIDUALS

A. Effects Upon Array Performance

Differential travel-time errors from a source of seismic energy to array elements would normally degrade an array in two respects. First, the signal buildup would be less effective. This is normally expressed as a degradation in main beam gain. Second, side lobe suppression would be less effective. This is often expressed as a rise either in the general side-lobe level, the peak side lobe or in the depth of the nulls.

The LASA/Montana array will suffer only the former degradation, however. Side-lobe control is exercised by the locations of the clusters, which are spaced by several wavelengths, rather than by the elements within each cluster. With only 21 clusters in an area on the order of 1500 square wavelengths, the number of degrees of freedom available for side-lobe control is very limited. The side-lobe pattern shown in Figure 136 confirms this fact. As a consequence the additional effect of timing errors is marginal. Thus, in the following paragraphs, we consider only the effect on array gain.

B. Steady State Loss in Gain

Assume that the travel-time characteristics of the sites of all elements in an array have been studied, that station calibrations have been obtained and that all timing biases have been removed. Assume, too, that the irreducible minimum arrival time uncertainty is approximately Gaussian with variance σ^2. This assumption means that if ΔT_i is the timing error at the ith site for a particular beam focus, the probability density distribution of ΔT is

$$p(\Delta T) = \frac{1}{\sqrt{2\pi}\,\sigma} e^{-(\Delta T)^2/2\sigma^2} \tag{7}$$

The assumption further implies that the same distribution holds for all other beams from the same array even though the timing errors at a given site may be independent from beam to beam.

---

[6]General Atronics Corporation, 1965, Seismic Detection and Classification Techniques Study, GAC Report 1400-2026-1, Semiannual Technical Report, April, Section VII.

Assume a steady-state sine wave of period τ which might be identified with the dominant seismogram period. Assume also an N-element array. Let the signal gain to the ith element be a_i and the timing error be ΔT_i. Then the array output when the array is focused at the source of period τ is

$$V = \sum_{i=1}^{N} a_i \cos 2\pi(t + \Delta T_i)/\tau \qquad (8)$$

$$= E \cos\left(\frac{2\pi t}{\tau} - \phi\right) \qquad (9)$$

where

$$E^2 = \left(\sum_{i=1}^{N} a_i \cos 2\pi \Delta T_o/\tau\right)^2 + \left(\sum_{i=1}^{N} a_i \sin 2\pi \Delta T_i/\tau\right)^2 \qquad (10)$$

$$\tan \phi = \frac{\sum_{i=1}^{N} a_i \sin 2\pi \Delta T_i/\tau}{\sum_{i=1}^{N} a_i \cos 2\pi \Delta T_i/\tau}$$

Define the relative array gain A as the ratio of the peak output E to its value in the absence of timing errors.

$$A = \frac{E}{E(\Delta T_o = 0, \text{ all } i)} = \frac{E}{\sum_{i=1}^{N} a_i} \qquad (11)$$

(Attention is paid only to the envelope E of the array output V and not to the entire ' .me function.)

The second sum in (10) has zero mean since $p(\Delta T)$ is unbiased. Thus for large N it always may be ignored. Furthermore, effective beamforming requires small timing errors, $\Delta T_i/\tau \ll 1$. Consequently most terms in the second sum are small and, therefore, even for small N this

151

term may be dropped. Hence we can approximate (10) by

$$E = \sum_{i=1}^{N} a_i \cos 2\pi \Delta T_i/\tau \tag{12}$$

Both ΔT and a are independent random variables having probability density distribution $p(\Delta T)$ and $q(a)$. (12) is a sum over both variables and may be written

$$E = \sum_{i=1}^{N} a_i \cos 2\pi \Delta T_i/\tau$$

$$= N< f(a, \ \Delta T)> \text{ave}$$

$$= N \iint a \cos \cdot \pi \Delta T/\tau \cdot p(\Delta T) q(a) d\Delta T \, da$$

$$= N \int a q(a) da \int \cos 2\pi \Delta T/\tau p(\Delta T) d\Delta T \tag{13}$$

The first integral

$$\int a q(a) da = \bar{a} \tag{14}$$

the average value of the signal gain. Using (7) the second integral is

$$\int_{-\infty}^{\infty} \frac{1}{\sqrt{2\pi}\sigma} \cos 2\pi \Delta T/\tau e^{-(\Delta T)^2/2\sigma^2} d\Delta T = e^{-2\pi^2 \sigma^2/\tau^2} \tag{15}$$

Thus the peak response of the array is

$$E = N\bar{a} e^{-2\pi^2 \sigma^2/\tau^2} \tag{16}$$

and the relative array gain (11) becomes

$$A = e^{-2\pi^2 \sigma^2/\tau^2} \tag{17}$$

The square of (17) is the relative power gain

$$A^2 = e^{-(2\pi\sigma/\tau)^2} \tag{18}$$

152

Expressed as a loss in db with respect to zero timing error across the array

$$\text{db loss due to timing error} = -10 \log_{10} A^2$$

$$= 170(\sigma/\tau)^2 \tag{19}$$

(19) is plotted in Figure 138. It is evident that the permissible tolerance is the order of $\sigma \sim 0.1\tau$. Beyond this value the array gain rapidly disappears.

C. Loss to a Transient

Assume that the seismic waveform $f(t)$ may be represented by a finite Fourier series of M terms.

$$f(t) = \sum_{j=1}^{M} b_j \cos\left(\frac{2\pi t}{\tau_j} + \phi_j\right) \tag{20}$$

Let each of the N-array elements have signal gain a_i and timing error ΔT_i. The array output is

$$V = \sum_{i=1}^{N} \sum_{j=1}^{M} a_i b_j \cos\left[\frac{2\pi(t + \Delta T_i)}{\tau_j} + \phi_j\right] \tag{21}$$

It is near maximum at $t = 0$ provided that the ϕ_j are zero or near zero, which is a reasonable assumption for classical P-type waveforms.* Thus the envelope becomes

$$E = \sum_{i,j=1}^{N,M} a_i b_j \cos\frac{2\pi \Delta T_i}{\tau_j} \tag{22}$$

By (13) and (14)

$$E = N\bar{a} \sum_{i,j=1}^{N,M} b_j \cos 2\pi \Delta T_i / \tau_i \tag{23}$$

and, from (11)

$$A = \frac{1}{NM\bar{b}} \sum_{i,j=1}^{N,M} b_j \cos\frac{2\pi \Delta T_i}{\tau_j} \tag{24}$$

---

*This argument is tied to the Fourier representation (20) as a cosine series. A similar argument would be appropriate for a sine series. Note that the specific transient used for the array calculation (Figure 136) was a sine series.

153

where $\bar{b}$ is the average value of the Fourier coefficients b_j. (24) is a sum of terms of form (12), each evaluating to (17). Thus

$$A = \frac{1}{M\bar{b}} \sum_{j=1}^{M} b_j e^{-2\pi^2 \sigma^2 / \tau_j^2}$$

(25)

In Section II a transient waveform was described which was used to test the beam pattern of LASA/Montana (see page 146 and Figure 136). It is interesting to evaluate the loss in array gain for that specific transient. That loss is shown by the circled points in Figure 138. Note that the circles are very close to the curve for the steady-state wave. Thus the simple expression (19) and the solid curve of Figure 138 may be taken as the approximate loss in array gain when τ is identified with the dominant period in the seismic wave.
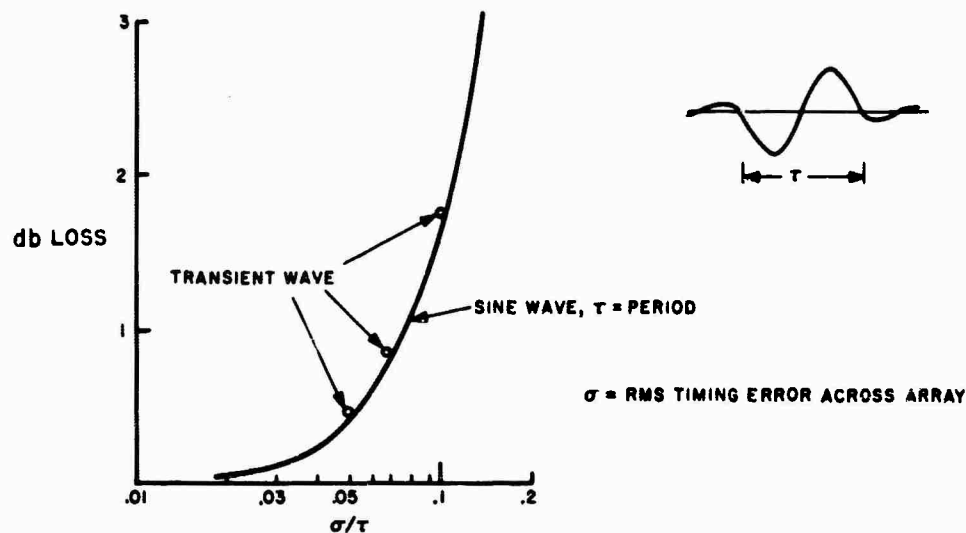
FIGURE 138. LOSS IN ARRAY GAIN DUE TO TIMING ERRORS

D. Conclusion

The rms tolerance on the irreducible minimum timing uncertainty of a seismic array is about one-tenth the dominant period of that portion of the seismic wave for which the beam is being formed. This results in a loss of less than 2 db. Beyond this error the array gain rapidly disappears.

154

16. MULTICHANNEL FILTER
by
L. A. Chamberlain, Texas Instruments, Inc.

The Multichannel Filter, shown in Figure 139, is a high speed special purpose digital processor designed specifically for the filtering problem. This particular unit will be installed in the LASA Data Center in Montana for special processing applications to be described in a later paper. As can be seen from the photograph, the MCF is contained in a single standard 19-inch relay rack eighty-three inches in height. The paper tape reader which is used in reprogramming the MCF is separately housed and is intended to be cart-mounted so that a single tape reader can service several MCF's.
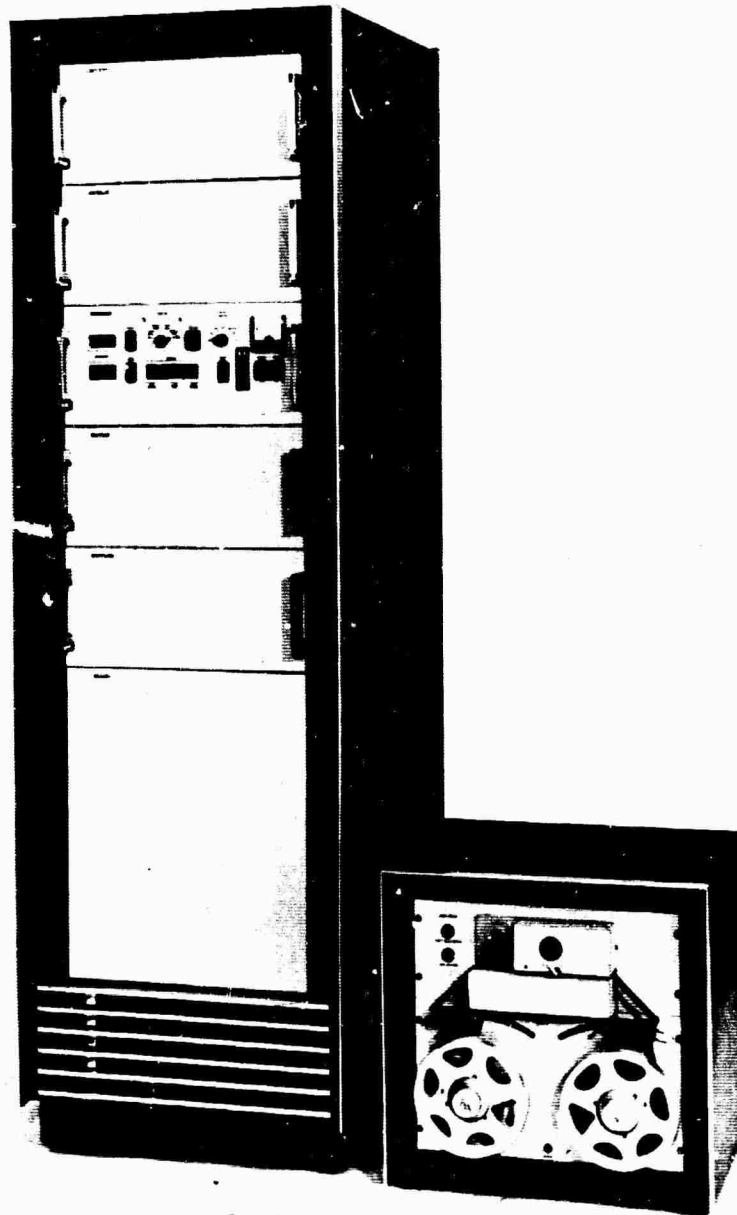
FIGURE 139. MULTICHANNEL FILTER (MCF)

The system logic is implemented using Texas Instruments Series 73 SOLID CIRCUIT® integrated semiconductor networks. The networks can be seen in Figure 140. Use of the integrated circuits has permitted the one-cabinet design and offers reliability improvement over more conventional implementations using discrete transistors, diodes and other components. All circuitry is mounted on printed circuit boards and the boards in turn plug into slide-mounted drawers allowing free access to the circuitry for maintenance and troubleshooting purposes. The system is self-contained, including its own power supply and cooling air blowers. Room air is utilized for cooling. The system operates from single phase 60 cps, 115 V power.
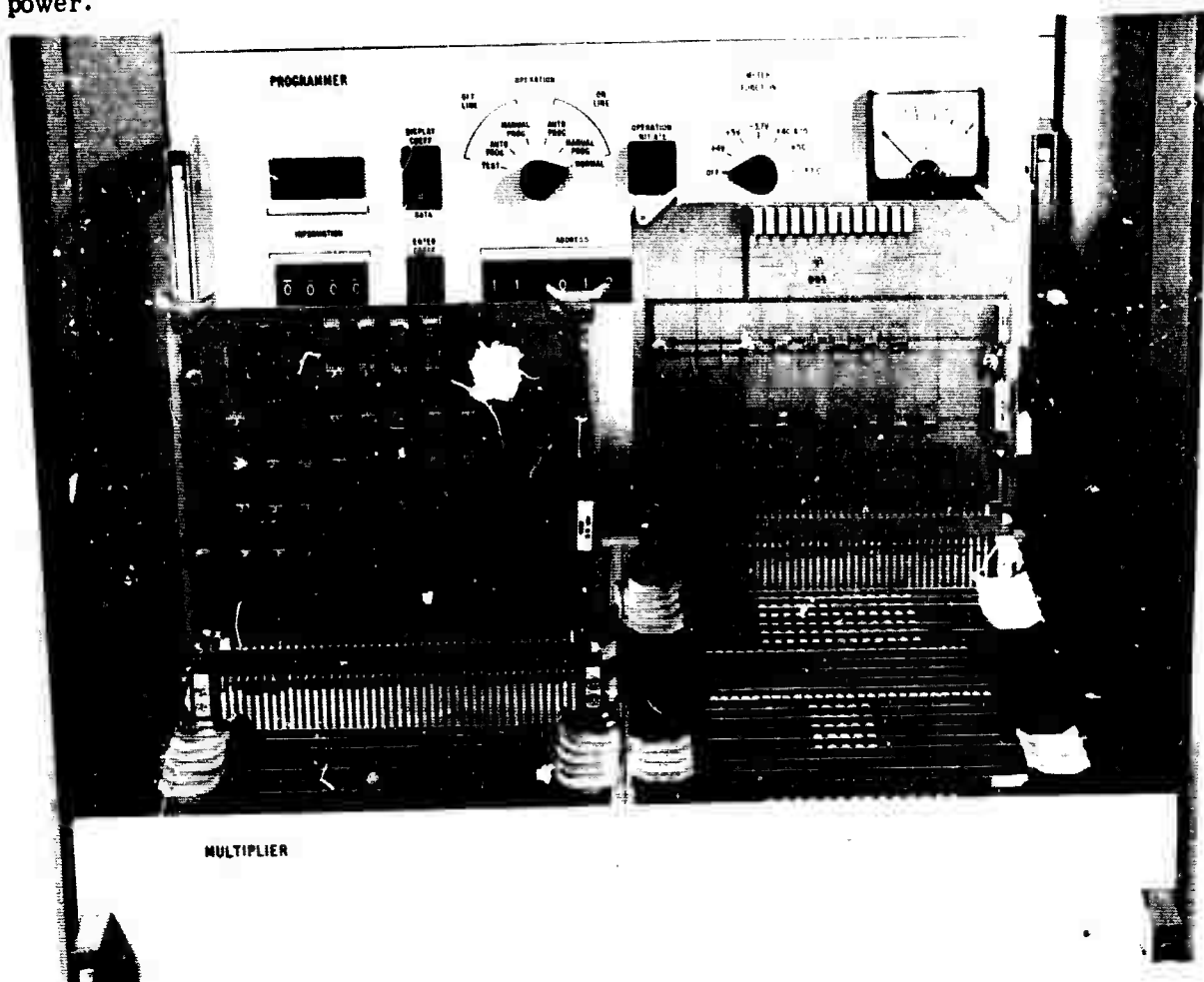
FIGURE 140. INTEGRATED SEMICONDUCTOR NETWORKS

Figure 141 lists the basic characteristics of the system. As can be seen, flexibility is provided to allow the number of inputs, outputs and points per filter to be varied. The primary restriction in selecting a format is that the product of the number of inputs, outputs and points per filter must not exceed the capacity of the memory of 8192 words.

®Registered Trademark of Texas Instruments, Incorporated

156

MCF SPECIFICATIONS

Number of Inputs	Up to 32 (25 normally used)
Number of Outputs	Up to 5
Input Word Length	12 bits, including sign*
Output Word Length	18 bits, including sign**
Number of Points per Filter	Up to 512
Quantization Precision of Filter Coefficients	12 bits, including sign
Memory Capacity	8192 words of 24 bits length
Sampling Rate	20 samples per second per channel
Basic Machine Cycle Time	2.5 microseconds

*NOTE 1: The received data word is of 15 bits length, however, only the most significant 12 bits are used in computation.

**NOTE 2: The actual word resulting from computations is of 25 bits length, however, only 18 bits are read out.

FIGURE 141. MULTICHANNEL FILTER SPECIFICATIONS

Figure 142 shows two typical formats and illustrates how, with a fixed number of inputs, a trade can be made between length of the filters and number of outputs. It should be noted here that all filters being applied at any given time must be of the same length. The number of outputs could be further reduced if even longer filters were desired. With a single output and 25 inputs, a maximum filter length of 327 points could be realized. To realize the longest possible filter, one of 512 points, the number of inputs, would have to be reduced to 16.

TYPICAL FORMATS

Number of Inputs	25
Number of Outputs	5
Points per Filter	65
Number of Inputs	25
Number of Outputs	4
Points per Filter	81

FIGURE 142. MCF, TYPICAL FORMATS

157

Figure 143 illustrates the operation performed by the MCF. To each input a separate independent filter is applied and the output of the filter is summed to produce a single output. Since the MCF system is capable of generating five outputs, the system includes 5 of the single multichannel filters illustrated in the figure. Please understand that this diagram is only a signal flow chart and does not reflect the actual hardware implementation. It should be re-emphasized that the filters, implemented by a digital computing routine, are completely independent of each other.

Figure 144 is a block diagram of the system. The Input Interface Section serves to interface the processor with the input data lines. For this particular application, serial digital data is received from a commercial telephone line data modem. The input data bit rate is 9600 bits per second and the format of each data frame, that is, one complete set of samples from each seismometer, is as follows. The data samples, comprising 25 successive words of fifteen
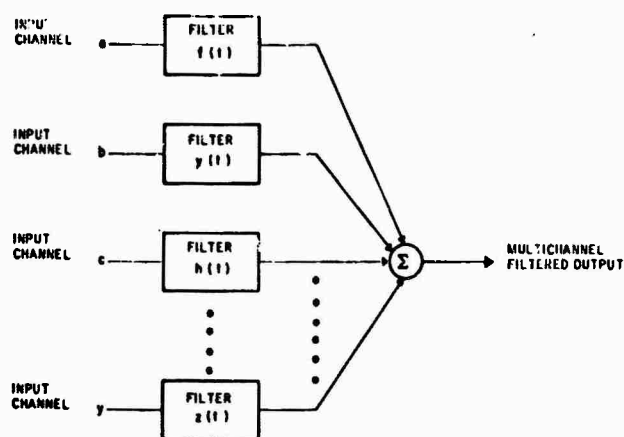
FIGURE 143. DIAGRAM SHOWING EACH SIGNAL PASSING THROUGH ITS OWN FILTER, WITH ALL SIGNALS SUMMED TO PRODUCE ONE OUTPUT
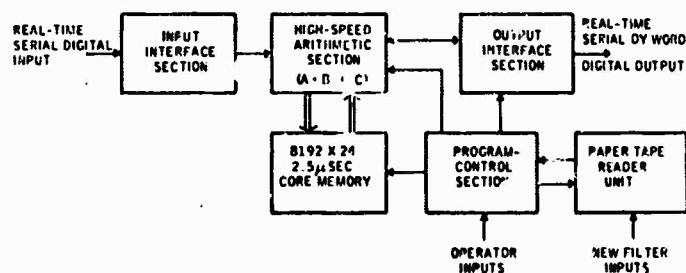
FIGURE 144. MIT MULTICHANNEL FILTER PROCESSOR BLOCK DIAGRAM

158

bits length is first received, followed by 105 bits of information which is not utilized by the processor. The fifteen bits representing each sample comprise 14 data bits (including sign) and one parity bit. A separate input line from the modem furnishes a frame synchronization pulse concurrent with the state of each data frame.

The code form utilized is straight binary with negative numbers expressed in binary two's complement form. The functions of the input interface section are to

1. receive the data and synchronize the system to the data;
2. check parity of each input word; and
3. furnish the data to the High-Speed Arithmetic Section.

The High-Speed Arithmetic Section, along with the associated core memory, is the heart of the MCF. The operation of a single multichannel filter is illustrated by the equations shown in Figure 145.

$$A_n = \sum_{k=1}^{K} \sum_{\ell=0}^{L} S_{n-\ell}^{k} a_{\ell}^{k}$$

Where

A_n = Output at time n

$S_{n-\ell}^{k}$ = The ℓth most recent data input from the kth channel

a_{ℓ}^{k} = A stored coefficient to be multiplied by $S_{n-\ell}^{k}$

K = Total number of input channels

L = Length of filter in points

FIGURE 145. MCF EQUATION

This equation illustrates the operations required to form a single output word. Since the MCF generates five outputs, five similar equations must be instrumented. Notice that the arithmetic operation performed is always of the form

$$A \cdot B + C$$

where A and B represent the product of a data sample and filter coefficient and C represents the accumulated sum of the products of filter points and data samples. Since there is a possible total of 8192 filter points, which may be divided into various combinations of inputs, outputs and filter points, there are 8192 possible arithmetic operations to be performed in one

data frame. Assuming a sampling rate of 20 samples per second per channel, fifty milliseconds is available for performing the 8192 operations, thus the maximum permissible operation time is about 7.1 microseconds. Further speed requirements are imposed by the input data format, which includes 105 bits of data not used by the processor in each frame of 480 bits. If input data is not separately buffered, a maximum operation time of about 5.8 microseconds is permitted.

The MCF is considerably faster than this, performing an operation in 2.5 microseconds, thus permitting increased sampling rates, should they ever become necessary.

The arithmetic section is simply a high-speed multiplier, which also adds the product formed to a previously accumulated sum of like products. Figure 146 is a diagram of the multiplier. Five separate accumulators, or filter registers, are provided to hold the five cumulative sums formed, one for each output. Use of five accumulators eliminates the need for operations being required to store the partial sums and greatly simplifies the control logic for the system.

To gain insight into the operation of the multiplier, consider a simple example, shown in Figure 147. The first example shown multiplies the numbers 26×29. For simplicity, numbers of five bits plus sign, or six bits, are used. Note that six summands, labeled W_1 through W_6, result.
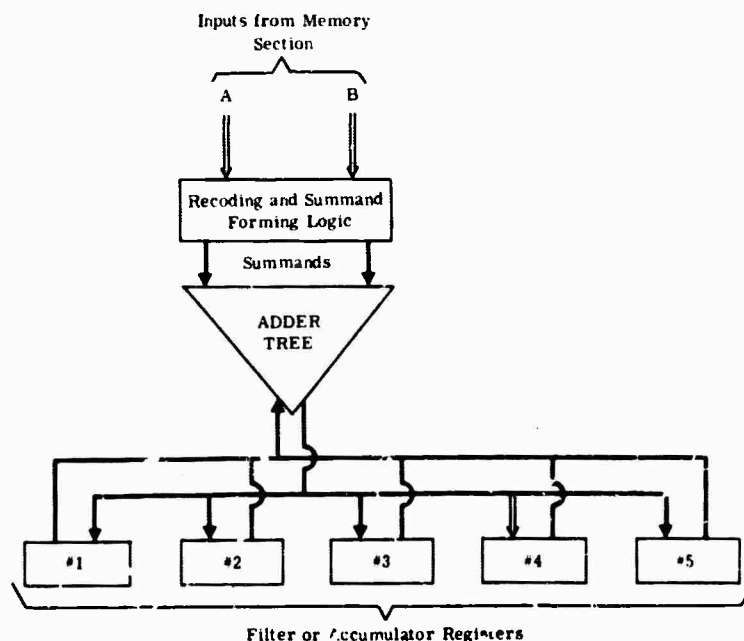
FIGURE 146. MULTIPLIER BLOCK DIAGRAM

(a) Straight Binary Multiplicatio ،

```
        0 1 1 0 1 0     Multiplicand        26
        0 1 1 1 0 1     N   ،plier          29
      0 1 1 0 1 0       " 1                 234
    0 0 0 0 0 0         W₂                    52
  0 1 1 0 1 0           W₃  ⟩ Summand'      754
0 1 1 0 1 0             W₄
0 1 1 0 1 0             W₅
0 0 0 0 0 0             W₆
0,1 0 1 1 1 1 0 0 1 0,  ————————————→ 754
Sign    Product
```

(b) Multiplication ᴏy Recoding

```
      0 1 1 0 1 0
      (+2)(-1)(+1)
      0 1 1 0 1 0         W₅
  1 1 1 1 0 0 1 1 0       W₃   (Note:  W₃ in 2's complement form)
    0 1 1 0 1 0 0    __   W₁
  0 1 0 1 1 1 1 0 0 1 0
```

FIGURE 147. MULTIPLICATION EXAMPLE

The MCF multiplier recodes the multiplier, as shown in the second example, ᴄᴏ that only 3 summands result. The recording scheme, which is beyond the scope of this short paper, is such that all multiplications performed are by +2, +1, 0. -0, -2. These are simple operations which require only shift and complement capability.

Within one clock time (2.5 microseconds) the multiplication, which consists of forming the summands and summing them, is completed. Actually, the multiplier can operate in less than one microsecond, the machine being limited in speed by the present core memory.

As stated above, the core memory is of 8!92 words capacity, each word being of 24 bits length. In addition to high speed in the multiplier, efficient utilization of the core memory is required to obtain the high operating speed of the system. Recall that the data and coefficient words are of twelve bits length. The memory stores one coefficient and one data word in one memory word. For example, the first memory location stores the most recent sample of data channel one and the first coefficient of one of the filters which is operated on the data channel. The second memory location stores the first coefficient of another filter to operate

on the same data channel. In an example format wherein five filters are applied to each input, the sixth memory address would contain the next most recent sample of input number one and the second coefficient of one of the filters. With the memory so configured, the 24 bit word read out gives the data and coefficient to be multiplied. Only one memory cycle, 2.5 microseconds, is required to fetch both words. After the read operation, the coefficient half of the word is restored in the location from whence it came, but the data sample is delayed and read back to the next data slot. Thus, the word representing the most recent sample for one iteration becomes the next most recent sample for the next iteration.

The output interface section accepts the output of the arithmetic section and makes it available to external equipment. At the end of each data frame, the output section accepts the contents of the five filter registers in the arithmetic section. To fit the requirements of the external equipment, only the 18 most significant bits of the 25-bit arithmetic unit output are transferred. The words are read to the external device in bit parallel, word serial fashion, that is, the 18-bit word representing the first output is presented as an 18-bit parallel word. When the receiving device acknowledges receipt of the word, the next 18-bit word is presented, and so on until all outputs have been read.

The program control section exercises control over the entire system and serves as the interface between the operator and the machine. To program the MCF, two operations are required. First, the format must be established. The format establishes the number of inputs, outputs and filter lengths. In this system, format is selected by inserting a printed circuit card. The alternatives existed to use cards, patchboards or switches to establish the format. The card method was selected since it was believed that formats would not often be changed and this method provides maximum assurance that incorrect formats will not be programmed and minimizes the chances of an inadvertent change.

The next operation is to load the filter coefficients. This may be done with either the paper tape reader or manual switches. The coefficient programming may be a complete loading of up to 8192 coefficients or as little as changing a single coefficient. The filters may be loaded while the machine is processing data or may be loaded off-line. The time required for a full 8192 coefficient load in the on-line mode, is approximately 5 minutes. Off-line loading is even faster.

In addition to its normal operating mode, the MCF has several test modes. These include

Step Test
Stop on Specified Address
Single Step

162

In the step test mode, a test input simulates a step function and is applied to all input channels. The outputs of the system can be examined to determine that proper response results. The stop on specified address mode is similar to the step test, except that the processor stops after a specified number of iterations. Verification of proper machine operation is then quickly obtained by reading the outputs and comparing them with known correct results. The single step mode permits advancing the MCF through its routine one step at a time for troubleshooting purposes. In addition to these test modes, the core memory is equipped with test circuitry to check it.

In conclusion, then, the MCF is a high-speed digital processor organized specifically to perform the filtering problem. Though a special purpose processor, it permits full flexibility in programming filter routines.

17. ON-LINE PROCESSING AND RECORDING
by
H. W. Briscoe
Lincoln Laboratory, Massachusetts Institute of Technology

I. INTRODUCTION

Before getting into the details of the current and proposed on-line processing for the ex-
perimental LASA, I want to spend a few minutes on our concept of the overall processing for
data from LASA and then summarize the terminology we will use for various processing
techniques.

A. LASA Processing System Concept

Figure 148 shows a block diagram of the LASA processing system. The various func-
tions will be divided into on-line and off-line operations. Initially, the off-line operations are
being performed at Lincoln Laboratory; but, as analysis procedures are evaluated, the most
effective will be implemented at the LASA Data Center.
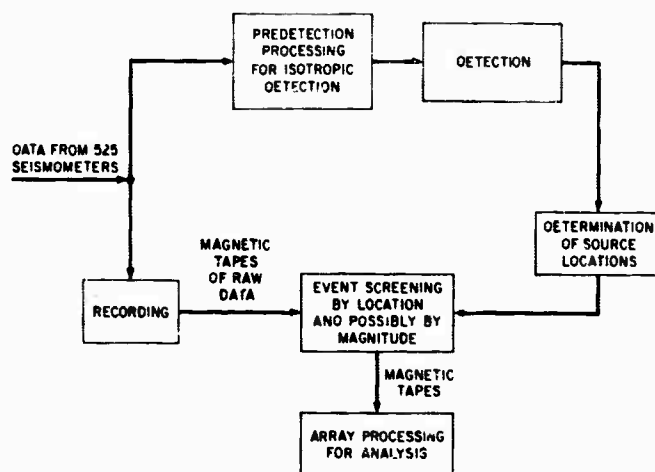
FIGURE 148. LASA PROCESSING SYSTEM BLOCK DIAGRAM

The on-line processing consists of a predetection processing stage to improve the signal-
to-noise ratio for detecting P waves, detection and determination of relative arrival time across
the array, source location for detected events, screening to select those events occurring in
areas of particular interest, and recording of raw and processed data for off-line processing.
Clearly, the predetection processing and detection must be done in real time or an ever-
increasing backlog of data will accumulate. The programs now operating in the PDP-7 in the
LASA Data Center include an experimental version of each of the operations except source
location.

164

Off-line processing at the Data Center will ultimately consist of optimum processing to use the full resolution of the array to extract waveforms of the most useful phases and parameters for discrimination between natural events and man-made explosions.

B. The Hierarchy of Linear Processing Techniques

During the experimental operation of the LASA, we are evaluating the relative costs and relative effectiveness of a series of linear processing procedures for predetection and post-detection processing. This work is being done off-line at Lincoln Laboratory and will be discussed in detail by P. E. Green, Jr. in a later paper. The terms we will use in this and succeeding papers to describe the various processing techniques are listed in Figure 149. Generally, there are adaptive procedures in which the parameters are varied with time in order to optimize the processing to reject the seismic noise as the character of the noise changes, and there are non-adaptive procedures designed from ideal noise and signal models. Parameter changes in the adaptive techniques can occur when the noise in the processed outputs reaches a certain level (for on-line operation), or the parameters may be completely redesigned for each event (for off-line analysis).

The straight sum consists of simply adding all the seismometer outputs together. It is an optimum processing for extracting signals with infinite horizontal phase velocity from uncorrelated noise. Delay and sum is the same as the straight sum except that each seismometer output is delayed to account for signal travel times of the wavefront to the stations and the individual station corrections before summing. Weighted delay and sum are the same as the above except that data from each seismometer essentially has a different gain. The gains can be determined to give a desired side-lobe response based on a hypothetical noise and signal model or can be based on periodically measured and updated noise and/or known signal parameters (adaptive). The filter and sum processing allows a different filter or frequency sensitive gain on each seismometer, and it can also be adapted to measured noise characteristics or based on a hypothetical model.

ARRAY PROCESSING

NON-ADAPTIVE	ADAPTIVE
STRAIGHT SUM	WEIGHTED DELAY AND SUM
DELAY AND SUM	FILTER AND SUM
WEIGHTED DELAY AND SUM	
FILTER ND SUM	

FIGURE 149. ARRAY PROCESSING TECHNIQUES

II. ON-LINE PROCESSING IN THE EXPERIMENTAL ARRAY

A. On-Line Equipment

Figure 150 shows the equipment that is now being installed at the experimental LASA Data Center. The current status of the installation has already been described by R. G. Enticknap. The equipment has been selected to provide a flexible capability to experiment with different procedures for accomplishing the on-line processing. Experimental on-line development, demonstration, and evaluation of each required step in on-line operation is possible with this equipment configuration although the implementation of an operational on-line processing capability will probably require addition of new equipment and possibly replacement of some of the existing equipment. For example, we will develop and demonstrate a predetection processing and detection logic and evaluate the resulting detection threshold using a single complete channel of processing and detection. We will also demonstrate and evaluate the ability to locate the source of an event as a function of the detection threshold using several raw seismometer traces or sub-optimum processed traces. We will then be able to specify the equipment required to combine the two techniques in an operational system and to accurately predict the performance of the operational system.
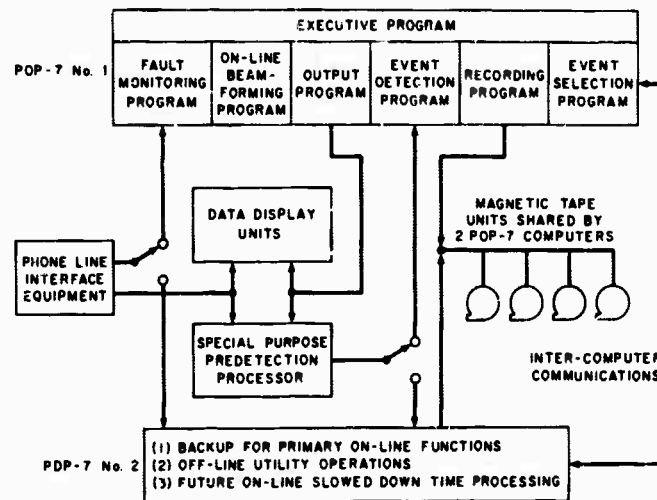
FIGURE 150. ON-LINE PROCESSING EQUIPMENT AT LASA DATA CENTER

The flexibility inherent in this equipment configuration ` be illustrated by describing a few of the on-line systems we expect to try. In each system the PDP-7 computers provide the central control and bookkeeping and also provide magnetic tape recordings of the raw and processed data, Develocorder recordings of key waveforms, and typewriter lists of system parameters and decisions such as arrival times of detected events. Source location will also be done

in a PDP-7 using raw sensor data, subarray sums, or processed data from the MCF or other PDP-7 programs.

1. Filter and sum predetection processing on the 25 seismometers in a single subarray will be performed using the Multi-Channel Filter (MCF) processor built by Texas Instruments, Inc. for Lincoln Laboratory. The output of the MCF will be used in the PDP-7 to perform detection and time picking. At the same time, a few high resolution beams (sum, delay and sum, or weighted sum and delay and sum) will be formed in the PDP-7 and detection and time picking on these resulting traces will also be performed in the PDP-7 to provide a comparison of the capability of beamforming and filter-and-sum processing for predetection processing. Evaluation of beam splitting techniques for source location can be performed off-line in the second PDP-7.

2. Filter and sum using 25 elements collected from an area larger than a subarray will be performed by selecting the data to be used in the PDP-7 and feeding the simulated super-subarray data from the PDP-7 to the MCF. The MCF output will go back to the PDP-7 for detection and time picking.

3. Filter and sum of precombined groups of seismometers from several subarrays may be tried by combining the seismometer groups in the PDP-7 and operating the MCF on the precombined data. MCF output would go back to a PDP-7 as in the experiments above.

The experiments listed above will be used to do competitive evaluation of various techniques on-line. As an illustration of system capacity, the system of programs operating in the PDP-7 at Billings performs:

1. Fault monitoring, including calibration of the seismometers
2. Recording of all data on magnetic tape
3. Formation of five beams from the 21 (or all operating) subarray sums
4. Detection of events on eight channels (raw traces or beams)
5. Bookkeeping and typewriter printout of results from 1 and 4.

This program system uses only about one-third of the available real-time, but uses the entire 8K memory of the first PDP-7. As a result, the second PDP-7 computer to be delivered at Billings will have twice the memory capacity. When the larger memory is available, this initial system will be augmented to implement the first system described above by addition of programs for source locations, Develocorder recording of selected data, and using the MCF processor. This system will be operated long enough to evaluate it and then changed to try other techniques.

I would like to spend the rest of my time considering in more detail the present state of our investigations into techniques for the on-line processing.

B. Predetection Processing

Figure 151 gives a summary of the requirements for predetection processing. The first requirement, real-time operation, limits the use of adaptive processes to those for which the processing required for adapting to changes in the model is either simple or for which the required changes are infrequent. If the resolution (beamwidth) of the predetection processing is so fine that many processed outputs are required for an isotropic capability, the equipment requirements for real-time operation may become unreasonable.

1. MUST OPERATE IN REAL TIME
2. MUST HAVE ISOTROPIC DETECTION CAPABILITY
3. MUST ALLOW SOURCE LOCATION FROM THE DETECTED DATA
4. MAY PRODUCE MODERATE SIGNAL DISTORTION

FIGURE 151. PREDETECTION PROCESSING CRITERIA

Predetection processing techniques that will be tried or have been tried include:

1. Straight sum — The analog sums formed at the subarray vaults at Sites B1 and F3 were compared with single seismometers for detection capability during experiments in May and June and did not seem significantly better than the single seismometers.

2. Delay and sum (beamforming)— For essentially the same complexity, beamforming can be done with adaptive or theoretical weighting instead of simply delay and sum. Since seismic noise is distinctly not random, side-lobe control using tapering offers important gains in signal-to-noise improvement. On-line beamforming experiments are being done using the PDP-7 to form a few high resolution beams. In order to get good isotropic signal-to-noise improvements by beamforming a large number of relatively high resolution beams will have to be used, and detection will have to be performed on each beam. Source location would be determined by the steering of the beam with the largest output.

3. Filter and sum— Filter and sum processing clearly provides the most versatile control of the processing for separating regions of signal and noise. With this form of processing it is possible to get both the wide acceptance band for isotropic P-wave surveillance and still get high noise rejection with only a few processed output traces. The cost, of course, is in length of computation. With the prototype digital MCF at Billings, it will be possible to perform the complex processing on-line in real time.

The load on the detection function is light because only a few processed channels are required for isotropic detection capability, and source location can be done explicitly using triangulation and can be less sensitive to failure of sensors or entire subarrays.

C. Detection

The detection logic now programmed for the PDP-7 is shown schematically in Figure 152. Data is bandpass filtered and rectified. The rectified channel is then integrated, delayed, and divided into the original rectified channel. The quotient is then tested to see if it goes above set threshold. The delayed channel provides an AGC so that the detection is not sensitive to gain changes. Figure 153(a) and (b) illustrates the event detector operation on a moderate sized event and a very weak event. If the bandpass filter is tuned to the characteristics of the input trace, the same logic can be used on processed or raw traces.
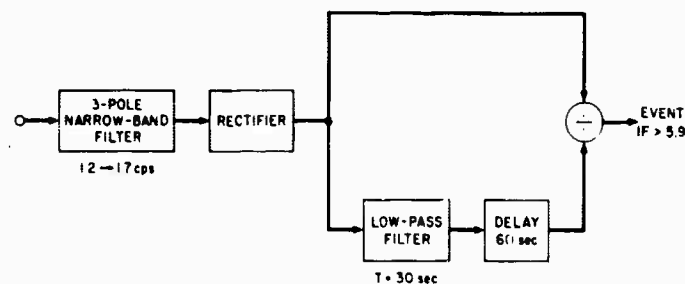
FIGURE 152. BLOCK DIAGRAM OF DETECTION LOGIC

Figure 154 shows a comparison of the event detector output and a human analyst both using raw seismometer outputs from subarrays B1 and F3 during the experimental operations in May and June.

The false alarm rate is high on a single trace, but a restraint requiring detection on three or more of five-to-seven event detector outputs (three sites are required for source location by triangulation) does an excellent de-ghosting job.

D. Source Location

The method used for source location is partly determined by the form of predetection processing and detection being used. If detection is done on individual processed or raw traces from widely separated seismometers or groups of seismometers, source location is done by a sort of triangulation using relative arrival times at the various points of detection. Experiments using the extended TFO array and the Weston College Network in New England have shown that if relative arrival times are picked to about 0.1 second and station corrections are applied to remove biased values, the source of a seismic disturbance can be located to $\pm 2^0$ in latitude and longitude with stations located at the extreme LASA subarrays. This accuracy is adequate

169
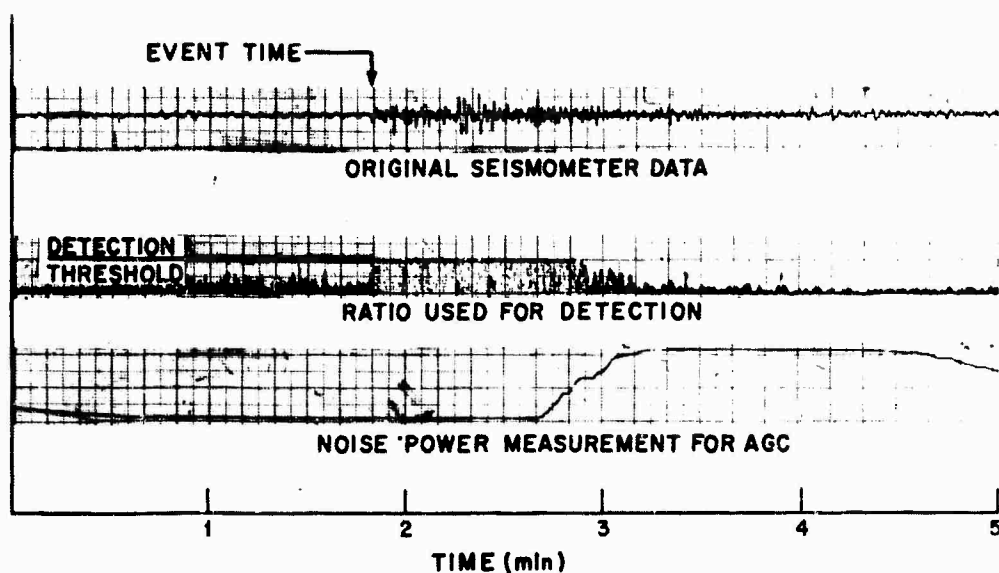
FIGURE 153(a). EVENT DETECTOR OPERATION ON A MODERATE TELESEISM FROM KODIAK ISLAND, ALASKA
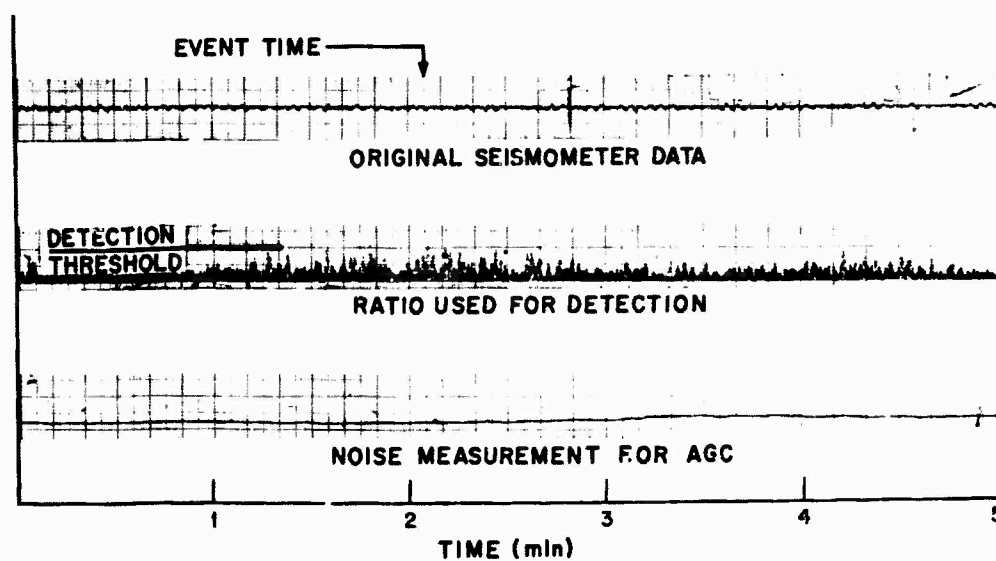
FIGURE 153(b). EVENT DETECTOR OPERATION ON A VERY WEAK TELESEISM FROM RAT ISLAND, ALEUTIAN ISLANDS

for reasonably effective screening of events and is comparable to the effective beamwidths of the LASA so optimum forms of array processing can be carried out with the source locations determined by the array itself.

170

As signal strength gets weak, the accuracy of arrival time determination by the event detector gets poor and errors of as much as a second (about one cycle of signal energy) have been observed on events that can be reliably detected. Several approaches for improving time picking are being considered. Variations in the detector logic are being investigated, and techniques involving correlations of the processed waveforms when an event is detected have been tried and show promise but are computationally costly. Where an event is detected at more than the minimum three stations, the redundant times can be used to improve the source location accuracy to partly compensate for errors greater than the 0.1 second objective for arrival time determination at each point being used.
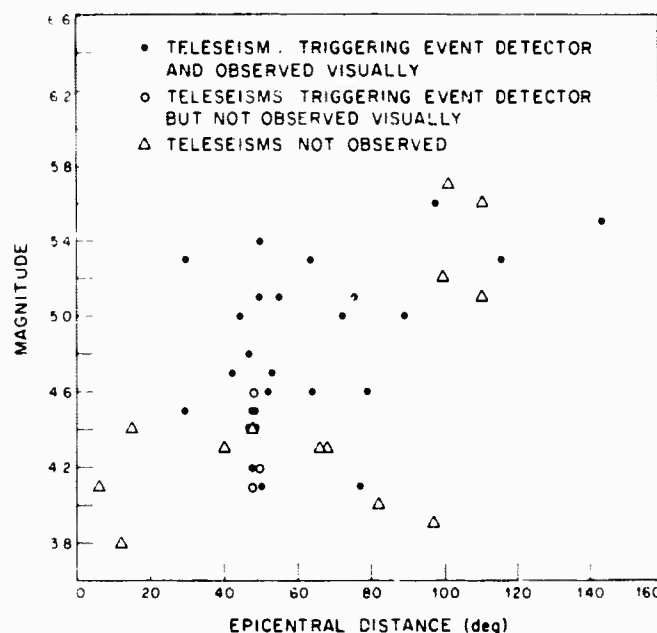
FIGURE 154. COMPARISON OF PERFORMANCE OF EVENT DETECTOR AND ANALYST

E. Recording

Because of the need to start with the raw data in order to realize the full resolution of LASA to detect each phase of arriving energy to be used in analysis of a suspicious event, we intend to save all the raw data from the experimental LASA on digital magnetic tape until detection, source location, and screening are completed. Those raw data tapes which do not contain detected events from potentially interesting areas will be written over since it would be impractical to save all the raw data. When an event is selected for off-line analysis, the recorded data tapes are removed from the system before they are written over. Each tape contains about 10 minutes of data, and 20 to 30 minutes of data including 5 to 10 minutes before the event must be saved for analysis of a detected event. Thus, using two tape drives for recording will

allow about 10 minutes delay for detection and screening before a tape must be removed or switched out of the system. Ten minutes is a long time for a computer, but an operator must move fast to change the tapes so it is likely that three or more drives will be necessary.

The processed traces from predetection processing will be saved on a Develocorder and a separate magnetic tape recording. Tapes containing on-line processed data from the entire period of operation of the array will probably be saved so that the output from LASA may include continuous recordings of processed data and recordings of all the raw data during interesting detected events or pre-requested time periods.

The on-line typewriter on the PDP-7 is used to record a variety of information for the use of the LASA Data Center personnel and the analyst. The printouts include, for example, equipment failures determined by the fault sensing programs, indications of parity checks from the magnetic tape recorders, and arrival times of detected events.

18. LASA OFF-LINE ARRAY PROCESSING RESULTS

by
J. Capon
R. J. Greenfield
P. E. Green, Jr.
Lincoln Laboratory, Massachusetts Institute of Technology

I. INTRODUCTION

For the last several months we have been processing digital array data from TFSO and LASA, the purpose being to establish tradeoffs between signal-to-noise enhancement achieved versus the complexity or cost of doing the processing. Only when these tradeoffs are well understood will it be possible to design with certainty the on-site processing hardware, make a statement about LASA system performance to be expected, or speculate about combinations of LASAs. The results described here are relevant to the predetection array processing which Briscoe described as necessary for on-line event screening and recording, just as much as to the question of off-line processing of 525-sensor LASA tape recordings. The unprecedentedly large aperture and large number of sensors mean that previously existing results on this subject are of only modest assistance in seeking the desired tradeoff relations. The tradeoffs to be discussed in this paper are between processing signal-to-noise ratio (SNR) gain and the following factors: number of sensors used, how often the noise statistics are measured, the length of the noise measurement interval, the length of filter functions, the inclusion of frequency filtering, and the amount of random variation in seismometer amplitudes and phases.

Array processing schemes, which map the set of N traces out of the seismometers onto a single output trace, can be divided into the various categories shown in Figures 155-158, and already discussed by Kelly. These are straight summation, delay-and-sum, weighted delay-and-sum, and filter-and-sum. We limit ourselves to linear processing with the understanding that nonlinear operations, if any, will be applied to the output trace after the SNR has been improved.
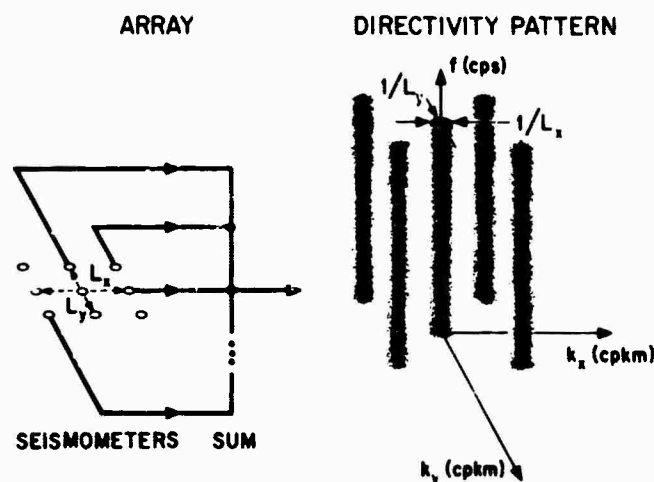
FIGURE 155. ARRAY PROCESSING, STRAIGHT SUM

173

ARRAY   DIRECTIVITY PATTERN
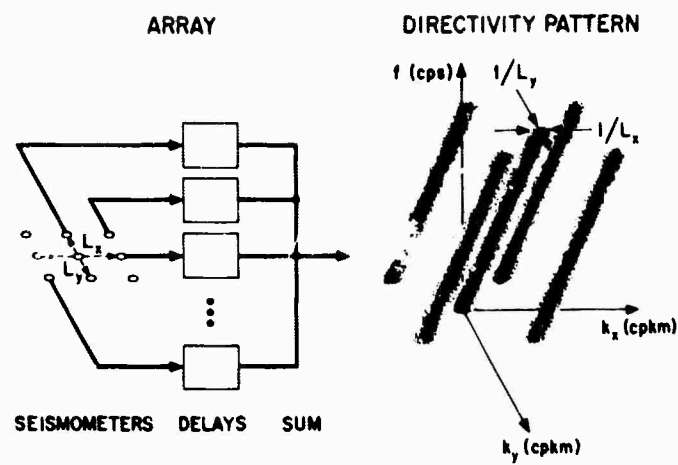
FIGURE 156. ARRAY PROCESSING, DELAY-AND-SUM

ARRAY   DIRECTIVITY PATTERN
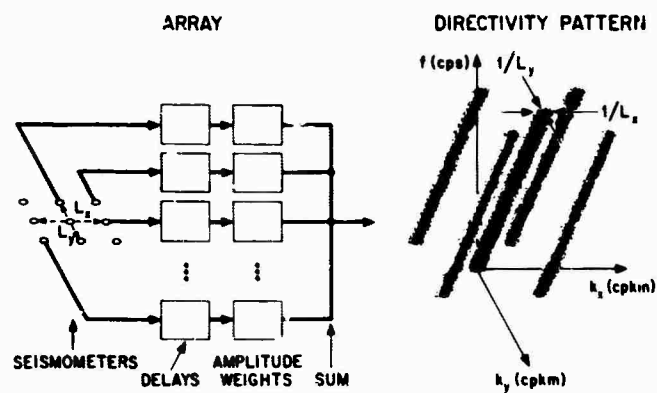
FIGURE 157. ARRAY PROCESSING, WEIGHTED DELAY-AND-SUM

ARRAY   DIRECTIVITY PATTERN
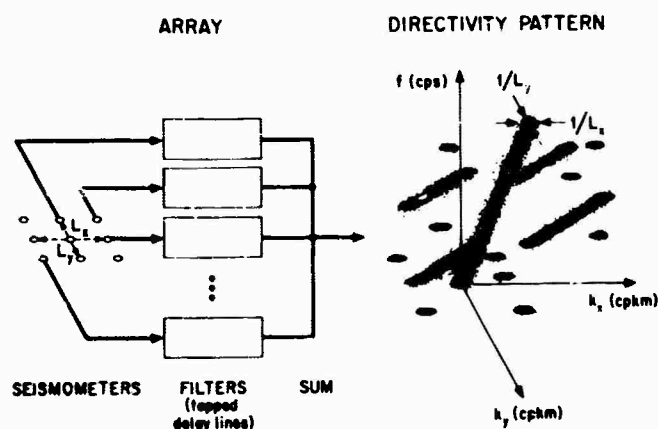
FIGURE 158. ARRAY PROCESSING, FILTER-AND-SUM

174

II. SNR AS A FUNCTION OF NUMBER OF SEISMOMETERS

Figure 159 shows a summary of the SNR gains achieved using various numbers of LASA sensors. SNR is defined as the ratio of the squared peak-to-peak amplitude of the largest initial P-wave oscillation to the noise power. To allow simple comparisons to be made between filter-and-sum, weighted delay-and-sum, and delay-and-sum, the issue of frequency filtering was deferred by using for the particular form of filter-and-sum processing the so-called maximum-likelihood procedure. This procedure, although involving frequency filtering of individual traces, produces an output trace in which no frequency distortion is present; that is, the sum of the N-filter frequency functions is flat in frequency. Another way of saying this is that the sum of the impulse responses of the filters is effectively an impulse. Frequency filtering before and after array processing will be discussed shortly as a separate issue.

The data in the figure are based on small samples, namely 2 runs for N = 6, 7 for N = 9, 4 for N = 25 (four subarrays on an event of August 27) and 1 for N = 100 (the maximum-likelihood outputs of the same four subarrays combined by delay-and-sum). The data should thus be taken as very tentative.

In attempting to find shortcut methods of approaching the full max-likelihood processing SNR gain for a given N without having to actually treat N individual seismometers, several attempts were made to pre-combine the 25 sensors in a subarray into groups by delayed summation of the members of a group. The smaller number of traces resulting from this were then subjected to max-likelihood processing. The results were very disappointing, as shown by the circle and star points in the figure, which are for the event of August 27 observed at subarray C4. The circle represents the result of delayed summing the members of each of
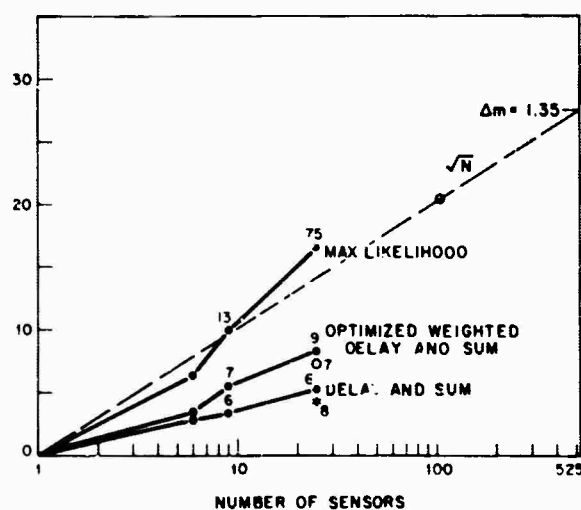
FIGURE 159. RATIO OF PROCESSOR OUTPUT SNR TO AVERAGE INPUT SNR FOR VARIOUS PROCESSING SCHEMES

175

four rings of seismometers in a subarray, then max-likelihood processing these four plus the center sensor. The star point shows the result of delayed summing within each of the six spokes of a subarray and then processing the six resulting traces. (The center sensor was included in one spoke.)

The small numbers underneath each point are the number of minutes of 7094 computer time required to do the complete processing job, including in the case of max-likelihood and weighted delay-and-sum, the time necessary to compute the $N \times N$ correlation matrix from a three-minute noise sample. The 75 minutes required per 25-element subarray subdivides as follows: 40 minutes for noise correlation matrix computation, 20 minutes for filter design and 10 minutes for processing of 25 input traces to produce the output trace. Five minutes of setup time are required in all cases. It is obvious that frequent noise recomputation and filter design is undesirable so that data on noise stationarity is important.

III. NOISE STATIONARITY

The best operational test of noise stationarity was considered to be to process the event of a given day with max-likelihood filter functions designed from noise on a different day to see how much SNR gain dropped because the filters were synthesized on the wrong noise. The insensitivity to this effect evidenced by the very limited data obtained to date is encouraging, especially when one can observe that simple statistics like power level change in a matter of hours.

Specifically, a November 1964 event at TFSO was processed using the 10 minutes of noise immediately preceding the event and a 10-minute noise sample 8 days earlier, and a 4 db loss was observed. This was repeated for a one-hour lapse and in this case no measurable loss was found. Two such pairings at LASA have been observed, roughly a 6 db drop for a May 13, 1965, event processed with filters designed from noise 14 days earlier, and a 6 db drop for an August 19, 1965, event processed with filters from noise occurring 8 days later.

IV. REQUIRED LENGTH OF NOISE MEASUREMENT INTERVAL

The duration of the correlation matrix measurement step in the processing, the most time consuming step, is proportional to the measurement interval. Therefore, it is important to know how short a measurement interval can be used. Figure 160 shows the results obtained in studying this question on an April 22 event at subarray B1, using nine sensors.

The height at which each bar is plotted is the rms noise level actually observed on the processed trace in the interval given by the location and length of the bar laterally. It may be seen that although the 0.5 and 1 minute filters give good noise reduction during their measurement intervals they do not work satisfactorily outside it. (Compare the results of the 2 and 3

176
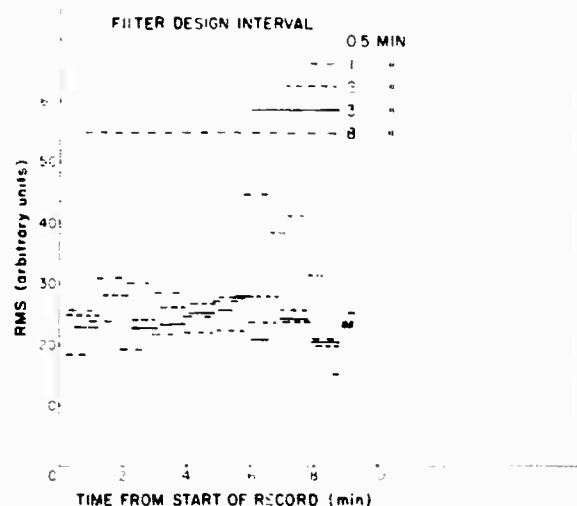
FIGURE 160. RMS NOISE LEVEL OF MAX-LIKELIHOOD TRACE vs TIME

minute filters.) From these studies we conclude that for nine seismometers 1 minute or less is definitely too short a measurement interval. Two minutes is marginal and three minutes is safe. If the measurement interval ends within 0.5 minutes of the event, it seems improbable that the filters designed on three minutes could, on the average, give filtering more than 0.5 db worse than the ones designed on eight minutes. This possible slight improvement does not justify the added computation time needed to obtain a filter based on eight minutes of noise. This entire experiment is being repeated for $N = 25$.

V. EFFECT OF FILTER LENGTH

The duration of the impulse response of each filter in the max-likelihood processor is the product of two quantities, NIP, the number of .05 second digital sampling intervals between adjacent filter sample points, and NFP, the number of filter sample points. If NIP is made too small, the impulse response duration for a given NFP is insufficient to give the desired frequency resolution and the long-period noise suppression will suffer; if it is too long, frequency aliasing introduces noise into the output. Experiments with NIPs of 1, 2, 5, and 10 with NFP fixed at 21 showed that for nine sensors, NIP = 2 gives the best compromise.

Figure 161 shows the effect of the filter length on SNR gain, using NIP = 2. Along the lower curve the filters are completely "physically realizable," that is, the sum of their impulse responses is zero for all values of delay except the first one at which the sum is unity. Along the top curve, the filters are unphysical in a "symmetrical" way: the sum of the impulse response is zero except at the very center sample point at which they sum to unity.

It is seen that the symmetrical arrangement is the best, as has been verified theoretically. (Separate experiments with the impulse at the tail rather than head of the sum of responses show that these two asymmetrical conditions are about equally poor.)

177
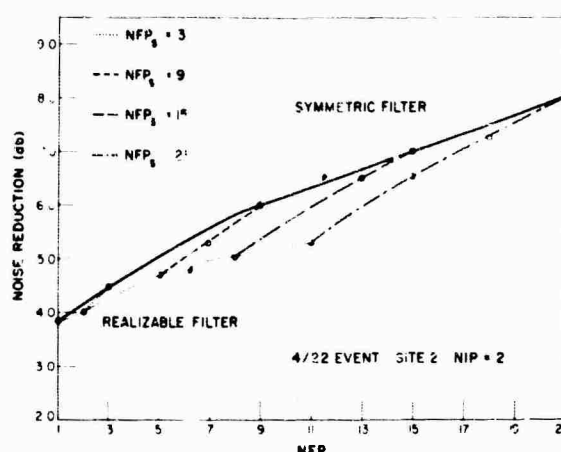
FIGURE 161. EFFECT OF FILTER LENGTH ON SNR GAIN

VI. EFFECT OF FREQUENCY FILTERING

Examination of one of the seismometer output traces or any of the processed traces shows that in both instances the frequency spectrum of signal and noise are different, the main power of the noise being mostly of longer period, especially in the input traces. Figures 162 and 163 show the results of a simple experiment designed to determine the SNR gains available by frequency filtering of all traces before processing and by frequency filtering the single trace afterwards. Nine input traces, the weighted delay-and-sum (WS), delay-and-sum (DS), and max-likelihood (ML) traces are shown in order without input trace filtering on the left and on the right with such filtering. High pass filters with a 0.5 cps cutoff were used. Note the signal distortion due to filtering. In Figure 163 the ordinate is in db relative to the average noise in the nine unfiltered traces. The run chosen was an event of April 22, 1965 at subarray B1 This had been a below-average run from the standpoint of SNR gain; it did not quite achieve $\sqrt{N}$ using max-likelihood processing. The results given in the left-hand column of data show the effect of filtering after the processing and the right-hand column the results for frequency filtering before the processing. (The filtering is portrayed by the heavy arrows.)

It is seen that the figure on SNR gain versus N quoted in one of the earlier figures in this paper can easily be bettered, if frequency distortion of the signal is allowed. Since the seismometer itself is already doing some of this, modest additional distortion of the signal such as just seen would appear to be perfectly permissible, particularly for predetection processing.

Incidentally, it is appropriate to remark here that if one follows the max-likelihood processing operation with a single Wiener filter (designed from the noise in the output trace and an assumed signal spectrum and SNR to effect an optimum compromise between noise and distortion), then the combined process is equivalent to the Wiener array processing introduced several years ago by Texas Instruments, Inc. Several experiments have been done using this form of postfiltering of the max-likelihood trace.

178

HEADER

220100005130

REFERENCE UNIT

1HRS 47MIN 15.5 0SEC

REEL 02Y257

LEVELS/INCH

250.3?
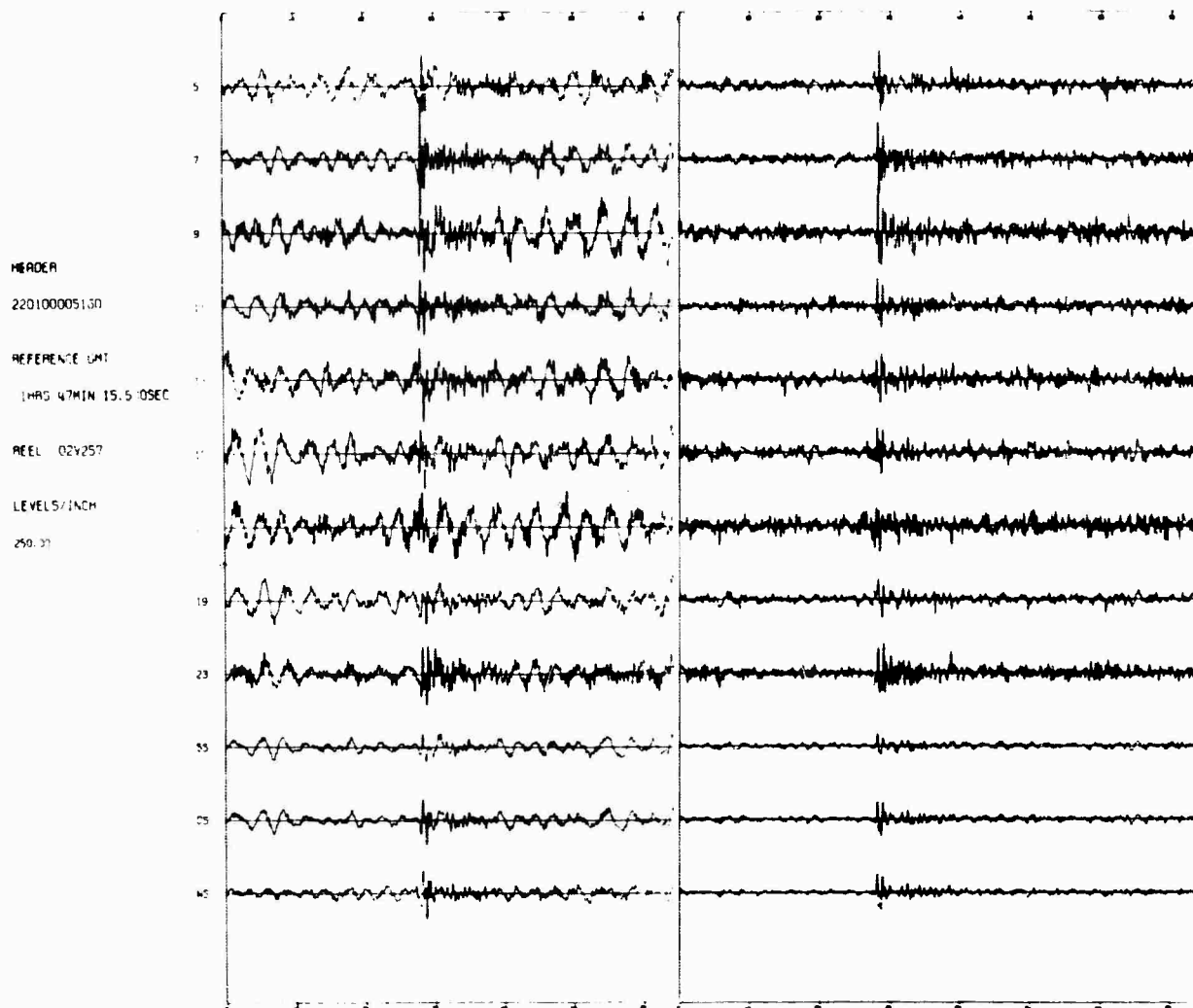
FIGURE 162. RESULTS OF PROCESSING NINE SIGNALS BY THREE METHODS WITHOUT AND WITH HIGH-PASS PRE-FILTERING
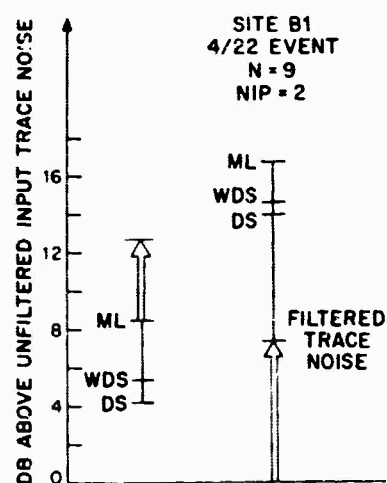
FIGURE 163. PROCESSING GAIN REALIZED BY THREE METHODS WITHOUT AND WITH HIGH-PASS PRE-FILTERING

179

VII. SENSITIVITY OF THE PROCESSING TO SEISMOMETER DIFFERENCES

Figure 164 shows the four N = 25 max-likelihood output traces of the event of August 27 for the four subarrays that were used to get the N = 100 point on the curve of SNR gains versus N shown earlier. The subarrays were F4, A0, C4 and F2, so that the entire 200 km aperture was spanned. (The traces were delayed and summed to produce the bottom trace using eyeball time delay picks since the appropriate station corrections were not yet available. The traces of the subarray outputs in the figure are shown as received, rather than time-shifted, with the delayed sum (DS) referenced to the F4 subarray trace.) Note that there is a 2.0 db loss in amplitude of the first positive half-cycle; this figure constitutes a reasonable operational measurement of coherence.

The seismometer output signal amplitudes were slightly different, rms deviations averaged over the four sites were ±14.5%. It is clear from Figure 164 that signal amplitude caused the processing no trouble.
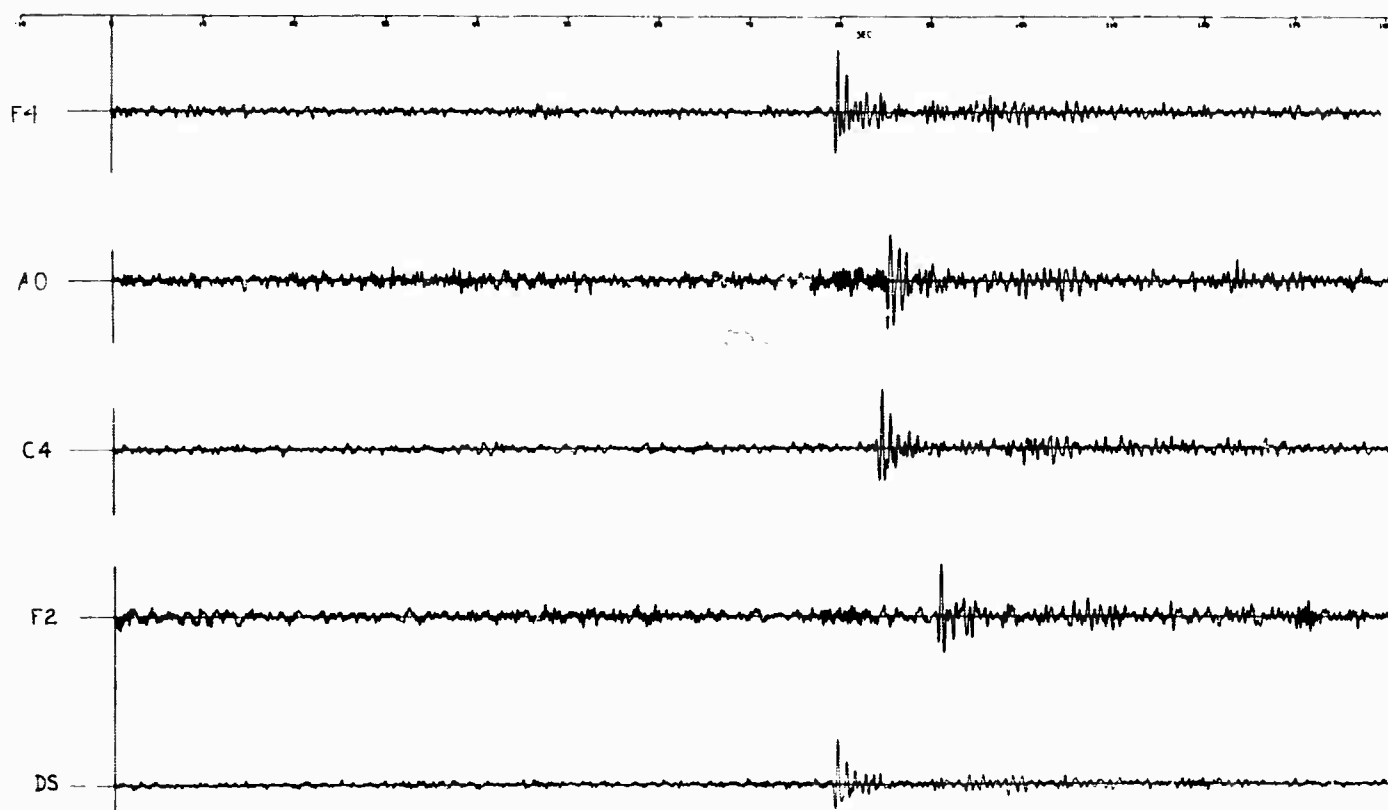
FIGURE 164. DELAY-AND-SUM (DS) OUTPUT OF FOUR LASA SUBARRAYS

180

19. A LASA SIGNAL PROCESSING SYSTEM
by
R. G. Baron, W. Vanderkulk and S. D. Lorenz[*]
International Business Machines Corporation
Federal Systems Division

INTRODUCTION

The purpose of this paper is to present a processing system that will modularly handle the full range of signal processing techniques under consideration for the Large Aperture Seismic Array (LASA) system. Two system configurations are presented. The first assumes that only subarray processing is performed at the array site, and an alternate system considers all processing performed at the array site.

SYSTEM FUNCTION

In order to provide a basis for processing system synthesis, it is assumed that the primary function of the LASA signal processing system is to utilize the full capability of the LASA seismometer field to detect, edit, record, and assist in classifying teleseismic events occurring in a specified azimuthal sector spanning 60° and at great circle distances between 30° and 94° from the LASA site. The event magnitudes of interest range from eight down to the full LASA processing capability. As a secondary function, the system may also be called upon to utilize the full array to monitor events outside of the aforementioned azimuthal sector and contained within specified portions of a vertical beam. The tertiary function is to monitor events external to the above mentioned areas of interest that are detectable on a subarray.

The detection, editing, and recording functions must be executed in real-time and serve to produce a tape recording of events of interest which must be analyzed in detail for the purpose of classification. Although this classification analysis is allowed to proceed off-line, reasonable bounds on the event backlog must be maintained.

Since classification relies in part on the analysis of the high-frequency contents of the signal (up to about 3 cps), preservation of the high-frequency signal phase and amplitude spectrum on the edited and recorded tape is required. On the other hand, detection demands a high-signal-to-noise ratio. Since the signal-to-noise ratio is expected to peak at or below 1.5 cps, it is only necessary to minimize signal power loss at or below 1.5 cps for the real-time detection function; while signal distortion and attenuation at the high frequencies (at or above 3 cps) can be permitted. The detection beams are referred to as "coarse beams" and the high fidelity beams employed for classification purposes are referred to as "vernier beams."

---

[*]At the LASA System Evaluation Conference, presentation papers were delivered by Vanderkulk and jointly by Baron and Lorenz. This paper combines the aforementioned to unify and consolidate the system concept described.

The beam coverage requirements to achieve the above mentioned functions will now be addressed. The array contains 21 subarrays of 25 seismometers each. A subarray is distributed over an area of 7 km diameter. The subarrays, although clustered near the center, are for the most part sparsely distributed over an area of 200 km diameter. Assuming a horizontal planar array of N elements whose element positions are denoted by the vectors $\overline{r}_n$ the loss for conventional beam forming in a homogeneous medium is

$$\text{Loss} = -20 \ \log_{10} \left| \frac{1}{N} \sum_n \exp\left[2\pi i \overline{r}_n \cdot \overline{\Delta k} \right] \right| \text{db}.$$

The vector $\overline{\Delta k}$ may be expressed as:

$$\overline{\Delta k} = f \left(\underline{u} - \hat{\underline{u}} \right)$$

where f is the signal frequency in cycles per second and $\underline{u}$ and $\hat{\underline{u}}$ are the wave number vectors at the positions of the received signal wave front and of the wave front to which the beam has been steered respectively. Figure 165 depicts beam pattern cross-section of the worst and best case azimuths. If u_x and u_y are the reciprocal horizontal velocity components, east and north respectively, the azimuth angle is:

$$\phi = \tan^{-1} \left(u_y / u_x \right)$$
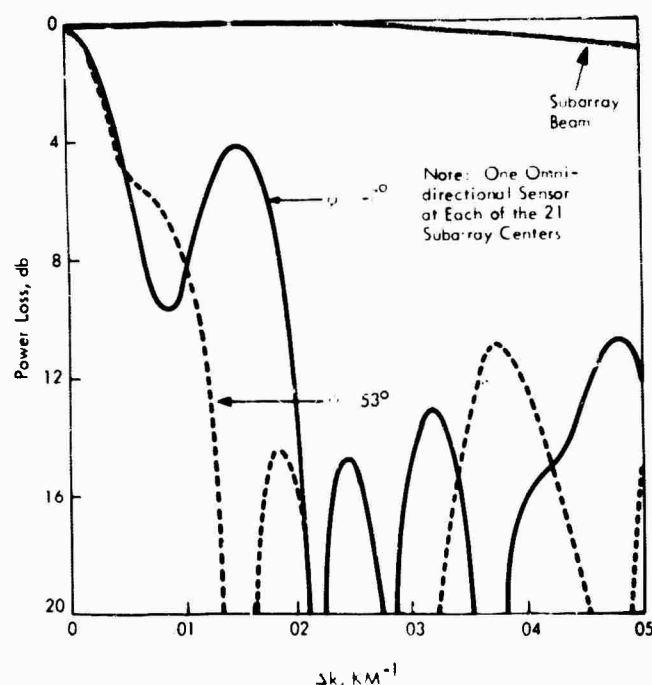
FIGURE 165. SINGLE FREQUENCY BEAM PATTERN

182

For small losses the following approximation holds:

$$\text{Loss} = A \, (\text{fr})^2 \, \text{db}$$

where r is horizontal component of $\underline{u} - \hat{\underline{u}}$ in sec/km. For subarray beams A ≈ 360 and for LASA beams A ≈ 2.07×10^5. It is noted that the beam loss contours are circles of radius r about the beam center coordinates ($\hat{u}_x$, $\hat{u}_y$).

The array geometry suggests step-wise processing: a subarray processing subsystem to generate inputs for the coarse and vernier array processing subsystems, which in turn, are employed for detection and classification record producing purposes respectively. In order to permit world-wide coverage, one vertical beam is generated for each subarray. A total of six beams per subarray, one vertical and five non-vertical, will yield a maximum beam coverage loss of approximately 1.0 db for frequencies up to 3.0 cps over the surveillance area defined by a 60° azimuth section in the u_x, u_y plane bounded by the radii 0.04 sec/km and 0.08 sec/km (these radii correspond to event ranges of 94° and 30° respectively), as shown in Figure 166.
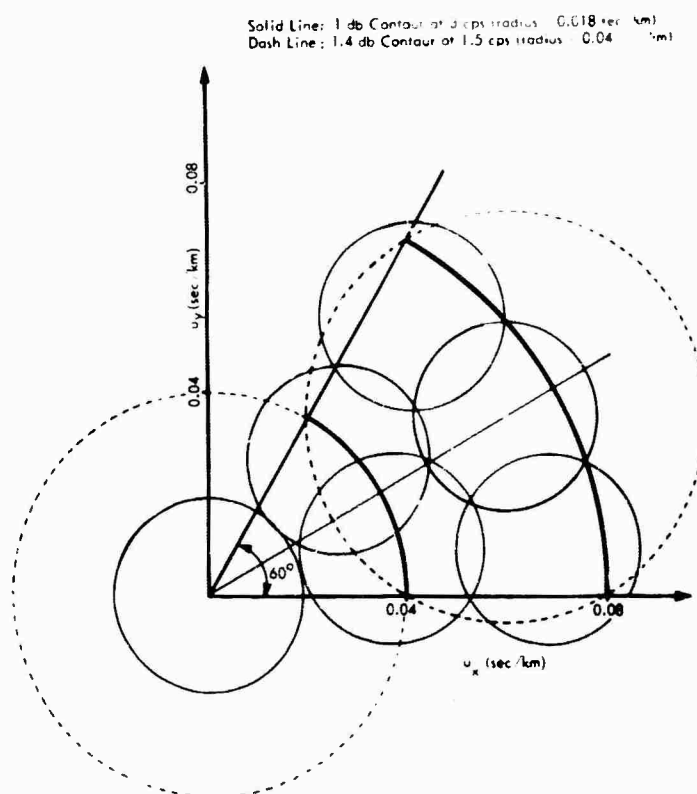
FIGURE 166. SIX SUBARRAY BEAMS

183

For detection, approximately 250 coarse ASA beams are proposed to assure an accumu-
lative loss of no more than 3.0 db at 1.5 cps over the surveillance area. Only two subarray
beams, one vertical and one non-vertical need be employed to form the coarse beams as de-
picted in Figure 166. Approximately 1.4 db loss is allowed in subarray beam forming and 1.6
db loss is allowed in coarse beam forming. An additional 50 beams may be generated from the
vertical subarray beam and directed to specific secondary surveillance regions in the world.

Upon event detection, the subarray beam whose center is nearest to the event location is
identified. The 21 subarray beams so obtained are employed to generate vernier or high
fidelty beams. The beam coverage required for the vernier beams need only cover the area of
event location uncertainty. Assuming a 9.0 db detection capability, the circle of radius 0.016
sec/km contains all losses that are less than 9.0 db down as determined from the wide-band
beam pattern shown in Figure 167. In order to maintain an accumulative loss of less than 3.0
db at 3.0 cps over the area of the aforementioned circle of uncertainty, about 300 vernier
beams are required.
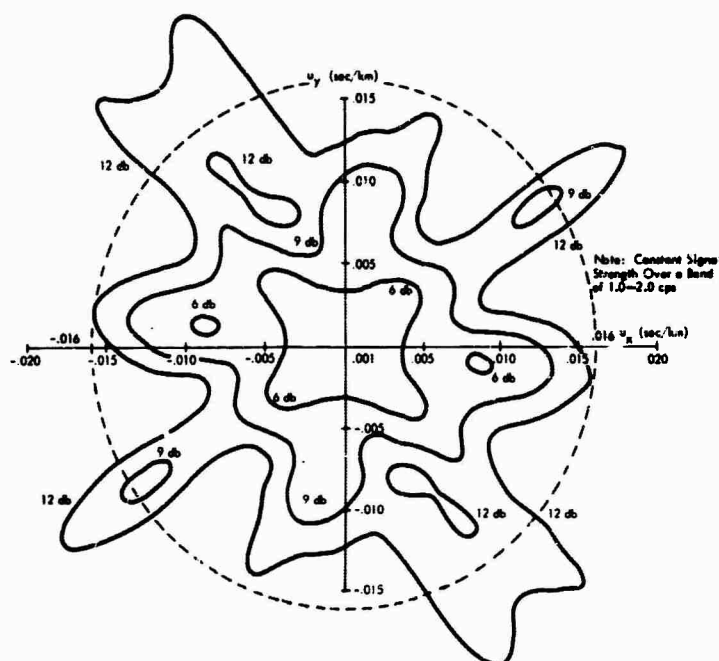
FIGURE 167. WIDE-BAND BEAM PATTERN CONSTANT LOSS CONTOURS

Due to the conservative manner of arriving at the beam coverage, the 6 subarray beams
and the 300 coarse and 300 vernier beams are felt to represent a reasonable upper bound on
the beam forming requirements for the function and coverage specified. The remainder of this
paper will demonstrate that even with this large beam forming requirement, the system opera-
tion and instrumentation is feasible, practical and reasonable.

184

SYSTEM DESCRIPTION

A block diagram of the LASA processing system showing the data flow interrelationships of the various subsystems is presented in Figure 168.

The Subarray Beam Former located physically at the LASA site, has as its function the real-time formation and transmission of 6 subarray beams for each of the 21 subarrays. In addition, the Subarray Beam Former also transmits the outputs of 21 padded seismometers (one from each subarray) to detect and record, without overloading, events with amplitudes up to 28,400 millimicrons.
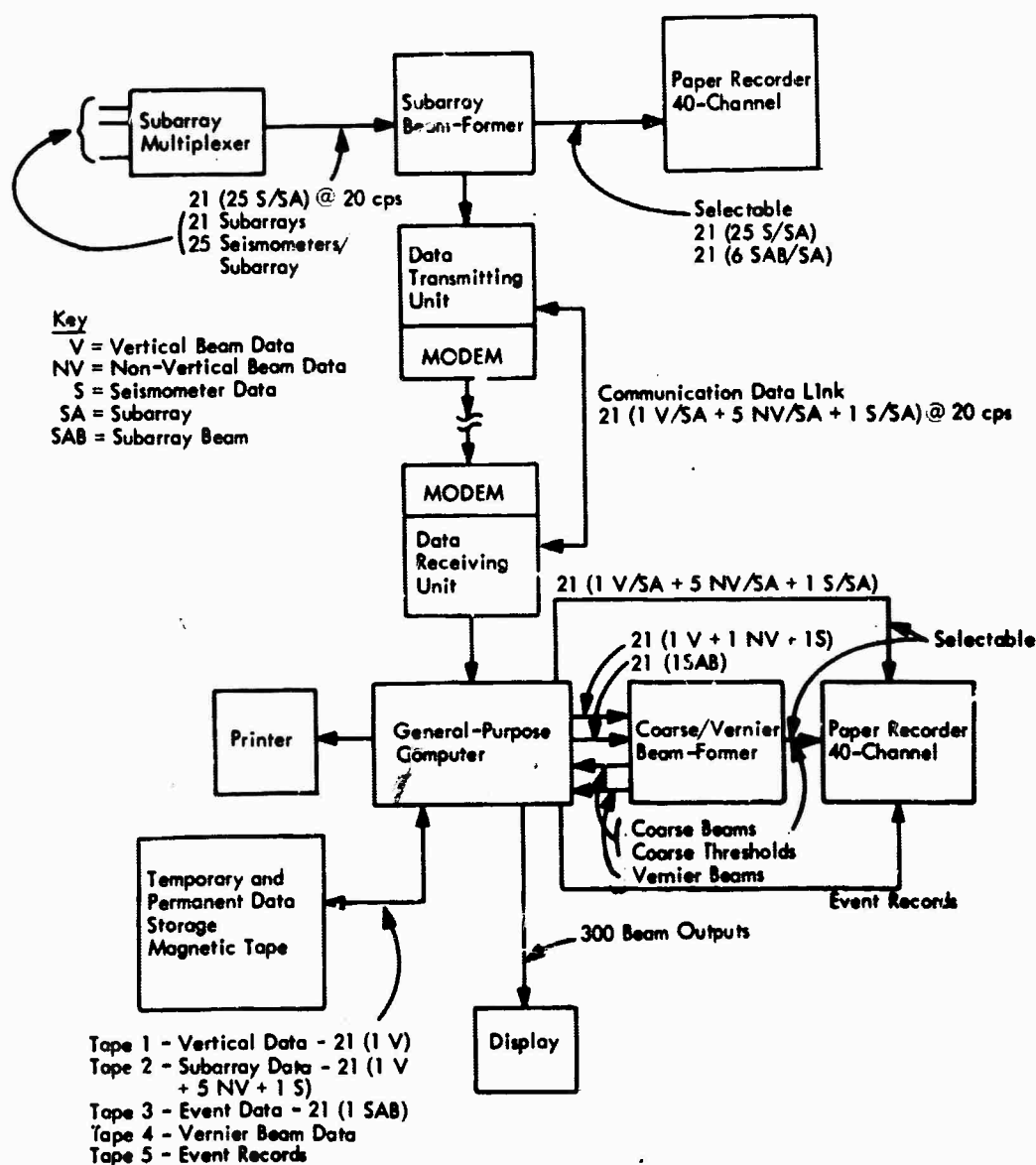
FIGURE 168. LASA PROCESSING SYSTEM

Part of the LASA signal processing function consists of detecting seismic events occurring in the surveillance region, using the full LASA detection capability. To this end, the Coarse Beam Former generates 300 LASA beams covering the surveillance region and certain other specified portions of the world. Each of these LASA beams is formed in real-time from one set of vertical or one set of non-vertical subarray beams. The coarse beam outputs are rectified and integrated to form signal and threshold detection outputs for interpretation by the General Purpose Computer. Rectification and integration is also performed on the 21 vertical subarray beams and the 21 padded seismometers. Since beam forming is a linear process, predetection band-pass filtering is allowed to be performed before coarse beam formation in the computer. Therefore, the real-time output of the Coarse Beam Former is 342 pairs of event and threshold signals presented to the General Purpose Computer for detection purposes. The magnitudes of the detected events will be as low as the General Purpose Computer is capable of detecting without an unduly high false-alarm rate.

The set of 21 vertical subarray beams are used to detect (substantially stronger) events occurring outside the surveillance region. By recording the arrival times of such an event at the various subarrays and by fitting a "least squares" planar wavefront to these data, the location of the event (or, more appropriately, its phase speed and azimuth at LASA) can be estimated. The set of 21 padded seismometers are monitored to localize, in the same manner, events which are strong enough to overload the unpadded seismometers.

Once an event has been detected and localized, it must be recorded on tape for further classification analysis by the Vernier Beam Former. To this end, the General Purpose Computer controls magnetic tapes with a "look-back" capability on the order of minutes and whose inputs are all subarray beam outputs (numbering 6×21) and the outputs of the 21 padded seismometers. The look-back feature allows the General Purpose Computer sufficient time to make a detection following the onset of the event arrival at LASA.

When a detection has been made, the General Purpose Computer initiates the transfer of the appropriate subarray outputs from the look-back tape onto an event tape. For events inside the surveillance region, one beam per subarray is recorded, namely the subarray beam whose center is nearest to the location of the detected event. For events detected outside the surveillance region, the 21 vertical subarray beams are recorded. In case of overloading of the unpadded LASA seismometers, the outputs of the 21 padded seismometers are recorded. For events detected on the vertical beams or on the padded seismometers, the event location is recorded in the form of the 21 subarray time delays corresponding to the best estimate of the event location as determined from the least squares wavefront calculation.

186

The Vernier Beam Former is an aid for the LASA classification function. The event tape generated under control of the General Purpose Computer serves as input, which is a subarray beam or equivalently a set of padded seismometer outputs. The output of the Vernier Beam Former is 300 LASA beams covering a small region centered about the event location as estimated and recorded by the General Purpose Computer. These vernier LASA beams are expected to allow more accurate event location, as well as detailed signal waveform examination. The Vernier Beam Former is allowed to operate in an off-line manner, provided reasonable bounds on the event backlog are maintained. The vernier outputs are recorded on magnetic tape which is denoted as the vernier tape.

The 300 vernier beams can now be displayed, permitting selection of the particular beams to be employed for classification purposes. The General Purpose Computer initiates this function by energizing a display. Ideally, an intensity modulated CRT with the appropriately biased beam amplitude displayed in u-space coordinates would appear as the wide-band beam pattern depicted in Figure 166. A uniform intensity display of beam amplitude vs beam number may well yield sufficient correlation to isolate the beams of interest. In either case, selection is at this time planned to be accomplished manually and the selected beam or beams may then be rerecorded on film, on tape, and/or on the paper recorder for subsequent manual or machine classification analysis.

SYSTEM INSTRUMENTATION REQUIREMENTS

The equipment requirements for the Subarray Beam Former, the Coarse/Vernier Beam Former and the General Purpose Computer will now be discussed.

Subarray Beam Former

The Subarray Beam Former receives its input from the 21 subarrays in a multiplexed serial format. Each subarray transmits 25 words of 15 bits (13 data bits + sign + parity) to the Subarray Beam Former within a 50 msec sampling frame. The Subarray Beam Former stores one word of data for each of the 525 seismometers during the frame. One padded seismometer from each subarray is not involved in the beamforming process and is stored only for convenience of transmission to the output of the unit. Data from the 504 remaining seismometers are stored in memory to form 1.0 second of time history.

The Subarray Beam Former forms 6 beams for each of the 21 subarrays. Functionally, it is 21 beam formers with processing independent from one subarray to another, using common data paths for practical convenience only. The Subarray Beam Former presents a 16 bit output to the transmission link. The word rate is about 2940 per second, approximately a 50 kc bit rate. In this configuration, any 40 of the 525 subarray outputs or 126 subarray beam outputs may be selected for display on a paper recorder.

187

Table 1 summarizes the real-time on-line processing load that is incurred under two different assumptions as to the type of processing performed. Conventional beam forming here denotes the simple delay and sum operation. Optimum processing is assumed to include a 50 point generalized convolution filter per seismometer, per beam, in addition to the delay and summing operation. The processing requirements are stated in terms of minimum storage and memory speed requirements, without allowance for control or operational programs in the general purpose sense. Storage includes data words and program words. The program words are limited to the delay definition words and filter coefficient words, if any. Since speed is stated in terms of memory cycles, it assumes that this is the limiting factor and the arithmetic element can perform its function within the memory cycle time. For conventional processing, where the arithmetic operation is addition, this is generally true. For optimum processing, where the arithmetic operation is a multiply and add, this is not true of general purpose computers.

TABLE 1
Subarray Beam Former Requirements

| | Memory Size | | | Memory |
| | Data | Program | Total | Speed |
Subarray Beams	(Words)	(Words)	(Words)	(kcps)
Conven. (1V + 5NV)	10,080	3,024	13,104	137
General. (1V (50 point)) and Conven. (5NV)	25,200	28,224	53,424	1,136

Thus, Table 1 demonstrates that optimum processing represents a heavy load that is not practical to perform in a conventional general purpose computer. However, such processing loads may be handled with currently available digital hardware organized as a special processor, or a modified general purpose computer utilizing special complex operating codes. For example, the operational sequences of conventional or optimum processing could be microprogrammed as a special instruction in a general purpose computer. It should also be pointed out that alternate parallel processing techniques may be required when arithmetic speed requirements are as high as indicated.

Coarse/Vernier Beam Former

Referring again to Figure 168, the Coarse/Vernier Beam Former receives data from the General Purpose Computer, forms coarse and vernier beams, and transmits the results back to the computer and to a paper recorder. The Coarse/Vernier Beam Former must accept three beams from each of the 21 subarrays. These are one vertical beam and one non-vertical beam for coarse beam forming, and one beam for vernier beam forming. To achieve full fidelity,

188

the vernier beams must be formed at a rate of 20 samples per second. The coarse beams need only be formed at a rate of 10 samples per second, because the detection function does not require high-fidelity beams.

The 300 coarse beams, 21 vertical subarray beams, and 21 padded seismometers are averaged over two time intervals, which range from 0.8 seconds to 12 seconds and 3.2 seconds to 48 seconds, and the results sent to the computer. The 300 vernier beams are averaged for a computer designated amount of time and sent to the computer for tape recording and subsequent display. In addition, a set of control words, sent from the computer to the beam former, indicates which of the beams are to be displayed on the paper recorder. The Coarse/Vernier Beam Former selects these outputs, converts them to analog form and transmits them to the paper recorder.

Utilizing the same basic assumptions as Table 1, Table 2 shows the speed requirements of the Coarse/Vernier Beam Former. The storage requirements may be computed as follows:

Data   = 20 sec × 20/sec × 21 subarrays × 3 sec = 25,200 words.
Program = 300 beams × 21 delays × 2 beam formers = 12,600 words.

TABLE 2
Coarse/Vernier Beam Former Requirements

	Beams	Memory Cycles	Subarrays	Rate (cps)	Memory Speed (/cps)
Input	3	1	21	20	1,260
Beamforming					
Coarse	300	2	21	10	126,000
Vernier	300	2	21	20	252,000
Output					
Coarse (Signal)	300	1	NA	1.25	375
Coarse Threshold	300	1	NA	0.3	90
Vernier	300	1	NA	0.25	60
Total					379,785

The memory speed (2.6 μsec) and size (37,800 words) are well within the state-of-the-art. Allowing for housekeeping and control, a conventional General Purpose Computer which operates at a speed of about 800 K instructions per second could perform the Coarse/Vernier Beam Former function. Such machines are available however, it again appears attractive to organize

available hardware as a special purpose processor or utilize special instructions in a smaller machine to obtain the required speed.

General Purpose Computer

Figure 169 illustrates the configuration for the General Purpose Computer Subsystem. The centralized control element for the system is a general purpose digital computer operating under stored program control. Data enters the computer subsystem by way of a communication channel from the Subarray Beam Former and transmission system.
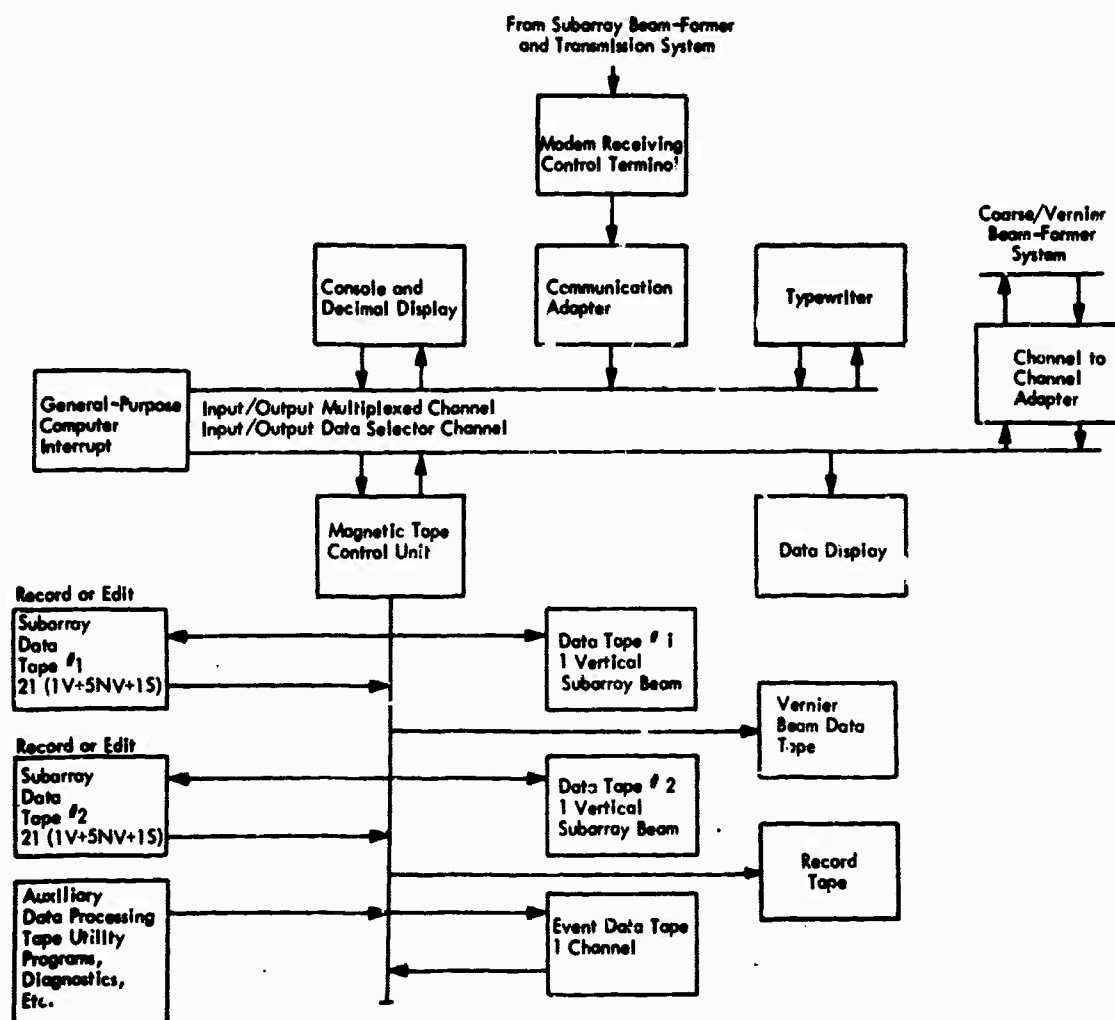
FIGURE 169. GENERAL PURPOSE COMPUTER SUBSYSTEM

Operation with the beam former is performed in conjunction with a common control channel. Only data is exchanged via the channels indicated. Control of devices and, specifically, the beam former requires execution by other means. This control can be satisfied by an interrupt channel capable of signaling start, stop, and control of data transmission in either direction between computer and beam former. Data is transferred within the computing system via

190

two types of channels: a data multiplexed channel and a data burst or selector channel. Control is handled by way of interrupts between devices and computer with the functions allocated as indicated. A 32 K word memory at 2.5 μsec per memory cycle is adequate. An add time of about 8 μsec, a multiply time of about 80 μsec, and tape speeds of 60 K characters per second are indicative of the speed requirements.

ALTERNATE SYSTEM CONFIGURATION

Examination of the processing system presented above reveals that the subarray processing may be the most vulnerable portion of the system from a practical and economical point of view. While optimum processing may well be needed for the high-fidelity beams, it is likely that conventional processing is adequate for the event detection process in the Coarse Beam Former. Thus, ideally, optimum processing should be performed off-line only after event detection, and the event detection would then require only two beams per subarray, formed conventionally. Such a system can be synthesized if event detection is allowed to be performed at the array site as functionally illustrated in Figure 170.
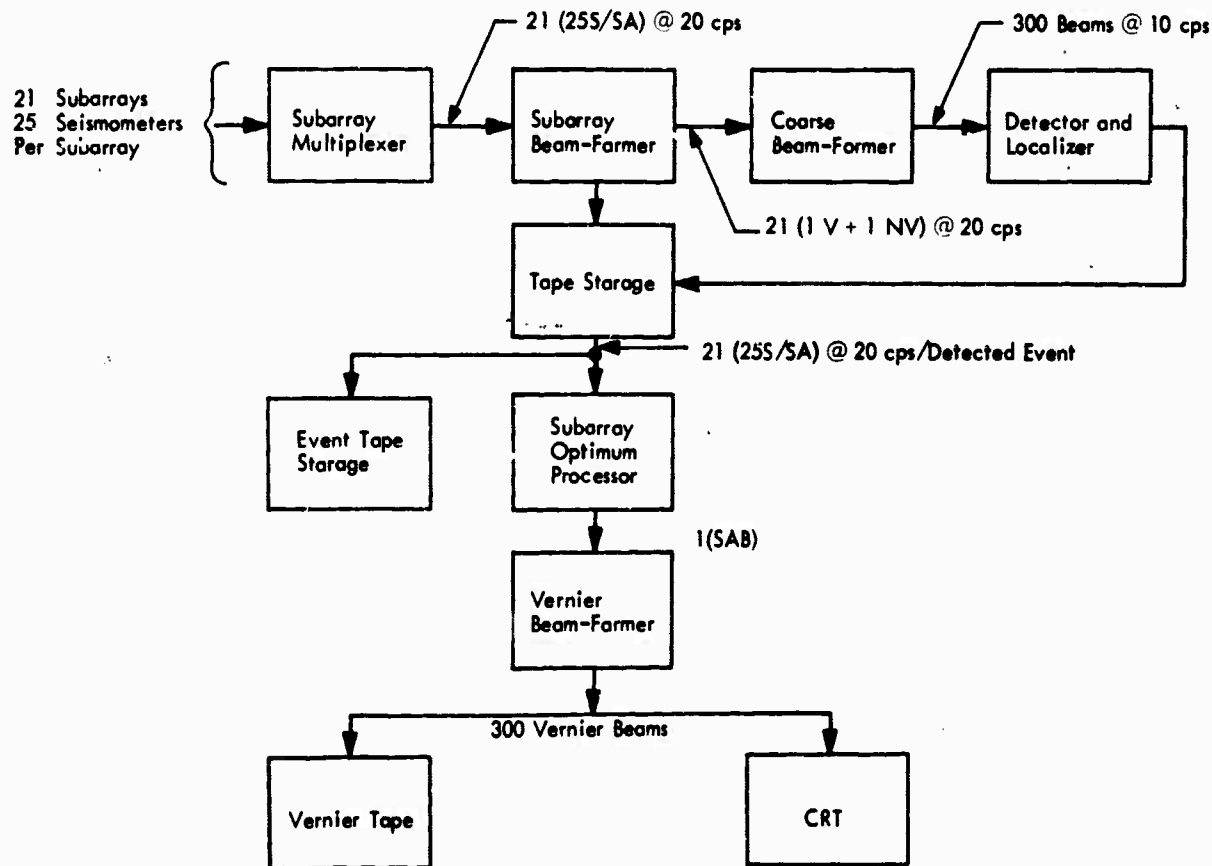
FIGURE 170. ALTERNATE LASA PROCESSING SYSTEM

The subarray multiplexer performs the same function as in the previous system. The Subarray Beam Former forms only the two beams, one vertical and one non-vertical, necessary as input to the Coarse Beam Former. The Coarse Beam Former and the detector and localizer are the same as before. Temporary tape storage is larger because of the necessity of storing all 525 seismometers, but this does not appear to be serious since these tapes may be re-cycled after concurrence that they do not contain data of interest.

The subarray processing requirement generated by this configuration is reduced, since optimum processing is performed only on detected events. Processing is reduced by a factor proportional to the fraction of time that events occur. If one assumes 4 hours of events per day, the optimum processing requirements are therefore reduced by a factor of 6 over the initial system.

We note here that the burdensome calculations leading to a machine speed of over 10^6 operations per second in the optimum Subarray Beam Former of the first system can be reduced to less than 2×10^5 operations per second, with little or no loss in detection capability and an equivalent performance in the generation of records for classification purpose.

CONCLUSION

While either system described herein is feasible, it is evident that array site oriented processing offers substantial economies in both processing and data transmission requirements. A key point in the system concept is the utilization of the full LASA capability for detection and coarse localization, combined with the relegation of optimum processing to non-real-time, off-line processing. These more sophisticated techniques are reserved for detected events where the higher potential gain may be needed to increase the chances of success in classification without placing an unreasonable load on the processing equipment.

It is pointed out that in the system parametrics, no consideration has been given to such items as sampling rates and quantum levels, nor to instrument sensitivity variations or filter implementation inaccuracies. Although when considered individually they may appear to be small, in the aggregate their effect on system performances and equipment specification through characteristic trade-offs should not be ignored.

Basic to any proposed processing system for such an array system as LASA must be processing flexibility and modular expandability. Since the upper bound on the system requirements can readily be met with existing equipments and state-of-the-art design, it is reasonable to base system configuration selection on detection and event record fidelity capability. The general purpose programmed machine, with special operations instrumented as required, offers not only the modular expandability but also sufficient flexibility to vary the processing

192

technique from an initially conservative method, to maximum system capability in accordance with a range of classification requirements without the need of major processing equipment redesign.

20. DISCUSSION OF LASA PROCESSING REQUIREMENTS
by
Milo Backus and George T. Baker
Texas Instruments, Inc.

This paper presents a possible processing system for a LASA installation. It is assumed that each LASA installation is a part of a network of such stations with the objective of world-wide monitoring of nuclear explosions and earthquakes. First, the general system concept and processing functions are presented. Second, the nature of seismic noise, seismic signal, and signal-to-noise ratio as they relate to seismic processing requirements are discussed. Next, details of the processing functions are examined. Finally, a summary of the system is presented.

GENERAL CONCEPT AND PROCESSING FUNCTIONS

A. On-Line Detection and Approximate Location

The total processing done on the data from a LASA and the nature and quantity of data permanently stored on magnetic tape are determined by the status of the seismic wave field at the time. For example, when ambient noise is present with no teleseismic events above a given magnitude threshold and the absence of such events is known, no further processing is required and only a limited amount of data need be stored. In the presence of a teleseismic event above the threshold, additional on-line processing dependent on the approximate location of the event would be carried out. A greater amount of data would be stored in the presence of a teleseismic signal with certain characteristics. In the presence of an abnormally high noise field, a large amount of the data [possibly up to the 525 channels] would be stored in order that maximum processing capability might be exploited. Therefore, the major on-line function of the processor must be determination of the status of the seismic wave field. The processor must detect teleseisms above a specified magnitude threshold, but need determine their location only to sufficient precision to permit additional on-line processing to extract more detailed information about the event.

B. Data Storage

An on-line temporary buffer storage for the full 525 channels is contemplated. The buffer storage must save the raw data from the 525 channels long enough for appropriate action to be taken for detected events. This period is probably on the order of one and one-half minutes.

Magnetic tape units are provided for permanent storage. World-wide P-wave outputs from the 21 subarrays would be stored for all data. On the basis of the detection logic a number of other storage operations would be provided, up to and including storage of the full 525 channels.

194

C. Post-Detection Processing

Post-detection processing would include immediate on-line processing of the buffered data to develop the best steered beam for each of the 21 subarrays based on the approximate location of the event. Additional processing of this data would include improved location and measurement of arrival time, and would accomplish signal extraction for subsequent measurement of classification parameters. In the case of larger teleseisms, special re-detection processing would be provided for locating possible smaller events which might be buried in a larger teleseismic arrival.

D. Built-In Learning Function

It is anticipated that the determination of the necessary corrections [particularly between subarrays] to provide maximum enhancement in the beam forming function will require a long period of time and the use of data from a large number of teleseisms. Large detected events would therefore undergo processing for upgrading of the beam former corrections.

E. Off-Line Network Processing

Finally, the function of combining information from a number of LASA stations must be performed to accomplish source classification.

F. General Implementation

A generalized picture of this processing concept is shown in Figure 171. The 525 channels from the subarrays are delivered to a special purpose processor which provides signal detection and preliminary location. In addition, the special purpose processor provides 21 processed
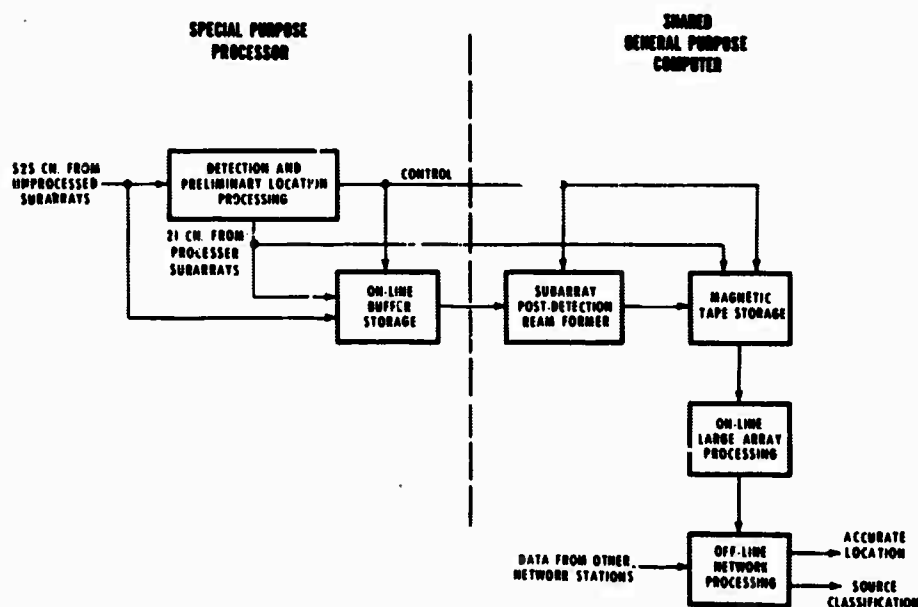
FIGURE 171. LASA PROCESSING SYSTEM CONCEPT

195

broadband subarray outputs for permanent magnetic tape storage. The detection and location information goes into control logic which determines the necessity for additional processing and programs permanent magnetic tape storage. Under the condition of an event detection, the 525 channels from the buffer go into a special subarray post-detection beam former aimed at the direction of the detected teleseism. This output is also stored on magnetic tape. Under certain conditions, the detection logic may direct that the full 525 channels be stored on magnetic tape. The subarray post-detection beam forming and subsequent additional processing are accomplished by a time-shared general purpose computer.

NOISE, SIGNAL, AND SIGNAL-TO-NOISE RATIO CHARACTERISTICS

A. Noise Characteristics

Figure 172 shows a summary of typical observed ambient noise spectra from a single seismometer at TFO, CPO, UBO, and Angela [References 1 through 4]. Power density is plotted in decibels relative to one $m\mu^2$/cps at one cps as a function of frequency. A solid zero db curve, which takes into account overall system response is shown for reference.
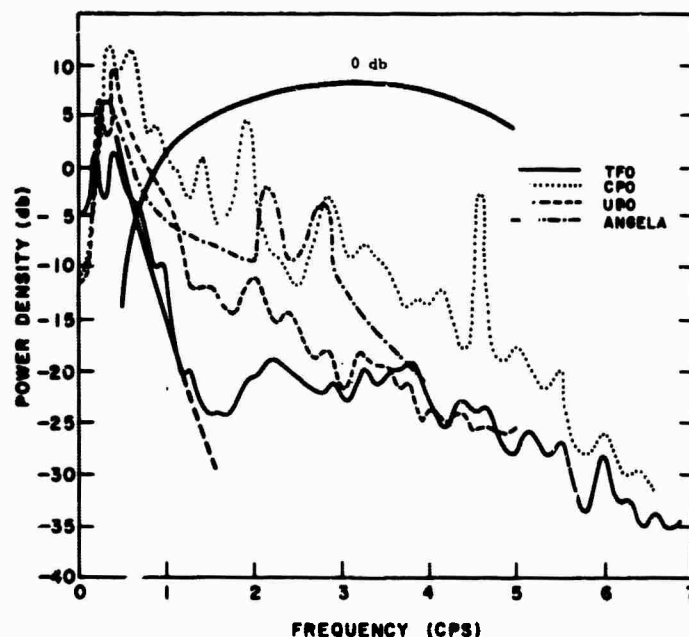
FIGURE 172. SPECTRA OF AMBIENT NOISE RECORDED ON A SINGLE SEISMOMETER AT VARIOUS LOCATIONS

1. Texas Instruments, Inc.: Large Aperture Seismic Array Final Specifications, August 1965

2. Texas Instruments, Inc.: Array Research, Semiannual Technical Report No. 1, May 1964

3. Texas Instruments, Inc.: Array Research, Semiannual Technical Report No. 2, Nov. 1964

4. Texas Instruments, Inc.: Array Research, Semiannual Technical Report No. 3, June 1965

Also shown is an estimate of the mantle P-wave noise spectrum from 0.5 cps to about 1.5 cps. This spectrum is an estimate of the mantle P-wave noise level at UBO, and is based on measurements of the ambient noise observed on a 10,000 foot vertical array [Reference No. 3]. On the basis of results obtained from analysis and processing of data from these four locations, it is postulated that a mantle P-wave noise component, with this general spectral shape and level exists at all four locations. For example, at TFO a single seismometer appears to be mantle P-wave noise limited over the frequenc range from about 0.6 cps to 1.2 cps. The other three stations have a significant amount of additional noise. Because this mantle P-wave noise propagates with high horizontal velocity [in fact, with the velocity in the range of the signals which we wish to detect] it can be regarded as a lower limit on the noise level output from a small dian eter (up to seven kilometers) subarray. This result appears to be roughly consistent with the findings obtained from studies at the other three locations. A very important implication is that the signal-to-noise improvement in the vicinity of 0.5 to 1.0 cps which can be obtained with a small subarray is limited to reduction to mantle P-wave noise level. Improvement can thus be expected to be large at noisy sites such as ..FO, and can be expecte to be negligible at very quiet sites such as TFO.

In the vicinity of 0.2 cps most stations are limited by the well known microseismic peak, made up of energy pr agating in the trapped modes. At frequencies above 1.5 cps, most of the systems are limited by what appears to be spatially random noise [with the seismometer spacing usually used in the subarrays]. In some locations, additional highly coherent energy peaks (2 cps at CPO) propagating as normal modes may dominate the high frequency range.

Figure 173 [Reference No. 1] shows some preliminary results obtained from two of the Montana LASA subarrays located at Angela and Hysham. Solid curves show the noise power density spectrum of a single seismometer, the noise power density spectrum of the simple summation (i.e., average) of approximately 10 subarray elements, and the output spectrum of a multichannel filter designed to pass distant teleseisms. The noise power density of the error output of a multichannel spatial interpolator filter, designed to interpolate the noise on one seismometer from the other approximately nine seismometers is shown as "Error Trace." The previously discussed mantle P-wave spectrum is shown for reference.

In the vicinity of 0.25 cps the trapped mode microseismic energy shows fair spatial predictability and the multichannel filter is capable of providing significant noise reduction. Because of the long wave length of trapped mode noise at this low frequency, the simple summation shows negligible improvement. In the vicinity of 0.5 to 0.75 cps the multichannel filter output is approximately at the mantle P-wave noise level. From 0.75 cps to 1.25 cps, some gain of the multichannel filter over the straight sum is shown, but the output is still above postulated mantle

197
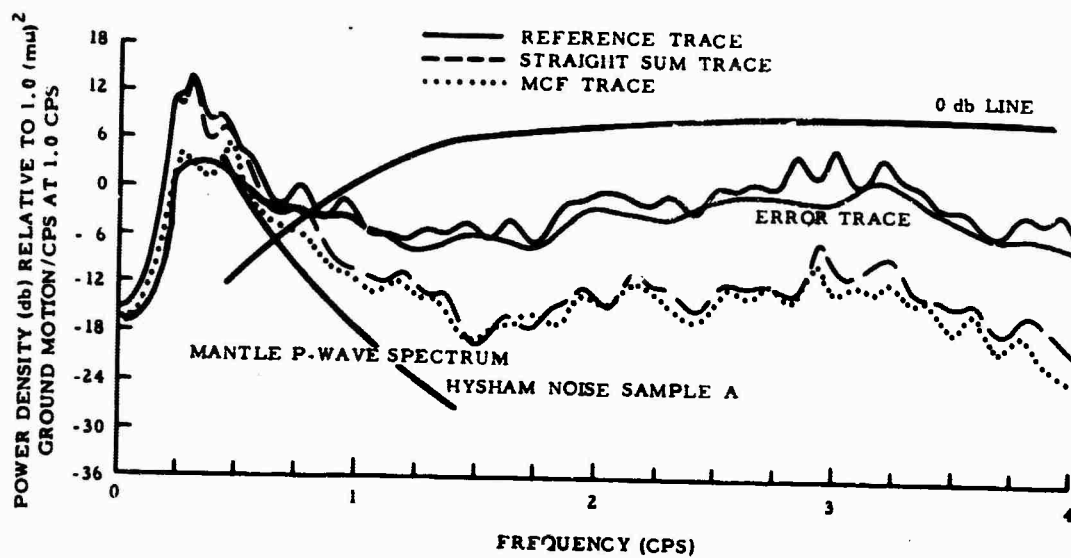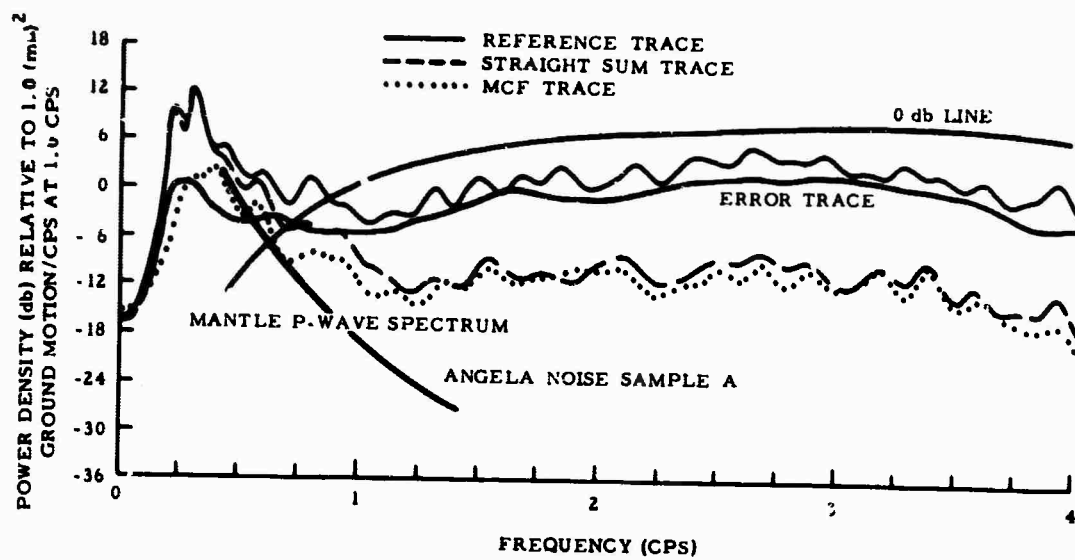
FIGURE 173. AMBIENT NOISE SPECTRA FROM ANGELA AND HYSHAM

198

P-wave level. (It is possible that additional gain might be realized from use of the full 25 elements of the subarray.) Above 1.5 cps multichannel filter and simple summation performance are nearly equivalent, and it appears that the noise problem above 1.5 cps may be regarded as spatially "almost random" noise for the element spacing in these subarrays.

Figure 174 shows a generalized model of the seismic noise field. In the vicinity of 0.2 cps exists the trapped mode microseismic peak, which at most locations has highly variable level as a function of time. Properly processed subarrays can provide significant gain against this microseism peak, but it is not clear whether the limited aperture subarray can get down to mantle P-wave noise limitation at this frequency. From 0.5 to 1.25 cps is the basic limiting mantle P-wave noise component, which appears to have a certain degree of uniformity from location to location in the continental U. S., and which appears to be relatively stable in level as a function of time. Overriding this limiting noise in some areas is a component of trapped mode noise, which varies substantially in level from one location to the next, and which may have significant variation in level as a function of time at a particular site. It is postulated that in this frequency range an appropriately processed subarray should be able to operate at a noise level corresponding to the mantle P-wave noise limit. Above 1.5 cps is found other noise, which may include coherent rejectable noise peaks, but is more often characterized by essentially spatially random noise [in the context of the usual element spacing employed in subarrays investigated to date].
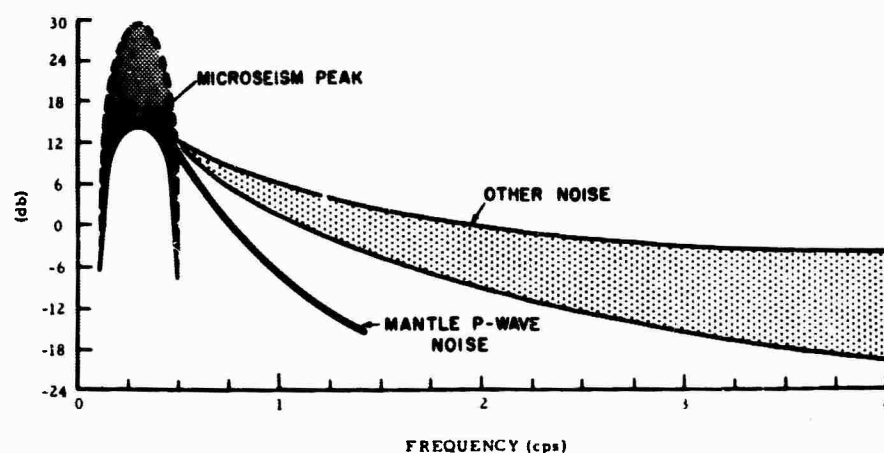
FIGURE 174. SCHEMATIC OF MONTA. ' LASA NOISE

The output of a subarray can be expected to include, at the low frequency end, mantle P-wave noise plus a residual component of trapped mode microseismic noise which is time variable. The subarray output from 0.5 cps to 1.25 cps can be expected to be relatively time-stable mantle P-wave noise. Above 1.5 cps a spatially random noise component, which may be fairly time-

variable and variable from subarray to subarray, would be dominant. This model provides a basis for considering the detection logic which might be applied to the 21 processed subarray outputs. Although this noise model is oversimplified, and no doubt lacks complete universality, its use in system design can probably lead to a more effective system than one based on the assumption that nothing whatever is known about the noise.

One major issue regarding the noise which is unclear at this time, but is relevant to the ultimate capability of the LASA concept is the question of the "fine structure" of the so-called "mantle P-wave noise." All that can be said presently is that the noise is made up of energy propagating at high horizontal velocity (8 km/sec or greater), with a depth dependence corresponding to energy travelling upward from below the crust at the receiving station, and that it appears to be a mixture of waves with different vector velocities at any instant in time. Mantle P-wave noise characteristics are consistent with the model of noise coming from a multitude of distant sources on or near the earth's surface, travelling through the earth in teleseismic P-wave paths. If indeed it is a mixture or "integral" of the disturbances over most of the earth's surface, it might be expected to be rather homogeneous in space and time, and rather uniformly distributed in k space, with a possible concentration of sources in the oceans [not significantly different from a uniform distribution]. Mantle P-wave noise undoubtedly includes also a multitude of very small earthquakes. To the extent that the latter energy source might dominate (certainly true some of the time), a fine structure related to the earth's seismicity might be found. The capabilities of the Montana LASA are required in order to determine the "mantle P noise" fine structure and its time characteristics, and hopefully it will soon yield answers to this question.

In this connection it is pertinent to examine some of the results of the study of world-wide seismicity conducted with 1963 data by Texas Instruments for the U.S. Coast and Geodetic Survey [Reference 5]. Table I presents the cumulative number of earthquakes having the indicated magnitudes and shows the mean time between direct P arrivals for depths less than 70 km.

TABLE I
Magnitude — Time Relationships

m_b	Cum. No.	Mean Time Between Direct P Arrivals
6	40	200 hours
5	1000	10 hours
4	$^*3 \times 10^4$	20 minutes
3	$^* 10^6$	30 seconds
2	$^*4 \times 10^7$	0.75 seconds

* extrapolated values

5. Texas Instruments, Inc., World-Wide Collection and Evaluation of Earthquake Data, Special Report No. 1, September 1965.

200

These findings tend to substantiate the hypothesis of a significant component of mantle P-wave noise being due to the almost continuous generation of very small earthquakes.

The general description of the noise presented here describes a base level noise. Added to this base level noise are the sequence of "detectable" discrete teleseisms, which must be treated as part of the "noise" as well as being treated as signals. This point of view is particularly necessary when one is attempting to operate at the low magnitude threshold contemplated, at least ultimately, for LASA. The probability of simultaneous teleseismic energy from more than one source increases rapidly with decreasing magnitude, and a statistical model of the teleseism "events" must be included in the LASA system noise model. A satisfactory description for system design would include frequency of occurrence, power spectrum, and energy envelope as a function of magnitude, as well as the geographical seismicity of the earth. Such a model has not yet been developed, as far as is known.

B. Signal Characteristics

Figure 175 shows a good example of teleseismic wave form as recorded from the Angela an and Hysham subarray outputs. The subarrays are separated by 100 kilometers. There is clearly a difference in wave form, but not such a radical difference as to require abandonment of coherent detection processing. The necessity of special time corrections dependent on azimuth and range for coherent beam formation has been reasonably well established.
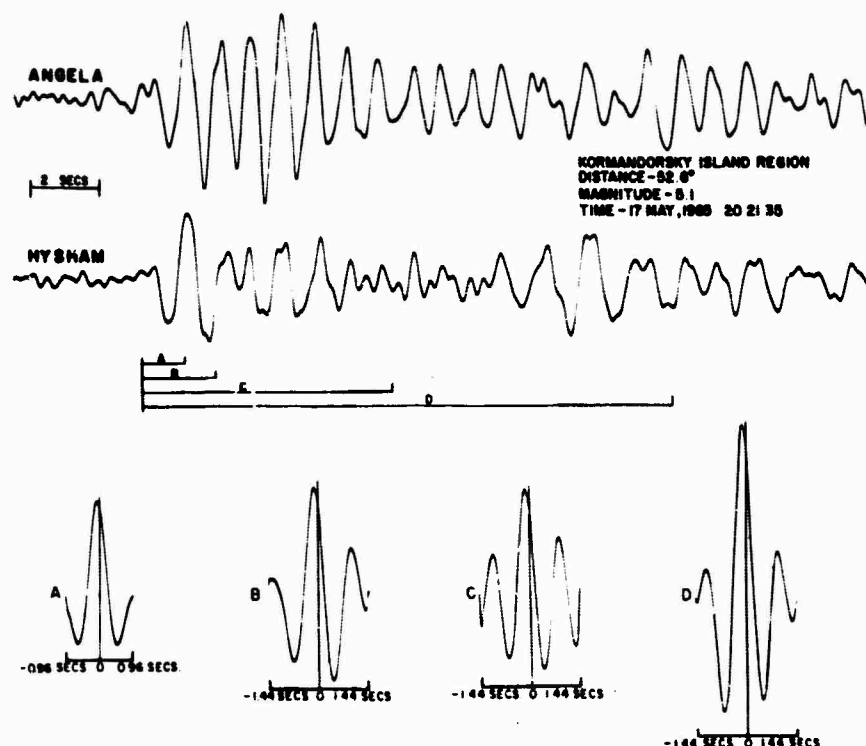
FIGURE 175. TELESEISMIC SIGNAL RECORDED AT ANGELA AND HYSHAM; CROSSCORRELATION vs CORRELATION GATE LENGTH

The following model of teleseismic signal seems to be appropriate. Teleseismic signal arrival will cause an increase in energy on each of the subarrays for at least a second or two — in some cases much longer. These energy increases will be initiated at times on the subarrays corresponding to propagation times for a high-velocity, predictably curved wave, with an error on the order of one second. The errors are probably invariant for a given source location, but have to be treated as unknowns in the initial operation of a LASA. They do, however, represent quantities that can be learned. The signal can be further characterized as a wave form which often has similarity of the first cycle recorded from each of the subarrays, and which arrives at times again corresponding approximately to a simple model with an azimuth- and range-dependent error of the order of a second. The remainder of the signal after the first cycle, which may often contain the major fraction of the teleseismic energy, can often be characterized as a dissimilar wave form on the subarrays. It is presumed that the degree of dissimilarity generally increases with increasing subarray separation. It is possible that the later portion of the teleseismic wave form can be represented as a constant wave form propagating across the array with teleseismic velocity, modified at each subarray by convolution with an operator which is smoothly dependent on range and azimuth, and which may contain a common component independent of range and azimuth. The validity of the latter hypothesis, and the degree of smoothness of the convolution operator with range and azimuth, represent a key issue in the ultimate capability of the LASA. However, it is apparent that reasonable utilization of the LASA array aperture can be accomplished while this question is being resolved.

C. Signal-To-Noise Ratio

The expected signal-to-noise ratio as a function of frequency is one of the most important parameters involved in the on-line detection problem. Of interest is the expected signal-to-noise ratio versus frequency on the processed subarray outputs. Figure 176 shows results of analysis of a small sample of teleseisms recorded from the 19-element array at the Cumberland Plateau Observatory, and originating from the Kurile Islands region. The measurements were made from data digitized from conventional station FM tape recordings of the output of an on-line multichannel-filter, isotropic processor which was operated at Cumberland Plateau Observatory. Signal-to-noise ratio energy contours are shown as a function of frequency and earthquake magnitude.

The general indication is that an upper frequency of importance for detection is on the order of 2.5 cps in the 4 to 5 magnitude range. The lower limit ranges from about 0.6 cps at magnitude 4 to about 0.3 cps at magnitude 5. Figure 177 is an example of the data from which this generalization was constructed and shows as points the upper and lower frequencies at which signal-to-noise ratio exceeds 0 db for each of the individual events. The frequencies are seen to be reasonably independent of magnitude over this range.

202
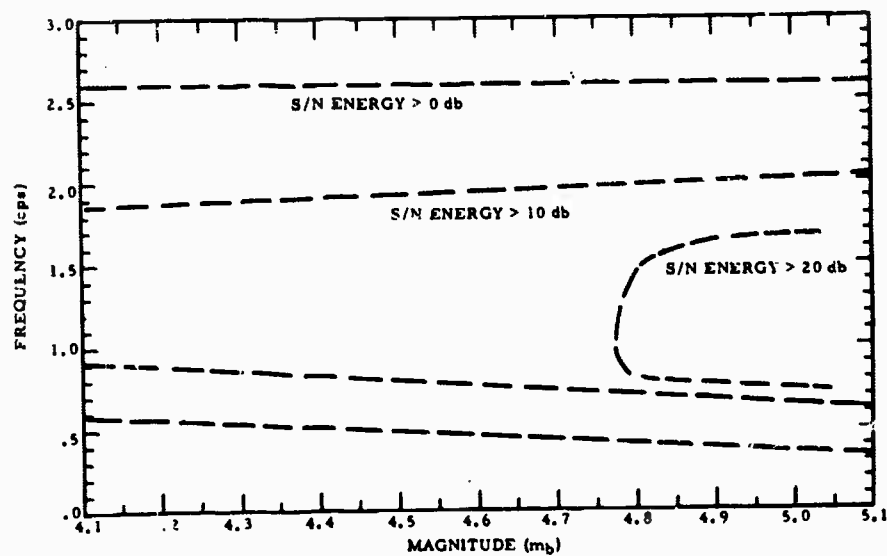
FIGURE 176. FREQUENCY BANDWIDTH vs MAGNITUDE WITH SIGNAL-TO-NOISE RATIO CONTOURS
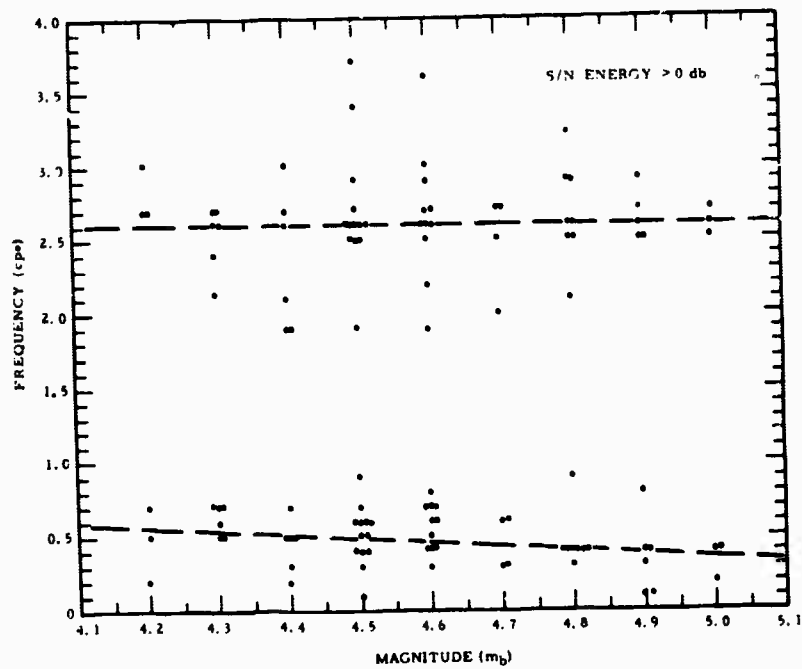
FIGURE 177. FREQUENCY BANDWIDTH vs MAGNITUDE FOR 60 KURILE ISLAND EVENTS

Figure 178 is a different presentation showing signal-to-noise ratio power as a function of frequency for a small number of events coming from many different directions at a Δ range of from 60⁰ to 75⁰. The same general bandwidth conclusion is supported by this data. One additional point to note in Figure 178 is that an individual event may have a fairly narrow peak in signal-to-noise ratio versus frequency but that different events peak at different frequencies. This imposes a requirement for broadband detection, as opposed to attempting to select a single very narrow frequency band for the detection process. Figure 179 is a similar plot for a number of events in many azimuths in the range from 20⁰ to 30⁰.

A similar single example is shown in Figure 180 for a Peruvian earthquake recorded from a single seismometer at the Tonto Forest Observatory. Although the signal drops rapidly with increasing frequency the noise also drops rapidly and a useful signal-to-noise ratio over the range from 0.25 cps to 2.5 cps is apparent, although the signal-to-noise ratio from 1.5 to 2.5 cps is lower than that at lower frequencies. It is known that a small array will provide signal-to-noise improvement in this high frequency range, whereas it will not provide much in the lower frequency range. This is an example of a fairly uniform signal-to-noise ratio over a broad frequency band.
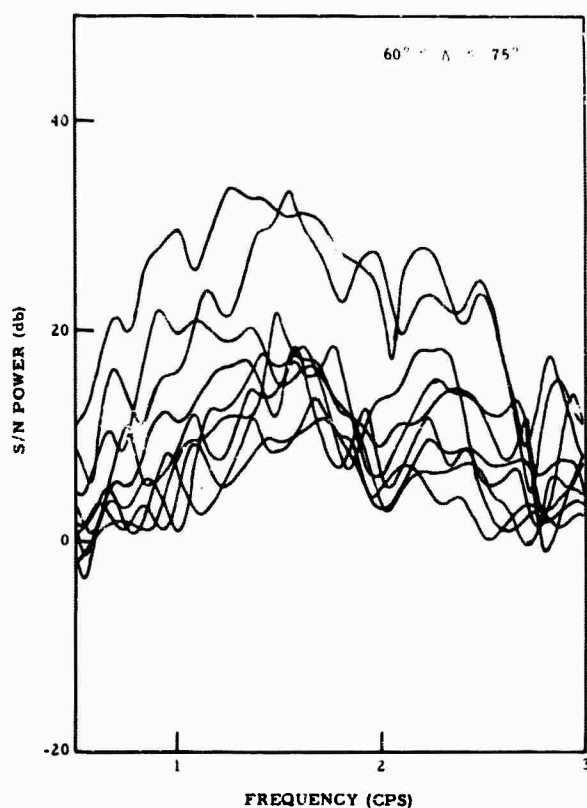
FIGURE 178. SIGNAL-TO-NOISE RATIO POWER DENSITY SPECTRA FOR 60⁰ ≤ Δ ≤ 75⁰
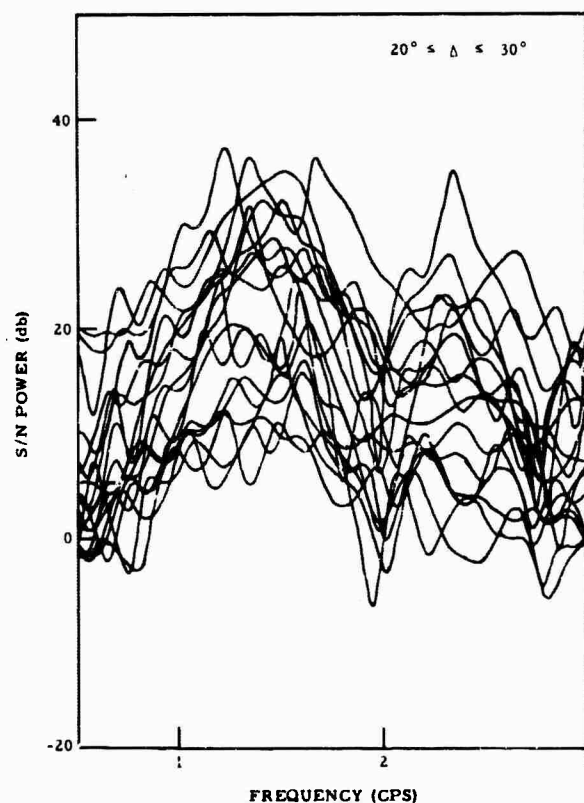
FIGURE 179. SIGNAL-TO-NOISE RATIO POWER DENSITY SPECTRA FOR 20⁰ ≤ Δ ≤ 30⁰

204
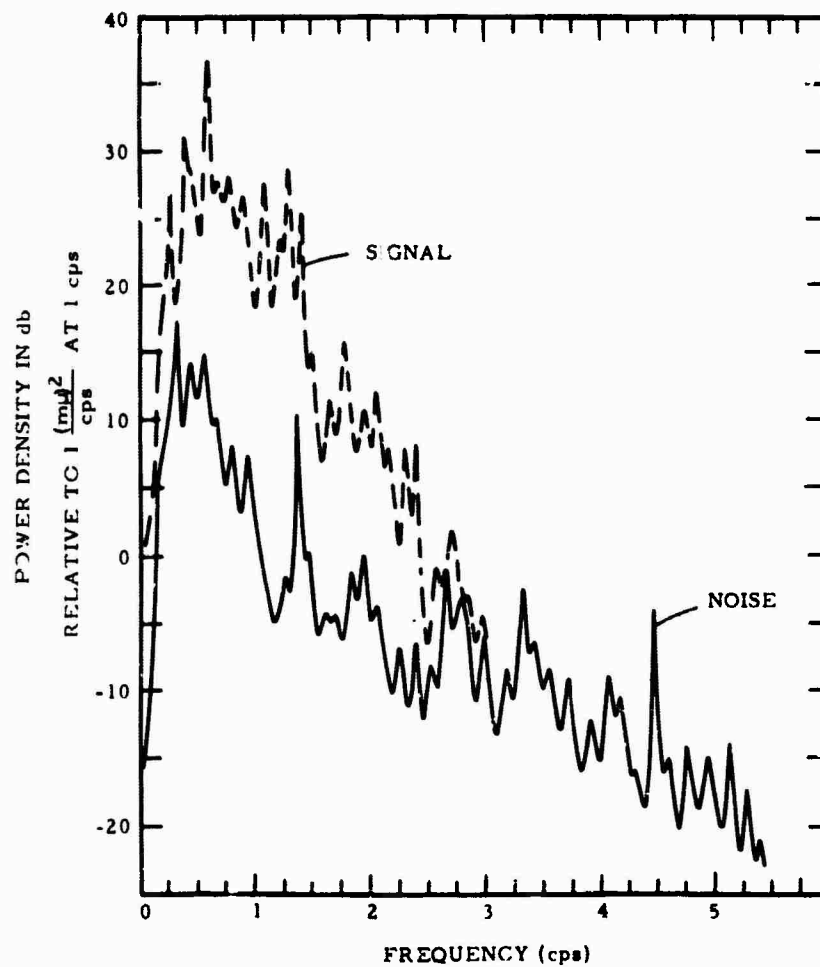
FIGURE 180. POWER DENSITY SPECTRA OF PERU EARTHQUAKE AND ACCOMPANYING NOISE RE-
CORDED AT TFO

D. Component and Subsystem Characteristics

In a description of the signal and noise field concerned with LASA processing, instrumental
parameters must also be considered. The transducing system should be regarded as a system
which does not have a precisely known response. The amplitude and phase response as functions
of frequency can be characterized statistically for purposes of processing design. Hopefully,
considerably lower variances in response can be achieved than those observed for the Montana
LASA in its present form. In addition, it is reasonably likely that at any given time one or
more of the 525 seismometers will not be operating properly. Distribution of the number of
expected inoperative seismometers at any given time is not yet available, but will be necessary
as a parameter in the processing design.

205

SUBARRAY PROCESSING

A. Subarray Processing Functions

Subarray processing is concerned with the following functions:

1. For purposes of detection, each subarray will be processed to provide, if possible, a mantle P-wave noise limited output preserving world-wide teleseisms over the 0.5 to 2.5 cps band.

2. Permanent magnetic recording should be provided of a broadband output from each sub-array preserving world-wide teleseisms. This will provide a capability for looking back into the past during time periods of interest when no event was detected on-line.

3. For purposes of refined location and classification of detected events, 21 subarray outputs should be provided with the teleseismic arrival enhanced broadband, i.e., up to about 8 cps. For economy, this function is proposed as a post-detection function.

4. Subarray processing of an adaptive nature possibly should be provided for the case of looking for events in the presence of very large teleseisms and/or in the presence of abnormal noise conditions [such as a particularly strong quarry blast]. Again this can be a post "detection" function if "abnormal noise" is included in the class of on-line "detection" conditions.

The initial discussion will be concerned with functions one and two, which are performed continuously, on-line.

B. Predetection Subarray Processing

1. One-Line Processing

Figure 181 shows a generalized block diagram for the suggested predetection subarray processing. The 25 channels from each subarray are combined into 5 to 8 ring summations and then put through a 5 to 8 channel multichannel filter designed to pass all teleseisms and to reject noise on the basis of long-term noise characteristics. The noise model might also include samples of intermittent types of noise characteristic for each particular subarray [e.g., quarry blast]. For some of the subarrays, a 25-channel filter might be required instead of the ring filter in the event that some subarrays have particularly strong local noise problems.
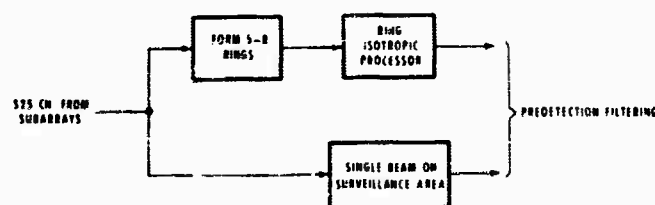
FIGURE 181. SUBARRAY PROCESSING

206

A second data route comprising simple time-shift-and-sum for a particular surveillance region is suggested. This would be used primarily for monitoring for aftershocks, and in some cases might provide additional high-frequency detection capability for the particular area of interest. Some of the reasons for this particular selection will be reviewed.

2. Alternatives

Figure 182 lists some of the subarray processing alternatives. The use of simple summation of subarray seismometer outputs would be good for very distant teleseisms but would provide excessive high-frequency loss over most of the Δ range of interest.

1. SIMPLE SUMMATION OF SUBARRAY SEISMOMETER OUTPUTS	• EXCESSIVE HIGH-FREQUENCY LOSS
2. OPTIMUM ISOTROPIC PROCESSING OF SEISMOMETER RINGS	• IMPROVED LOW-FREQUENCY SIGNAL-TO-NOISE RATIO
	• REDUCED SUSCEPTABILITY TO QUARRY BLASTS AND LOCAL DISTURBANCE
	• REQUIRE 6 TO 9 FILTERS PER SUBARRAY, INCLUDING PRE-DETECTION FILTER
3. TIME-SHIFT-AND-SUM BEAM FORMING FOR SURVEILLANCE REGION	• IMPROVED HIGH-FREQUENCY SIGNAL-TO-NOISE RATIO FOR BEAM CENTER
	• REQUIRES 1 PRE-DETECTION FILTER PER SUBARRAY PER BEAM
4. BROADENED SUBARRAY BEAM FOR SURVEILLANCE REGION	• SAME AS 2, EXCEPT BETTER HIGH-FREQUENCY SIGNAL-TO-NOISE RATIO
	• REQUIRES 25 FILTERS FOR SUBARRAY

FIGURE 182. SUBARRAY PROCESSING ALTERNATIVES

The second alternative [which is the proposed isotropic processing of seismometer ring outputs] can provide improved low-frequency signal-to-noise ratio for detection and definitely improved signal-to-noise ratio at the noisier sites. It can provide a single output which preserves broadband all P waves of interest, and it can provide reduced susceptibility to quarry blasts and local disturbances. The cost is the requirement of six to nine filters per subarray, including the predetection filter.

The third alternative is the use of time-shift-and-sum beams for the surveillance region. Time-shift-and-sum appropriate for some particular source can provide improved high-frequency signal-to-noise ratio relative to an isotropic beam. However, a large number of beams would be required to cover the world up to 2.5 cps. Since each beam output would have to be processed by a predetection filter, the hardware requirement for this type of processing is probably more costly than that involved in isotropic ring processing. Its low-frequency performance would also be poor. The reason for including a single steered beam (from each subarray) in the system discussed is the slightly better potential high-frequency performance.

A fourth possibility is to form directional beams for particular surveillance regions on a multichannel filter basis. This approach would provide all of the advantages of the isotropic processing in signal-to-noise improvement and could provide better signal-to-noise ratio at the higher frequencies. However, it would require 25 filters for each subarray for each beam, would have to be time adaptive, and is probably excessively expensive relative to its potential gain. This degree of complexity in on-line subarray processing might ultimately prove worthwhile if

(a) the magnitude threshold is lowered to the point that interfering events are the dominant "noise" a major fraction of the time.

(b) a very marked fine structure in the mantle "P" noise is discovered.

(c) intra-array equilization is of major importance.

In the present system, this kind of processing is relegated to intermittent "post-detection" use for handling "special problems."

Figures 183 and 184 provide an illustration of the relative characteristics of these different kinds of subarray processing. An on-line output is shown from the 19-channel array at CPO; the array has a diameter of 3.7 kilometers. The event is a quarry blast with an initial P-wave arrival having a horizontal velocity of 8 kilometers per second. The illustration may be scaled to the LASA problem to correspond to the behavior of a 16 km/sec teleseism on a 7 kilometer diameter subarray.

The upper 12 traces show time-shift-and-sum outputs of the array steered in 12 different azimuths at P-wave velocity. The next trace labeled TIP is the output of a multichannel filter designed to pass P waves from all directions; this trace has a one-second time delay. The summation trace [labeled sum 19] is also shown. The P-wave arrival can be seen on the 343^0 simple beam steering output and is well preserved. It is apparent that about 12 beams were necessary to insure that the signal would be adequately preserved. It is preserved as well on the single isotropic processor, and would be preserved this well independent of its direction of propagation.

High-frequency loss on the simple sum is quite apparent. Note the improved low-frequency microseismic noise reduction achieved by the isotropic beam former. A slightly improved high-frequency noise reduction on the beam steering relative to the isotropic processor can be noted, however. Figure 184 shows the same set of outputs at the time of arrival of the surface wave. It is apparent that the time-shift-and-sum beam steering has very poor rejection of the surface wave relative to the isotropic processor, and the simple sum is intermediate.

208
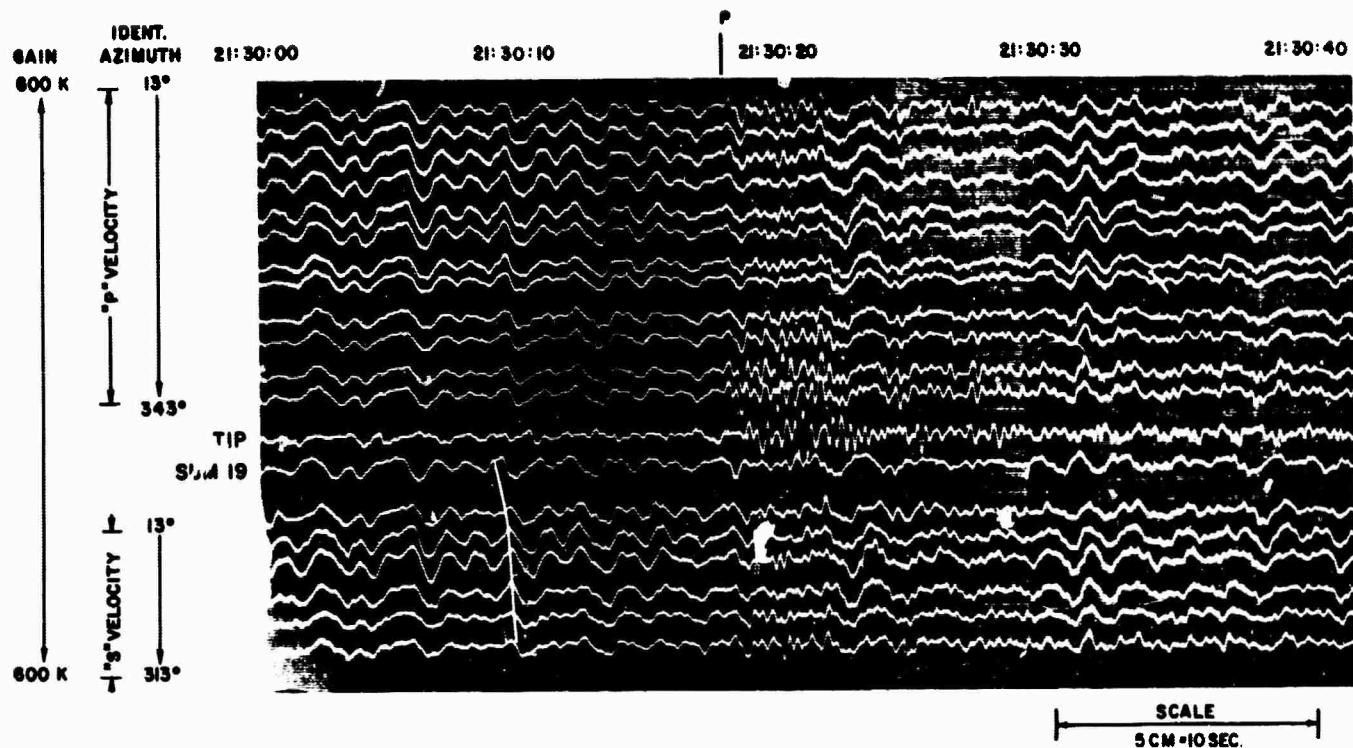
FIGURE 183. QUARRY BLAST RECORDED AT CPO WITH BEAM STEERING, SUMMATION, AND ISO-
TROPIC PROCESSOR OUTPUT 21:30:00 - 21:30:40
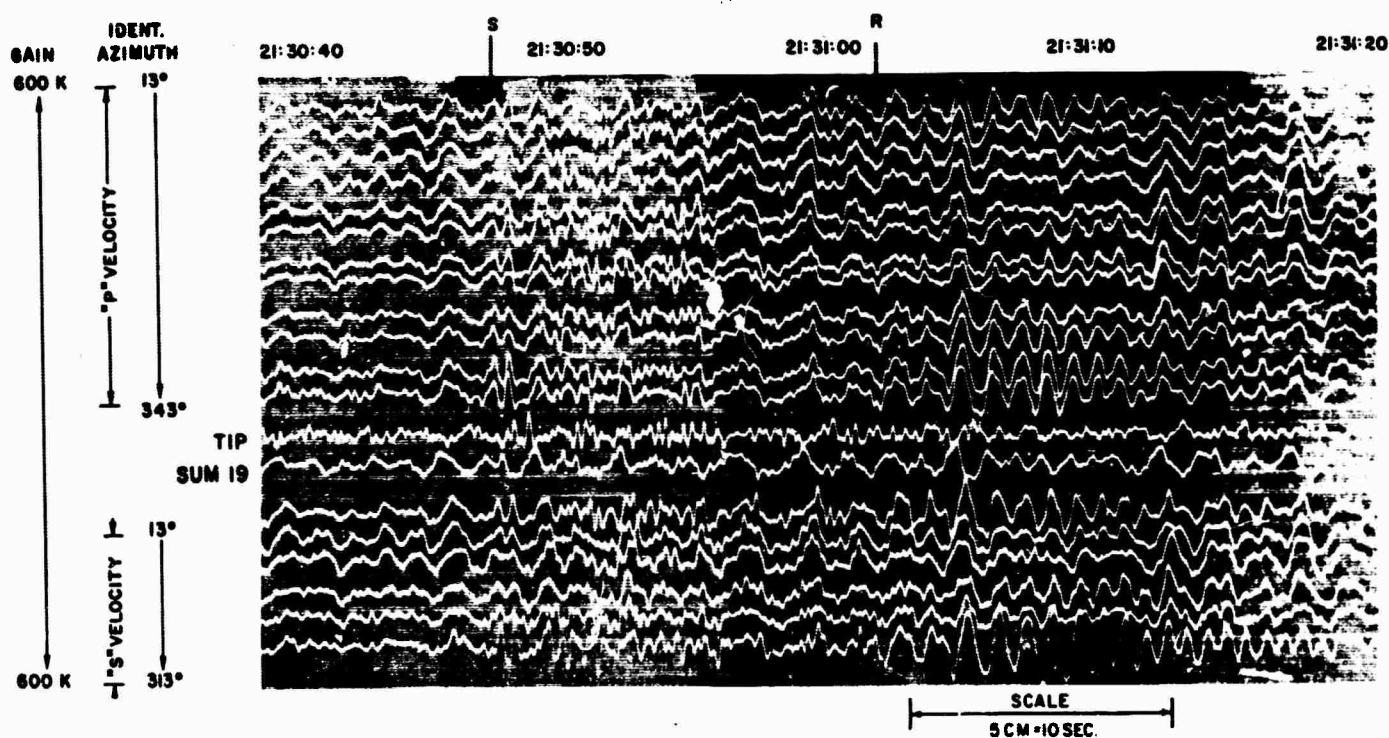
FIGURE 184. QUARRY BLAST RECORDED AT CPO WITH BEAM STEERING, SUMMATION, AND ISO-
TROPIC PROCESSOR OUTPUT, 21:30:40 - 21:31:20

3. Subarray Beam Broadening With Increasing Frequency

The beam broadening effect of an isotropic processor in preserving a broad class of signals, and the resultant loss incurred in high-frequency signal-to-noise ratio improvement deserves additional illustration. Figures 185 and 186 show wave-number responses at five different frequencies for a Montana LASA subarray operated under two conditions. On the right-hand side simple summation is illustrated; on the left-hand side an isotropic processor output designed simply to broaden the beam in the presence of spatially random noise is shown. The noise model did include mantle P-wave noise below one cps. The wave-number scale for each diagram is arbitrary. A solid disc is shown representing all of the teleseisms propagating at velocities from 12 kilometers per second to infinity, together with the 3 db loss contour for the subarray output beam. The signal picture also includes an insert illustrating a 60° azimuthal sector of events in an epicentral range of 30° to 90°.

SUBARRAY ISOTROPIC PROCESSOR   SUBARRAY SUMMATION
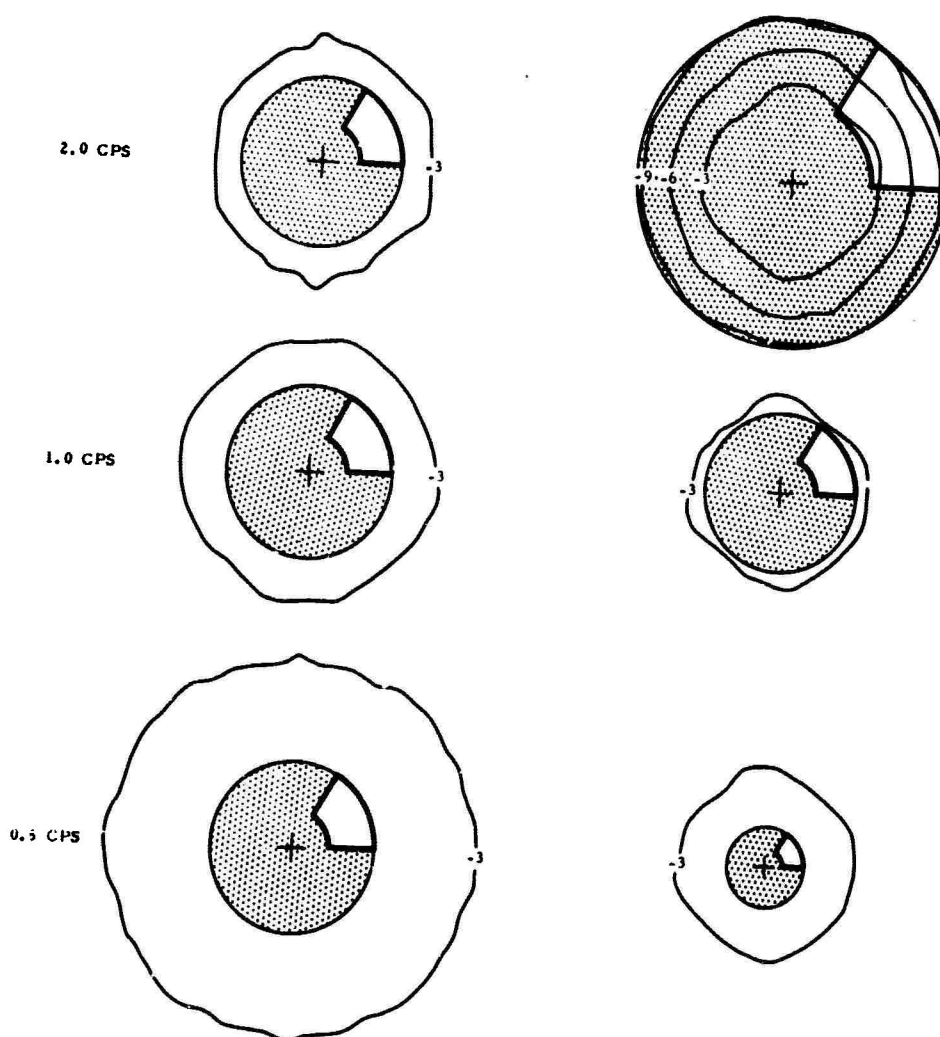
FIGURE 185. BEAMWIDTH COMPARISONS BETWEEN SUBARRAY SUMMATION AND ISOTROPIC PROCESSOR AT 0.5, 1.0 AND 2.0 cps

210
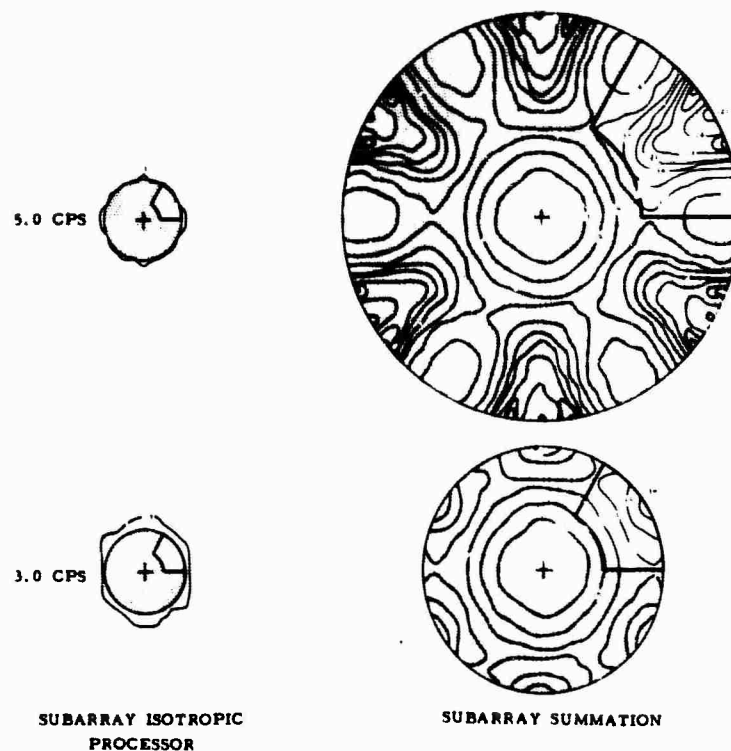
FIGURE 186. BEAMWIDTH COMPARISONS BETWEEN SUBARRAY SUMMATION AND ISOTROPIC PROC-
ESSOR AT 3.0 AND 5.0 cps

Simple summation is seen to be adequate up to one cps but is clearly inadequate at two cps
and above. The adequacy of signal preservation for the isotropic processor is apparent up to
five cps. In this simple noise model, the isotropic processor simply broadens the subarray
beam width as the frequency increases. As a result of broadening the beam width, random
noise rejection is reduced. In fact the reduction, relative to simple summation, can be esti-
mated from the plots because the power loss relative to simple summation is proportional to
the ratio of the processor beam area in wave-number space to that of a simple beam.

The signal-to-noise improvement for random noise was calculated explicitly for this proc-
essor and is shown in Figure 187. Note that there is about 5 to 6 db loss [relative to $\sqrt{N}$] at 3 cps.
This reduction is much better than the 6 to 15 db loss at 3 cps which would be incurred with a
simple sum [Figure 186]. The signal-to-noise improvement relative to the model used in the
design, which was dominantly mantle P-wave noise below one crs, is also shown but is not par-
ticularly relevant to this discussion.

Figures 188 to 190 show similar results for a beam designed to monitor a limited surveil-
lance region comprising events in the 30° to 90° range over a 60° azimuthal wedge. Beam

211

width relative to such a surveillance region is shown at five frequencies for a time-shift-and-sum beam versus a multichannel filter beam. The simple beam is quite adequate up to three cps, and in the presence of purely spatially random noise could provide at three cps about five db better signal-to-noise ratio than an isotropic processor.
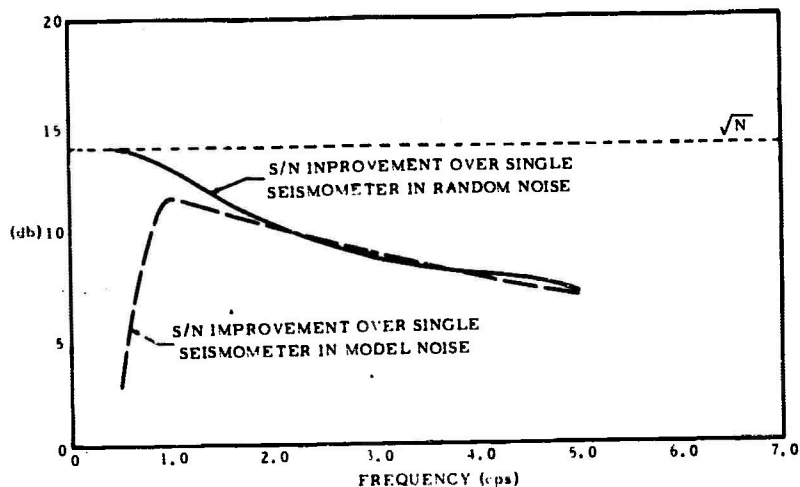
Signal Model: Al' velocities above 12 km/sec

Noise Model: As above

FIGURE 187. SIGNAL-TO-NOISE RATIO IMPROVEMENT

These observations provide the rationale for post-detection subarray beam forming to preserve signal energy up to 8 cps for classification and refined location.

4. Summary of Expected Performance

The general expected performance of the subarray isotropic processor is as follows:

(a) It should be capable of eliminating trapped mode noise that lies within the subarray unit cell in wave-number space. In most locations it should be able to accomplish this using ring processing.

(b) It should be capable of providing a single subarray output for world-wide coverage with no significant signal distortion up to any desired frequency. Limitations lie in the acceptance for detection of a higher random noise level at high frequency on the subarray output than would be tolerated, for example, for signal extraction prior to source classification studies. On the basis of our knowledge of signal-to-noise ratio, this is not a serious compromise as far as detection is concerned, but clearly necessitates the logic of a specially directed post-detection subarray beam former, and suggests the luxury of one special purpose simple beam former in the detection system.
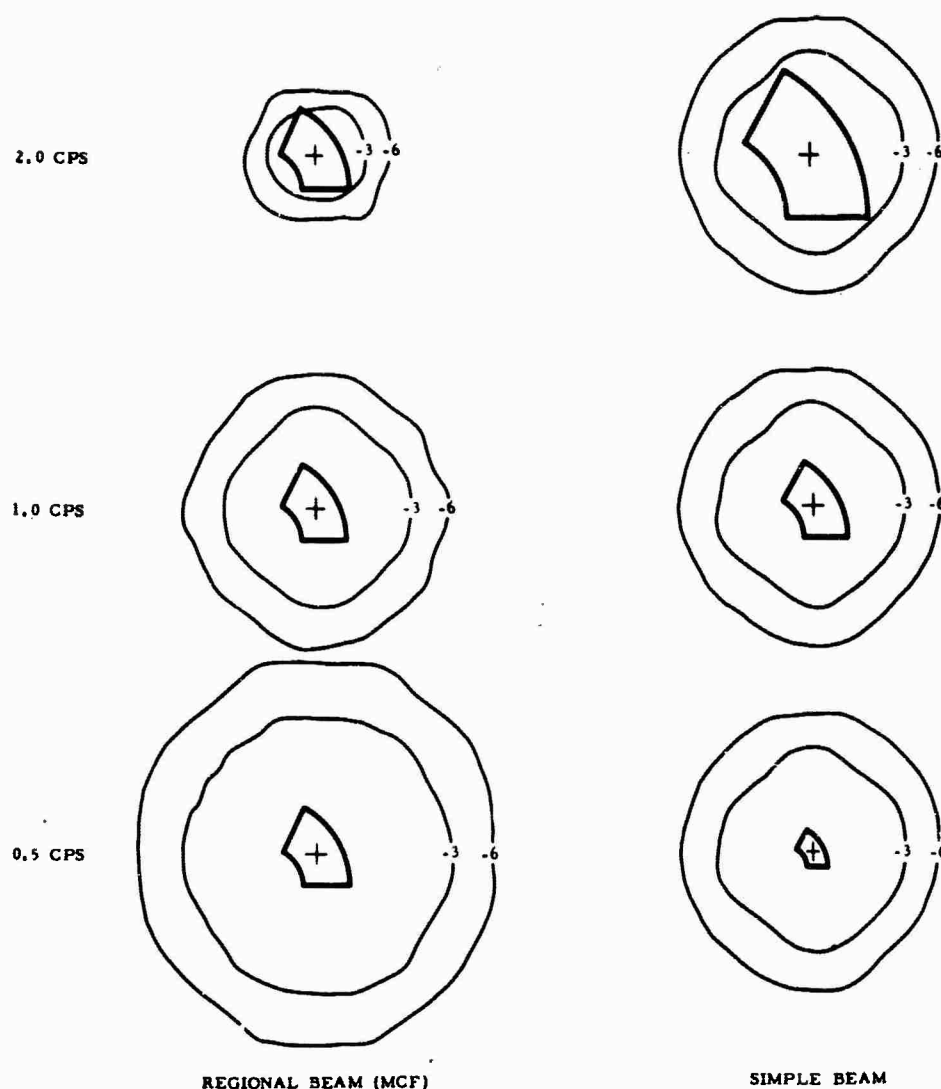
FIGURE 188. BEAMWIDTH COMPARISONS BETWEEN SIMPLE BEAM STEERING AND DIRECTIONAL MULTICHANNEL FILTER (MCF) AT 0.5, 1.0, AND 2.0 cps

5. Ring Processing

The selection of ring processing versus 25-channel general multichannel filtering is primarily based on cost. Except under special noise conditions, theory and experiment indicate that the improvement in a 25-channel isotropic processor versus a processor using ring sums is probably not worth the additional cost. [Experimental results are found in References 2 through 4.] Theoretical reasons include the following:

(a) The signal model is isotropic.

(b) Noise rejection is on the basis of propagation velocity. While there may exist dominant noise directions (e.g., from local disturbances), noise waves may be expected to arrive from all directions.

213

5.0 CPS

3.0 CPS

REGIONAL BEAM (MCF)   SIMPLE BEAM
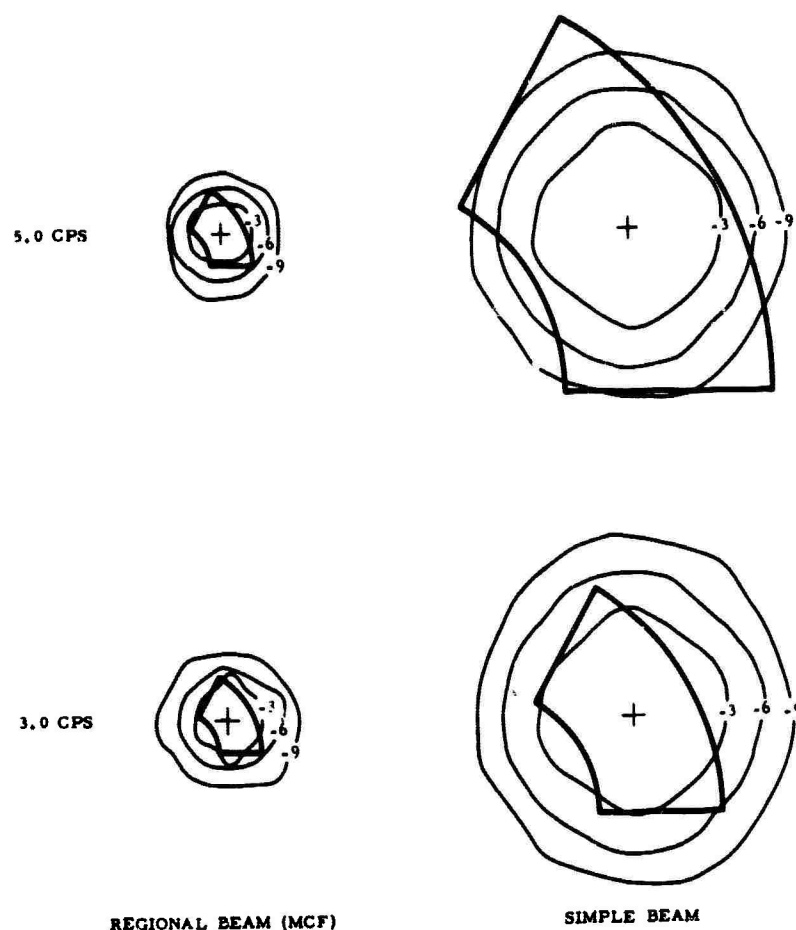
FIGURE 189. BEAMWIDTH COMPARISONS BETWEEN SIMPLE BEAM STEERING AND DIRECTIONAL MCF
AT 3.0 AND 5.0 cps
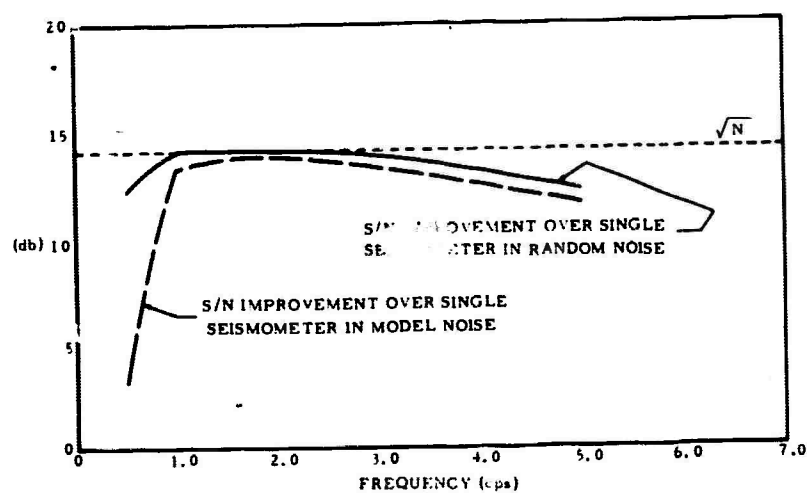
Signal Model: All velocities between 12 km/sec and 24 km/sec

Noise Model: All velocities greater than 12 km/sec in interval
from 0 to 2 cps plus random noise at all frequencies

FIGURE 190. SIGNAL-TO-NOISE RATIO IMPROVEMENT

214

(c) The fact that the signal model is isotropic limits the degree to which directional noise characteristics can be exploited. In other words, isotropic rejection of a given velocity can be accomplished nearly as effectively as directional rejection, if there is adequate separation in absolute velocity of the noise.

(d) The main need for deviating from rings would be the presence of a very strong local noise source, non-planar across the subarray. A small number of subarrays falling in this category may be expected and they would require non-ring subarrays.

6. Adaptive Processing

A second system consideration is the possible need for time-adaptive subarray processing. On the basis of experimental evidence [References 2, 3, and 4] and considerations similar to those given above, it is reasonable to expect that a time-invariant multichannel filter would generally be adequate except under special noise conditions. The capability to determine when special noise conditions exist and the ability to provide special processing [probably adaptive] for those situations should be considered a requirement of the system. For normal on-line operation, it would be necessary to redesign the on-line multichannel filters only occasionally if an adequate noise ensemble were used in the filter design.

7. Subarray Processing Problems

A summary of some typical subarray processing problems together with possible system solutions or comments is presented below.

Problem	System Solution or Comment
1. To cover the world beyond 30° with beam steering, it would require a dozen beams from each subarray to cover up to 3 cps (or about a hundred subarray beams to preserve signals up to 8 cps) to avoid signal rejection due to the 7-km subarray aperture.	1. Use a single isotropic processor output which will preserve signals up to any desired frequency, world-wide.
2. Because of the 7-km subarray aperture, 4.5 km/sec surface waves are not effectively attenuated by the array.	2. By use of a ring multichannel filter processor the effective subarray beam pattern can be modified at the low frequencies to provide additional attenuation of surface wave noise.

Problem	System Solution or Comment
3. Although world-wide signals may be preserved in a single output with a multichannel filter processor the random noise rejection of the subarray at higher frequencies would not be as good as it would for a time-shift-and-sum beam in the proper direction.	3. The capability of a multichannel filter at the higher frequencies will generally be better than predicted for random noise, but because of the signal beam broadening, will not have the signal-to-noise capability of a directed beam. In the detection problem, however, the frequency range 0.5 to 3 cps is of maximum interest, and adequate performance over this range is obtainable without subarray multiple beam forming. Subarray directed beam forming is desirable, however, for post-detection processing, although after detection it is necessary to form only a single beam. If it is desired to extend the maximum signal-to-noise ratio to higher frequencies for detection, the subarray geometry should be modified. The accuracy with which the location of the event must be known is equal to the subarray beam width at the highest frequency of interest for classification. This would correspond to a beam selection from LASA at 1/20 the maximum frequency. An 8-10 cps limit would thus dictate the use of about 100 beams for detection, or a 5 cps limit would require about 30 beams to define location adequately for post-detection processing.
4. Very strong local noise sources may exist in the vicinity of some subarrays such that the ring-processed output would be at a significantly higher noise level than the other subarrays.	4. High-noise subarrays may be processed on a non-ring basis and/or may require additional seismometers near the center of the subarray. The criterion determining this action should be long-term noise spectrum equivalence from all subarrays in the 0.2 to 4 cps frequency range.

216

Problem	System Solution or Comment

5. Disturbances which are local in time and space will occur and raise the noise level significantly.

5. The basic noise spectrum for a subarray will be known. The power output of each subarray will be monitored. When a few subarrays show significant excess noise, they will not be used in the detection beam former. If all show significantly higher noise than normal, all 525 channels will be recorded for off-line special detection processing. Noise sources producing propagating noise ma也 also be specifically gathered and used in the subarray filter design, so long as basic performance is not affected. All subarray thresholds should be set to insure a constant detection capability.

6. Seismometers or even entire subarrays may be out of operation part of the time.

6. In the use of ring processors, we have found that having one or two seismometers out is not critical to operation unless the subarray is performing at a very great increase over $\sqrt{N}$ in signal-to-noise improvement. By monitoring subarray output power, any situation could be detected where inoperative seismometers were limiting performance. Special action would be initiated as for case 5.

7. In the presence of large teleseisms the detection capability of the LASA for other events would be severely restricted.

7. By detecting world-wide, a logic for handling this situation may be used. All events below some power level (i.e., such that subarray outputs were within 6 db of noise level) would require no special treatment. Events from 6 db to 20 db higher than

Problem	System Solution or Comment
	subarray noise could be post-detection-processed using the normal subarray processing with special re-detection large array processing. Events greater than 20 db above the noise level [i.e., events larger than magnitude 5 or unexpected very large local events] would be retained in 525 channels for special post-detection subarray processing.
8. Ambient noise characteristics may change with time.	8. In ring processing, the noise propagation velocity is exploited, and that is time invariant. However, provision for adaptive (or slow time scale) subarray processing should probably be included.

8. Options Required for the On-line Predetection Subarray Processing

In considering the design of an on-line subarray processor, a number of contingencies should be provided for. In a quiet LASA site it might be more effective to have 42 subarrays of 12 seismometers each (3-4 ring configuration) rather than 21 subarrays of 25 seismometers each (5 to 8 ring configuration). In one case we would have 42 subarray outputs, ich formed from up to 4 inputs. In the second case we would have 21 outputs, each formed from up to 8 inputs. In addition, the possibility that some of the subarrays might require 25-channel filtering to handle special noise conditions should be provided for.

It is also possible that other types of subarray systems might be capable of accomplishing in some areas the functions of the existing subarrays in the Montana LASA. Two examples are vertical seismometer arrays and combinations of vertical and horizontal component seismometers. The processing requirements would basically involve the use of an on-line multi-channel filter providing an output preserving all teleseisms and rejecting trapped mode type noise.

The degree of generality required to satisfy any combination of the above contingencies is not great and special purpose processing equipment could be designed in the face of these contingencies.

218

ON-LINE DETECTION SYSTEM

We now proceed to an examination of the on-line detection system which basically operates upon 21 data channels, one from each subarray. Figure 191 shows a partial block diagram indicating some of the major features in a possible detection system. The major functions shown include the application of predetection filters to the 21 data channels, followed by a large aperture array beam forming function, followed by measurement of average power on the beam outputs (with square law detectors) upon which the detection logic is based. Not shown, but also important is the monitoring of the power output of the 21 channels before beam forming. This on-line detection system should accomplish the following objectives:

1. Provide detection and crude location on-line of all teleseismic events above a specified magnitude level.

2. Recognize any time period that the threshold detection requirement is not being satisfied in order that a command may be given to reprocess or store the 525-channel data on magnetic tape.
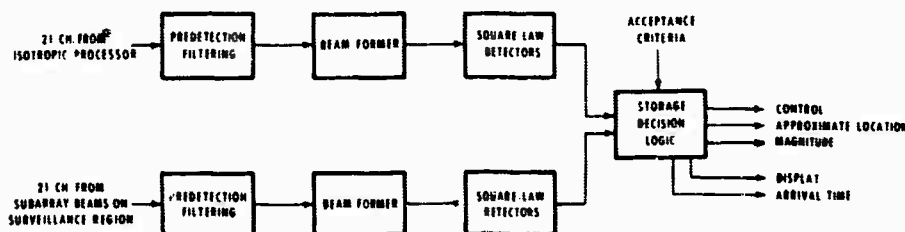
FIGURE 191. DETECTION SYSTEM

The precision requirement on the location function is primarily determined at this stage by the beam width of a subarray at the maximum frequency of interest for classification and fine location. With the Montana LASA subarray an upper frequency of 4 cps would involve decisions among about 25 areas covering the earth. A requirement of 8 cps would impose a requirement of 100 beams and areas for this approximate location. It is important that this on-line detection system be able to monitor its own detection capability.

A. Predetection Filtering

Figure 192 lists some of the objectives which should be accomplished by the predetection filter. If there is a difference in response to teleseisms from one subarray to the next which includes a component reasonably independent of range and azimuth, the predetection filtering should compensate for this difference. Such a difference can exist as a result of local coupling and/or the local shallow layering. By accomplishing this function in an average sense, spectra for noise and for teleseismic signals should be expected to be fairly uniform from one sub-

219

- COMPENSATE FOR AVERAGE SITE
  RESPONSE DIFFERENCE

- PROVIDE UNIFORMITY OF SPECTRA FOR
  NOISE AND AVERAGE SIGNAL FROM ONE
  SUBARRAY TO THE NEXT

- ACCOMPLISH AVERAGE TIME CORRECTIONS

- WHITEN AND BANDPASS LIMIT NOISE
  SPECTRA OVER DETECTION BANDWIDTH

- COMPENSATE FOR SYSTEM PHASE
  DISTORTION

- PROVIDE FOR LARGE ARRAY BEAM
  SHAPING

FIGURE 192. PREDETECTION FILTERING

array to the next, at least in the frequency range where the subarray output is mantle P-wave noise limited. Included in this site response difference would be any average time corrections, i.e., components of time correction independent of azimuth and range.

Since the ensemble signal-to-noise ratio can probably be expected to be fairly uniform over a frequency range of from 0.5 to 2.5 cps, or at least over the octave from 1 to 2 cps, and since a square law detector is contemplated, the predetection filter should also accomplish whitening of the noise spectrum over the detection bandwidth. It is expected that the subarray noise spectrum, at least over a limited frequency range and except under abnormal conditions, should have a reasonably time-stationary spectrum. However, at the present state of our knowledge the capability to modify the whitening filter function adaptively should be included in the system.

Because a square law detector is contemplated and because a relatively short integration time might be appropriate (at least for some of the functions), the predetection filter should compensate for system phase distortion such as that introduced by the seismometer response.

Predetection filtering can also provide for frequency-dependent large array beam shaping. The intrinsic time-shift-and-sum beam width of the large array is such that a very large number of beams would be required to cover the teleseismic world at the upper detection frequency of interest. However, only about 100 beams at most are required to satisfy the precision requirements on location determination. Therefore, beam broadening can result in the simplification of the system (by reducing the number of beams required) without significant loss in performance. This is especially true for the Montana LASA in which there is a concentration of subarray elements in a small aperture.

220

In its simplest form, the large array beam shaping function consists of introducing low-pass filtering on the outer subarray outputs such that they are not included in the beam forming process at higher frequencies. The degree of complexity of this detection beam former might range from a simple system (though potentially capable of ample performance) in which the data is reduced to one bit (polarity) data before input to the beam former, up to the point where it is introduced in more finely quantitized form (e.g., 2-12 bits) and in which the beam forming includes crude beam-dependent cross equalization. In any case, it is apparent that in forming a beam a simple plane wave assumption is not adequate and that an empirical table of time shifts would be required for each beam. It is expected that the time shifts used initially would form an imperfect beam but upgraded values could be "learned" to great precision over a period of a year or two.

In both channels of the detection processor, the short term average power of each of the beam outputs would be monitored for decision purposes.

B. Decision Logic

Decisions will be made on the basis of the power output from the 21 filtered subarrays and the power output from the beams. Two seconds would likely be an appropriate integration time, thus one test per second would be adequate. There is no requirement for accurate arrival time determination in the detection function.

1. Use of the Subarray Power Output

By comparing the relative power output of the 21 subarrays the presence of abnormal noise levels on one or more can be detected and abnormally noisy subarrays excluded from the beam former in the detection system. When there is an increase in short term average power on all of the subarrays within a 20 second time period, this may be interpreted as a signal or as the presence of abnormally high noise over the entire installation. On the basis of the power increase on subarray outputs a predictable power level increase should occur on one of the beam former outputs if a signal is present. If such an increase in beam former output is not detected and if the subarray output level exceeds an established threshold, a control unit would call for the recording of 525-channel data to determine the nature of the problem, and possibly apply on-line reprocessing for detection.

During the early operation of the system when the time corrections are imperfectly known, a signal loss will occur in the beam former For signals which can be detected on the basis of the 21 subarray power outputs the beam forming performance can be quantitatively monitored, and the postulated upgrading of the beam forming function can be quantitatively measured. If the coherent beam forming problem is very severe during the initial operation, incoherent beam

221

forming could be accomplished on the power outputs of the 21 subarray channels. This system might also be useful for those events which have their maximum power after the first few cycles and which therefore might require more complicated cross-equalization filtering in the coherent beam former. In considering a teleseismic arrival it is also of interest to note that the subarray power output would increase during the arrival of all teleseismic phases, but the power would be transferred from one beam to another in the beam output as different phases come in. It is assumed that the so-called signal-generated noise would be substantially reduced by the subarrays and will be low compared to actual signals on subarray outputs.

It is assumed that the detection system would at all times be in one of three states:

(a) An ambient state in which a reasonable fraction of the subarrays are at normal power level and in which no signals are detected on the beam outputs and in which it can be said with reasonable certainty that no events above threshold are occurring anywhere in the world. Under this condition, at least in later operation, only the 21 broadband isotropic subarray outputs would be permanently recorded on magnetic tape.

(b) An abnormal noise condition in which no teleseismic signals are being detected but in which the power output of the 21 subarrays is at a level such that it can be said that if a teleseism abo.. threshold occurred, it would not necessarily be detected. Under this condition, which probably should occur infrequently with a magnitude four threshold, the 525 raw data channels would be recorded on magnetic tape for "off-line" processing, or for adaptive subarray processing.

(c) The condition in which a teleseismic signal is being detected and its approximate location is known. Under this condition if the event were a small teleseism below some specified power level, the post-detection subarray beam forming would be initiated and carried out for all expected teleseismic phases of interest. In this condition the 21 isotropic processor subarray outputs as well as the post-detection subarray beam outputs would be recorded on a magnetic tape.

In the event of teleseisms with a power above some specifiable level, it would be possible to say that had another teleseism above the surveillance threshold arrived from another part of the world at the same time, it would not have been detected in the on-line detection system because of the interfering large teleseism. [This level may be raised by use of knowledge of the side-lobe pattern of the LASA in the detection logic.] In this situation special re-detection processing would be initiated on the data which had been recorded on magnetic tape. At a still higher teleseismic power level, at which special subarray processing would be required to detect smaller events in the presence of the large teleseism, the full 525 channels of data

222

would be recorded on magnetic tape. Again, with a system threshold of magnitude 4 this would probably be a fairly infrequent occurrence.

Particularly in the early stages of operation and/or for special research projects, the requirement to record the full 525 channels of data for any specifiable class of events should definitely be included in the detection and decision logic. For example, one might wish to record the full raw data for all events from magnitude 4 to 5 from some particular geographical region; or one might wish to record the full raw data in the presence of all quarry blasts coming from a northerly direction. This type of requirement could readily be accommodated within the general framework of the main system.

The decision logic would also control subsequent processing to be performed on the 525-channel or the 21- to 42-channel data being recorded on magnetic tape. For example, all events above some power level might go into a learning program designed to upgrade the beam forming capabilities of the LASA. Events within another power level range might be automatically routed to a fine location and classification system. Generally the initial additional processing required of any "non-ambient" data could be routed and controlled by the detection logic.

C. Large Array Beam Forming

Figure 193 lists some of the items to be considered in the problem of large array beam forming. For the detection function, it is probably unnecessary to input fully quantitized data into the beam former inasmuch as it appears that adequate dynamic range can be provided using polarity data only. It is very likely necessary to include azimuth-dependent station corrections in large array detection beam forming as well as post-detection beam forming, but the azimuth and range dependence can be more coarsely characterized for the large array detection beam forming than for the post-detection beam forming. It has been pointed out that beam shaping (i.e., high-frequency beam broadening) can readily be accomplished independent of azimuth by appropriately designing the predetection filters.

It is most likely that azimuth-dependent multichannel filters for beam forming would not be required in the detection system, but very likely would be required in the post-detection large array beam forming. Examples of possible need are for:

1. Potential exploitation of mantle P-wave noise fine structure if such exists.

2. Azimuth-dependent cross-equalization from subarray to subarray (potentially required if more than the first cycle or two of the signal is required for classification).

3. Detection of small events in the presence of large events (the use of adaptive location dependent multichannel filters is probably required in the post-detection processing).

223

- USE POLAR. Y DATA ONLY OR FULLY QUANTIZED DATA

- ACCOMPLISH AZIMUTH-DEPENDENT STATION CORRECTIONS

- USE SIMPLE BEAM STEERING BASED ON PLANE WAVE ASSUMP-
  TION, OR

- USE AZIMUTH-DEPENDENT MULTICHANNEL FILTERS TO PROVIDE
  - REDUCED NUMBER OF BROADENED BEAMS
  - POTENTIAL EXPLOITATION OF MANTLE P-WAVE NOISE
    FINE-STRUCTURE (IF SUCH EXISTS)
  - POTENTIAL AZIMUTH-DEPENDENT CROSS-EQUALIZATION

FIGURE 193. BEAM FORMING

MAGNETIC TAPE STORAGE

Figure 194 illustrates schematically the major storage requirements. Approximately 1.5 minute buffer storage for the raw and partially processed data is required in order that the decision logic can have time to determine the appropriate course of action. On-line magnetic tape storage includes a unit to record the 21 isotropic processor output channels continuously, a second tape unit to record possibly 42 channels from many of the detected events for post-detection processing, a tape unit with capability to record 525 channels of data when required for future processing, and enough additional tape units to accomplish the processing required on the general purpose computer and to insure the system does not become saturated. On all of the on-line tape units annotated data concerning the results of the detection logic (location, magnitude, and arrival time) should also be recorded.
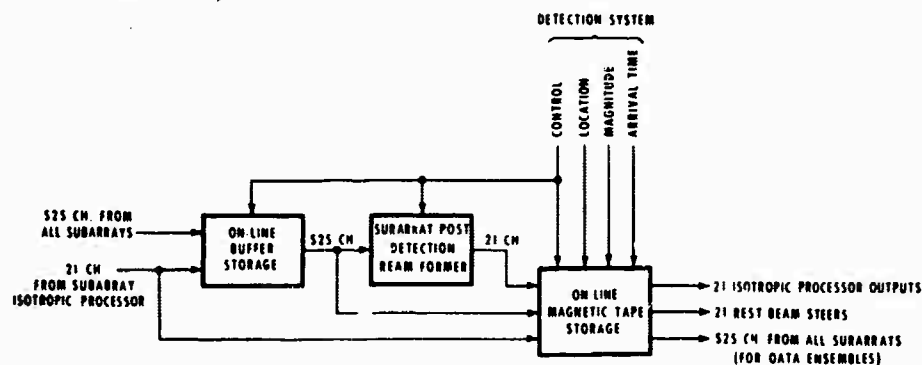
FIGURE 194. MAGNETIC TAPE STORAGE

224

Some indication of the volume of data that would be subject to recording is gained from Table I which indicates that world-wide a magnitude four event occurs on the average every 20 minutes and a magnitude three event every 30 seconds.

A. Post-Detection Large Array Processing

The full requirements for post-detection large array processing will not be fully specified for the next several years. At this point it is clear, however, that a reasonably powerful general purpose computer is required. An example of more mundane processing which might be done on some of the simpler events is shown on Figure 195.
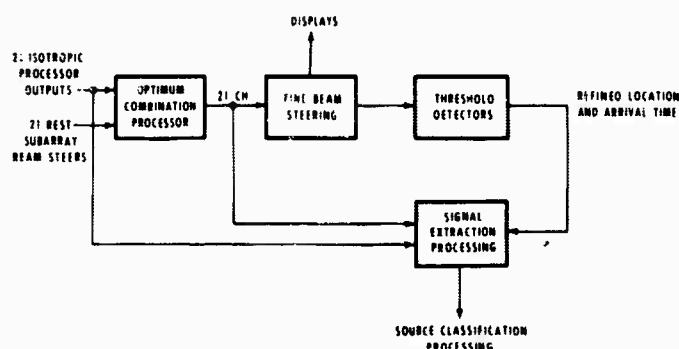
FIGURE 195. ON-LINE LARGE ARRAY PROCESSING

For a small detected event there would be stored on tape 21 isotropic processor outputs plus the 21 subarray outputs resulting from post-detection subarray beam forming, as well as the initial estimates of location, magnitude, and arrival time obtained from the detection logic. The two outputs from a given subarray could be combined by a two-channel filter as indicated in Figure 195. The resulting signal would probably be a close approximation to what would have resulted had an optimum 25-channel directional filter been applied to the subarray data. Because of the large beam width of the subarray at low frequencies, an optimum processor cannot make much use of the knowledge of the direction of the signal. Thus, an isotropic processor is near optimum at the lower frequencies even for a signal of known direction. At the higher frequencies, where noise in general is spatially random from one seismometer to the next in the subarray, time-shift-and-sum is the optimum 25-channel filter for extraction of a signal from a known direction. The output resulting from a two-channel filter shown in Figure 195 would thus in general be similar to the isotropic processor output at the lower frequencies, and would essentially represent the post-detection subarray beam output at the higher frequencies. The transition frequency range would be dependent on the local subarray noise characteristic. For example, at a noisy site like CPO, transition would probably occur above 3 cps.

225

At a very quiet site like **TFO** the transition might occur between 1 and 2 cps. At those frequencies in the higher frequency range where local coherent noise peaks were present, the two-channel filter would revert to the isotropic processor in the vicinity of the noise peak. The net result of the post-detection processing is 21 channels of near optimum subarray output data which can now be treated for refined location, improved signal wave form extraction, arrival time estimation, and the measurement of classification parameters.

SUMMARY

Figure 196 summarizes in block diagram form most of the elements of the system discussed. Much of the processing which has to be done on-line all of the time to all of the data has been discussed in moderate detail. Because of the large number of computations required and the degree to which the system can be defined at this time the use of a special purpose detection processor seems appropriate.
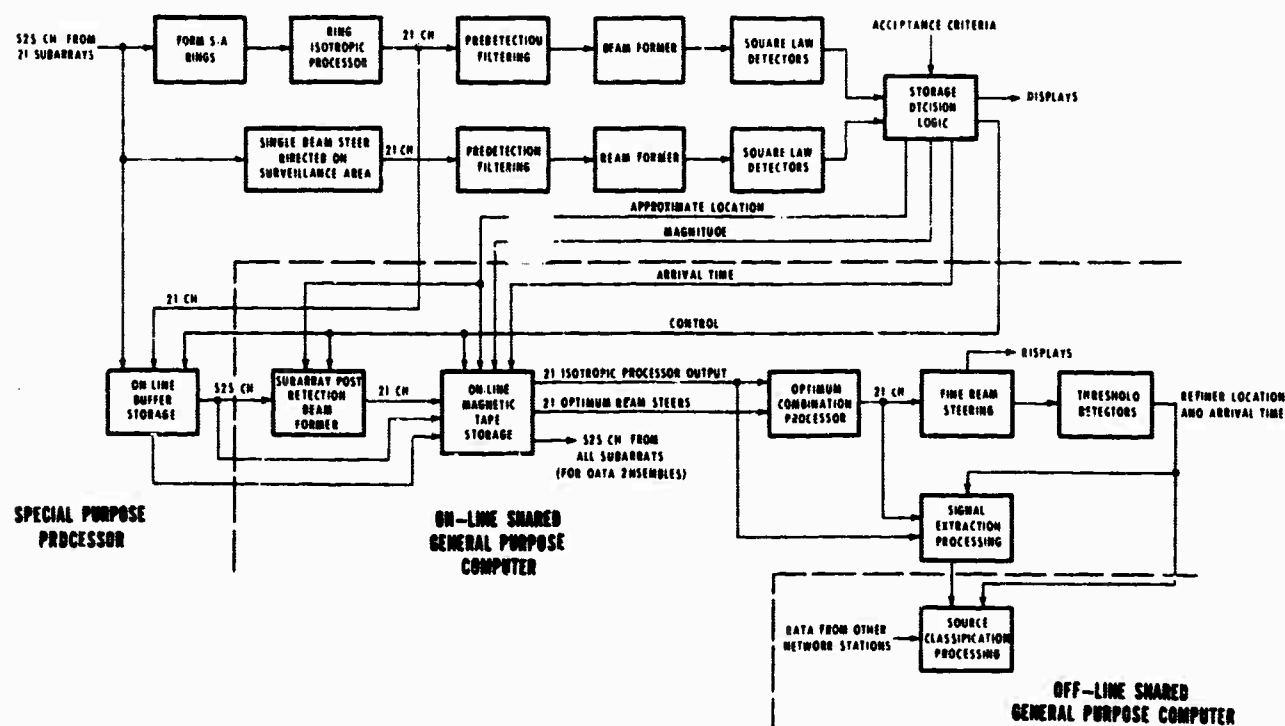
LASA PROCESSING SYSTEM

FIGURE 196. LASA PROCESSING SYSTEM

For processing that is only applied intermittently to a portion of the data, the use of an appropriate magnetic tape storage facility and a time-shared general purpose computer appears to be appropriate. However, it does seem necessary that for a practical system the bulk of the post-detection processing must be accomplished automatically under computer control, essen-

tially "on-line" using the general purpose computer. This automatic processing should include refined location, phase separation, re-detection processing, arrival time determination, measurement of classification parameters, production of a system log, and such service functions as subarray noise analysis and filter design. It should also include an automatic learning capability which would use information from the large teleseisms to continuously upgrade the LASA performance. It should be clear from the discussion that the system discussed, in addition to including certain special purpose computing equipment, peripheral equipment and displays, will require a very major software development.

The introduction of off-line processing not under automatic control would be introduced at the network processing level.

21. HIGH FREQUENCY SIGNAL CONTENT IN SEISMIC EVENTS
by

M. A. Rubenstein and J. Aein, Institute for Defense Analyses
J. Beardwood, General Atronics, Corp.

The Story is Still SIGNAL-TO-NOISE RATIO

In examining the problem of detecting nuclear underground explosions by seismic means at teleseismic distances it has become clear that "informed" opinion regards detection at (high frequency) (i.e., >5 cps), to be very unpromising. This view is based on the argument that even if high frequencies existed at the source the properties of the earth attenuate these frequencies so that it is impractical to consider their use in detection and in diagnostics at teleseismic distances.

Over the years much data has been assembled to indicate that the high frequency content of explosions fall off inversely as a power of distance from the explosion. USC&GS and USGS have had on-going programs which support this view. These measurements were made at near-in distances (50 km to 800 km from the shot).

In addition to shot data, most of the earthquakes examined supported the view that high frequencies were attenuated by the earth at teleseismic distances. The question remained; perhaps large magnitude earthquakes ($m_b > 5$), that could be detected at teleseismic distances, did not generate high frequencies or that the instrumentation was not sensitive enough and/or did not have the dynamic range to record high frequencies in the presence of stronger low frequencies. Furthermore, for many years the observations of earthquakes were made by measuring long-period surface waves which did not show "high-frequency energy."

During the past few years a small number of investigators have continued to raise the question of the presence of high-frequency signals associated with nuclear events. In particular, Prof. Rocard in France, has tailored his seismometers to give peak response at 4.5 cps in order to discriminate against 1 cps signals.* Interesting events were detected using this type of instrumentation. ARPA (Dr. Bates) requested IDA to examine the "unique" results that Prof. Rocard obtained.

It soon became apparent that the facts on "high frequency" energy of seismic events were difficult to obtain. Furthermore, the crucial issue was not "high frequency" energy alone, since no adequate relationship existed for amplitude or magnitude conversion to energy; but rather our old friend Signal-to-Noise Ratio. In fact, the discussion based solely on energy tended to obscure the important factor that for our purposes it was the ratio of signal power density to noise power density that was important.

---

*The VESIAC Lakewood Conference on High Frequency also considered the matter.

With this in mind IDA requested the General Atronics Corporation to analyze a detected Soviet nuclear explosion for "high frequency" content. The first results showed no detectable energy above 2.5 cps. A closer examination** of the data showed that the magnetic recording did not have the noise characteristics nor the dynamic range (<30 db) to permit "high frequencies" to be recorded in the presence of stronger 1 cps signals. Further investigation showed that most of our VELA UNIFORM events at teleseismic ranges were recorded at low speed tapes with inherent frequency and dynamic range limitations.

After a discussion with Dr. Paul Green of Lincoln Laboratories, who also felt that the "high frequency" question had to be answered, IDA began to push further in the investigation of the problem of high-frequency content of signals obtained at teleseismic distances. One nuclear event had been recorded at the Tonto Forest Observatory using a high quality digitized recording system designed by M.I.T. The digitized data covered a spectral band from 1 to 8 cps with a 75 db dynamic range. During a visit to Lincoln Laboratories, IDA requested that this event be analyzed to see if any usable high-frequency signal could be observed. The answer is a very clear YES!

General Atronics Corporation in their letter of 11 August 1965, reported that the signal power density to noise power density was approximately +9 db over the 1 cps to 8 cps frequency band as observed with 0.25 cps bandwidth filters. Figures 197 and 198 are the pertinent data for a magnitude 5.6 shot detonated at Semipalatinsk. It should be noted that these data were taken from a single shallow buried vertical seismometer of the Tonto Forest array. The readers attention is invited to the noise power density spectrum which falls by -14 db in going from 1 cps to 7.75 cps. The signal-to-noise ratio maintained itself at a mean value of approximately +9 db over the frequency band when measured with 0.25 cps filters.

Furthermore, this data, taken on a near surface based seismometer, does not suppress high-frequency ambient seismic noise as well as other buried instruments. A recent report on a LASA Seismometer buried at 200-foot depth shows that at 3 cps the ambient seismic noise is -22 db as compared with that at 0.5 cps; at 5 cps the noise advantage is -43 db!! (See Figure 199 AFTAC LASA Report of 3 August 1965.)

The availability of seismic information in the broad band covering from 0.5 cps to at least 8 cps and probably higher raises the following interesting possibilities:

1. New scientific research on earthquakes and geologic events at teleseismic distances.

2. For LASA the potential for very fine beams with good side-lobe characteristics and perhaps smaller arrays.

**Dr. J. Aein of IDA has investigated and determined these facts (report forthcoming).
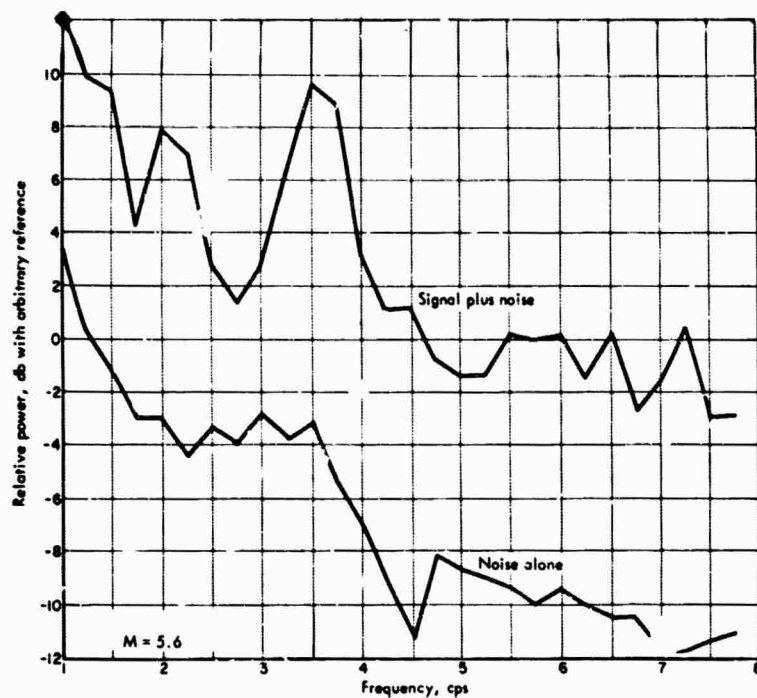
FIGURE 1 Power Density Spectra (Instrument response included)

FIGURE 197. POWER DENSITY SPECTRA

FIGURE 198. S/N vs FREQUENCY

230

3. Diagnostic studies comparing the spectral distribution of shots and earthquakes. In this connection, Dr. J. DeNoyer postulated such a discrimination. (IDA paper P-30 in 1963.)

4. Seismic concealment.

5. The crucial issue of cavity decoupling as a function of frequency.

Since this note is based on limited data it is essential that VELA UNIFORM instrumentation consistent with answering questions similar to those raised above, be employed as a regular part of the program. This recommendation has been made to ARPA.
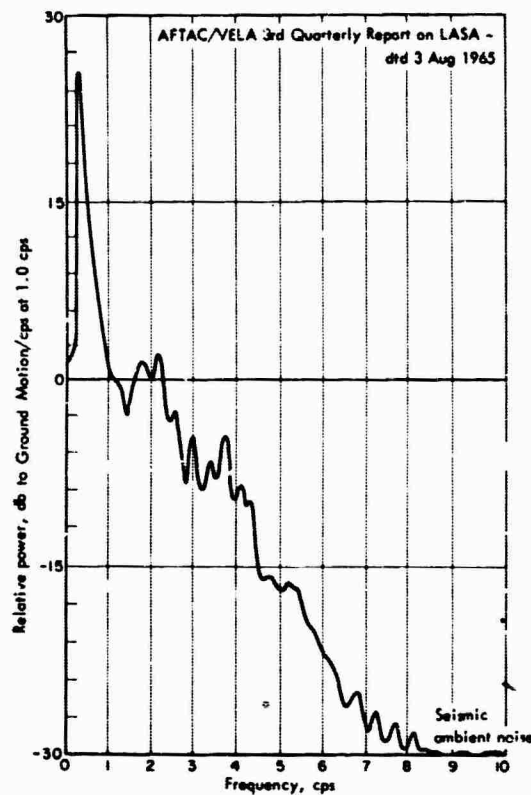
FIGURE 199. POWER DENSITY SPECTRA OF SYSTEM NOISE TESTS FOR SEISMOMETER BURIED AT 200 FT

22. PRELIMINARY PLANS: SDL PROCESSING OF LASA DATA

by

W. C. Dean
Seismic Data Laboratory, Teledyne, Inc.

Most computer processing of LASA data will involve velocity filtering. In order to velocity filter teleseismic P waves over a large array, we must know the P-wave travel times to each seismometer in the array. Initial attempts to velocity filter an array of 100 km to 200 km in extent assuming a single velocity wave front have not successfully aligned the P-wave signals. One explanation is that there exists a velocity (or time delay) anomaly at each site due to the structure. Experience with TFSO has shown that when signal arrival times are adjusted by the site travel-time anomalies, the expected velocity will provide the proper signal alignment.

There are two basic approaches to velocity filtering 525 inputs. The first involves alignment by computer cross correlations on the received signals. This method eliminates the necessity of measuring the travel-time anomalies altogether. However, it works only for strong signals since for weak signals the cross correlations will be aligning noise. The second approach is to calibrate the array by measuring the travel-time anomalies at each site for all regions of interest. This method permits beams to be focused on particular regions prior to signal detection.

Measurement of the travel-time anomalies can be done by either cross-correlation computations (reading the time of the peak of the cross-correlation function between the seismograms of a signal recorded at two sites) or by film analysis (reading the time delay of some prominent feature of the signal recorded at two sites). Experience with TFSO shows that the travel-time anomalies determined by film analysis and by computer cross correlation are in agreement. We recommend film analysis since it is faster. Moreover the travel-time anomalies can be expected to vary for different azimuths and epicentral distances. Therefore it is cheaper and more convenient to save the large quantities of LASA data necessary to calibrate the array in all desired azimuths and distances on film rather than magnetic tape.

Motivated primarily by the necessity to calibrate the LASA array, we plan the following analyses at the SDL:

1. Film Catalog

The objectives of this study are to create a log of events detected at LASA for subsequent posting and processing; to compare the list of events detected at LASA independently of other stations with other lists such as the USC & GS list in numbers, magnitudes, signal-noise ratio, location, etc.; and to monitor the performance of on-line beams or other on-line processors.

232

Many large events or events with large signal-to-noise ratios from each seismic region of interest are required. Large events permit accurate measurements of the relative arrival times between subarrays. Many events from any given region permit averaging out the effects of inaccurate epicenters.

The data would include several LASA inputs on 1 or 2 Develocorders. For example, the primary Develocorder might display the individual traces from the 500-foot wells at the center of all subarrays but those in the B-ring. A second Develocorder. if available, might display the summation traces from a similar set of subarrays. Either or both Develocorders might display one or more beams or other special processor outputs when they become available on-line.

The procedure would be similar to that practiced at Seismic Observatories now. All signals detected would be entered by their arrival times, t_o, amplitudes, A, and periods, T, together with phase identification where possible. This data recorded at the center and each outside subarray permits computing an approximate epicenter, azimuth, and range, as well as the event magnitude. These data and computations would be filed chronologically on tape for future searching.

2. Travel-Time Anomalies at LASA

The objectives of this study are to test how accurately LASA can be beamed for all events from any given region, to determine departures from expected travel-time curves for each site vs azimuth and distance, and to develop digital programs to account for the travel-time anomalies.

The data required would be the same Develocorder film data used for the event catalog.

The procedure is the same as that outlined by Chiburis (Experience with the TFSO Extended Array). Using the event epicenter obtained from the USC & GS, or from the arrivals at the four outside subarrays at LASA, or from a network of VELA array stations, we compute the time intervals between the expected arrival time at the center of each outer subarray with the expected arrival at the center subarray. We compute similar intervals for measured arrivals. The travel-time anomaly for each outer subarray is the average of the differences between measured and expected time intervals for events from one particular epicentral region. Errors in epicenter locations must be either averaged out over many events or systematically accounted for as outlined by Chiburis.

3. LASA Beam Forming

The objectives of this study are to compare various methods of forming LASA beams, to compare LASA's beam response in signal-to-noise ratio with that of single seismometers or

single subarrays, and to measure the beam response for signal-epicenters not on the center of the beam.

The data would be that saved on magnetic tape by the LASA computers.

The procedure would be to form a beam toward a single event by using the average travel-time anomalies for events from that region, by using the travel-time anomalies measured for that particular event on film, by aligning this event from cross correlations over 5, 10, and 20 seconds of the P-wave signals. In addition the individual and average film travel-time anomalies should be compared with the equivalent anomalies computed from cross-correlation alignments. Partial beams should be formed using only the center and outside four subarrays, using all but the outside four subarrays, all but the outside eight subarrays, and so forth comparing the signal waveforms and signal-to-noise ratios in each case. Beams formed by using only single elements in each subarray with those using all 25 should be compared in a similar way.

4. Analysis of Array Noise by Coherence Functions

A. Coherence Functions of Linear Systems

One area currently under study at SDL for increased understanding of seismic noise in arrays is that of multiple coherence functions. In the investigation of any kind of random phenomena, there is always the need to subject the procedures and results to critical statistical analysis. For random time functions, this appears difficult in the time domain. However, in the frequency domain, methods are available. The distributional results of the multivariate complex Gaussian statistical analysis due to Goodman[1] are applicable in describing the statistical variability of estimators for the spectral density matrix of a stationary Gaussian multiple time series and also for describing the variability of estimators of certain functions of the elements of these matrices. Among this class of functions are the frequency response functions and coherence functions for multiple input linear systems.[2] Multichannel frequency response functions have been used in processing of seismic array data. However, the role of the coherence functions and their distributional properties for multichannel systems have not been developed for these applications. The coherences of a multiple input linear system are functions of frequency which are direct analogues of the various correlations of classical multivariate statistical analysis.

To describe coherence functions in the terminology of filters, we speak of projecting $x_o(t)$ on $x_1(t)$ whenever x_1 is passed through an optimal linear filter (non-realizable or non-real-

[1] N. R. Goodman, "Statistical Analysis Based on Certain Multivariate Complex Gaussian Distribution (An Introduction)," Ann. Math. Stat., 34, pp. 152-177, 1963.

[2] Loren D. Enochson, Frequency Response Functions and Coherence Functions for Multiple Input Linear Systems, NASA contractor report, NASA CR-32, April 1964.

time filters are allowed) for which the desired output is x_o. This filter has the frequency response function

$$H = \frac{P_{10}}{P_{11}}$$

where P_{10} is the cross power spectrum of x_o and x_1 and P_{11} is the spectrum of x_1. The output of the filter, which we call the projection of x_o on x_1 and denote by $x_{o/1}$, then has power spectrum

$$H^2 P_{11} = \frac{\left|P_{10}\right|^2}{P_{11}}$$

The fraction of the power of x_o contained in this output is the ordinary coherence of x_o and x_1, and is denoted by γ_{10}^2. We then have

$$\gamma_{10}^2 = \frac{\left|P_{10}\right|^2}{P_{00}P_{11}}$$

Whenever γ_{10}^2 is unity, an exact linear filter relationship exists between x_1 and x_o.

Whenever there are n inputs $x_1, \ldots, x_n$, then x_o may be projected on all n simultaneously. In this case, n filters $H_1, \ldots, H_n$ are determined such that the sum of their outputs, the projection, is an optimal approximation to x_o. Here the matrix $H = (H_1, \ldots, H_n)^T$ (where the superscript T indicates the transpose) of filters is given by

$$H = P^{-1}P_o$$

where P is the matrix of the cross power spectrum of $x_1, \ldots, x_n$, and where $P_o = (P_{10}, P_{20}, \ldots, P_{n0})^T$. Here the summed output which we denote by $x_{o/z}$ has the power spectrum

$$P_o^{*T}P^{-1}P_o$$

The fraction of the power of x_o which is contained in $x_{o/z}$ is called the multiple coherence of x_o with $x_1, \ldots, x_n$, and is denoted by γ_{z0}^2. The multiple coherence is given by

$$\gamma_{z0}^2 = P_o^{*T}P^{-1}P_o / P_{00}$$

when the multiple coherence is one, an exact linear filter relationship exists between $x_1, \ldots, x_n$ and x_o. The multiple coherence is useful as a detector of unidentified inputs to a linear

system. For, until all significant inputs are identified, the output power is not accounted for with the result that the multiple coherence is less than unity.

Another kind of coherence function which appears to be useful in the study of noise in seismic arrays is partial coherence. The statement, "the partial coherence of x_o and x_1 with the effects of $x_2, \ldots, x_n$ removed" means that the projection of x_1 on $x_2, \ldots, x_n$ has been subtracted from x_1, the projection of x_o on $x_2, \ldots, x_n$ has been subtracted from x_o and then the ordinary coherence of the residual functions has been calculated. Several input channels $x_1, \ldots, x_m$ could each have their projections on $x_{m+1}, \ldots, x_n$ removed and then a multiple-partial coherence calculated. Partial coherences may be used to uncover unsuspected linear relationships which are masked by known ones involving much larger power.

B. Application of Coherence Functions to Seismology

Arrays of seismometers produce multiple time series which can be studied with the methods of coherence functions. When the noise at an array consists of a single component which propagates coherently across an array, the time function output of any one element will be approximately a linear filter transformation of the output at any other element. When the noise consists of n uncorrelated components, all coherent across the array, then n elements outputs will be sufficient to approximate one additional output. The noise at the center element obtainable by linear filtering from all the other elements (assuming that there are sufficiently many) constitutes the coherent noise. The other part is incoherent. The multiple coherence of all other elements with the center one will be the fraction of the noise which is coherent. The coherent noise may be controlled by multilinear filtering. The incoherent part must be overpowered by the numbers of elements used. From the number of elements required to maximize the multiple coherence, one knows the number sufficient to do the multilinear filtering. Comparing this with the number needed to control the incoherent noise indicates the required numerical size of the array.

Multilinear filters may be synthesized in the time domain or frequency domain. Use of the complex Gaussian distribution allows confidence intervals to be determined for the results in the frequency domain.[3,4]

---

[3] N. R. Goodman. Measurement of Matrix Frequency Response Functions and Multiple Coherence Functions, Technical Report No. AFFDL-TR-6. 56, June 1965.

[4] L. D. Enochson and N. R. Goodman, Gaussian Approximation to the Distribution of Simple Coherence, Technical Report No. AFFDL-TR-65-57, June 1965.

C. Results of Computational Experiments

Numerical experiments under controlled conditions have been made at SDL.[5,6] It has been found that frequency response functions, in terms of gain and phase may be accurately determined. They remain stable and reliable under various complicating conditions. The multiple coherent function is computationally stable, and may be determined accurately. It may be used as an indicator of the presence of unaccounted for variables. The partial coherence function is computationally delicate and unstable. Longer record lengths and narrow filter bandwidths tend to stabilize the results. Particular sensitivity of the partial coherence functions to time delays between the inputs has been observed.

5. Signal Correlations Across LASA

The objectives of this study are to find the P-wave correlations with distance and frequency for teleseismic signals across LASA. The section to follow describes results from a similar study applied to data from TFSO.

A. Signal and Noise Correlations at TFSO

Velocity filtering tends to enhance signals of the same shape and tends to smear, average, or cancel signals of different shapes. A measure of the similarity in shape between waveforms is given by correlation coefficients which is simply the maximum value of the normalized cross-correlation function. Plotting the correlation coefficient versus separation between the seismometers provides a measure of correlation versus distance over the array. Filtering the seismograms through narrow bandpass filters before correlating provides a measure of correlation versus frequency.

In this study the signals used were P waves from ten teleseismic earthquakes. Noise samples were chosen from these same seismograms just prior to the onset of the signals. The events were chosen for the largest signal-to-noise as possible which still avoided clipping on the magnetic tapes. The array configuration is shown on Figure 200.

The signal and noise correlations decrease as both frequency and distance increase. Figure 201 shows the average correlations between all pairs of seismometers at the TFSO extended array for all ten teleseismic events. Both signal and noise correlations are high for small distances (less than 3 km). Noise correlations decrease faster than signal correlations with increasing distance so that signal correlations exceed noise correlations for all distances greater

[5]L. D. Enochson, G. P. Thrall and J. C. Bradford, Seismic Partial Coherency Study, SDL Report, 28 April 1965.

[6]L. D. Enochson and J. C. Bradford, Numerical Experiment with Partial and Multiple Coherences, SDL Report, August 1965.

237
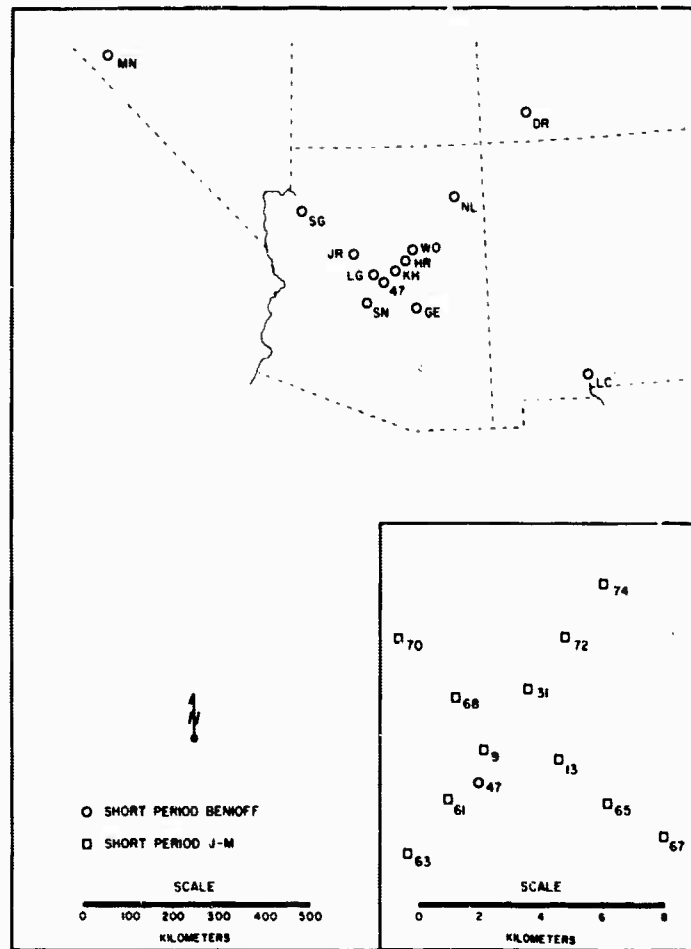
FIGURE 200. MAP OF THE TFSO AND EXTENDED ARRAY SEISMOMETERS

than 3 kilometers. The large drop in correlations for both signals and noise beyond 10 kilometers is not due to a change in instruments (J-M to Benioff seismometers), but more likely to a change in local site structure. All correlations in this report are corrected for changes in instrument responses.

The decline of correlations with distance ceases after the noise correlations are between 0.2 and 0.4. By our method of computing correlations, this range is just the level of correlations that we would expect from random functions. Generally, the noise appears to be random for seismometer separations equal to and larger than 30 kilometers. The signal correlations at all frequencies are above values expected from random functions for all distances covered by the extended array (up to 800 kilometers).

238
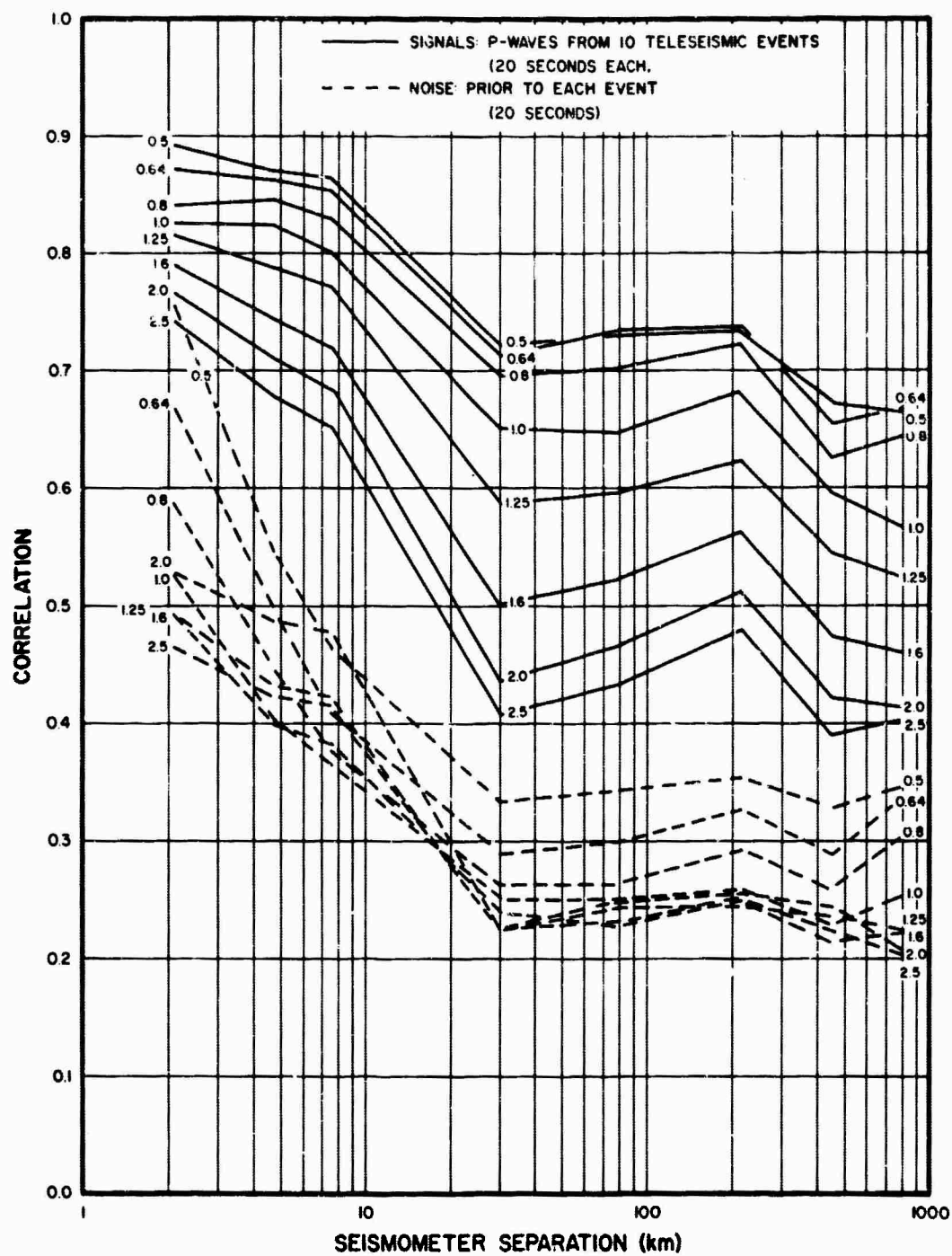
FIGURE 201. AVERAGE SIGNAL AND NOISE CORRELATIONS vs DISTANCE AND FREQUENCY AT TFSO
EXTENDED ARRAY FOR 10 TELESEISMIC EVENTS

239

The prominence of signal over noise with distance is shown by the correlations at 0.5 and 1.0 cps and their confidence limits shown on Figures 202 and 203. The lower confidence limit for signal correlations is above the upper confidence limit for noise correlations for all distances greater than 3 kilometers. The maximum dominance of signal correlations over noise correlations occurs for seismometer separations between 10 and 100 kilometers.

The signal correlations presented in Figure 201 show averages of all seismometer pairs irrespective of their orientation with the signal direction. Seismometer pairs oriented normal to the signal direction might be expected to correlate higher than pairs with the same separation oriented in line with the signal direction. Figure 204 shows signal and noise correlations from all 10 events versus distance and frequency for all seismometer pairs normal to the signal direction. Figure 205 is a similar plot for pairs in line with the signal direction. There is little difference in the two. Figure 206 shows the average broadband correlations and confidence limits of signals for : seismometer pairs, for pairs normal to signal direction, and for pairs in line with the signal direction. The signal confidence regions overlap for all distances indicating essentially no difference between in-line and normal correlations.

The large drop in correlations occurring for distances greater than 10 kilometers was thought to be due to the change of instruments at the LRSM sites (Benioff seismometers) over those at the TFSO sites (J-M seismometers). Such is not the case. All J-M seismograms for the correlation computations have been filtered to convert them to the Benioff response. Moreover, the effect of correlating a J-M and a Benioff seismogram instead of two Benioffs decreases the correlations by only .02 to .03, insufficient to account for the large decrease seen for distances beyond 10 kilometers. The drop in correlations is more likely due to the large differences in structure between the TFSO array and the outlying LRSM sites.

B. Correlation Computations

The philosophy behind our method of computing correlations for teleseismic signals is the following: We want to determine quantitatively the largest dimensions of a seismic array for which the ordinary array processing of velocity filtering and mixing the seismograms reinforces teleseismic P waves and cancels the noise. Moreover, we wish to determine this correlation as a function of frequency as well as distance. Since velocity filtering aligns the onset of the P waves and adds, the signals reinforce if they possess the same shape. A measure of similarity in shape of two seismic traces, $Z_m(k)$, and $Z_n(t)$, is given by the correlation coefficient, $\phi_{mn}(o)$, which will be the maximum value of the cross-correlation function when the signals are properly aligned.

240
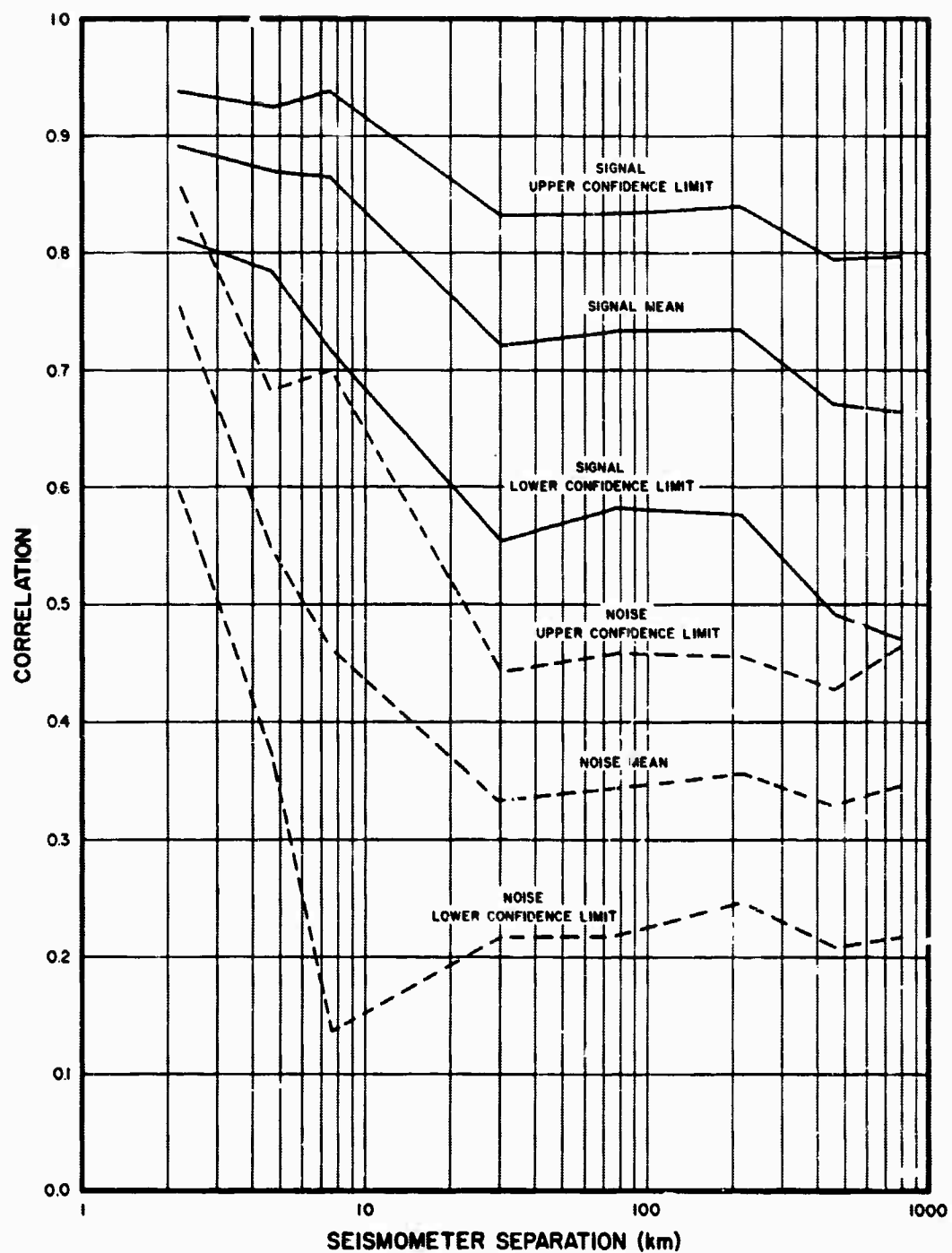
FIGURE 202. AVERAGE SIGNAL AND NOISE CORRELATIONS AT 0.5 cps vs DISTANCE AT TFSO EX-
TENDED ARRAY FOR 10 TELESEISMIC EVENTS
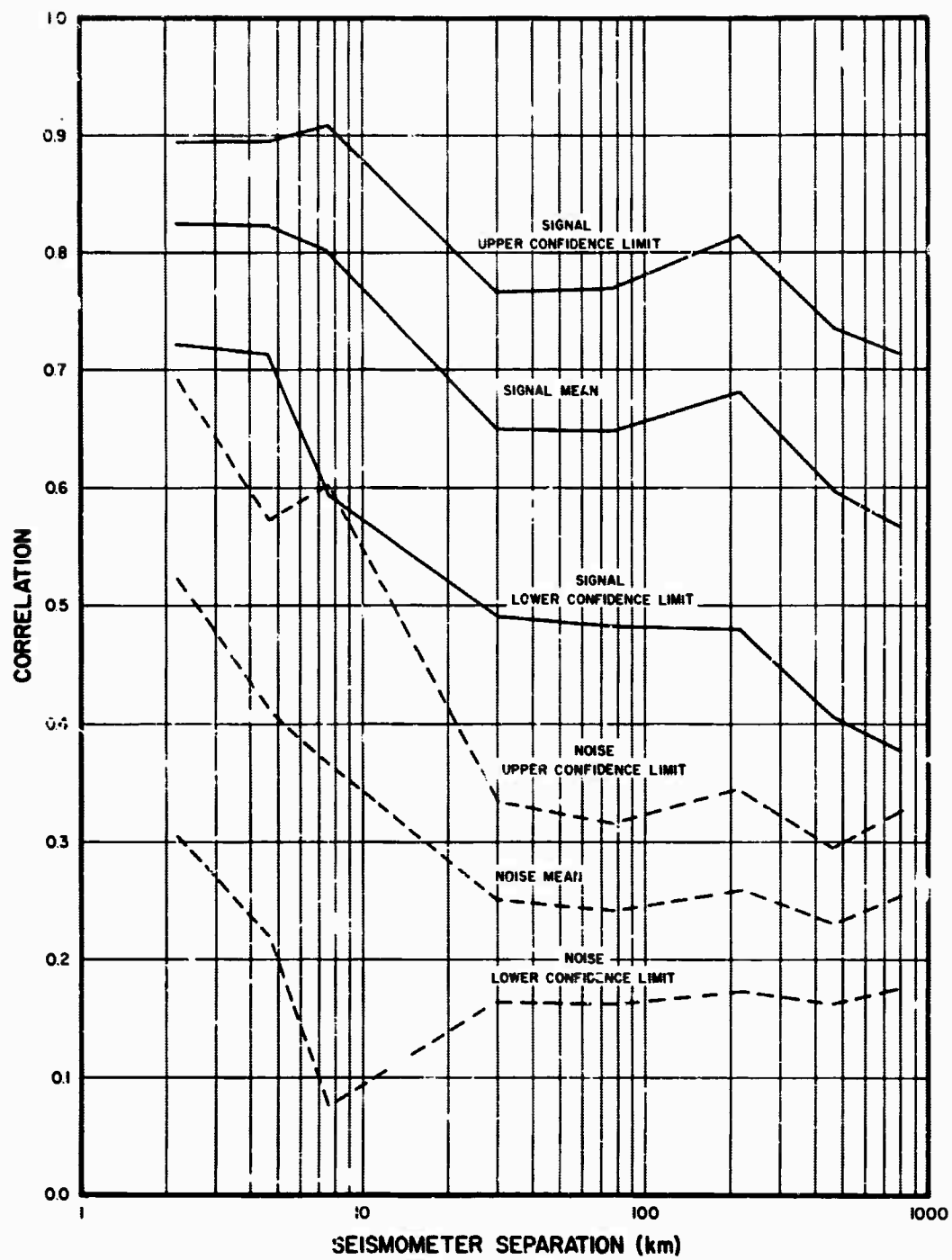
FIGURE 203. AVERAGE SIGNAL AND NOISE CORRELATIONS AT 1.0 cps vs DISTANCE AT TFSO EX-
TENDED ARRAY FOR 10 TELESEISMIC EVENTS

242
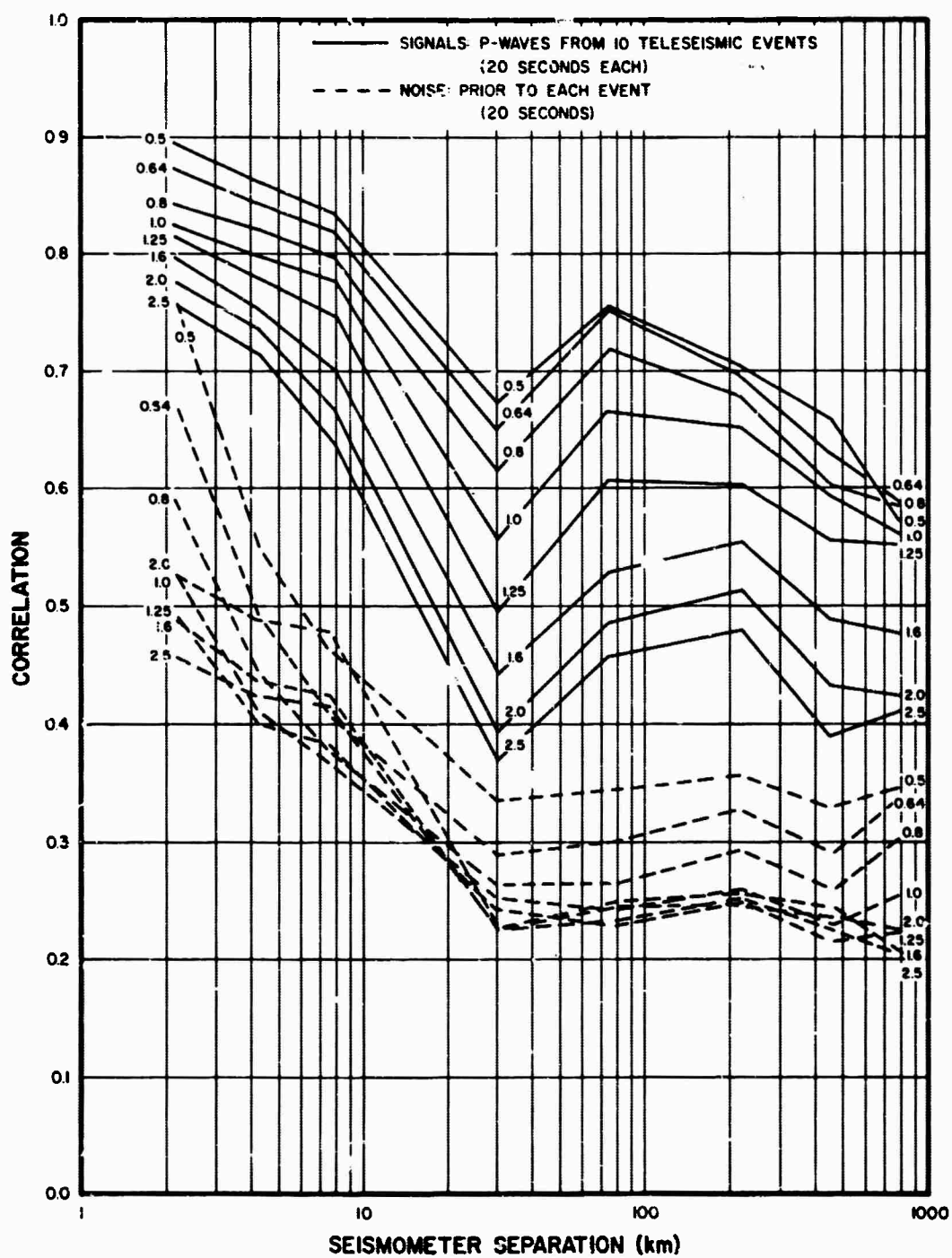
FIGURE 204. AVERAGE SIGNAL AND NOISE CORRELATIONS vs DISTANCE AND FREQUENCY FOR SEISMOMETER DISPLACEMENTS NORMAL TO SIGNAL DIRECTION

243
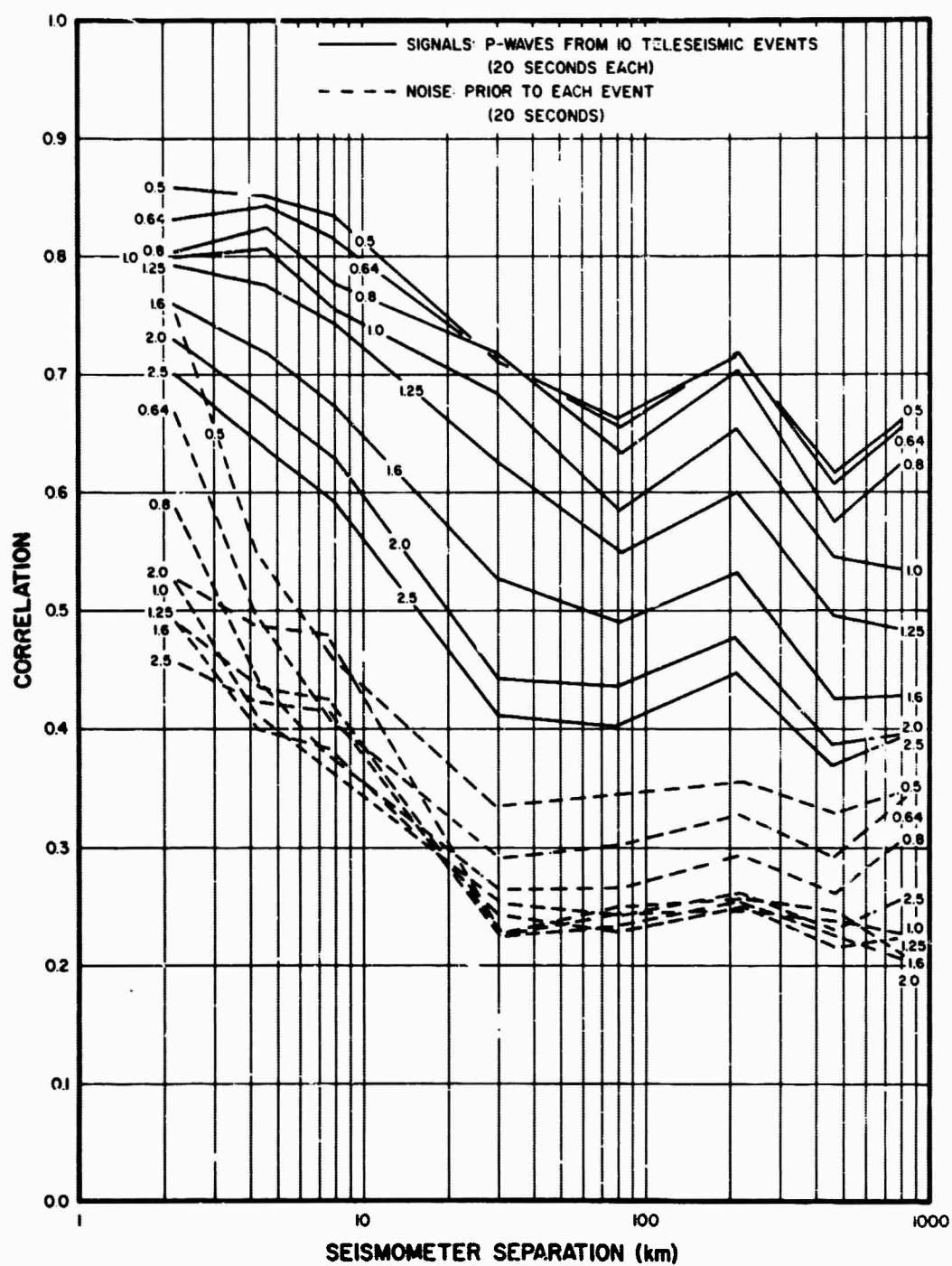
FIGURE 205. AVERAGE SIGNAL AND NOISE CORRELATIONS vs DISTANCE AND FREQUENCY FOR SEISMOMETER DISPLACEMENTS IN-LINE WITH SIGNAL DIRECTION

244
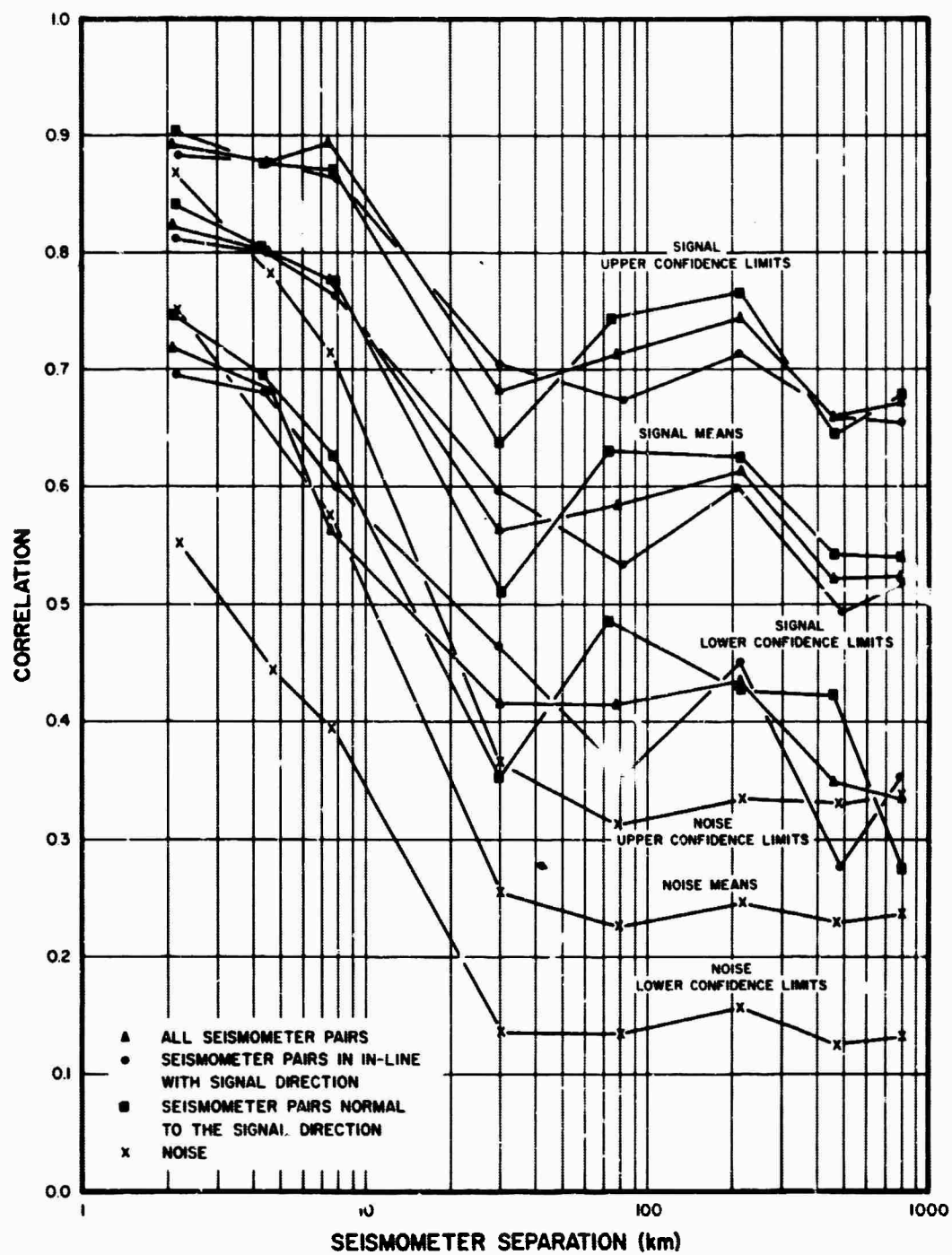
FIGURE 206. BROADBAND SIGNAL AND NOISE CORRELATIONS vs DISTANCE AT TFSO EXTENDED ARRAY FROM 10 TELESEIMIC EVENTS

245

$$\phi_{mn}(\tau) = \frac{\frac{1}{T} \int_{t_0}^{t_0+T} Z_m(t) Z_n(t + \tau) dt}{\left[\frac{1}{T} \int_{t_0}^{t_0+T} Z_m^2(t) dt \; \frac{1}{T} \int_{t_0}^{t_0+T} Z_n^2(t) dt \right]^{1/2}}$$

where $-1 \leq \phi_{mn}(o) \leq 1$. In fact, proper alignment will be indicated when the maximum of $\phi_{mn}(\tau)$ occurs at $\tau = o$.

The time interval, T, used for most of these correlation computations was 20 seconds. The choice was governed by a compromise between choosing an interval to keep random correlations low and positive correlations high (i.e., many degrees of freedom) and choosing an interval short enough to contain strong P-wave signals throughout. To enable a direct comparison, the noise correlations were computed by the same method using 20 second samples of noise prior to the P-wave signals. The only modification was that noise cross-correlation functions were computed over more lags than the signals hunting for a maximum in the correlation function. Thus the array alignments for the maximum noise correlations were chosen close to, but not the same as, the signal alignments.

To determine how two seismic signals correlate at a particular frequency, the two traces are first filtered by a narrow band filter and the correlation coefficient formed from the outputs. The narrow band filters used in this study were recursive digital filters approximating the response,

$$\frac{\frac{\omega_0}{Q} s}{s^2 + \frac{\omega_0}{Q} s + \omega_0^2}$$

with the Q = 2.5 and resonant frequencies of 0.5, 0.64, 0.8, 1.0, 1.25, 1.6, 2.0, and 2.5 cps.

C. Statistical Averages

Correlation coefficients were computed for all possible pairs of seismometers in the TFSO extended array. Due to the array geometry some seismometer separation intervals were repeated, or almost repeated, many times while other distance intervals were not represented. Figure 207 shows an example of all the individual correlations computed for one frequency for one event. In plotting average correlations with distance, therefore, both the correlation values and their associated distances were averaged. The entire distance range, 1 kilometer to 1600

246
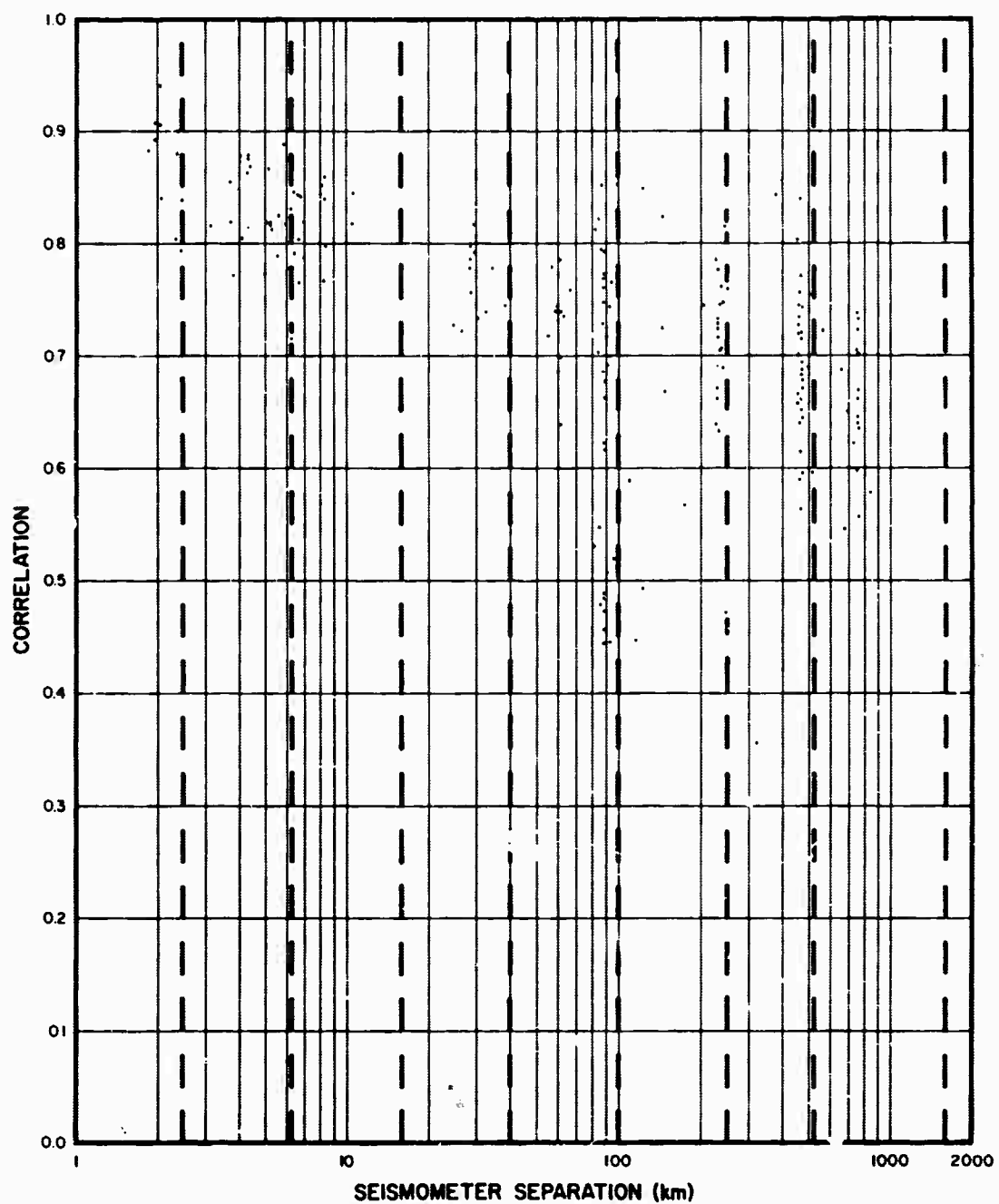
FIGURE 207. INDIVIDUAL CORRELATIONS vs DISTANCE AT 0.5 cps FOR A PERU EVENT RECORDED
AT TFSO EXTENDED ARRAY

247

kilometers, was divided into eight intervals which are more or less equal on a logarithmic scale (see Figure 207). All distance intervals of computed correlations within each of these distance ranges were averaged to find some average separation. The average correlations were the means of all correlations within one distance interval.

The confidence limits of the average correlations are akin to standard deviations. However since the correlations are bounded by unity, they are not normally distributed. Consequently, the ordinary methods for standard deviations will not be correct. Fisher[7] has shown that a new variable, z, defined from the correlations, r, as

$$z = 1/2 \; \ln(1 + r) - \ln(1 - r)$$

will be distributed almost normally and be practically independent of the value of the correlation in the population from which the sample is drawn. Confidence limits for the correlations are found by computing upper and lower bounds in a single standard deviation away from the mean in the z variable and converting back to correlation, r, by the transformation.

$$r = \tanh(z)$$

The means computed in the z variable will be slightly higher than the means computed on the correlations directly.

The sample interval of 20 seconds is a compromise between a short interval insuring that the P-wave signal is strong throughout, and a long interval to give many degrees of freedom to the correlation computations. Figure 208 shows the broadband correlations versus distance for several different sample intervals from 5 seconds to 22 seconds. The longer sample intervals give lower correlations; the shorter intervals give higher correlations and are more erratic. However, all choices show the same general trend of descending correlation with distance.

By our method of computing signal and noise correlations, purely random functions can be expected to correlate appreciably above zero. In fact, if the filters are narrow enough, purely random, uncorrelated inputs will give sinusoidal outputs which are virtually unchanging over any 20-second interval. The maximum of the cross-correlation function between two such samples will be almost unity.

If we can assume that the expected rms value of the cross correlation between two random functions[8] is given by

$$\sigma_{rms} = \left(E\left[\phi_{12}^{2}(t) \right] \right)^{1/2} = (1 + BT)^{-1/2}$$

---

[7]Snedcor, G. W., Statistical Methods, Iowa Univ. Press, 1937, pp. 175-180, presents a description of Fisher's transformation.

[8]Laning, J. H. and R. Battin, Random Processes in Automatic Control, McGraw-Hill, N. Y., 1956, pp. 160-163.

248
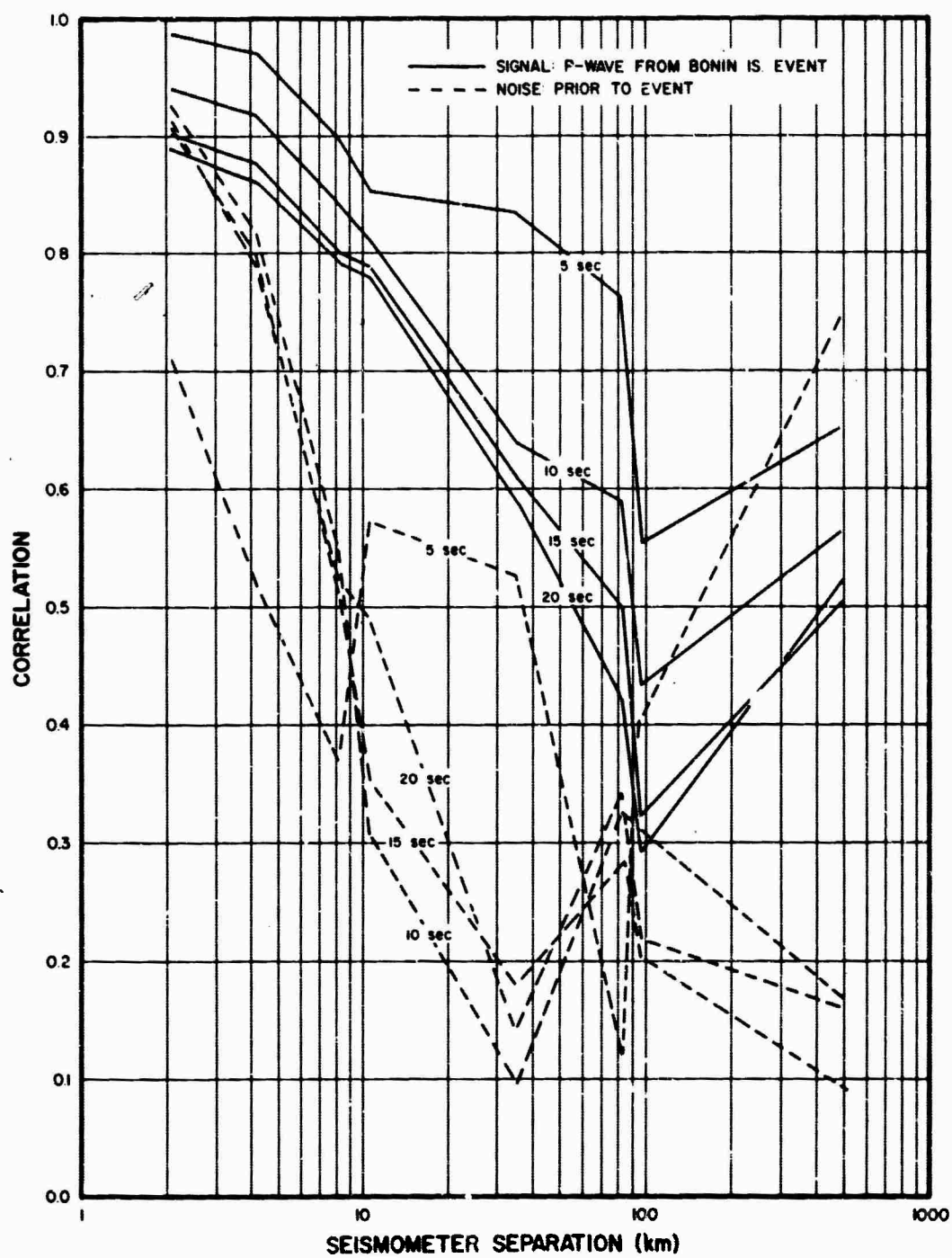
FIGURE 208. BROADBAND SIGNAL AND NOISE CORRELATIONS vs DISTANCE FOR DATA SAMPLES OF
5, 10, 15, and 20 SECONDS DURATION AT TFSO EXTENDED ARRAY

249

where T = sample interval = 20 seconds

B = the bandwidth

f_0 = resonant frequency

$Q = \dfrac{f_0}{\Delta_f} = 2.5$, a constant

and $B \cong 2\Delta f = \dfrac{2f_0}{Q} = .8f_0$

then we have the following table of expected correlations from random functions:

f_0(cps)	Expected rms of random correlations
0.5	.33
0.64	.30
0.8	.27
1.0	.24
1.25	.22
1.6	.20
2.0	.17
2.5	.16

Local maxima of the correlation functions will be somewhat higher than the expected rms values given above.

Beyond 10 to 15 kilometers the noise correlations level off at just the levels we would expect from random correlations. Conversely the signal correlations are significantly above the level expected from random functions even for seismometer separations of 1000 kilometers.

The results of this correlation study show that:

1. Signal and noise correlations decrease as distance and frequency increase.
2. The correlations of the signals are significantly greater than the correlations of the noise for all distances greater than 3 kilometers.
3. The noise correlations equal that expected from uncorrelated random functions for distance equal to and greater than 30 kilometers.
4. The signal correlations are significantly greater than random correlations for all distances spanned by the extended array.
5. There is no difference in correlations between signals from two seismometers normal to or in line with the signal direction.
6. The largest gain in signal correlations over noise correlations occurs at TFSO for seismometer separations of 10 to 100 kilometers.

More elaborate data processing schemes on LASA data will be studied at the SDL. However the calibration of the LASA array and the preliminary noise and signal studies just outlined will command the bulk of our attention at the SDL initially.

250

23. HARDWARE REQUIREMENTS FOR LASA CENTRAL SIGNAL PROCESSING SYSTEM

by

Richard G. Baldwin, Texas Instruments, Inc.

I. INTRODUCTION

During the last several months, a number of LASA signal processing schemes have been described. Therefore, a discussion of hardware requirements for a LASA could be very broad.

In order to limit the breadth of this discussion, only one such system will be considered. That system is the one presented by Dr. Milo Backus and Mr. George Baker included elsewhere in this conference report.

A block diagram of the total system is given in Figure 209. The system is seen to consist of three major parts:

- A special purpose (SP) digital computer which includes facilities for filtering and beam forming in real time on-line.
- A general purpose (GP) computer operating in a time shared on-line mode.
- A general purpose computer operating in a completely off-line mode.

The first two parts will be considered in terms of the requirements for performing each function, where each block in Figure 209 describes a particular function.

This system will operate in the following manner. Data will be read from 21 separate data lines and stored on a one-million word drum. This drum will act as a temporary buffer to save 1.5 minutes of data while a decision is being made whether or not to record the data or magnetic tape.

The SP computer will provide pre detection processing, detection processing, and decision logic to activate the on-line GP computer. The SP computer will also provide location and time information about a detected signal.

The GP computer will act on the location information to beam steer each of the 21 subarrays so that their beams are centered on the proper location, using history data from the drum storage. These beams, along with the 525 outputs from the individual seismometers and 21 multichannel filtered outputs from the SP computer on the drum buffer may be recorded on the magnetic tape.

Later, the GP computer will use the data on the magnetic tape to perform more sophisticated signal processing, off-line, but not in real time.
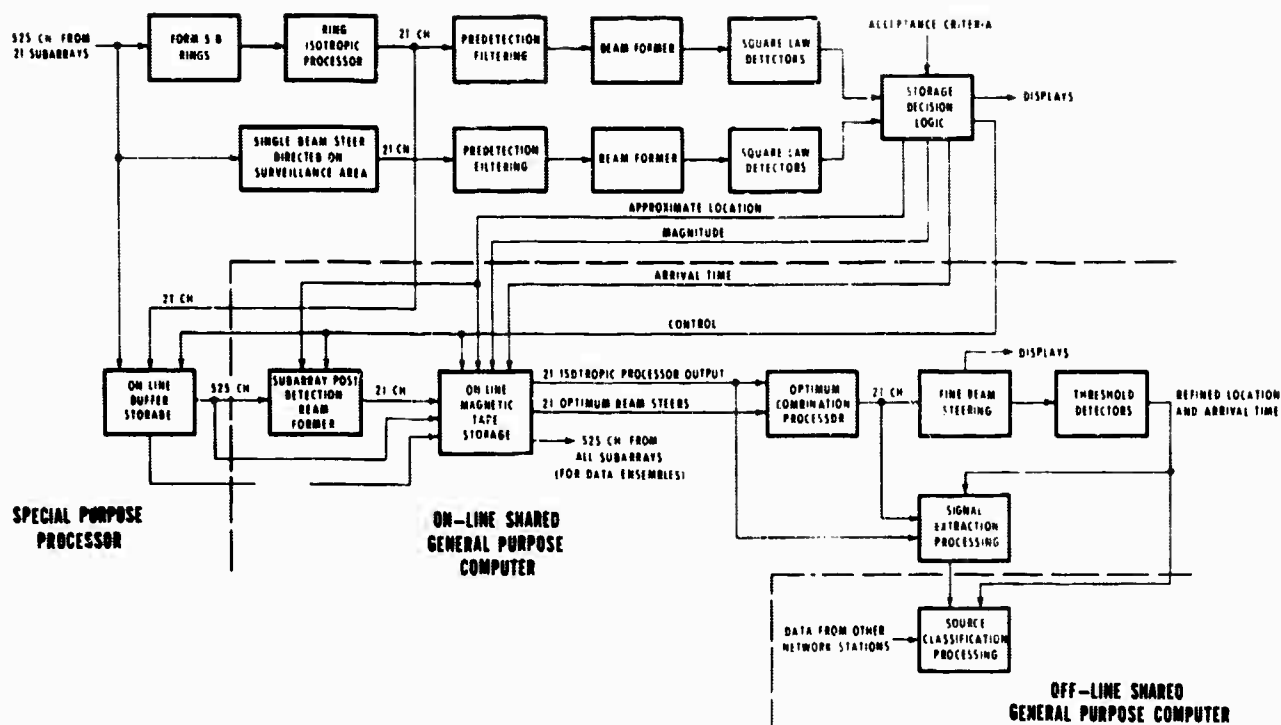
FIGURE 209. LASA PROCESSING SYSTEM

Finally, network analysis from more than one LASA will be performed on an off-line GP machine.

II. SPECIAL PURPOSE DIGITAL COMPUTER

A. Ring Sum Data Reduction

The first function to be considered is the addition of seismometer outputs from the sub-arrays. This addition will be performed in such a way that all the seismometers which fall on a particular ring in a subarray will be added together to produce a single time function. This will produce eight time functions for each subarray. It may also be desirable to add certain rings so as to produce five, six or seven outputs per subarray, or to make use of all individual seismometers.

The requirements for this function are shown in Figure 210. The computer must be able to read serial data from 21 parallel data lines and provide whatever skew compensation is necessary.

Probably the most severe requirement is the input data rate. Each line runs at 9600 bits per second, so that data must be transferred into the computer at a rate of 201,600 bits per second.

252
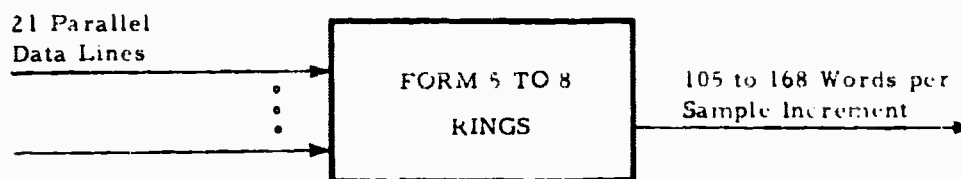
REQUIREMENTS:

1. Read serial data from 21 parallel data lines and compensate for skew if required.

   WORD LENGTH: 15 bits/word
   FRAME LENGTH: 32 words/frame
   INPUT RATE   =   9600 bits/second/data line
                 =   640 words/second/data line
                 = 13,440 words/second

2. Save first 25 words from each frame on each data line.

   INPUT DATA STORAGE: 525 words

3. Select appropriate words for summing on rings.

   OUTPUT DATA STORAGE: 105 to 168 words.

FIGURE 210. DATA RATE AND STORAGE REQUIREMENTS TO FORM RING SUMS

The input data rate problem has been solved in the existing Montana system being operated by Lincoln Laboratory. Therefore, feasibility of solution is not a problem here.

This computer must be capable of operating on the first 25 words from each 32-word frame on each data line and forming five to eight sums from each set of 25 words.

It may be necessary to provide storage for all 25 words from each of the 21 data lines, in which case 525 words of storage would be required. However, it may be possible to get by with only 21 words of core memory storage.

This would entail collecting 21 data words simultaneously in a set at input registers, transferring these 21 words into memory as soon as all 21 are completely received, and then adding each of the 21 into the proper accumulator location while another set of 21 input words is being collected in the input registers. At a 9.6 KC bit rate, 1562.5 μsec are required to collect a 15-bit word in each input register. Therefore, ample time will be available to perform the ring sums. It is quite possible that the input registers could be eliminated and the data could be taken from the drum (to be discussed later) and summed.

253

B. Single Beam Steer

The next function to be considered is that of forming a single beam steered output for each subarray directed on a particular surveillance area. (See Figure 211.) This would consist of simply time-shifting the seismometer outputs prior to summing.

```
525 CH From          SINGLE BEAM STEER
21 Sub Arrays  ──►  DIRECTED ON SURVEILLANCE  ──►  21 CH
                           AREA
```
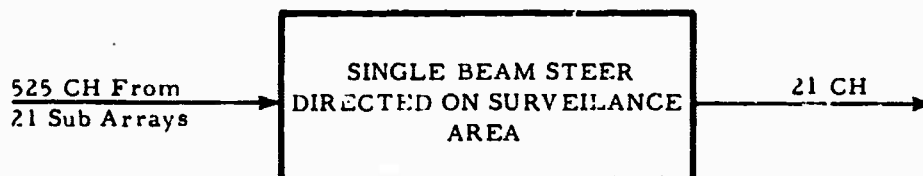
REQUIREMENTS:

Read serial data from 21 parallel data lines and form a single time-shifted beam steer output for each sub array.

   Maximum time delay = 0.5 sec = 10 samples

   Total history storage required = 5250 samples

   Arithmetic requirements = 525 additions each 50 ms

   Required addition time = 95 μ sec

THIS FUNCTION COULD BE READILY COMBINED WITH THE RING
FORMING FUNCTION AND PERFORMED IN A SMALL GP MACHINE.

FIGURE 211. BEAM STEERING REQUIREMENT FOR A SINGLE BEAM PER SUBARRAY

At teleseismic distances, the longest time delay that would be required within any particular subarray would be about 0.5 seconds or ten samples. This would require a total history storage of 5250 samples. However, considerable history will be stored on the magnetic drum and it will not be necessary to store history in a core memory.

Each 50 msec it will be necessary to access the drum and perform an addition 525 times. This will allow 95 μsec to access the drum and add. Once each 50 msec it will be necessary to transfer accumulated sums to the predetection filtering function.

C. Multichannel Filtering

The next function to be considered is multichannel filtering of ring summed data, as shown in Figure 212.

It has been assumed that filters of 100 points in length are desired to operate on eight time functions from each ring-summed subarray. In order to perform this function, it must

254

```
                          ┌─────────────┐
105 to 168 Words          │    RING     │    21 Words per Sample
──────────────────────►   │  ISOTROPIC  │    Increment
per Sample Increment      │  PROCESSOR  │    ──────────────────►
                          └─────────────┘
```

REQUIREMENTS:

Apply digital filter to each input channel and sum on sub arrays.

ASSUME: Filter length = 100 points
         Number rings = 8

Multiplications and additions required to form each independent output point = 800

Multiplications and additions required to form 21 independent output points = 16,800

Time available for 16,800 multiply and add = 0.05 sec

Necessary multiply and add time = 2.97 μsec

For 5 rings per sub array and 100 points per filter, necessary multiply and add time is 4.75 μsec/multiplication

THESE MULTIPLY AND ADD SPEEDS ARE WITHIN THE CAPABILITIES OF THE TI DIGITAL MCF.

FIGURE 212. MULTICHANNEL FILTERING REQUIREMENTS FOR RING SUMMED DATA

be possible to multiply a filter point coefficient by a data word and add the result to an output accumulator in 2.97 msec.

Texas Instruments has developed a digital multichannel filter system (as described by Leo Chamberlin elsewhere in this report) which will multiply two 12-bit numbers in less than one microsecond. This system is speed limited by a 2.5 μsec memory and could run with a faster memory if necessary.

This machine would certainly be adequate to perform the multichannel filtering since 2.97 μsec are available for the multiply and add operation. If only five rings are used for each subarray, 4.75 μsec are available for a multiply and add operation.

This MCF should not be constrained to operate on rings but should be capable of treating all 25 channels of selected subarrays. Further, the system should be capable of changing any particular subarray from ring operation to 25-channel operation automatically under computer control. A short time period of contaminated data during the changeover would be acceptable since all raw data could be stored on magnetic tape during this time.

255

This system should also be capable of operating on up to 42 input subarrays and providing 42 MCF filtered outputs.

Now assume that the MCF is designed to operate with a 1.5 μsec cycle time. This is believed to be within the state-of-the-art of available memories, multipliers, etc. This system would be capable of performing 33,000 multiplications during each 50 msec sample period. Operating with a full 525 input channels, the system would be capable of utilizing 63 filter points on each input channel. If the system were operated with a 32,000 word memory, 60-point or three-second filters could be used.

D. Predetection Filtering

The next function to be considered is the predetection filtering stage as shown in Figure 213. This would consist simply of filtering the 21 outputs from the multichannel filtered subarrays and the 21 outputs from the beam-steered subarrays to produce 42 new outputs which have been shaped in frequency.

REQUIREMENTS:

Read 42 input functions, apply 42 separate digital filters to produce 42 separate output functions reduced to polarity data after filtering.

ASSUME: Filter length = 100 points

Multiplications and additions per frame = 4200

Required multiply and add time = 11.9 μsec

THIS FILTERING OPERATION COULD BE DONE IN THE SAME ARITHMETIC UNIT AS THE MCF AND STILL STAY WITHIN THE SPEED OF THE TI DIGITAL MCF.

FIGURE 213. PREDETECTION FILTERING REQUIREMENTS

Once again, assume 100-point filters on 42 channels. This would require 4200 multiply and add operations per 50 msec. If this is combined into the arithmetic unit used to perform the eight-channel multichannel filter operation discussed previously, then a total of 21,000 multiply and add operations would be required in each 50 msec period. This would require that a multiply and add operation be performed in 2.38 μsec.

256

Although this is faster than the memory speed in the existing system, it is still well within the capabilities of the arithmetic unit of the existing digital multichannel filter system.

The next function is one of beam forming using polarity data. Therefore, the output data from the predetection filtering stage need be stored as polarity data only.

E. Polarity Beam Forming

The polarity beam forming function shown in Figure 214 will use two sets of 21-channel polarity data to form many time-shifted sum beams. The number of beams required is approximately 120.

The maximum time delay required for a 12 km/sec signal is about 17 seconds. Therefore, it will be necessary to store 340 one-bit history data words per input channel, or a total of 14,280 one-bit words.
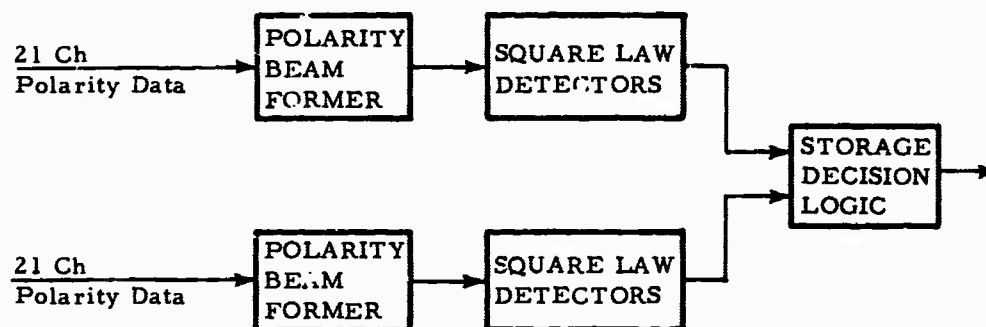
REQUIREMENTS:

Form 20 to 30 beams from each set of 21-channel polarity data, square the results or compute the absolute value, integrate, and apply decision logic.

Maximum time delay approx 17 sec or 340 one-bit words per channel.

History storage requirements = 14,280 one-bit words for beam forming.

Beam Steer Accumulator word length = 5 bits

Absolute value word length = 5 bits

Integration storage possibly one second or about 1000 5-bit words

Learning program for location, magnitude, and arrival time estimates.

FIGURE 214. POLARITY BEAM FORMING REQUIREMENTS

257

If, at a given time, all the 21 inputs add in phase, the output for a particular beam will be 21. This can be accumulated in a five-bit register. If it were desired to form 300 beams from each 21-channel input set, it would be necessary to perform 600 additions of 21 one-bit words each 50 msec. This would allow 3.96 μsec for accessing and adding each new one-bit word to the accumulated sum.

F. Square Law Detectors

The detection function will operate on many separate data channels, square (or take absolute value), and integrate over a predetermined time interval. If it is assumed that a one-second integration is required, and 600 beams need be formed, then it will be necessary to store 12,000 five-bit words. It would probably be desirable to make use of drum storage for this function.

G. Storage Decision Logic

This function will monitor the outputs from the square law detectors and compare them with a preset threshold level. Whenever a detector output exceeds the preset threshold, a signal will be transmitted to an on-line tape recorder to cause the information temporarily stored on the drum buffer to be transferred to the magnetic tape. The length of recording on magnetic tape will be controlled by the detection logic.

Information pertinent to the location of the signal will be transmitted to a post-detection beam former to be discussed later.

Information pertinent to the magnitude and time of arrival of the signal will be recorded on the magnetic tape and also printed on an available on-line printer.

In addition, this function will monitor other parts of the system and command permanent recording of all raw data in the event of trouble.

Possibly this should be a stored program section which can be upgraded with time as more knowledge is accumulated relative to the characteristics of the signals of interest.

H. On-Line Buffer Storage

Considerable mention has been made of a magnetic drum buffer storage unit. The purpose of this unit is to provide bulk storage as needed by the system.

In particular, this drum will provide temporary storage for about 1.5 minutes or 983,000 words of raw data (see Figure 215). Upon command from the decision logic mentioned previously, raw data will be transferred to the magnetic tape recorder for permanent storage. In addition, the drum will be used for temporary storage of partially processed data as mentioned previously.

258

```
              21 Ch MCF
              Outputs
                 |
                 v
              +----------+
              | ON-LINE  |------> 525 Ch
525 Ch Raw Data -----> | BUFFER   |
              | STORAGE  |------> 21 Ch
              +----------+
```
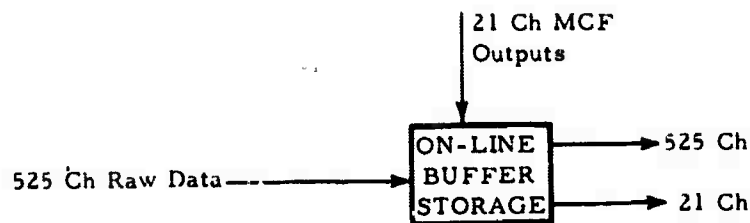
REQUIREMENTS:

Desired data buffer approx 1.5 min or 90 samples per channel or
982,800 samples for 546 channels

THIS BUFFER CAPABILITY COULD PROBABLY BE ACHIEVED WITH
A DRUM

FIGURE 215. ON-LINE BUFFER STORAGE REQUIREMENTS

III. ON-LINE SHARED GENERAL PURPOSE COMPUTER

A general purpose computer will be utilized on-line to do post-detection processing in
non-real time where applicable.

A. Subarray Post-Detection Beam Former

Upon command from the decision logic section of the system, the general purpose com-
puter will terminate the current off-line processing and go under control of the on-line system.
Location information will be used to specify the time delays required to beam-steer each sub-
array with the beam centered on the appropriate location. Fully quantized wide-band data will
be used and the results will be permanently stored on magnetic tape.

A maximum history storage of 5250 samples will be required (available from the drum)
and the required addition time will be 95 μsec. This will be a real-time function, and is shown
in Figure 216.

B. Optimum Combination Processor

This function would provide multichannel processing for 42 input functions considering
them in pairs. The processing would not necessarily be accomplished in real time since the
input data would be available from magnetic tape. The requirements for an assumed filter
length of 100 points are shown in Figure 217. If it were desired to do the filtering in real time,
11.8 μsec would be available for each multiply and add operation.

259
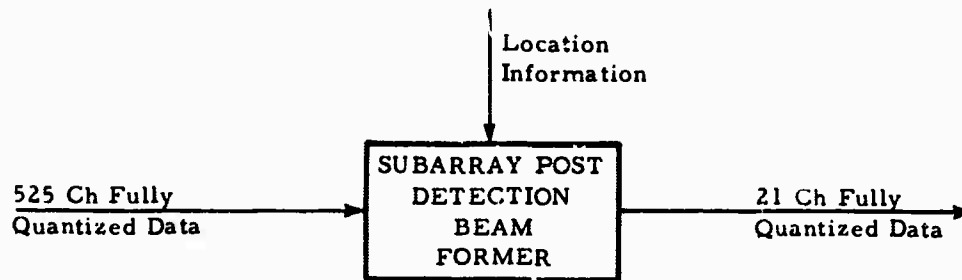
REQUIREMENTS:

Act on location information and form the appropriate best beam
for each subarray using fully quantized wide-band data.

   Maximum time delay = 0.5 sec = 10 samples

   History storage for beam steer = 5250 samples

   Required addition time = 95 μsec

THIS FUNCTION PERFORMED IN A SHARED ON-LINE GENERAL
PURPOSE COMPUTER.

FIGURE 216. SUBARRAY POST-DETECTION BEAM FORMER REQUIREMENTS
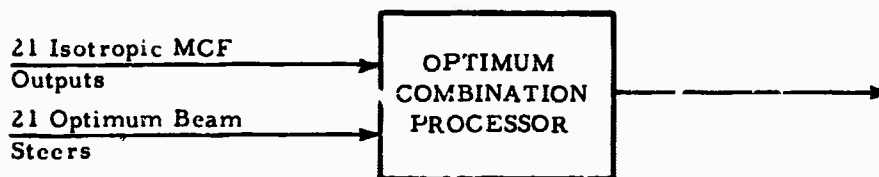
REQUIREMENTS:

Provide multichannel processing for 42 input functions, considering them
in pairs.

ASSUME: Filter Length = 100 points

Multiplications and additions required for one pair = 200

Total multiply and add required = 4200/50 msec

Required multiply and add time = 11.8 μsec

THIS FUNCTION COULD BE PART OF AN ON-LINE SHARED GP
COMPUTER

FIGURE 217. OPTIMUM COMBINATION PROCESSOR REQUIREMENTS

260

C. Signal Extraction, Fine Beam Steering, etc.

The full requirements for post-detection large array processing have not yet been fully specified. It is clear, however, that a reasonably powerful general-purpose computer will be required, since this computer should be capable of designing multichannel filters in the time domain.

IV. SUMMARY

The hardware requirements for a specific on-line LASA processing scheme have been described. It is apparent that some of the assumptions which were made regarding filter length, etc., may not agree with the values which will be used in a final system design. However, it is believed that the information which has been presented serves to illustrate that such a system is, in fact, feasible.

24. SDL LASA HARDWARE AND SOFTWARE

by

J. B. Wellen

Seismic Data Laboratory, Teledyne, Inc.

This report describes briefly the equipment and computer programs at the Seismic Data Laboratory (SDL) as they may relate to the processing of LASA data.

Figure 218 shows configuration as of June 1965.
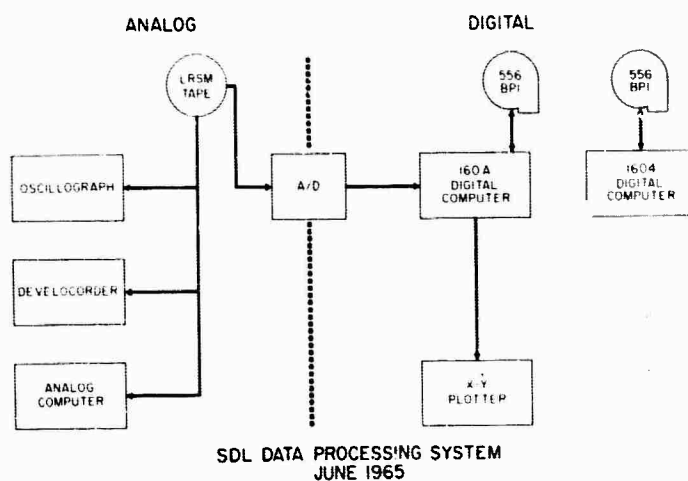
FIGURE 218. SDL DATA PROCESSING SYSTEM, JUNE 1965

The primary input to this system has been analog FM tapes recorded at the LRSM site and VELA UNIFORM observatories. Two kinds of requests have been made for this data:

Analog

- oscillograph or Develocorder playouts
- copies of original tapes
- analog computer processing such as particle motion studies, correlograms, and non-linear combination of traces
- preparation of composite tapes of shots, earthquakes, or other events of special interest

Digital

- analog-to-digital conversion of selected portions of the analog tapes
- copies of existing digitized data

In order to efficiently work with digitized data from LASA, the SDL data processing system was expanded as shown in Figure 219. Additions include:

- a magnetic tape drive which can read the 800 bits per inch tape generated at LASA.

262

- a 200 million bit disk file providing random access of data to both the 160A and 1604 computers.
- a digital-to-analog conversion system which will play out 26 channels of data simultaneously at 10 times real time.
- activation of a satelliting capability, allowing information to be exchanged directly between the 160A and 1604.
- a type of servo control which allows two Sangamo analog tape transports to be synchronized to each other during playback. Since data from 22 of LASA's sensors will be recorded on analog tape using 2 transports, this device will minimize problems due to variations in record and playback speeds.

SDL DATA PROCESSING SYSTEM
DECEMBER 1965
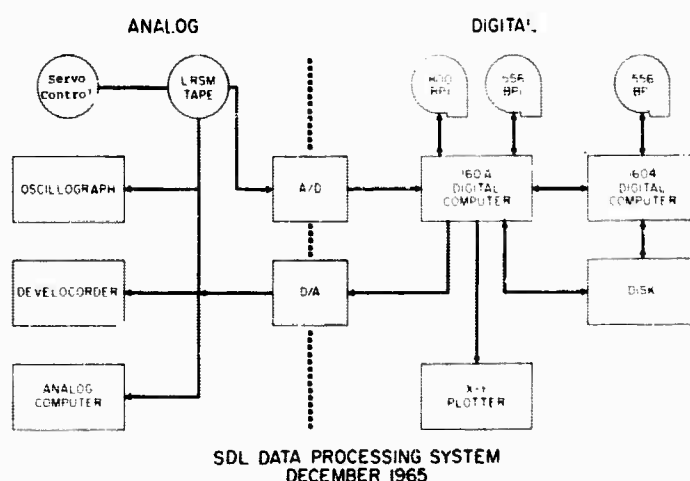
FIGURE 215. SDL DATA PROCESSING SYSTEM, DECEMBER 1965

Most of the LASA programming at SDL is designed to condense the data from 525 multiplexed channels to a smaller number (21) of time series, or to reformat the data for plotting or input to standard seismic signal analysis programs.

A program has been written to read a multiplexed LASA tape and to input from cards, parameters such as starting time, time interval to process, angle of incoming signal, and velocity. The output tape contains the phased sum of each subarray (21 phased sums) in a segmented format of 50 seconds from each subarray. Inoperative seismometers or subarrays, and distorted channels are not summed in. This is accomplished by checking the status words written on the tape by the computer at LASA, or by inputting the status from cards. At present we are determining which seismometers are to be deleted by plotting about 10 seconds from each of the 525 channels on the x-y plotter. This procedure will be speeded up by a program which will read portions of a LASA tape onto the disk and plot selected channels using the D/A system.

263

We have not yet decided which tape format would be most useful to users of LASA data both in SDL and within the VELA UNIFORM community. The problem of finding the best tape format for the digitized LRSM data was resolved by providing VELA users with a binary tape which could be read on an IBM 729 tape drive. Each user was then free to choose the optimum format for his own special studies and convert the tapes to that format.

The SDL LASA tape format will be determined after we assess our own retrieval problems with this data.

25. TRANSMISSION REQUIREMENTS FOR A WORLDWIDE LASA NETWORK

by

Harry Urkowitz, General Atronics Corporation

SUMMARY

Data transmission requirements for a worldwide LASA network depend upon the mode of operation. This paper presents a standard mode of operation, consisting of transmission of detected-event reports for those events whose seismic magnitude is equal to or greater than 4.0. If the world data center to which the material is transmitted desires a processed and cleaned-up seismogram representing one particular event, this would be transmitted, upon request, by electromagnetic signalling (teletype, for example). The requirements for detected events result in less than 200 binary digits per event. A processed seismogram would require, for complete data transmission, approximately 28 minutes. Since this does not happen often, it is concluded that standard teletype of 100 words per minute would be sufficient for this purpose.

Other modes of operation are considered. One of these modes, consisting of automatic transmission of processed seismograms (one from each LASA site) of detected events, would require the addition of a teletype link to the presumably existing command and control channel. An extreme mode of operation includes sending raw data to the world data center either from all of the individual seismometers or from each of many preformed beams. The requirements for these modes are measured in megabits per second. Transmitting only cluster or subarray outputs to the world data center would require a transmission facility of about 9.6 kilobits per second. These latter modes would probably require installation of new transmission facilities.

I. Introduction

This paper is limited to a discussion of the data transmission requirements from large aperture seismic array (LASA) installations throughout the world to a world data processing center not necessarily located in the United States. The problems of intra-site data locations are not considered here. It is presumed, however, that considerable sophisticated signal processing will be accomplished at each of the LASA sites. The data transmission requirements naturally depend on just how the worldwide net will be operated, the character and amount of information to be transmitted from the LASA sites to the world data center, and the speed with which these data must be transmitted.

To make this discussion definite a mode of LASA net operation will be assumed which appears to be reasonable. In addition, the appendix contains alternative modes of operation and

their data transmission requirements. It may be noted that most of these alternatives place rather heavy demands on data transmission.

The standard mode of operation assumed for the body of this paper is outlined as follows:

1. There will be 10 to 12 LASA sites throughout the world.

2. A seismic magnitude threshold is set and events whose estimated magnitude is below this threshold number will be neglected. This magnitude is arbitrarily set at 4 for this discussion.

3. A detailed event bulletin will be prepared for all detected events. This bulletin will be transmitted to the world data center within 24 hours after detection.

4. On request from the world data center, the LASA installation would submit a processed data tape consisting of a completely processed seismogram representing the completely processed output of the entire site. This data tape will have its information transmitted by electromagnetic signalling (teletype, for example).

5. The outputs of all seismometers as well as the outputs of subarrays of seismometers at the LASA installations will be recorded on magnetic tape. Some of these records will be kept for a short time and others will be kept indefinitely, as follows:
   a. All 525 seismometer output tapes will be kept for 10 days. Unless instructions to the contrary are received from the world data center, these tapes will be recycled for re-use.
   b. Tapes kept indefinitely will be those of the 21 subarray outputs and tapes containing processed events which exceed the magnitude threshold.

6. The world data center would automatically prepare seismic bulletins for transmission to all of the LASA installations; these bulletins would be based upon all information received at the world data center.

II. Transmission Requirements

A. Detected-Event Reports

The data transmission requirements are given in terms of the number of bits necessary to convey specific types of information. In the case of a detected-event report the following types

266

of information together with their bit requirements are given:

Parameters	Bit Requirements
Magnitude	6 bits
Time of onset (to within 1/10 second)	20 bits
Focal depth estimate	7 bits
Approximate epicenter	17 bits
Complexity parameters	10 bits
Amplitude	8 bits
Dominant period	10 bits
Other identification parameters (including significant phases and times)	40 bits

The sum is 118 bits per detected event. To provide for future contingencies the bit requirement is given as less than 200 bits per detected event.

To estimate the capacity necessary for sending event reports from the LASA installations to the world data center, it is generously assumed that the number of events of magnitude 4 or greater per day is about 50. This comes out to less than 10,000 bits per day necessary for reporting detected events.

A standard teletype word is capable of transmitting 30 data bits per word. At a standard speed of 100 words per minute, or 50 bits per second, 10,000 bits requires 200 seconds. Thus, using standard teletype transmission, the necessary transmission time during the day for such reports would be less than 200 seconds.

B. Processed Seismogram

On request from the world data center a processed seismogram of some specific event exceeding the threshold would be radioed to the world data center. For this processed or cleaned-up seismogram, we assume that the average duration will not exceed 10 minutes, and that the necessary dynamic range above threshold will be 40 decibels or 7 binary digits. Assuming a sampling rate of 20 samples per second, this comes to 84,000 bits per event. A standard teletype word is capable of transmitting 30 data bits per word, meaning 2800 teletype words per event. At a standard teletype speed of 100 words per minute the expected maximum duration of transmission time for answering the request from the world data center would be 28 minutes. Presumably this would not happen many times during the day. In addition, the assumed duration is very likely overly generous.

C. Automated Bulletin from the World Data Center

Although the automated bulletin from the world data center would have information concerning detected events from all of the LASA installations, it is unlikely that this bulletin would contain significantly more information than that from each of the LASA installations. It is therefore estimated that the data transmission requirements for the automated bulletin would be less than 10×200 or 2000 bits per event. In a standard teletype format this would take less than 40 seconds to transmit.

D. Comment

Under the assumption of the existence of a control and command channel of at least standard teletype quality, one may conclude that there is sufficient capacity to handle this mode of operation. If the command and control channel has voice quality transmission, then there is no doubt that it will be of sufficient capacity to handle this mode of operation. The figure of 50 detected events per day is probably excessive. It is used for illustration to show that the command and control channel will probably be sufficient for the data transmission requirements under the above mode of operation.

III. Conclusions

The standard mode of operation assumed here is that each LASA installation transmits routinely reports on events exceeding a threshold of seismic magnitude 4.0. Upon request from the world data center, a complete, cleaned-up, or processed seismogram would be transmitted to the world data center, for closer scrutiny. Under this mode of operation, the data transmission requirements are quite modest and can probably be handled by an existing or contemplated control and command channel which would be installed along with the LASA sites.

Other modes of operation are considered in the appendix. Each of these modes of operation are characterized by the transmission of considerably more data from the LASA site to the world data center. The mode which includes automatic transmission of detected events (events exceeding a given seismic threshold) could be accomplished by the addition of one teletype link in addition to the control and command channel. The other forms of operation, including transmitting all of the raw data from individual seismographs or from each subarray, result in greatly increased bandwidth requirements which cannot be satisfied with standard teletype transmission facilities.

268

APPENDIX
OTHER MODES OF OPERATION

A.1. Automatic Transmission of Detected Events

In this mode of operation it is assumed that the processing ability of the LASA installation is used to provide a single clean seismogra... and only events which exceed the threshold will have complete data transmitted to the world data center. To get approximate numbers, it is assumed that each LASA installation will have to handle on an average of ten events per day of magnitude equal to or greater than 4 and that the average duration of each of these events is five minutes, giving a total of 50 minutes during the day in which threshold will be exceeded, and requiring automatic transmission to the world data center. Assuming a range of 40 db or 7 binary digits above the threshold level, with a sampling rate of 20 samples per second, the requirement is for 420,000 bits per event on an average. Assuming the standard teletype word of 30 data bits per word, this comes out to 14,000 teletype words per event. This would take 140 minutes during the day to transmit. This requirement can be met by facilities of the type that are in existence, such as the DCA net or the Command and Control Channel which has been presumed, but it u .es a sizable portion of the communication capacity for the worldwide installation when all other stations are taken into account. This would strain the existing channel. If this mode is to be adopted it would be better to have a separate transmission channel for this purpose. This could be accomplished by the addition of one more teletype link.

A.2. Extreme Operation. All Raw Data.

The extreme in data transmission requirement occurs when it is desired to send all raw data back to the world data center for processing, regardless of what may be done at the individual LASA sites. Presuming that this extreme would use the Lincoln Laboratory format for transmitting the data, this would consist of 20 frames per second from each cluster, each frame consisting of 32 15-bit words. Since there are 21 clusters at each site, the total data rate requirement for sending all these data is 200,000 bits per second. Taking into account all of the LASA installations, the requirement for data transmission to the world data center would amount to 1.2 megabits per second. Clearly, this would call for extreme measures in providing the necessary data capacity. This could be handled with combinations of microwave relays, troposcatter relays, and coaxial cable land li es, but these have their own problems in site accessibility, installation, etc. The other possibility consists of a satellite communication network in which a bandwidth of about 2 megacycles per second is set aside for this purpose.

A.3. Cluster Outputs

A mode of operation requiring a smaller data rate is to send back one channel from each cluster to the world data center. Sampling at the rate of 20 samples per second, taking into

269

account the increase in dynamic range due to adding the outputs of individual instruments the data rate requirement is now 9.6 kilobits per second.

This rate is also excessive for use with the probably existing command and control channel, and would therefore require a net of its own. Good quality leased land-lines could provide the necessary capability but in many parts of the world these lines are not available. It is not known at the present time whether or not the use of the existing land lines and the installation of others, together with microwave relay links, troposcatter links, or HF links could be fitted together economically to provide the necessary capacity.

A.4. Data From Preformed Beams

Still another mode of operation is the formation of preformed beams at each site, with a separate data channel for each beam. Only the beam outputs would be transmitted to the world data center. Again using the sampling rate of 20 samples per second, taking into account the increase in dynamic ranges due to beam formation, the data rate requirement is 10^5 bits per second for each group of 300 beams. Taking into account all of the LASA installations, the data rate requirement is of the order of 1 or 2 megabits per second depending on the number of beams at each site. This requirement is approximately the same as that of Section A.1 above.

26. THE PROTOTYPE STATION
by
H. Sonnemann, ARPA

PREFACE

The third day of the LASA Evaluation Conference was devoted to a discussion of the prototype station. For completeness I am including my remarks which formed the basis for the discussions.

The prototype station specifications tabulated at the end of this conference report resulted from the effort of all participants. They were arrived at by considering each part of the system as it was presented. The spirited discussions by those present aided immeasurably in achieving a realistic system specification. I want to express my appreciation to all the conference attendees for their contribution to the discussions.

Although what follows will read like a self-contained presentation, I want to reiterate that it served primarily as a vehicle for the discussions. The tabulated specifications are the result, and supercede any of my remarks which may be at variance with the end product.

INTRODUCTION

The aim of this portion of the meeting is to establish the basic requirements of a prototype station. With the continuing pressures on ARPA to be ready to build additional LASA stations, it is necessary to establish a basis for generating station specifications at an early date, preferably today.

It seems to me that we are in no better position today than we were at the time of decisions for the Montana LASA to arrive at optimum station parameters. At best we have increased our confidence in the general scheme, have a better feel for the physical plant, some further inputs on the geometry of this type of array, and a general outline of the processing that is likely to be useful.

Most of you are probably aware that the Air Force has set up a program office for LASA at the Electronic Systems Division, Hanscom Field, in Lexington, Massachusetts, to be specifically responsive to requirements for additional LASA installations. Their first order of business will be to establish specifications to be able to implement additional installations if this requirement is established. To accomplish this they must be furnished with the basic criteria for the station complex. The group gathered here today seems uniquely qualified to arrive at the best criteria based on the information available to date.

To serve as a basis for discussion, I will go through the various elements of the system and set forth my interpretation of the requirement. This will be in terms of the need to arrive at specifications. As a result, I expect that a significant portion of what follows will be painful to the scientific ear since the requirements listed will be far from optimum and will be based on insufficient data. I intend to arrive at a general station design, which will subsequently be modified as the specific location, and new inputs from the Montana installation dictate. In contrast to this, one could postulate a station design tailored to each site on the basis of the terrain, geology, detailed noise study, etc. I do not feel that this approach can be implemented in a real time scale. The general station design, however, can be modified to take into account peculiarities of the particular location, provided it is recognized at this time that provisions must be made to accomplish such modifications to the general design as the need arises. This implies somewhat greater flexibility in stations specifically tailored to the site. It will hopefully, however, discourage special modifications which tend to make a station incompatible with the remainder of the network. It seems to me vital that the eventual desire to achieve network operation be kept in mind at all times, so that modifications to a general station design will be made only if it is compatible with the network requirement. This will further compromise the optimum design, at least initially.

The most straightforward way to consider all the elements of the system is from the input to the output so I will procede in that order.

SITES

The choice of the general areas in which an array is to be installed will be a compromise choice between technically desirable locations and other factors not related to the scientific requirements. I will merely assume that there is sufficient area available to install a full array, that the background noise level is within tolerable limits, and that the terrain is such that boreholes can be drilled, and data lines installed.

ARRAY CONFIGURATION

The basic array configuration will cover an area of 200×200 km. It will consist of 21 clusters of 25 instruments, each cluster covering an area of approximately 7 km in diameter. All cluster instrument outputs will be cabled to a central location for further data transmission and/or processing.

Note that I have said nothing about the layout of the clusters within the area. This is an item that must be considered today. Hopefully we can arrive at a recommendation. Again, I must stress that I fully recognize that tomorrow's results in Montana may change this recommendation. To alleviate fears that we will back ourselves into a corner, I would suggest that

the specifications we establish today be reviewed periodically by this group and upgraded to reflect our latest scientific knowledge.

Once we have arrived at an array configuration let us ask how we would modify this configuration if we did not have sufficient area to install the entire array. Would we reduce the diameter of it, or would we slice the outer ring? I would expect that we would reduce the diameter since this would minimize the degradation. But is the difference between a reduced diameter array and one with the outer ring removed sufficient to warrant the installation of the outer ring? Again, it presumably depends on how far the array diameter must be reduced to fit the array into the available terrain. Possibly we can arrive at a consensus of the maximum reduction in the diameter before the outer ring should be dropped, or the array considered to be too small to be in the LASA category.

BOREHOLES

We have now had some experience with 200 ft and 500 ft boreholes, both cased and uncased. There seems to be little difference between the cased and uncased borehole seismic signals. We have found in Montana that there was considerable difficulty in installing the uncased instruments because of almost immediate hole collapse. It has also become evident that if uncased boreholes are used, we must have all instruments on site prior to the drilling of the boreholes, and that in the case of instrument problems it is difficult to recover the instruments. Further, new boreholes must be drilled to reinsert the instruments. I want to suggest that the specifications require that the boreholes be cased, not so much because this is a technical necessity, but because it appears logistically very desirable. It will permit the drilling and casing to go forward independent of the instrument delivery, and as a bonus will permit the recovery of instruments and reinsertion of new ones in case of trouble, or if it is found in the future that the characteristics are to be modified, or additional instruments added in the boreholes.

BOREHOLE DEPTH

The minimum borehole depth presumably will depend on the local geological structure, so that this depth can not be specified. It appears reasonable though to cite the Montana experience and use the 200 ft depth as a good compromise for sedimentary areas. In granite a much shallower depth is undoubtedly satisfactory.

SEISMOMETERS

At this time we can cite the general specifications of the HS-10-1 as meeting our requirements. We need not be restricted to the HS-10-1, since I am sure, that we will be able to ask for competitive bids on seismometers when the need for them arises. I do feel, however, that the maximum case diameter should be that of the HS-10-1.

273

You may recall that the units we are using in Montana are double cased units. To date it has not been demonstrated that this is a necessity or adds appreciably to the performance of the units. We can carry this requirement as an option until we have more performance data from Montana. At the time a decision must be made this requirement should be reviewed. My own feeling at this time is that the double case is not required.

BOREHOLE CABLE

To date the PE-23 borehole cable has proved satisfactory. It is considerably cheaper than the armored cable which is generally used. There are problems in the cable seal to the seismometer. This has been overcome by Geospace and UED, although the process is cumbersome. I would recommend that the PE-23 cable be retained, and some effort expended to adapt other acceptable seismometers to it.

WELL-HEAD VAULT

The present well-head vault appears satisfactory.

WELL-HEAD TERMINATION

The Teledyne well-head termination appears satisfactory. Provisions should be added to tamperproof it.

AMPLIFIER

The Texas Instruments RA-5 amplifiers appear satisfactory. A new configuration which is truly balanced is now available from TI. This unit should be tested in the near future. It should further reduce the susceptibility to lightning, which is most troublesome in the power circuit. The new unit might be substituted for this in the near future, if it proves superior.

CABLES TO CENTRAL VAULT

The PE-23 cable to the central vault is satisfactory and should be specified for future installation. This cable can be installed underground or carried on poles. The preferred installation will be underground.

CENTRAL VAULT

The central vault design appears to be satisfactory. The underground construction is very desirable to stabilize the environment, and keep surface structures which could be vandalized to a minimum.

LIGHTNING PROTECTION, TERMINATION

The modified lightning system has not been completely evaluated but appears to be close to, or to be the solution.

Termination panels appear satisfactory.

274

AMPLIFIER POWER

Common power for each leg of the cluster has worked satisfactorily. The modified lighting protection system seems to have reduced to incidence of lightning damage sharply. The new amplifier configuration with the balanced to ground power system recently developed by TI should reduce potential lightning damage.

PRIME POWER

The requirements for prime power at each central vault need to be reviewed. Specifically, this prime power requirement should be divided into the requirement of the sub array terminal equipment and the auxiliary power needed if provisions for a LRSM or digital van are to be made. Only 1 KW is required for the subarray equipment. This requirement would have to be modified if an underground structure can not be used for the central vault and air-cooling, air-conditioning or heating is required.

The 8-hour standby capability should be reviewed for each particular installation area to determine if it is adequate in view of local power outages. As a planning item, the 8-hour figure seems reasonable.

Consideration should be given at this time to supplying prime power by fuel cells, local generators, etc. for areas which do not have commercial power, where commercial power cannot be readily furnished, or where theft or sabotage make it unreliable. Recommendations should be in hand for auxiliary power systems which can be serviced at 30-60 day intervals.

DATA TRANSMISSION AND RECORDING

From the construction phase we must now move to the data transmission and data recording phase of the prototype station. Again, as in the previous section, I will go through the systems from the front, that is the input section to the output of the data transmission system, up to and ncluding the recording of the 525 channels.

The first element we encounter is the isolation amplifier which converts the signal from a balanced to an unbalanced configuration. Following this, we have an amplifier to provide an unfiltered output and subsequently another stage of amplification and a filter section which cuts off the upper frequency response of the system at 5 cps to prevent aliasing in the subsequent signal manipulation. I will choose for the moment to consider the five cycle cut-off adequate with due deference to the arguments presented by Mr. Rubenstein on the desirability to retain a good high-frequency response. The 20 per second sampling rate is consequently satisfactory. A point of discussion might be whether the 80 db dynamic range is really necessary. It would

seem to me that to retain the flexibility in the system it is advisable to keep this dynamic range, unless other considerations force a cutback because of the limitations of the data transmission system beyond the modem at the central telemetry vault of the subarray.

There is at least one situation which I could postulate that might force us to consider ways to reduce the bit rate transmitted from a subarray to the central data acquisition facility. Since consideration is being given at this time to the possible installation of additional LASA stations outside the continental United States, I can envision situations where the data transmission system is vulnerable, that is subject to tampering or sabotage. Obviously, the open-wire line which we are using in Montana is most vulnerable. A radio relay could be used without out degradation of the data rate, where such an installation is feasible. In the worst case, we might be forced to bury the data transmission cables from the subarray to the data acquisition facility in a manner similar to the method now used to transmit the signals from each sensor to a subarray vault. This procedure would be somewhat painful and expensive due to the higher cable costs and the many repeaters which will be required in the line. A substantial cost saving might therefore be realized if the data rate can be reduced. We can achieve this by reducing the dynamic range, or what may turn out to be a more desirable procedure, by combining some of the sensors at the subarray prior to transmission to the central data acquisition facility. I think this is another logical point for discussion. It seems it would be desirable to have a consensus on procedure if such an eventuality should arise.

Once the signals have been digitized we will transmit them to the central data acquisition facility with equipment of the type now being used in Montana. I am sure that with a few more months of experience some of the minor problems which have been experienced can be ironed out.

At the central data acquisition facility, all the signals are being received, passed through an appropriate interface, and recorded on the PDT-7 computer tapes. Again, our present experience seems to indicate that this general approach is satisfactory.

We have now recorded all our signals on digital tapes. I will not dwell on the processing, or the exact processed outputs available from the computer, because with the recording of the 525 channels we have arrived at one goal, the objective to give us the data in a form which will permit any likely processing scheme to be applied.

Two additional points need to be considered prior to delving into the details of the processing system. One is the matter of calibration, and the other, which could rightly be considered part of the processing problem, the question of tape recycling time.

Our initial experience at Billings has indicated that it is entirely practical to carry out routine calibration on computer command or manually, as desired. To date, insufficient information is available to make a positive statement on the need for providing calibration coils in the seismometers. One could argue that it's an unnecessary complication in the system, or one could take the position that it is an aid in remote troubleshooting. From a cost standpoint it will probably not add a significant amount to the overall cost of the program. From a trouble-shooting standpoint it will permit the isolation of any potential difficulty to the amplifying system, the seismometer, or the coupling between the seismometer and the ground. My own inclination at this point is to say that the potential benefit of the calibration coil outweighs its additional cost. We might discuss the intervals of calibration, the types of signals to be applied, whether it is necessary to undamp the seismometer to calibrate, etc., but I do not feel that these issues form a basic problem of the prototype station. A word should be said about a re-cycle time of the tapes, even though this subject will come up again in discussing the network problems. It would seem to me that if all the data is to be recorded, which would require approximately 150 reels per day, a 10-day recycle time of tapes should be adequate to insure that significant events will not be erased prior to notification that the tape should be saved.

PROCESSING

We have now arrived at the more difficult sector of the prototype station, namely, to set forth guidelines for the processing equipment to be included in a station design. I recognize that we do not have sufficient data from the Montana installation to make very specific recommendations on hardware. We do have, however, a number of proposals for methods of processing the data which were presented yesterday. I think that we could take those as a basis for the discussion and arrive at a general outline of the likely form that the LASA prototype station processing would take.

Before we consider the prototype station processing I would like to depart from the subject for a moment to interject a network consideration which will interplay with the prototype station processing configuration. The question has come up, with regard to station capabilities of additional stations, on the extent of the processing to be performed locally. You have heard in the discussion of the network communications problem some of the constraints imposed by the system data rates. This certainly makes it advantageous to limit the real-time data transmission to outputs which have been partially or completely processed. In our discussions within ARPA, it has been tentatively agreed that each LASA station should have a capability to completely process the data. This would include subarray processing, if required, the formation of several beams pointing at specific areas, the formation of a packet of beams such as proposed by IBM to obtain area surveillance, provisions for threshold detectors to detect spe-

cific events, and if it appears desirable, a provision for vernier beams to refine the signals of interest to improve the chances of identification. Thus, we would have individual station capabilities to detect, locate, and possibly identify an event. For the purposes of this discussion I would like to exclude the portion of the processing which would require that the signal which was detected, located, and possibly identified, be taken off-line and further processed by the station equipment, or special equipment provided for the purpose of further enhancing the signal to achieve positive identification of the nature of the event.

This to me means that the basic station processing equipment must be capable of making a detection in real time.

I presume that I am correct in making the statement that some processing of the sub-array signals will be desirable. The extent of this processing certainly will depend to a large extent on the nature of the signal characteristics and background at each specific site. The output of the subarray then will be one or more processed outputs which form the input of the large array processor.

The processing equipment should be able to make a detection, epicenter location, and if possible, to say something about the identity of the signal. This we would like to achieve on-line. We have heard a number of proposals for processing the data, from which we can hope-fully extract in block diagram form the basic function of the prototype station on-line processing system.

278

27. SUMMARY OF STATION PARAMETERS

PARAMETER	SPECIFICATION FOR PROTOTYPE STATION
1. Array diameter	1. 100-200 km
2. Number of subarrays	2. Twenty-one, distributed approx. as in Montana. Distribution should be studied to remove close-in sidelobes from vicinity of main lobe.
3. Elements/subarray	3. 25 elements distributed as in Montana. Although some areas may not require as many elements, the present distribution will permit near optimum subarray processing subsequent to the installation. This will permit installation of the array after minimum noise surveys insure that the general area is seismically suitable.
4. Depth of burial of seismometers	4. 200 feet from surface appears to be a good compromise to achieve surface noise attenuation, yet keep drilling costs nominal. [500 feet would give a slight improvement over 200 feet during high winds or traffic. Deeper depths begin to show signal attenuation and interfering mode problems.] In fast and homogeneous media shallower burial in acceptable.
5. Elevation tolerance	5. Subarray datum ±.05 seconds from mean, for subarray without system correction. [It was concluded that if the terrain forces systems corrections, these should be made in the computation rather than by varying the borehole depth.]
6. Array area reduction	6. If geography dictates that the array diameter must be reduced, the 21 subarrays should be retained. The minimum diameter for the array should not fall below 60 km.
7. Boreholes	7. Boreholes should be cased, although there appears to be no seismic justification, it is very desirable logistically and for instrument maintenance to have cased boreholes. Casing the boreholes will permit the drilling operations to proceed independently of the instrument installation, and will subsequently permit repair and/or replacement of the seismometers. Boreholes should be nominally dry.

8. Seismometer	8. HS-10-1-ARPA Geospace or equivalent
A. Diameter	A. Not to exceed 4 3/4"
B. Natural period	B. 1 Hertz nominal, consistent between units
C. Phase	C. $\pm 10^0$ between units with $\pm 5^0$ tilt from 0.1-10 Hz. [It is desirable to meet these specifications with $\pm 10^0$ tilt to save drilling costs.]
D. Tilt	D. Must operate within specifications at $\pm 5^0$ tilt
E. Damping	E. 0.7 critical (nominal)
F. Double case (outer case insulated from inner case)	F. Appears not to be required. Further evaluation desirable
G. Calibration coil	G. Should be retained to permit remote calibration
H. Dynamic range, distortion, spurious modes	H. HS-10-1-ARPA satisfactory. Should be further investigated for HS-10-1-ARPA and checked for equivalent units.
9. Seismometer cable	9. Type 885P Ansonia Wire and Cable Co. (equivalent to REA specification type PE-23 with 10 mil copper shield.)
10. Pre-amplifier	10. Texas Instruments RA-5 with balanced, isolated input, balanced, ground referenced output and single ended output is currently in use. The balanced, ground referenced power configuration is desirable for future units to reduce susceptibility to lightning to a minimum.
11. Well-head vault configuration	11. The present Montana configuration appears to be satisfactory.
12. Interconnections with subarray terminal	12. Type 885P (PE-23) appears to be satisfactory. Only one six pair cable is required for the installation. The second pair provides redundancy, is useful for a permanent telephone link from the well-head to the subarray terminal and permits isolated power, calibration or special circuitry to be added at minimum cost. Both cables are laid in the same trench simultaneously.
13. Central vault (subarray terminal)	13. Satisfactory, except for stairway, which should be 3 ft wide for better equipment access.
14. Subarray terminal configuration and equipment [subarray electronics module-SEM and modulator-demodulator-MODEM] consisting of:	14.
A. Operational amplifiers (NEXUS CLA-5)	A. Satisfactory

280

B. Filters

C. Multiplexer and analog-digital converter (ADAGE VMX 32B/VS-13-AB/SA3/OP3/Two's complement)

D. Output formatter

E. Control module and calibration oscillator

F. Modulator-demodulator (MODEM) modulator, transmitter and receiver, Western Electric Co. Data set 303AID with type 809 modulator. [Leased from Telephone Co.]

15. Open wire and microwave data link

16. Data center
   A. Modulators-Demodulators (leased MODEMS)
   B. Phone line input system (PLINS)
   C. Master clock and timing signal generators
   D. General purpose computers (2) Digital Equipment Corp. PDP-7

   E. Monitor consoles
   F. Status boards

B. Satisfactory
C. Satisfactory

D. Satisfactory
E. Satisfactory

F. Satisfactory

15. Satisfactory

16.
   A. Satisfactory

   B. Satisfactory
   C. Satisfactory

   D. Satisfactory for recording, threshold detection, some beamforming as well as calibration and test programming. Can be programmed for additional on-line tasks, but will have to be supplemented with special purpose or additional general purpose computers for multi-channel filtering, most likelihood processing, epicenter location, and multiple coarse and/or fine beams, if these tasks are to be implemented in real or near real time.
   E. Satisfactory
   F. Satisfactory

28. SUMMARY OF LASA PROCESSING REQUIREMENTS

LASA PROCESSING REQUIREMENTS

PARAMETER	REQUIREMENT
1. Prototype station recording	1. As outlined in station requirements
2. Subarray processing	2. Present indications are that this is desirable to maximize array performance. The exact processing cannot be specified at this time. Minimum requirements will be for subarray sums. Probably filtered sums, steered sums and multi-channel filtered sums will be required.

3. Beamforming
  A. Coarse beams
  B. Vernier beams
	3. Entire world, on-line, real time
	  A. On-line magnitude 4
	  B. Off-line

4. Threshold detection	4. Detection on beams, not on subarrays
5. Epicenter location	5. On coarse beams, refined by vernier beams, and when sufficient signal is present on subarray
6. Event identification	6. Should be computer programmed. Initially analysis of event of interest will most likely be done visually from vernier beam outputs.
7. Station corrections	7. Upgrade automatically

8. Displays	8.
	  A. Provisions to make off-line records of events of interest for analysis.
	  B. Automated bulletin, preferably prepared in near real time (less than 24 hr lag for daily bulletin)

282

29. LASA STATION DATA STORAGE REQUIREMENTS

PARAMETER	REQUIREMENTS
1. Data storage	1.
A. All time	A1. 21 subarray outputs
	A2. Event tapes of 525 channels for events of magnitude 4 and above*
	A3. Processed data tapes
B. Ten days	B. 525 channel tapes*

---

*These requirements need to be re-examined, because they will incur high tape costs and extensive storage requirements.

30. LIST OF ATTENDEES

LASA Systems Evaluation Conference
14-16 September 1965

ACDA

Dr. Henry Myers

AFSC

Lt. Col. John J. Brunelly

AFTAC

Maj. Walter J. Davis
Mr. Jack F. Evernden
Mr. Doyle Northrup
Maj. Jack T. Pantall
Maj. Frank. F. Pilotte
Dr. Carl F. Romney

ARPA

Dr. John M. DeNoyer
Dr. Robert A. Frosch
Mr. Harry Sonnemann
Mr. Donald Clements

ESD (USAF)

Mr. John F. Asselta
Col. Charles Johnson
Col. David Kyzer

General Atronics

Mr. Joseph T. Beardwood
Dr. Bernard D. Steinberg
Mr. Harry Urkowitz
Mr. Andrew E. Zeger

IBM

Mr. Robert Baron
Mr. Stephen Lorenz
Mr. Felix Rosenthal
Dr. Woulter Vanderkulk

IDA

Dr. Joseph Aein
Dr. Walter D. Barfield
Dr. Milton U. Clauser
Dr. Robert A. Fox
Mr. David Katcher
Dr. William D. Montgomery
Dr. Elliott W. Montroll
Dr. Ivan Nelson
Mr. Francis Porzel
Mr. Albert M. Rubenstein
Dr. Jack P. Ruina
Mr. Alex Tachmindji
Dr. Benson Tucker
Prof. Eugene Herrin

MIT/Lincoln Laboratories

Mr. Howard J. Briscoe
Mr. Ronald G. Enticknap
Dr. Paul E. Green
Dr. Edward J. Kelly

Teledyne

Mr. E. F. Chiburis
Dr. William Dean
Dr. Edward A. Flinn
Mr. C. Boyd Forbes
Mr. Martin G. Gudzin
Mr. Jack H. Hamilton
Mr. R. A. Hartenberger
Mr. Charles E. Horn
Mr. Otto K. Kowallis
Mr. Vernon R. McLamore
Mr. Richard Obenchain
Mr. R. J. Swain
Dr. Robert Van Nostrand
Mr. J. B. Wellen
Mr. G. T. Young

UKAEA

Mr. Frank E. Whiteway
Dr. Frank H. Panton (British Embassy)

Texas Instruments

Dr. Milo M. Backus
Mr. George T. Baker
Mr. Richard G. Baldwin
Mr. L. A. Chamberlain
Mr. Harry R. Lake
Dr. Lawrence Strickland

BLANK PAGE

DOCUMENT CONTROL DATA · R&D

(Security classification of title, body of abstract and indexing annotation must be entered when the overall report is classified)

1 ORIGINATING ACTIVITY (Corporate author)	2a REPORT SECURITY CLASSIFICATION
ADVANCED RESEARCH PROJECTS AGENCY	Unclassified
	2b GROUP

3 REPORT TITLE

"Large Aperture Seismic Array (LASA)
First LASA Systems Evaluation Conference"

4 DESCRIPTIVE NOTES (Type of report and inclusive dates)

5 AUTHOR(S) (Last name, first name, initial)

Conference Proceedings

6 REPORT DATE	7a TOTAL NO OF PAGES	7b NO OF REFS
February 1966	xii + 284	25

8a CONTRACT OR GRANT NO.	9a ORIGINATOR'S REPORT NUMBER(S)
In-House	
b PROJECT NO	
c	9b OTHER REPORT NO(S) (Any other numbers that may be assigned this report)
d	

10 AVAILABILITY/LIMITATION NOTICES

11 SUPPLEMENTARY NOTES	12 SPONSORING MILITARY ACTIVITY
	OSD/ARPA/NTRO

13 ABSTRACT

This conference report consists of a compilation of papers describing the LASA installation in Montana. This includes the ground installation, data transmission and data acquisition systems. In addition, the proposed long-period seismometer installation is discussed, as well as potential on-line and off-line processing systems for the Billings Data Center. Preliminary results from the installation are reported along with results from Tonto Forest Seismological Observatory with instruments spaced over similar distances. An extensive series of papers describe the beam pattern analyses for the LASA installation and present theoretical data which will bear on the array geometry if additional arrays are to be constructed. Finally, prototype station requirements are developed, reflecting the current assessment of the desirable station configuration.

DD FORM 1 JAN 64 **1473**

14	KEY WORDS	LINK A		LINK B		LINK C	
		ROLE	WT	ROLE	WT	ROLE	WT
	LASA						
	Large aperture array(s), seismic						
	Buried arr						
	Array equip nt						
	Beam patte alysis						
	Array geomet,						

INSTRUCTIONS

1. ORIGINATING ACTIVITY: Enter the name and address of the contractor, subcontractor, grantee, Department of Defense activity or other organization (corporate author) issuing the report.

2a. REPORT SECURITY CLASSIFICATION: Enter the overall security classification of the report. Indicate whether "Restricted Data" is included. Marking is to be in accordance with appropriate security regulations.

2b. GROUP: Automatic downgrading is specified in DoD Directive 5200.10 and Armed Forces Industrial Manual. Enter the group number. Also, when applicable, show that optional markings have been used for Group 3 and Group 4 as authorized.

3. REPORT TITLE: Enter the complete report title in all capital letters. Titles in all cases should be unclassified. If a meaningful title cannot be selected without classification, show title classification in all capitals in parenthesis immediately following the title.

4. DESCRIPTIVE NOTES: If appropriate, enter the type of report, e.g., interim, progress, summary, annual, or final. Give the inclusive dates when a specific reporting period is covered.

5. AUTHOR(S): Enter the name(s) of author(s) as shown on or in the report. Enter last name, first name, middle initial. If military, show rank and branch of service. The name of the principal author is an absolute minimum requirement.

6. REPORT DATE: Enter the date of the report as day, month, year; or month, year. If more than one date appears on the report, use date of publication.

7a. TOTAL NUMBER OF PAGES: The total page count should follow normal pagination procedures, i.e., enter the number of pages containing information.

7b. NUMBER OF REFERENCES: Enter the total number of references cited in the report.

8a. CONTRACT OR GRANT NUMBER: If appropriate, enter the applicable number of the contract or grant under which the report was written.

8b, 8c, & 8d. PROJECT NUMBER: Enter the appropriate military department identification, such as project number, subproject number, system numbers, task number, etc.

9a. ORIGINATOR'S REPORT NUMBER(S): Enter the official report number by which the document will be identified and controlled by the originating activity. This number must be unique to this report.

9b. OTHER REPORT NUMBER(S): If the report has been assigned any other report numbers (either by the originator or by the sponsor), also enter this number(s).

10. AVAILABILITY/LIMITATION NOTICES: Enter any limitations on further dissemination of the report, other than those imposed by security classification, using standard statements such as:

(1) "Qualified requesters may obtain copies of this report from DDC."

(2) "Foreign announcement and dissemination of this report by DDC is not authorized."

(3) "U. S. Government agencies may obtain copies of this report directly from DDC. Other qualified DDC users shall request through

_____ ."

(4) "U. S. military agencies may obtain copies of this report directly from DDC. Other qualified users shall request through

_____ ."

(5) "All distribution of this report is controlled. Qualified DDC users shall request through

_____ ."

If the report has been furnished to the Office of Technical Services, Department of Commerce, for sale to the public, indicate this fact and enter the price, if known.

11. SUPPLEMENTARY NOTES: Use for additional explanatory notes.

12. SPONSORING MILITARY ACTIVITY: Enter the name of the departmental project office or laboratory sponsoring (paying for) the research and development. Include address.

13. ABSTRACT: Enter an abstract giving a brief and factual summary of the document indicative of the report, even though it may also appear elsewhere in the body of the technical report. If additional space is required, a continuation sheet shall be attached.

It is highly desirable that the abstract of classified reports be unclassified. Each paragraph of the abstract shall end with an indication of the military security classification of the information in the paragraph, represented as (TS), (S), (C), or (U).

There is no limitation on the length of the abstract. However, the suggested length is from 150 to 225 words.

14. KEY WORDS: Key words are technically meaningful terms or short phrases that characterize a report and may be used as index entries for cataloging the report. Key words must be selected so that no security classification is required. Identifiers, such as equipment model designation, trade name, military project code name, geographic location, may be used as key words but will be followed by an indication of technical context. The assignment of links, rules, and weights is optional.